Technical report on UK supplementary modelling assessment under the Air Quality Standards Regulations 2010 for 2022

Report for The Department for Environment, Food and Rural Affairs, The Welsh Government, The Scottish Government and The Department of the Environment for Northern Ireland

Ricardo Energy & Environment/R/3475

ED 12633 | Issue Number 1 | Date 14/02/2024

Customer:

The Department for Environment, Food and Rural Affairs, The Welsh Government, The Scottish Government and The Department of the Environment for Northern Ireland

Customer reference:

ecm_61369

Contact:

Sally Whiting
Ricardo Energy & Environment
Gemini Building, Harwell, Didcot, OX11 0QR, United Kingdom

t: +44 (0) 1235 75 3186

e: sally.whiting@ricardo.com

Ricardo is certificated to ISO9001, ISO14001 and OHSAS18001

Author:

Katherine L Pugsley, John R Stedman, Daniel M Brookes, Andrew J Kent, Rebecca J Morris, Sally L Whiting, Jasmine V Wareham, Abigail Pepler, Thomas M Thorp, Sam Gorji, Oliver Marshall

Approved By:

John Stedman

Date:

14 February 2024

Ricardo Energy & Environment reference:

Ref: ED12633- Issue Number 1

Executive summary

The United Kingdom's (UK) air quality regulations require that the UK undertakes air quality assessments on an annual basis under the Air Quality Standards Regulations 2010 (AQSR) (*legislation.gov.uk*, 2010).

The UK annual air quality assessment for the year 2022 has been undertaken in accordance with the requirements of the AQSR. The assessment takes the form of comparisons of measured and modelled air pollutant concentrations with the limit values, critical levels, target values and long-term objectives set out in the regulations. The AQSR includes a requirement to deduct the contribution to ambient PM from natural sources. The results were published and made available to the public in September 2023 in the form of e-Reporting Data flows (specifically Data flow G on attainment) (*UK-Air*, 2023).

The AQSR sets limit values for the ambient concentrations to be achieved for:

- sulphur dioxide (SO_2)
- nitrogen dioxide (NO_2)
- particles (PM_{10})
- lead (Pb)
- benzene (C_6H_6)
- carbon monoxide (CO)

The AQSR also includes:

- critical levels for the protection of vegetation to be achieved for ambient concentrations of sulphur dioxide (SO_2) and oxides of nitrogen (NO_x)
- a target value, a limit value, an exposure concentration obligation and exposure reduction targets for fine particles ($PM_{2.5}$)
- target values and long-term objectives for ozone (O_3)

AQSR sets target values for the ambient concentrations to be achieved for:

- Arsenic (As)
- Cadmium (Cd)
- Nickel (Ni)
- Benzo(a)Pyrene (B(a)P)

The UK has been divided into 43 zones for air quality assessment. There are 28 agglomeration zones (large urban areas) and 15 non-agglomeration zones. The status of the zones in relation to the limit values, critical levels, target values and long-term objectives has been assessed.

This report provides a summary of key attainment results from the e-Reporting publication for the AQSR pollutants and technical information on the modelling methods that have been used.

The results of the assessment against limit values are summarised in Table E1. This shows that 9 zones have not achieved full compliance with the annual NO_2 limit value in 2022.

Table E2 summarises the results of the assessment for O_3 in terms of the numbers of zones with exceedances of the target values and long-term objectives. Ozone concentrations typically show considerable variation from year to year as a result of variation in weather conditions.

Table E3 shows that there were no exceedances of the target value, limit value or exposure concentration obligation for $PM_{2.5}$.

The results of the assessment against the target values for As, Cd, Ni and B[a]P are presented in Table E4. Three zones have not achieved full compliance with the annual Ni target value and two zones have not achieved full compliance with the annual B(a)P target value in 2022.

Table E1. Summary results of air quality assessment for 2022: comparison with limit values and critical levels

Pollutant	Averaging time	Number of zones exceeding limit value
SO_2	1-hour	None
SO_2	24-hour	None
SO_2	Annual[1]	None
SO_2	Winter[1]	None
NO_2	1-hour[2]	None
NO_2	Annual	9 zones (1 measured + 8 supplementary assessment)
NO_x	Annual[1]	None
PM_{10}	24-hour	None
PM_{10}	Annual	None
Lead	Annual	None
Benzene	Annual	None
CO	8-hour	None

1 - Critical levels rather than LVs applying to vegetation and ecosystem areas only.
2 - No modelling for 1-hour LV

Table E2. Summary results of air quality assessment for 2022 for O_3: comparison with target values and long-term objectives

Pollutant	Averaging time	Number of zones exceeding target value	Number of zones exceeding long term objective
O_3	8-hour	none	43 zones (37 measured + 6 supplementary assessment)
O_3	AOT40	none	11 zone (5 measured + 6 supplementary assessment)

Table E3. Summary results of air quality assessment for 2022 for $PM_{2.5}$: comparison with target value and limit value and exposure concentration obligation

Pollutant	Averaging time	Number of zones exceeding target value
$PM_{2.5}$	Annual target value (25 µg m^{-3})	None
$PM_{2.5}$	Annual limit value (20 µg m^{-3})	None
$PM_{2.5}$	Exposure concentration obligation (20 µg m^{-3})	Not exceeded

Table E4. Summary results of AQSR air quality assessment for 2022: comparison with target values

Pollutant	Averaging time	Number of zones exceeding target value
As	Annual	None
Cd	Annual	None
Ni	Annual	3 zones (3 supplementary assessment: Sheffield, South Wales, Yorkshire & Humberside)
B(a)P	Annual	2 zones (2 supplementary assessment: Swansea, South Wales)

Table of contents

1 Introduction

1.1 The UK air quality regulations and the EU ambient air quality directives

The United Kingdom's (UK) air quality regulations require that the UK undertakes air quality assessments on an annual basis under the Air Quality Standards Regulations 2010 (AQSR) (*legislation.gov.uk*, 2010).

Prior to 2020 the UK's air quality assessment was undertaken under the European Union directives. The European Union directives on ambient air quality were established to assist member states to achieve protection and improvement of the environment. These directives require member states, which previous to 2020 included the UK, to undertake air quality assessments, and to report the findings of these assessments to the European Commission on an annual basis. Historically this was done according to:

- The Air Quality Framework Directive (1996/62/EC)
- The four Daughter Directives 1999/30/EC, 2000/69/EC, 2002/3/EC and 2004/107/EC.

In June 2008, a new directive came into force: The Council Directive on ambient air quality and cleaner air for Europe (2008/50/EC), which is known as the 'Air Quality Directive' (AQD). This directive consolidated the first three Daughter Directives, and was transposed into AQSR Regulations in England, Scotland, Wales and Northern Ireland in June 2010. The 4th Daughter Directive (AQDD4), 2004/107/EC was also transposed into the AQSR 2010.

The UK annual air quality assessment for the year 2022 has been undertaken in accordance with the requirements of the AQSR. The assessment takes the form of comparisons of measured and modelled air pollutant concentrations with the limit values, critical levels, target values and long-term objectives set out in the regulations. The AQSR includes a requirement to deduct the contribution to ambient PM from natural sources. The results were published and made available to the public in September 2023 in the form of e-Reporting Data flows, specifically Data flow G on attainment) (*UK-Air*, 2023). The 2022 UK submission on air quality is summarised by the annual Air Pollution in the UK reports (Air Pollution in the UK, 2023), which comprise a compliance assessment summary report and a full report, which, in addition, presents air quality modelling data and measurements from the UK national air quality monitoring networks.

The air quality assessment has been reported via the following e-Reporting Data:

- B: Zones and agglomerations
- C: Assessment regime
- D: Assessment methods
- E: Primary validated assessment data
- G: Attainment

Information on the supplementary assessment methods (modelling, diffusion tubes and objective estimations) has been provided in Data flows C and D and results have been provided in Data flows E and G.

The AQSR sets limit values (LVs) for the ambient concentrations to be achieved for:

- sulphur dioxide (SO_2)
- nitrogen dioxide (NO_2)
- particles (PM_{10})
- lead (Pb)
- benzene (C_6H_6)
- carbon monoxide (CO)

The AQSR also includes:

- critical levels (CL) for the protection of vegetation to be achieved for ambient concentrations of sulphur dioxide (SO_2) and oxides of nitrogen (NO_x)
- a target value (TV), a limit value, an exposure concentration obligation (ECO) and national exposure reduction targets (NERT) for fine particles ($PM_{2.5}$)

- target values (TVs) and long-term objectives (LTOs) for ozone (O_3)

The AQSR sets target values to be achieved for:

- arsenic (As)
- cadmium (Cd)
- nickel (Ni)
- polycyclic aromatic hydrocarbons with benzo(a)pyrene (B(a)P) as an indicator species

The number of monitoring sites required for compliance defined within the AQSR is reduced if other means of assessment, in addition to fixed monitoring sites, are available for inclusion in the annual air quality assessment. Air quality modelling has been carried out to supplement the information available from the UK national air quality monitoring networks. Diffusion tube data from the UK Urban NO_2 Network (UUNN) was included as part of the supplementary assessment for 2022. The diffusion tube data can be found on UK-Air (*UK-Air*, 2023), there is also a report for 2022 (Environment Agency/Joint Air Quality Unit, 2022).

1.2 This report

This report comprises technical information on the modelling methods that have been used for the assessed year, a summary of key attainment results from the e-Reporting submission for the AQSR pollutants, and key comparisons of findings for measured and modelled air pollutant concentrations with the limit values, critical levels, target values and long-term objectives set out in the regulations. The results of the air quality assessment for 2022 are summarised in Section 2.

Sections 3 to 11 of this report describe the Pollution Climate Mapping (PCM) modelling methods that have been used to calculate concentrations of SO_2, NO_x, NO_2, PM_{10}, $PM_{2.5}$, C_6H_6, O_3, heavy metals (Pb, As, Cd, Ni) and B(a)P for 2022 as part of the assessment of compliance with the limit values, critical levels, target values and long term objectives for each pollutant. This includes:

- A summary of the limit values, critical levels, target values and long-term objectives set out in the regulations for each pollutant.
- Details of the modelling methods including summaries of inputs, assumptions and schematic flow diagrams of the modelling process
- Source apportionment information
- Information on the verification of the models used and comparisons with data quality objectives.

The assessment for CO is described in Section 8. Prior to 2011 a modelling assessment was completed for CO. However, as ambient concentrations throughout the UK have been well below the limit value and assessment thresholds for many years, models are no longer required for CO and the supplementary assessment for 2022 has been based on objective estimation, as it was for 2011-2021.

1.3 Assessment regime and definition of zones

The regulations include a requirement to undertake preliminary assessments of ambient air quality. The objectives of these assessments were to establish estimates for the overall distribution and levels of pollutants, and to identify additional monitoring. The preliminary assessment (Bush, 2000) carried out for 1st Daughter Directive (AQDD1), 1999/30/EC, defined a set of zones to be used for air quality assessment in the UK. The preliminary assessment for the UK for AQDD4 was reported by (Bush, 2007). The AQD includes a similar requirement for continued assessment under Article 4, the preliminary assessment for the UK fulfilling this requirement was reported by (Vincent, Bush and Telling, 2010). The AQSR continues the requirement for the establishment of zones and agglomerations. Table 1.1 contains details of area, population and urban road length contained in each UK zone and agglomeration. The population data are from the 2021 census for England and Wales and mid-year estimates for 2021 for Scotland and Northern Ireland derived from data provided by National Records of Scotland and Northern Ireland Statistics and Research Agency. Output area totals have been assigned to 1 km grid squares using residential information from OS address base. The zones and agglomerations map for the UK is presented in Figure 1.1.

Figure 1.1 - UK zones and agglomerations for 2022

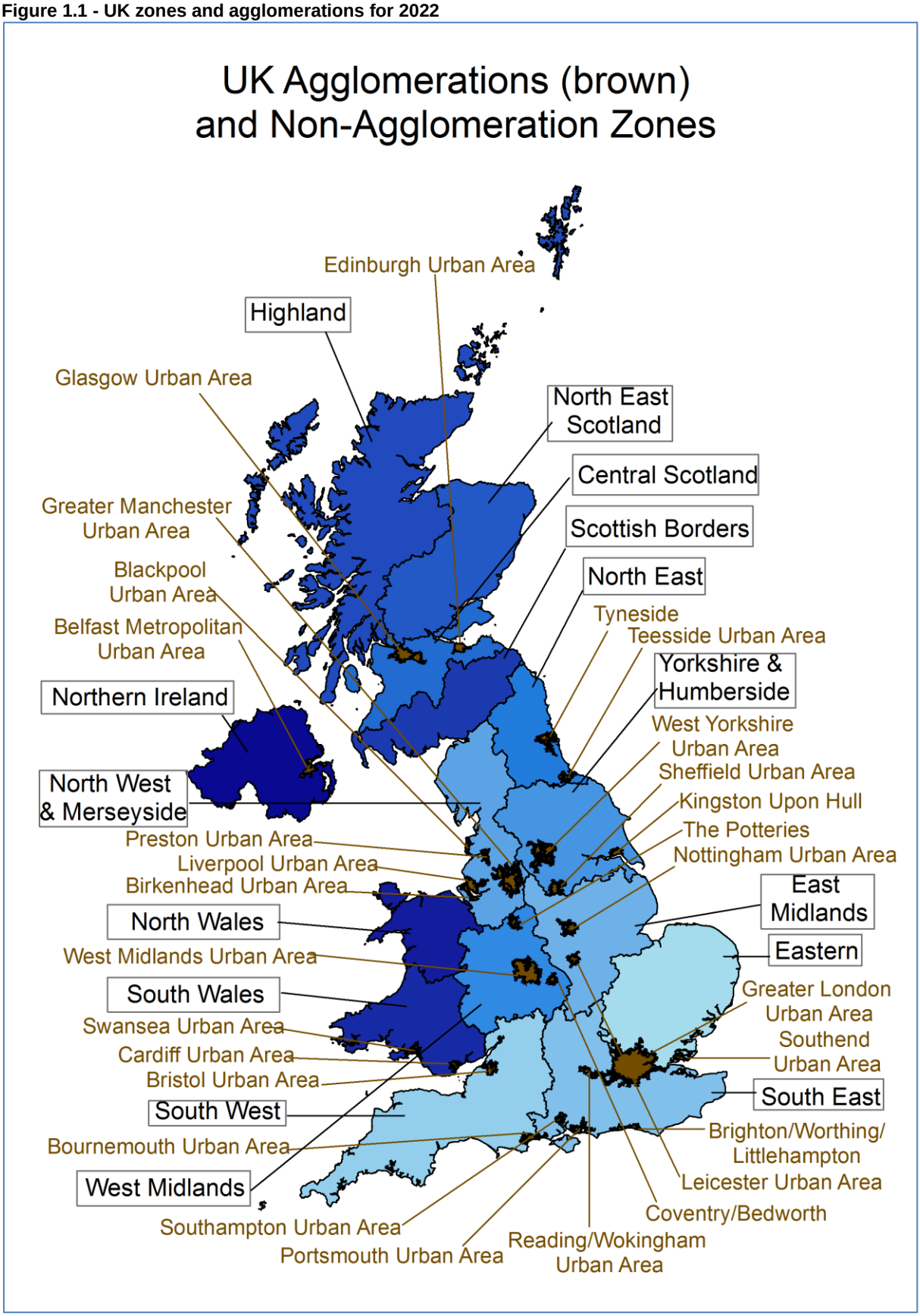

Agglomeration zones (brown)
Non-agglomeration zones (blue)

Table 1.1 - Zones for Air Quality Standards Regulations reporting.

Zone	Zone code	Ag or non-ag*	Population	Area (km^2)	Number of urban road links	Length of urban road links (km)
Greater London Urban Area	1	ag	9613389	1618	1879	1989
West Midlands Urban Area	2	ag	2446358	605	383	575
Greater Manchester Urban Area	3	ag	2242420	554	569	695
West Yorkshire Urban Area	4	ag	1397924	352	287	425
Tyneside	5	ag	783588	222	164	216
Liverpool Urban Area	6	ag	777268	199	243	218
Sheffield Urban Area	7	ag	588087	163	107	161
Nottingham Urban Area	8	ag	625777	155	129	133
Bristol Urban Area	9	ag	589880	139	113	130
Brighton/Worthing/Littlehampton	10	ag	432517	94	56	83
Leicester Urban Area	11	ag	471614	101	61	83
Portsmouth Urban Area	12	ag	405576	98	58	79
Teesside Urban Area	13	ag	318965	120	53	63
The Potteries	14	ag	293009	91	122	140
Bournemouth Urban Area	15	ag	398461	122	53	77
Reading/Wokingham Urban Area	16	ag	334368	82	67	77
Coventry/Bedworth	17	ag	337034	76	31	41
Kingston upon Hull	18	ag	285875	85	40	55
Southampton Urban Area	19	ag	315105	79	59	78
Birkenhead Urban Area	20	ag	290578	97	71	89
Southend Urban Area	21	ag	252560	67	31	55
Blackpool Urban Area	22	ag	231802	75	47	55
Preston Urban Area	23	ag	221642	60	35	42
Glasgow Urban Area	24	ag	1145391	367	293	410
Edinburgh Urban Area	25	ag	512576	134	71	119
Cardiff Urban Area	26	ag	340581	86	42	69
Swansea Urban Area	27	ag	208659	84	34	65
Belfast Metropolitan Urban Area	28	ag	566561	217	51	232
Eastern	29	nonag	5817324	19537	523	683
South West	30	nonag	4738809	24564	393	520
South East	31	nonag	7218104	19178	796	1026
East Midlands	32	nonag	3786511	15472	384	494
North West & Merseyside	33	nonag	3654607	13585	605	748
Yorkshire & Humberside	34	nonag	3206926	15040	340	449
West Midlands	35	nonag	2870322	12229	340	397
North East	36	nonag	1544454	8441	157	184
Central Scotland	37	nonag	2011449	10046	327	526
North East Scotland	38	nonag	1149406	19066	180	272
Highland	39	nonag	396347	44091	58	97
Scottish Borders	40	nonag	264354	11437	57	59
South Wales	41	nonag	1807537	12753	191	284
North Wales	42	nonag	749961	8766	68	127
Northern Ireland	43	nonag	1337717	14558	101	247
Total			**66981392**	**254905**	**9669**	**12570**

* ag = agglomeration zone; non-ag = non-agglomeration zone

The status of zones in relation to the limit values, target values, critical levels and long-term objectives for the AQSR pollutants have been reported to via e-Reporting (*UK-Air*, 2023) and a summary of the results of the assessments are included in Section 2. The status has been determined from a combination of fixed monitoring data from the Automatic Urban and Rural Network (AURN), Heavy Metals Network and Polycyclic Aromatic Hydrocarbons Network; indicative monitoring data from the UK Urban NO_2 Network (UUNN); and model results. A comparison of the results of similar assessments carried out since 2001 (Stedman, Bush and Vincent, 2002; Stedman *et al.*, 2003, 2005, 2006; Bush, Targa and Stedman, 2006; Bush *et al.*, 2007; Kent and Stedman, 2007, 2008; Kent, Grice, Stedman, Bush, *et al.*, 2007; Kent, Grice, Stedman, Cooke, *et al.*, 2007; Grice *et al.*, 2009; Yap *et al.*, 2009; Grice, Brookes, *et al.*, 2010; Grice, Cooke, *et al.*, 2010; Kent, Stedman and Yap, 2010; Walker *et al.*, 2010, 2011; Brookes *et al.*, 2011, 2012, 2013, 2015, 2016, 2017, 2019b, 2019a, 2020, 2021; Pugsley *et al.*, 2022, 2023) has been reported in Air Pollution in the UK 2022 (Air Pollution in the UK, 2023).

1.4 Monitoring sites

The fixed monitoring stations operating during 2022 for AQSR reporting have been listed within e-Reporting Data flow C (Assessment Regimes), which can be found on UK-AIR (*UK-Air*, 2023). Not all sites had sufficient data capture during 2022 for data to be reported. The data quality objective (DQO) for AQSR measurements is 90% data capture. The Implementing Provisions on Reporting (IPR) guidance (IPR 2013) states that when checking for compliance the minimum data quality objective can be reduced to take into account the proportion of time taken in a calendar year for planned maintenance and calibration. The IPR states that an estimation of this time is 5%, which makes the data quality objective 85%. For the purposes of compliance reporting all measurements from monitoring sites with at least 85% data capture for the entire year have been included. These have been supplemented with monitoring sites with data capture of 75%-84%. These results have been classified in the assessment as 'indicative', rather than fixed in this instance, for the zones they represent. Monitoring stations with at least 75% data capture have been included in the modelling analysis to ensure that a greater number of operational monitoring sites have been used for model calibration and verification purposes.

Measurements from the UK Urban NO_2 Network with at least 85% data capture have also been included in the compliance assessment as part of the supplementary assessment. These measurements have not been used in model calibration.

The monitoring data for the sites used in the assessment for heavy metals and B(a)P are summarised in Appendix 2 - Monitoring sites for As, Cd, Ni, Pb and B(a)P.

1.5 Data quality objectives for modelling results and model verification

The AQSR sets data quality objectives (DQOs) for modelling uncertainty, within supplementary assessment under the AQSR. Uncertainty is defined in the AQSR as the maximum deviation of the measured and calculated concentration levels for 90% of individual monitoring points over the period considered by the limit value (or target value), without taking into account the timing of events. The uncertainty of modelling should be interpreted as applicable in the region of the appropriate LV or TV. The fixed measurements that have been selected for comparison with the modelling results should be representative of the scale covered by the model. Final guidance clarifying the recommended methods for assessing model performance with respect to the DQOs has yet to be agreed. The comparisons with monitoring data presented in this report have therefore included data from all sites including those with measured values not in the vicinity of the LVs or TVs and a highly detailed assessment of the spatial representativity of the sites has not been carried out.

Under the AQSR, DQOs have been set at 50% for hourly averages, daily averages and 8-hour averages of SO_2, NO_2, NO_x, CO and O_3. DQOs have been set at 30% for annual averages of SO_2, NO_2 and NO_x. For PM_{10}, $PM_{2.5}$ and Pb the DQO for annual averages is 50%. DQOs have not been defined for daily averages of PM_{10}. DQOs have been set at 60% for annual averages of As, Cd, Ni and B(a)P.

The models used to calculate the maps of NO_x, NO_2, PM_{10}, $PM_{2.5}$, C_6H_6, O_3, and B(a)P presented in this report have been calibrated using data from the national monitoring network sites. Data from these sites alone does not allow an independent assessment of the validity of the mapped estimates

in relation to the DQOs for modelling. Measurement data from sites not included in the calibration are described as 'verification sites' in this report and are used in addition to the national monitoring network sites to make this assessment, except for C_6H_6 and B(a)P where no independent data are available. Data from sites quality assured by Ricardo under contract and not part of the national network, including Local Authority sites with data available from the Air Quality England website, Scottish Air Quality Archive monitoring sites, Welsh Air Quality Network monitoring sites, Northern Ireland Automatic Urban Network sites, and Heathrow Airwatch sites, have therefore been used for the verification of the modelled estimates. The description 'Verification Sites' is used to describe the independent monitoring sites included in the verification analysis. Monitoring data has also been obtained for the London Air Quality Network (LAQN) and other local authority monitoring networks for which data are provided by Imperial College London (ERG). The 'Verification Sites' used for the 2022 assessment are listed in Appendix 1 - Monitoring sites used to verify the mapped estimates.

The model used to calculate maps of SO_2 presented in this report is not calibrated because modelled values provide a reasonably good fit to measured concentrations and to avoid the risk of overfitting for the high percentile metrics. Modelled results have therefore been compared to and verified using a combination of national network monitoring data along with the 'Verification Sites' listed in Appendix 1 - Monitoring sites used to verify the mapped estimates. The models used to calculate maps of air pollution from heavy metals (Pb, As, Cd, Ni) presented in this report are also not calibrated. Results have been compared to and verified using national network monitoring data for those sites that are listed in Appendix 2 - Monitoring sites for As, Cd, Ni, Pb and B(a)P in order to ensure that the model assumptions and parameter values selected provide good agreement with measurements. Sites with data capture of at least 75% have been included in the verification analysis. Model verification results are listed in the sections on each pollutant.

1.6 Air quality modelling

Full details of the modelling methods implemented are given in Sections 3 to 11 including summaries of inputs, assumptions and schematic flow diagrams of the modelling process. A brief introduction is presented here.

1.6.1 Background concentration maps

Maps showing background concentrations for NO_X, SO_2 and C_6H_6 have been calculated at a 1 km x 1 km resolution for the relevant metrics set out in the AQSR. These maps have been calculated by summing contributions from the following sources:

- Large point sources[1] – modelled using the air dispersion model ADMS and emissions estimates from the UK National Atmospheric Emissions Inventory 2021 (NAEI 2021).
- Small point sources – modelled using the small points model and emissions estimates from the NAEI 2021.
- Emissions Trading Scheme[2] (ETS) point sources – those above the large point source modelling threshold or with emission release characteristics are modelled as large point sources, those below the modelling threshold are modelled using the small points model and emissions estimates from the NAEI 2021.
- Distant sources – characterised by the rural background concentration.
- Area sources[3] related to domestic combustion – modelled using a time varying dispersion kernel and emissions estimates from the NAEI 2021.
- Area sources related to combustion in industry – modelled using the small points model and emissions estimates from the NAEI 2021.
- Area sources related to road traffic – modelled using a dispersion kernel using time varying emissions and emissions estimates from the NAEI 2021.
- Other area sources – modelled using a dispersion kernel and annual emissions estimates from the NAEI 2021.
- Fugitive point source emissions – modelled using fugitive source kernel model and an estimate of the fugitive component of emissions derived from the NAEI 2021 (C_6H_6 only).

1 km x 1 km background concentration maps for B(a)P have been calculated using a similar approach except that a regional background has not been included and area sources related to industrial

[1] Point source emissions are defined as emissions of a known amount from a known location (e.g. a power station).
[2] Emissions Trading Scheme point emissions estimates for Air Quality pollutants based on reported carbon emissions
[3] Area source emissions are defined as 'diffuse emissions' from many unspecified locations (e.g. emissions from domestic heating, or from shipping).

combustion and ETS point sources not meeting the large point source modelling criteria have been modelled using an area source dispersion kernel.

For PM_{10} and $PM_{2.5}$ a similar approach has been used to generate 1 km x 1 km background concentration maps. For these pollutants, the following additional contributions have also been included:

- Secondary inorganic aerosol – derived by interpolation and scaling of measurements of SO_4, NO_3 and NH_4 at rural sites.
- Secondary organic aerosol – semi-volatile organic compounds formed by the oxidation of non-methane volatile organic compounds. Estimates derived from results from the NAME model.
- Regional primary particles – from results from the TRACK model and emissions estimates from the NAEI 2021 and EMEP.
- Regional calcium rich dusts from re-suspension of soils – modelled using a dispersion kernel and information on land use.
- Regional iron rich dusts from re-suspension – assumed to be a constant value, estimated measurements made in the vicinity of Birmingham.
- Iron rich dusts from re-suspension due to vehicle activity – modelled using a dispersion kernel and vehicle activity data for heavy duty vehicles.
- Sea salt – derived by interpolation and scaling of measurements of chloride at rural sites.
- Residual – assumed to be a constant value.

A similar approach has also been used for Pb, As, Cd and Ni to generate 1 km x 1 km background concentration maps. For these pollutants, the following additional contributions have also been included:

- Regional concentrations – derived from estimates of primary PM from regional sources calculated using the TRACK model and emissions estimates from the NAEI 2021 and EMEP.
- Re-suspension from bare soils – derived from estimates of re-suspension of PM modelled using a dispersion kernel and information on land use.
- Re-suspension as a result of vehicle movements – derived from estimates of re-suspension of PM modelled using a dispersion kernel and vehicle activity data for heavy duty vehicles.

1.6.2 Roadside concentration maps

Maps showing modelled roadside concentrations of NO_X, PM_{10}, $PM_{2.5}$ and C_6H_6 have been calculated for 9135 urban major road census points (A-roads and motorways) across the UK. Some of the lengths of road associated with each census point cross zone boundaries and thus a total of 9669 road links have been included in the analysis. The road lengths have been split between zones for assessment where a road has length in more than one zone. These roadside concentrations have been calculated by adding a 'roadside increment' concentration component (derived from the road link emission) to the modelled background concentration for each road. This roadside increment concentration has been calculated using the PCM Roads Kernel Model (PCM-RKM). The PCM-RKM, based upon dispersion kernels generated by the ADMS-Roads dispersion model, represents a more process-based approach than the previous empirical method (e.g. Brookes et al. 2015). It provides a more robust assessment, whilst retaining the link with measurement data by using AURN measurement data to calibrate this component of the model. Full details of the PCM-RKM are provided in Appendix 8 – The PCM Roads Kernel Model.

The PCM model provides roadside concentrations for major urban roads. The assessment of roadside concentration for 2022 incorporates an updated classification of urban and rural roads in England, Scotland and Wales. This classification uses an updated evidence base – 2011 Census data for built-up areas in England and Wales and similar data for Scotland, and underlying mapping from OS Open Roads – to provide an improved assessment of the road network in urban and rural areas. Details can be found in the NAEI mapping report (Tsagatakis *et al.*, 2023). The revised underlying mapping was first implemented for the 2018 compliance assessment modelling and the updated classification of urban and rural roads was first implemented for the 2019 compliance assessment modelling.

1.6.3 NO_2 maps

Background and roadside NO_2 concentration maps have been calculated by applying a calibrated version of the updated oxidant-partitioning model. This model describes the complex inter-relationships between NO, NO_2 and O_3 as a set of chemically coupled species (Jenkin, 2004, 2012; Murrells *et al.*, 2008).

1.6.4 Key input data

Emissions inventory data used in this modelling is taken from the NAEI 2021 (Ingledew *et al.*, 2023). Emission estimates for area and point sources (taking into account plant closure) have been scaled forward from 2021 to 2022. Work carried out to calculate emissions from aircraft and shipping within the PCM model is described in Appendix 6 – Method for calculating and mapping emissions from aircraft and shipping. Dispersion modelling has been done using ADMS 5.2 using meteorological data from the Weather Research and Forecasting (WRF) Model see Appendix 4 – WRF meteorology. UK national network monitoring data has been used to calibrate the background and roadside models, as discussed above in Section 1.5. Further details on inputs and assumptions are provided in Sections 3 to 11.

1.6.5 Ozone maps

Maps of the O_3 metrics specified in the AQSR have been calculated using a different modelling approach to the approach used for other pollutants in this report. This is because of the complex chemistry involved in the production and destruction of O_3. An empirical method based on a combination of interpolation of O_3 measurements at rural sites and model results for NO_x is used to model O_3 concentrations. This is described in Section 9.

1.7 Air quality in Gibraltar in 2022

Air quality monitoring and assessments are also undertaken in Gibraltar and the results of the assessment are published and made available to the public. Further information on air quality monitoring in Gibraltar can be found at http://www.gibraltarairquality.gi.

2 Results of the air quality assessment for 2022

The results of the air quality assessments for AQSR pollutants SO_2, NO_2 and NO_X, PM_{10}, $PM_{2.5}$, Pb, C_6H_6, CO, O_3, As, Cd, Ni and B(a)P have been listed in Table 2.1 to Table 2.6.

These tables summarise information from e-Reporting Data flow G (Attainment) published on UK-Air (*UK-Air*, 2023) relating to compliance with the respective LV, TV or LTO. The tables have been completed as follows:

- Where all measurements were within the relevant LVs in 2022, the table shows this as "OK".
- Where compliance was determined by supplementary assessment, this is shown as "OK (s only)".
- Where locations were identified as exceeding a LV, this is identified with ">LV". In general, where the status of a location was determined by supplementary assessment, this is indicated by (s only) as done here for compliance.

A similar approach has been used to summarise results in relation to critical levels (CLs), TVs and LTOs. Zones that complied with the relevant CLs, LVs, TVs or LTOs are shaded blue, while those in exceedance are shaded red. For O_3, exceedances of the LTO but not the TV are shaded purple. "n/a" means that an assessment is not relevant for a zone, such as for the vegetation critical level in agglomeration zones.

Measurements are regarded as the primary basis for the compliance status if both measurements and supplementary assessment estimates show that a threshold has been exceeded. Where locations have been identified as exceeding by modelling this indicates that modelled concentrations were higher than measured concentrations or that measurements were not available (or not required for that zone as determined by a 5-yearly assessment of concentrations relative to lower and upper assessment thresholds in the AQSR) and modelled values were therefore used. Modelled concentrations may be higher than measured concentrations because the modelling studies provide estimates of concentrations over the entire zone. It is possible that the locations of the monitoring sites do not correspond to the location of the highest concentration in the zone, for example, there may be no roadside monitoring sites in a zone. Compliance can be determined by modelling where measurements including diffusion tube indicative measurements from the UUNN are not available for a zone. Where AURN and/or UUNN measurements of NO_2 concentrations are available for a specific road link, the measured concentration is used in preference to the modelled concentration for the compliance assessment for that road link. The order of priority is AURN in preference to UUNN in preference to modelling.

CO concentrations were not modelled as part of the compliance assessment due to the sparsity of the monitoring network, low concentrations, and very low risk of limit value exceedance. Therefore in zones where measurements were not available compliance has been determined through objective estimation. These are represented as '(s only)' in the tables below as objective estimation is treated as a modelling approach in e-Reporting. The objective estimation process is explained further in Section 8.

Table 2.2 shows that nine zones have not achieved full compliance with the annual NO_2 limit value in 2022. All zones were compliant with the hourly limit value in 2022. The 1-hour limit value of 200 µg m^{-3} as a 98th percentile was not exceeded in 2022.

Table 2.3 shows that all zones were compliant with both the daily mean limit value and annual mean limit value for PM_{10} before subtraction of natural sources (required by the AQSR). The exposure concentration obligation for the average of annual mean $PM_{2.5}$ concentrations measured in urban areas of 20 µg m^{-3} was also met (see Section 6.6). Compliance with the $PM_{2.5}$ Limit Value and National Exposure Reduction Target (NERT) was also achieved in 2022.

Table 2.4 shows that all zones were compliant with the limit values for lead, CO and benzene.

Table 2.5 shows that the TV for health was met and the LTO for health for O_3 was exceeded in 43 zones. The TV for vegetation was met in all zones and the LTO for vegetation for O_3 was exceeded in 11 zones in 2022.

Table 2.6 shows that two zones have not achieved full compliance with the annual B(a)P target value and three zones have not achieved full compliance with the annual Ni target value in 2022.

Table 2.1 - List of zones and agglomerations in relation to limit value and critical level exceedances for SO_2 in 2022

Zone	Zone code	SO_2 LV for health (1hr mean)	SO_2 LV for health (24hr mean)	SO_2 CL for vegetation (annual mean)	SO_2 LV for vegetation (winter mean)
Greater London	UK0001	OK	OK	n/a	n/a
West Midlands	UK0002	OK	OK	n/a	n/a
Greater	UK0003	OK	OK	n/a	n/a
West Yorkshire	UK0004	OK	OK	n/a	n/a
Tyneside	UK0005	OK (s only)	OK (s only)	n/a	n/a
Liverpool Urban	UK0006	OK	OK	n/a	n/a
Sheffield Urban	UK0007	OK (s only)	OK (s only)	n/a	n/a
Nottingham	UK0008	OK	OK	n/a	n/a
Bristol Urban	UK0009	OK (s only)	OK (s only)	n/a	n/a
Brighton/Worthin	UK0010	OK (s only)	OK (s only)	n/a	n/a
Leicester Urban	UK0011	OK (s only)	OK (s only)	n/a	n/a
Portsmouth	UK0012	OK (s only)	OK (s only)	n/a	n/a
Teesside Urban	UK0013	OK	OK	n/a	n/a
The Potteries	UK0014	OK (s only)	OK (s only)	n/a	n/a
Bournemouth Urban Area	UK0015	OK (s only)	OK (s only)	n/a	n/a
Reading/Woking ham Urban Area	UK0016	OK (s only)	OK (s only)	n/a	n/a
Coventry/Bedwor	UK0017	OK (s only)	OK (s only)	n/a	n/a
Kingston upon	UK0018	OK	OK	n/a	n/a
Southampton	UK0019	OK	OK	n/a	n/a
Birkenhead	UK0020	OK (s only)	OK (s only)	n/a	n/a
Southend Urban	UK0021	OK (s only)	OK (s only)	n/a	n/a
Blackpool Urban	UK0022	OK (s only)	OK (s only)	n/a	n/a
Preston Urban	UK0023	OK (s only)	OK (s only)	n/a	n/a
Glasgow Urban	UK0024	OK (s only)	OK (s only)	n/a	n/a
Edinburgh Urban	UK0025	OK	OK	n/a	n/a
Cardiff Urban	UK0026	OK	OK	n/a	n/a
Swansea Urban	UK0027	OK	OK	n/a	n/a
Belfast Urban	UK0028	OK	OK	n/a	n/a
Eastern	UK0029	OK	OK	OK (s only)	OK
South West	UK0030	OK (s only)	OK (s only)	OK (s only)	OK (s only)
South East	UK0031	OK	OK	OK	OK
East Midlands	UK0032	OK	OK	OK	OK
North West &	UK0033	OK (s only)	OK (s only)	OK (s only)	OK (s only)
Yorkshire &	UK0034	OK	OK	OK (s only)	OK (s only)
West Midlands	UK0035	OK (s only)	OK (s only)	OK (s only)	OK (s only)
North East	UK0036	OK (s only)	OK (s only)	OK (s only)	OK (s only)
Central Scotland	UK0037	OK	OK	OK (s only)	OK (s only)
North East	UK0038	OK (s only)	OK (s only)	OK (s only)	OK (s only)
Highland	UK0039	OK (s only)	OK (s only)	OK (s only)	OK (s only)
Scottish Borders	UK0040	OK (s only)	OK (s only)	OK (s only)	OK (s only)
South Wales	UK0041	OK	OK	OK (s only)	OK (s only)
North Wales	UK0042	OK	OK	OK (s only)	OK (s only)
Northern Ireland	UK0043	OK	OK	OK (s only)	OK (s only)

Table 2.2 - List of zones and agglomerations in relation to limit value and critical level exceedances for NO_2 and NO_X in 2022

Zone	Zone code	NO_2 LV for health (1-hr mean)	NO_2 LV for health (annual mean)	NO_x CL for vegetation (annual mean)
Greater London Urban Area	UK0001	OK	> LV	n/a
West Midlands Urban Area	UK0002	OK	> LV (s only)	n/a
Greater Manchester Urban Area	UK0003	OK	> LV (s only)	n/a
West Yorkshire Urban Area	UK0004	OK	> LV (s only)	n/a
Tyneside	UK0005	OK	OK	n/a
Liverpool Urban Area	UK0006	OK	> LV (s only)	n/a
Sheffield Urban Area	UK0007	OK	> LV (s only)	n/a
Nottingham Urban Area	UK0008	OK	> LV (s only)	n/a
Bristol Urban Area	UK0009	OK	> LV (s only)	n/a
Brighton/Worthing/Littlehampton	UK0010	OK	OK	n/a
Leicester Urban Area	UK0011	OK	OK	n/a
Portsmouth Urban Area	UK0012	OK	OK	n/a
Teesside Urban Area	UK0013	OK	OK	n/a
The Potteries	UK0014	OK	OK	n/a
Bournemouth Urban Area	UK0015	OK	OK	n/a
Reading/Wokingham Urban Area	UK0016	OK	OK	n/a
Coventry/Bedworth	UK0017	OK	OK	n/a
Kingston upon Hull	UK0018	OK	OK	n/a
Southampton Urban Area	UK0019	OK	OK	n/a
Birkenhead Urban Area	UK0020	OK	OK	n/a
Southend Urban Area	UK0021	OK	OK	n/a
Blackpool Urban Area	UK0022	OK	OK	n/a
Preston Urban Area	UK0023	OK	OK	n/a
Glasgow Urban Area	UK0024	OK	OK	n/a
Edinburgh Urban Area	UK0025	OK	OK	n/a
Cardiff Urban Area*	UK0026	OK	OK	n/a
Swansea Urban Area	UK0027	OK	OK	n/a
Belfast Urban Area	UK0028	OK	OK	n/a
Eastern	UK0029	OK	OK	OK
South West	UK0030	OK	OK	OK
South East	UK0031	OK	> LV (s only)	OK
East Midlands	UK0032	OK	OK	OK
North West & Merseyside	UK0033	OK	OK	OK (s only)
Yorkshire & Humberside	UK0034	OK	OK	OK
West Midlands	UK0035	OK	OK	OK (s only)
North East	UK0036	OK	OK	OK (s only)
Central Scotland	UK0037	OK	OK	OK (s only)
North East Scotland	UK0038	OK	OK	OK (s only)
Highland	UK0039	OK	OK	OK (s only)
Scottish Borders	UK0040	OK	OK	OK (s only)
South Wales	UK0041	OK	OK	OK (s only)
North Wales	UK0042	OK	OK	OK
Northern Ireland	UK0043	OK	OK	OK (s only)

Table 2.3 - List of zones and agglomerations in relation to limit value exceedances for PM_{10}, limit value and target value exceedances for $PM_{2.5}$ in 2022 (after subtraction of contribution from natural sources where applicable)

Zone	Zone code	PM_{10} LV for health (24-hr mean)	PM_{10} LV for health (annual mean)	$PM_{2.5}$ LV for health (annual mean)
Greater London Urban Area	UK0001	OK	OK	OK
West Midlands Urban Area	UK0002	OK	OK	OK
Greater Manchester Urban Area	UK0003	OK	OK	OK
West Yorkshire Urban Area	UK0004	OK	OK	OK
Tyneside	UK0005	OK	OK	OK
Liverpool Urban Area	UK0006	OK	OK	OK (s only)
Sheffield Urban Area	UK0007	OK	OK	OK
Nottingham Urban Area	UK0008	OK	OK	OK
Bristol Urban Area	UK0009	OK	OK	OK
Brighton/Worthing/Littlehampton	UK0010	OK (s only)	OK (s only)	OK
Leicester Urban Area	UK0011	OK	OK	OK
Portsmouth Urban Area	UK0012	OK	OK	OK
Teesside Urban Area	UK0013	OK	OK	OK
The Potteries	UK0014	OK	OK	OK
Bournemouth Urban Area	UK0015	OK (s only)	OK (s only)	OK
Reading/Wokingham Urban Area	UK0016	OK	OK	OK
Coventry/Bedworth	UK0017	OK	OK	OK
Kingston upon Hull	UK0018	OK	OK	OK
Southampton Urban Area	UK0019	OK	OK	OK
Birkenhead Urban Area	UK0020	OK	OK	OK
Southend Urban Area	UK0021	OK	OK	OK
Blackpool Urban Area	UK0022	OK	OK	OK
Preston Urban Area	UK0023	OK	OK	OK
Glasgow Urban Area	UK0024	OK	OK	OK
Edinburgh Urban Area	UK0025	OK	OK	OK
Cardiff Urban Area	UK0026	OK	OK	OK
Swansea Urban Area	UK0027	OK	OK	OK
Belfast Urban Area	UK0028	OK	OK	OK
Eastern	UK0029	OK	OK	OK
South West	UK0030	OK	OK	OK
South East	UK0031	OK	OK	OK
East Midlands	UK0032	OK	OK	OK
North West & Merseyside	UK0033	OK	OK	OK
Yorkshire & Humberside	UK0034	OK	OK	OK
West Midlands	UK0035	OK	OK	OK
North East	UK0036	OK	OK	OK
Central Scotland	UK0037	OK	OK	OK
North East Scotland	UK0038	OK	OK	OK
Highland	UK0039	OK	OK	OK
Scottish Borders	UK0040	OK (s only)	OK (s only)	OK (s only)
South Wales	UK0041	OK	OK	OK
North Wales	UK0042	OK	OK	OK
Northern Ireland	UK0043	OK	OK	OK

Table 2.4 - List of zones and agglomerations in relation to limit value exceedances for lead, benzene and CO in 2022

Zone	Zone code	Lead LV for health (annual mean)	Benzene LV for health (annual mean)	CO LV for health (8-hr mean)
Greater London Urban Area	UK0001	OK	OK	OK
West Midlands Urban Area	UK0002	OK	OK	OK (s only)
Greater Manchester Urban Area	UK0003	OK (s only)	OK	OK (s only)
West Yorkshire Urban Area	UK0004	OK (s only)	OK	OK
Tyneside	UK0005	OK (s only)	OK	OK (s only)
Liverpool Urban Area	UK0006	OK (s only)	OK	OK (s only)
Sheffield Urban Area	UK0007	OK	OK	OK (s only)
Nottingham Urban Area	UK0008	OK (s only)	OK	OK (s only)
Bristol Urban Area	UK0009	OK (s only)	OK (s only)	OK (s only)
Brighton/Worthing/Littlehampton	UK0010	OK (s only)	OK (s only)	OK (s only)
Leicester Urban Area	UK0011	OK (s only)	OK (s only)	OK (s only)
Portsmouth Urban Area	UK0012	OK (s only)	OK (s only)	OK (s only)
Teesside Urban Area	UK0013	OK (s only)	OK	OK (s only)
The Potteries	UK0014	OK (s only)	OK	OK (s only)
Bournemouth Urban Area	UK0015	OK (s only)	OK (s only)	OK (s only)
Reading/Wokingham Urban Area	UK0016	OK (s only)	OK (s only)	OK (s only)
Coventry/Bedworth	UK0017	OK (s only)	OK (s only)	OK (s only)
Kingston upon Hull	UK0018	OK (s only)	OK (s only)	OK (s only)
Southampton Urban Area	UK0019	OK (s only)	OK	OK (s only)
Birkenhead Urban Area	UK0020	OK (s only)	OK (s only)	OK (s only)
Southend Urban Area	UK0021	OK (s only)	OK (s only)	OK (s only)
Blackpool Urban Area	UK0022	OK (s only)	OK (s only)	OK (s only)
Preston Urban Area	UK0023	OK (s only)	OK (s only)	OK (s only)
Glasgow Urban Area	UK0024	OK (s only)	OK	OK (s only)
Edinburgh Urban Area	UK0025	OK (s only)	OK (s only)	OK
Cardiff Urban Area	UK0026	OK (s only)	OK (s only)	OK
Swansea Urban Area	UK0027	OK	OK	OK
Belfast Urban Area	UK0028	OK	OK	OK
Eastern	UK0029	OK	OK	OK (s only)
South West	UK0030	OK	OK	OK (s only)
South East	UK0031	OK	OK	OK (s only)
East Midlands	UK0032	OK	OK	OK (s only)
North West & Merseyside	UK0033	OK (s only)	OK	OK (s only)
Yorkshire & Humberside	UK0034	OK	OK	OK (s only)
West Midlands	UK0035	OK	OK	OK (s only)
North East	UK0036	OK (s only)	OK	OK (s only)
Central Scotland	UK0037	OK	OK	OK (s only)
North East Scotland	UK0038	OK (s only)	OK (s only)	OK (s only)
Highland	UK0039	OK (s only)	OK (s only)	OK (s only)
Scottish Borders	UK0040	OK	OK (s only)	OK (s only)
South Wales	UK0041	OK	OK	OK (s only)
North Wales	UK0042	OK (s only)	OK (s only)	OK (s only)
Northern Ireland	UK0043	OK (s only)	OK (s only)	OK (s only)

Table 2.5 - List of zones and agglomerations in relation to target value and long-term objective exceedances for ozone in 2022 (*Met TV, > LTO means that the target value was achieved but the long-term objective was not)

Zone	Zone code	O_3 TV and LTO for health (8-hr mean)	O_3 TV and LTO for vegetation (AOT40)
Greater London Urban Area	UK0001	Met TV, > LTO	Met TV, > LTO
West Midlands Urban Area	UK0002	Met TV, > LTO	OK
Greater Manchester Urban Area	UK0003	Met TV, > LTO	OK
West Yorkshire Urban Area	UK0004	Met TV, > LTO	OK
Tyneside	UK0005	Met TV, > LTO	OK
Liverpool Urban Area	UK0006	Met TV, > LTO	OK
Sheffield Urban Area	UK0007	Met TV, > LTO	OK
Nottingham Urban Area	UK0008	Met TV, > LTO	OK
Bristol Urban Area	UK0009	Met TV, > LTO	OK
Brighton/Worthing/Littlehampton	UK0010	Met TV, > LTO	Met TV, > LTO (s only)
Leicester Urban Area	UK0011	Met TV, > LTO	OK
Portsmouth Urban Area	UK0012	Met TV, > LTO	Met TV, > LTO (s only)
Teesside Urban Area	UK0013	Met TV, > LTO	OK
The Potteries	UK0014	Met TV, > LTO	OK
Bournemouth Urban Area	UK0015	Met TV, > LTO	Met TV, > LTO (s only)
Reading/Wokingham Urban Area	UK0016	Met TV, > LTO	Met TV, > LTO (s only)
Coventry/Bedworth	UK0017	Met TV, > LTO	OK
Kingston upon Hull	UK0018	Met TV, > LTO	OK
Southampton Urban Area	UK0019	Met TV, > LTO	Met TV, > LTO (s only)
Birkenhead Urban Area	UK0020	Met TV, > LTO	OK
Southend Urban Area	UK0021	Met TV, > LTO	OK
Blackpool Urban Area	UK0022	Met TV, > LTO	OK
Preston Urban Area	UK0023	Met TV, > LTO	OK
Glasgow Urban Area	UK0024	Met TV, > LTO (s only)	OK
Edinburgh Urban Area	UK0025	Met TV, > LTO (s only)	OK (s only)
Cardiff Urban Area	UK0026	Met TV, > LTO	OK
Swansea Urban Area	UK0027	Met TV, > LTO	OK
Belfast Urban Area	UK0028	Met TV, > LTO (s only)	OK
Eastern	UK0029	Met TV, > LTO	Met TV, > LTO
South West	UK0030	Met TV, > LTO (s only)	Met TV, > LTO
South East	UK0031	Met TV, > LTO	Met TV, > LTO
East Midlands	UK0032	Met TV, > LTO	Met TV, > LTO
North West & Merseyside	UK0033	Met TV, > LTO	OK
Yorkshire & Humberside	UK0034	Met TV, > LTO	OK
West Midlands	UK0035	Met TV, > LTO	Met TV, > LTO (s only)
North East	UK0036	Met TV, > LTO	OK
Central Scotland	UK0037	Met TV, > LTO	OK
North East Scotland	UK0038	Met TV, > LTO (s only)	OK
Highland	UK0039	Met TV, > LTO	OK
Scottish Borders	UK0040	Met TV, > LTO	OK
South Wales	UK0041	Met TV, > LTO	OK
North Wales	UK0042	Met TV, > LTO	OK
Northern Ireland	UK0043	Met TV, > LTO (s only)	OK

Table 2.6 - List of zones and agglomerations where levels exceed or do not exceed target values for arsenic, cadmium, nickel and benzo(a)pyrene in 2022

Zone	Zone code	As TV	Cd TV	Ni TV	B(a)P TV
Greater London Urban Area	UK0001	OK	OK	OK	OK
West Midlands Urban Area	UK0002	OK	OK	OK	OK
Greater Manchester Urban Area	UK0003	OK (s only)	OK (s only)	OK (s only)	OK
West Yorkshire Urban Area	UK0004	OK (s only)	OK (s only)	OK (s only)	OK
Tyneside	UK0005	OK (s only)	OK (s only)	OK (s only)	OK
Liverpool Urban Area	UK0006	OK (s only)	OK (s only)	OK (s only)	OK
Sheffield Urban Area	UK0007	OK	OK	> TV (s only)	OK
Nottingham Urban Area	UK0008	OK (s only)	OK (s only)	OK (s only)	OK
Bristol Urban Area	UK0009	OK (s only)	OK (s only)	OK (s only)	OK
Brighton/Worthing/Littlehampton	UK0010	OK (s only)	OK (s only)	OK (s only)	OK (s only)
Leicester Urban Area	UK0011	OK (s only)	OK (s only)	OK (s only)	OK (s only)
Portsmouth Urban Area	UK0012	OK (s only)	OK (s only)	OK (s only)	OK (s only)
Teesside Urban Area	UK0013	OK (s only)	OK (s only)	OK (s only)	OK
The Potteries	UK0014	OK (s only)	OK (s only)	OK (s only)	OK (s only)
Bournemouth Urban Area	UK0015	OK (s only)	OK (s only)	OK (s only)	OK (s only)
Reading/Wokingham Urban Area	UK0016	OK (s only)	OK (s only)	OK (s only)	OK (s only)
Coventry/Bedworth	UK0017	OK (s only)	OK (s only)	OK (s only)	OK (s only)
Kingston upon Hull	UK0018	OK (s only)	OK (s only)	OK (s only)	OK (s only)
Southampton Urban Area	UK0019	OK (s only)	OK (s only)	OK (s only)	OK
Birkenhead Urban Area	UK0020	OK (s only)	OK (s only)	OK (s only)	OK (s only)
Southend Urban Area	UK0021	OK (s only)	OK (s only)	OK (s only)	OK (s only)
Blackpool Urban Area	UK0022	OK (s only)	OK (s only)	OK (s only)	OK (s only)
Preston Urban Area	UK0023	OK (s only)	OK (s only)	OK (s only)	OK
Glasgow Urban Area	UK0024	OK (s only)	OK (s only)	OK (s only)	OK
Edinburgh Urban Area	UK0025	OK (s only)	OK (s only)	OK (s only)	OK
Cardiff Urban Area	UK0026	OK (s only)	OK (s only)	OK (s only)	OK
Swansea Urban Area	UK0027	OK	OK	OK	> TV (s only)
Belfast Urban Area	UK0028	OK	OK	OK	OK
Eastern	UK0029	OK	OK	OK	OK
South West	UK0030	OK	OK	OK	OK
South East	UK0031	OK	OK	OK	OK
East Midlands	UK0032	OK	OK	OK	OK
North West & Merseyside	UK0033	OK (s only)	OK (s only)	OK (s only)	OK
Yorkshire & Humberside	UK0034	OK	OK	> TV (s only)	OK
West Midlands	UK0035	OK	OK	OK	OK (s only)
North East	UK0036	OK (s only)	OK (s only)	OK (s only)	OK (s only)
Central Scotland	UK0037	OK	OK	OK	OK
North East Scotland	UK0038	OK (s only)	OK (s only)	OK (s only)	OK (s only)
Highland	UK0039	OK (s only)	OK (s only)	OK (s only)	OK
Scottish Borders	UK0040	OK	OK	OK	OK (s only)
South Wales	UK0041	OK	OK	> TV (s only)	> TV (s only)
North Wales	UK0042	OK (s only)	OK (s only)	OK (s only)	OK (s only)
Northern Ireland	UK0043	OK (s only)	OK (s only)	OK (s only)	OK

3 NO_2/NO_X

3.1 Introduction

3.1.1 Limit values

Two limit values for ambient NO_2 concentrations are set out in the Air Quality Standards Regulations (AQSR) (*legislation.gov.uk*, 2010). These have been specified for the protection of human health and came into force from 01/01/2010. These limit values are:

- An annual mean concentration of 40 µg m^{-3}.
- An hourly concentration of 200 µg m^{-3}, with 18 permitted exceedances each year.

A critical level for NO_X for the protection of vegetation has also been specified in the regulations:

- An annual mean concentration 30 µg m^{-3} (NO_x as NO_2).

Because this critical level is designed to protect vegetation, it only applies in vegetation areas as defined in the regulations.

Results of the assessment in terms of comparisons of the modelled concentrations with the annual mean limit value for NO_2 and critical level for NO_X have been reported in accordance with the AQSR and published on UK-AIR (*UK-Air*, 2023)[4].

3.1.2 Annual mean modelling

Annual mean concentrations of NO_X and NO_2 have been modelled for the UK for 2022 at background and roadside locations. Figure 3.1 and Figure 3.2 present maps of annual mean NO_2 concentrations for these locations in 2022. These maps have been used for comparison with the annual mean NO_2 limit value described above. To calculate NO_2 annual mean maps, NO_X annual mean concentration maps at background and roadside locations were first calculated.

The modelling methods for annual mean NO_X and NO_2 have been developed over several years (Stedman and Bush, 2000; Stedman, Bush, *et al.*, 2001; Stedman, Goodwin, *et al.*, 2001; Stedman, Bush and Vincent, 2002; Stedman *et al.*, 2003, 2005, 2006; Bush, Targa and Stedman, 2006; Bush *et al.*, 2007; Kent and Stedman, 2007, 2008; Kent, Grice, Stedman, Bush, *et al.*, 2007; Kent, Grice, Stedman, Cooke, *et al.*, 2007; Grice *et al.*, 2009; Yap *et al.*, 2009; Grice, Brookes, *et al.*, 2010; Grice, Cooke, *et al.*, 2010; Kent, Stedman and Yap, 2010; Walker *et al.*, 2010, 2011; Brookes *et al.*, 2011, 2012, 2013, 2015, 2016, 2017, 2019b, 2019a, 2020, 2021; Pugsley *et al.*, 2022, 2023).

[4] https://uk-air.defra.gov.uk/compliance-data

Figure 3.1 - Annual mean background NO2 concentration, 2022 (µg m-3)

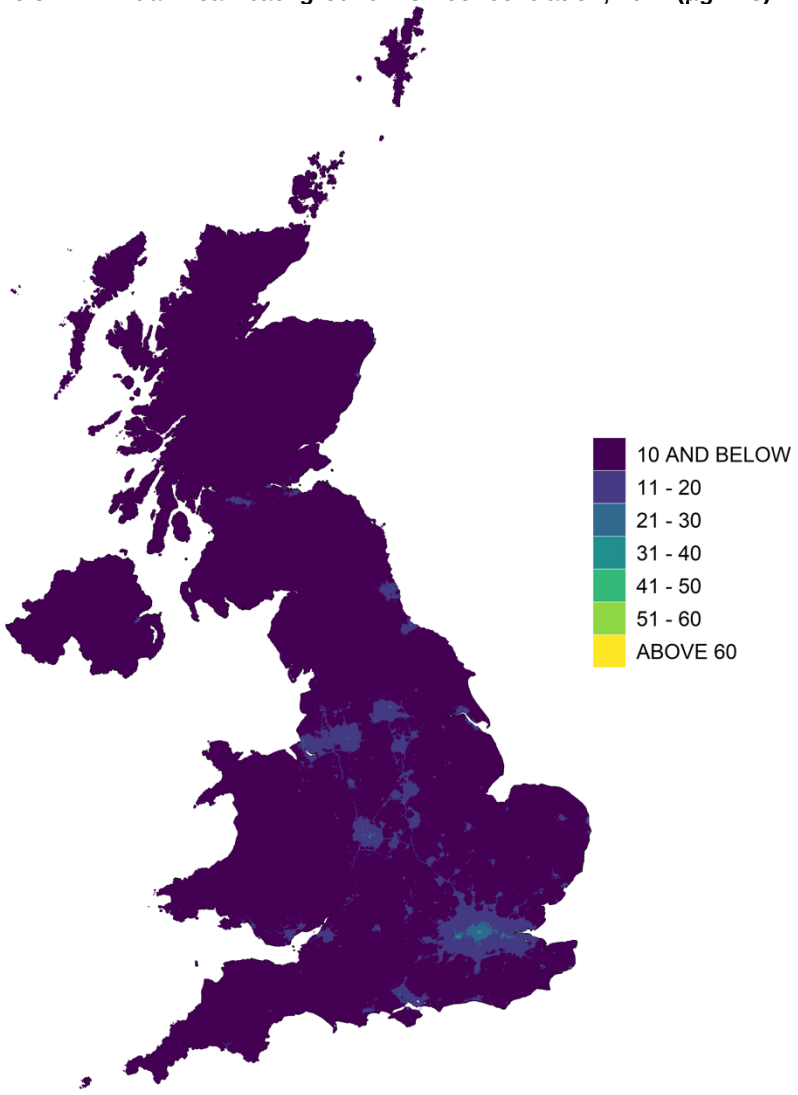

Figure 3.2 - Urban major roads, annual mean roadside NO_2 concentration, 2022 (µg m^{-3})

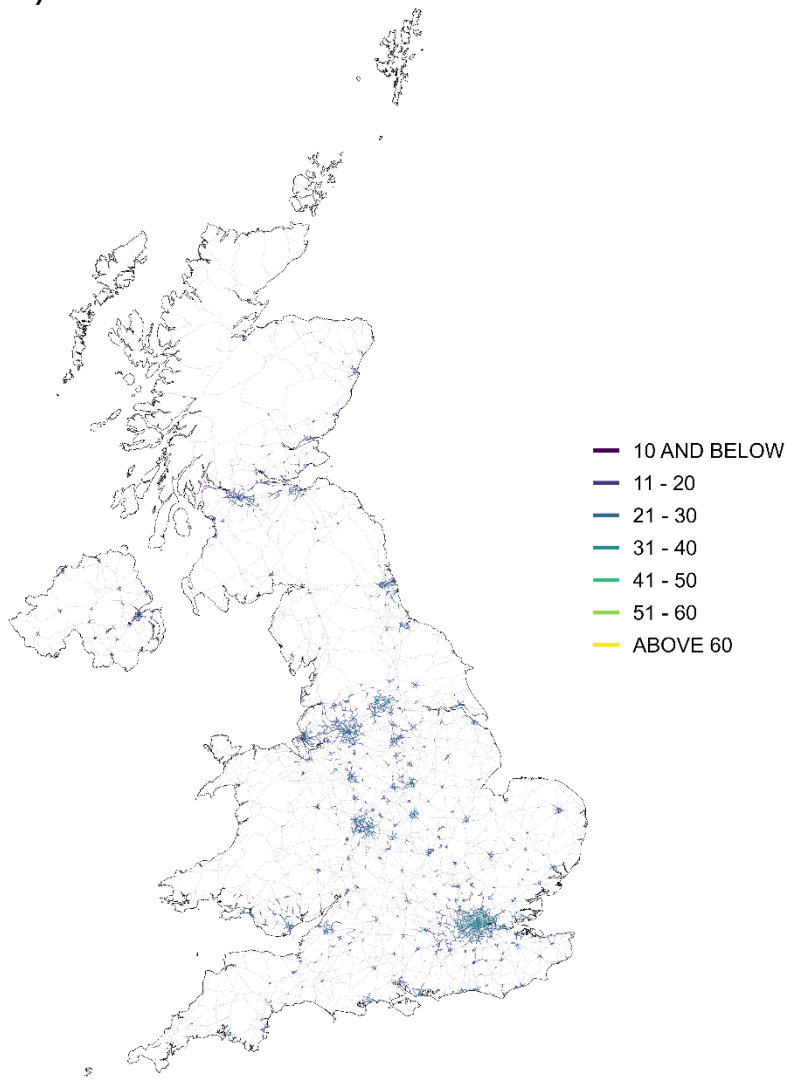

Figure 3.3 - Annual mean map of NO_X concentrations for comparison with the NO_X vegetation critical level, 2022 (µg m^{-3}, as NO_2)

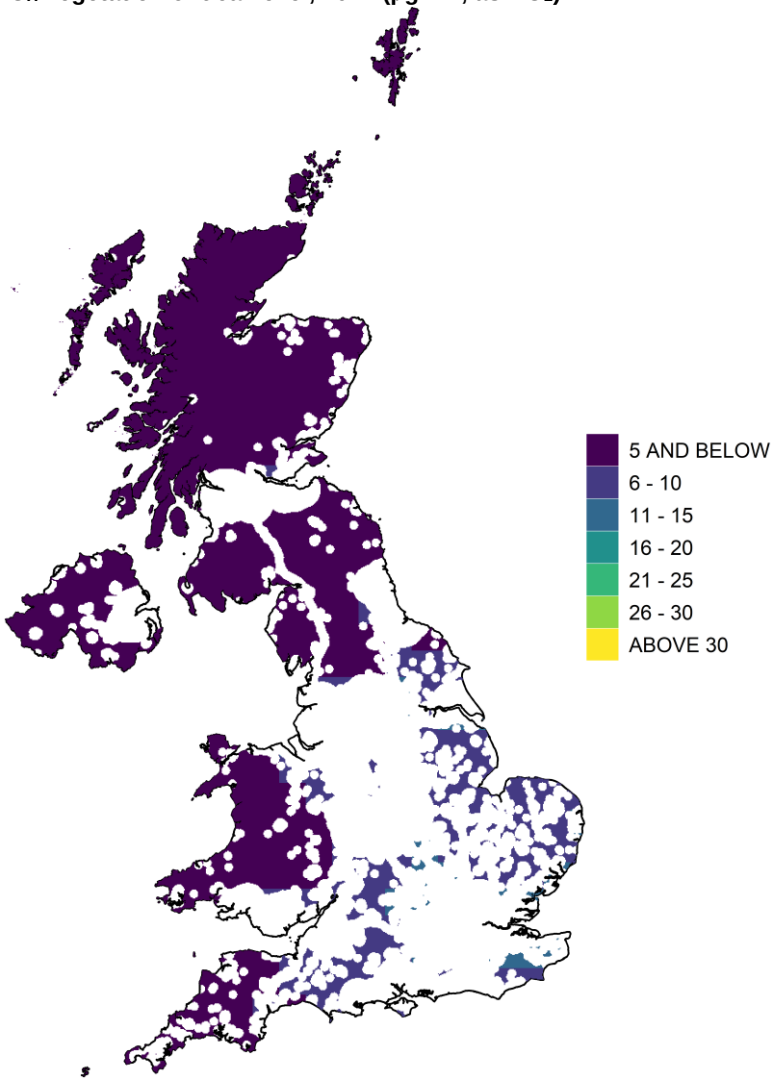

Figure 3.4 - Plot of annual mean against 99.8th percentile hourly NO_2 concentrations in 2022

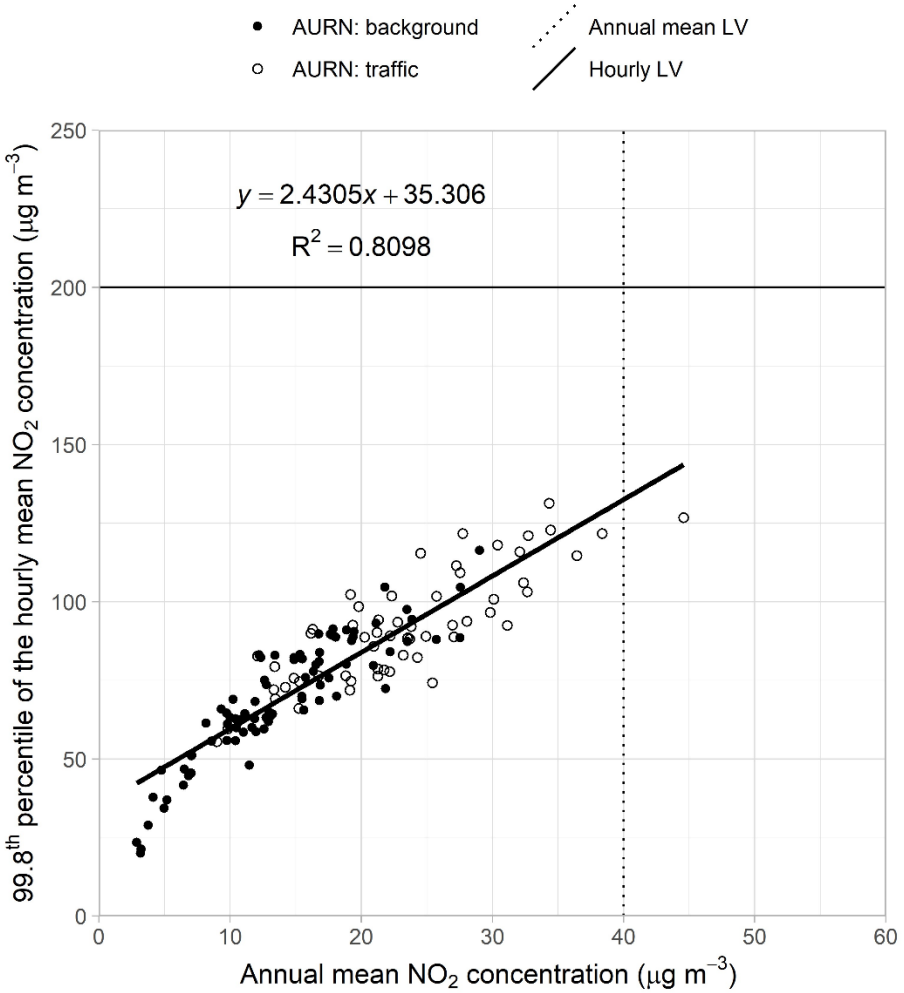

3.1.3 Overview of the PCM model for NO_x and NO_2

Figure 3.5 shows a simplified flow diagram of the PCM model for NO_x and NO_2. A summary of the PCM model method, input, and assumptions for NO_x and NO_2 is presented in Table 3.1.

Figure 3.5 - Flow diagram for PCM NO_x and NO_2 model

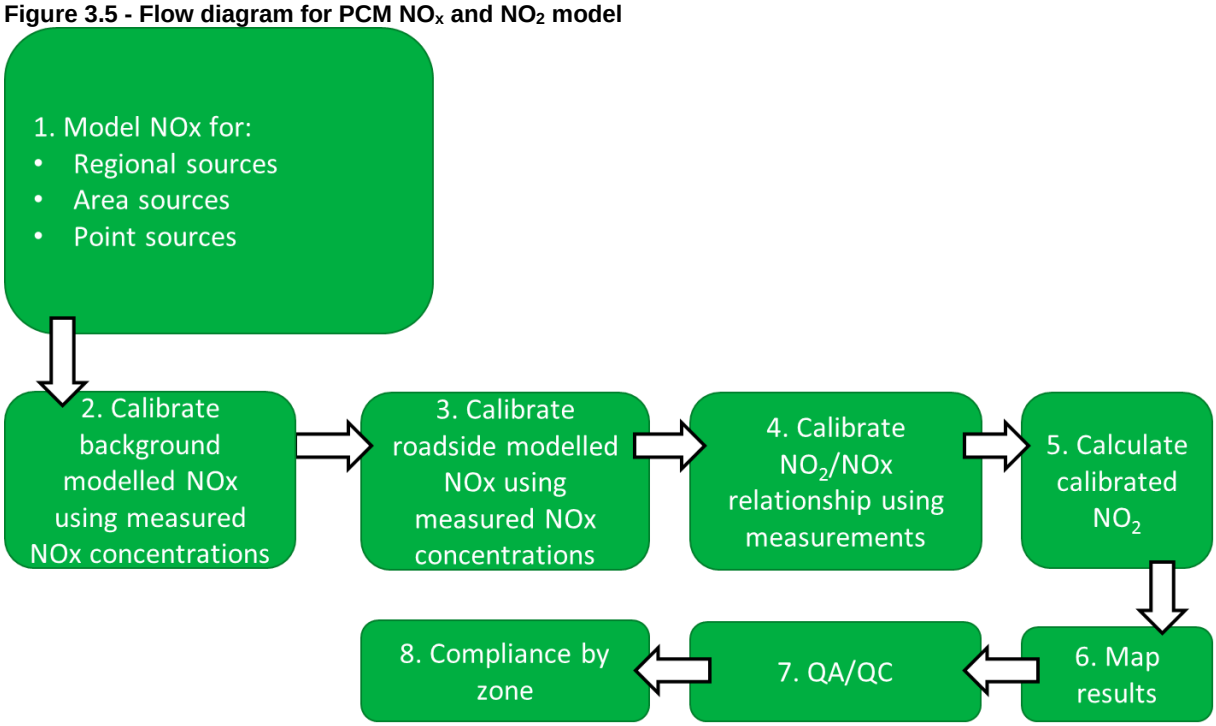

Table 3.1 - PCM model method, input and assumptions summary for NOx and NO_2

Heading	Component	Details
General	Pollutant	NO_x and NO_2
	Year	2022
	Locations modelled	Background and traffic locations
	Metric	Annual mean
Input data	Emission inventory	NAEI 2021 (scaled to 2022)
	Energy projections	Energy Projections 2022
	Road traffic counts	2022 (scaled from 2021 where not available)
	Road transport activity projections	DfT (2022) car sales projections, TfL traffic projections for London (2023)
	Road transport emission factors	COPERT 5.4 (COPERT 5.4, 2020)
	Measurement data	2022
	Meteorological data	WRF (see Appendix 4 – WRF meteorology)
Model components	Regional	Interpolated from Rural NOx measurements adjusted for local contribution
	Large point sources	389 sources modelled using ADMS 5.2
	Small point sources	PCM small points model
	ETS point sources	PCM small points model
	Large ETS point sources	75 sources modelled using ADMS 5.2
	Area sources	PCM dispersion kernels generated using ADMS 5.2. Time varying emissions for road transport and domestic sources. PCM small points model for industrial combustion emissions.

Heading	Component	Details
	Roadside increment	PCM Roads Kernel Model using ADMS-Roads 5.0
Calibration	Model calibrated?	Yes
	Number of background stations in calibration	79
	Number of traffic stations in calibration	55
Pollutant specific	Method used to calculate NO_2 from NO_x	Oxidant partitioning model, calibrated for 2022
	Source of f-NO_2 assumptions	NAEI 2023

3.1.4 Outline of the annual mean model for NO_X

The 1 km x 1 km annual mean background NO_X concentration map has been calculated by summing the contributions from:

- Large point sources
- Small point sources
- Distant sources (characterised by the rural background concentration)
- Local area sources
- Point sources with emissions estimates for air quality pollutants based on reported carbon emissions (ETS points)

The area source model has been calibrated using data from the national automatic monitoring networks (AURN) for 2022. At locations close to busy roads an additional roadside contribution has been added to account for contributions to total NO_X from road traffic sources. The contributions from each of these components are described in Section 3.3.

3.1.5 Outline of the annual mean model for NO_2

NO_2 concentrations have been calculated from the modelled NO_X concentrations derived using the approach outlined above using a calibrated version of the updated oxidant-partitioning model described in Section 3.4. This model describes the complex inter-relationships between NO, NO_2 and ozone as a set of chemically coupled species (Jenkin, 2004, 2012; Murrells *et al.*, 2008). This approach provides additional insights into the factors controlling ambient levels of NO_2 (and O_3), and how they may vary with NO_X concentration.

3.1.6 Annual mean NO_X concentration in vegetation areas

The background NO_X map has also been used to generate a map of annual mean NO_X concentrations in vegetation areas for comparison with the NO_X critical level described above; this map is shown in Figure 3.3. This map has been calculated by removing non-vegetation areas from the background NO_X map and calculating the zonal mean of the 1 km x 1 km grid squares for a 30 km x 30 km grid so that it complies with the criteria set out in the AQSR. Mean concentrations on a 30 km x 30 km grid have been used to prevent the influence of any urban area appearing unrealistically large on adjacent vegetation areas. Thus, the modelled concentrations in vegetation areas should be representative of approximately 1000 km^2 as specified in the AQSR for monitoring sites used to assess concentrations for the vegetation critical level.

3.1.7 Assessment for the 1-hour limit value

Hourly concentrations for comparison with the 1-hour limit value have not been modelled due to the considerable uncertainties involved in modelling at such a fine temporal scale.

The annual mean limit value is expected to be more stringent than the 1-hour limit value in the majority of situations (Air Quality Expert Group (AQEG), 2004). This is illustrated in Figure 3.4 which is a scatter plot of annual mean NO_2 in 2022 against the 99.8th percentile of hourly mean concentration (equivalent to 18 exceedances in the same year). Observed concentrations were lower relative to the limit value for the 99.8th percentile than for the annual mean.

3.1.8 Covid-19 pandemic impacts for aircraft and air support

2020, and to a lesser extent 2021, were exceptional years for air quality because of the substantial changes (mostly reductions) in emissions activity caused by the national and regional lockdowns that were introduced as a result of the Covid-19 pandemic. Emissions estimates from the 2021 NAEI have been used to estimate emissions for 2022 for the modelling for the 2022 compliance assessment and additional steps have been taken to capture the impact of the exceptional changes in activity in two related sectors.

Levels of activity do not typically vary by a large amount from year to year and in previous years emissions used in the compliance assessment modelling have been calculated by scaling forward emission estimates by one year based on emission projections from the NAEI. For the 2022 assessment this approach has been used for all sectors except aircraft and air support, which didn't return to normal levels of activity in 2021 and therefore there was significant difference between activity levels in 2021 and 2022. The large changes in activity levels for these sectors during 2021 and 2022 have therefore been accounted for in the compliance assessment modelling by applying scaling factors for aircraft and air support of 2.155 and 2.094 respectively. These were derived from CAA aircraft movement statistics (CAA, 2022).

3.1.9 Chapter structure

This chapter describes modelling work carried out for 2022 to assess compliance with the NO_X critical level and annual mean NO_2 limit value. Emission estimates for NO_X are described in Section 3.2 Section 3.3 describes the NO_X modelling methods. Details of the methods used to estimate ambient NO_2 from NO_X are presented in Section 3.4. Verification of and source apportionment for the modelling results are presented in Section 3.5.

3.2 NO_X emissions

The NO_X modelling is underpinned by the UK National Atmospheric Emissions Inventory 2021 (NAEI 2021) NO_X emissions estimates (Ingledew *et al.*, 2023). Emissions projections have been provided by the NAEI (Personal communication from Ben Pearson, 2023) based on BEIS EEP 2022 energy and emissions projections (BEIS, 2022). Emissions have been projected to 2022 from 2021.

Figure 3.6 shows the UK total NO_X emissions for 2022, with the coding described in Table 3.2. The figure shows that NO_X emissions in 2022 are dominated by four main sources:

- SNAP 7: Road transport (exhaust emissions) (27.6%)
- Combustion point sources (SNAP codes 1, 2 and 3) (27.3%)
- SNAP 8: Other Transport & mobile machinery (ships) (12.3%)
- SNAP 3: Combustion in industry (10.9%)

Figure 3.6 - Total UK NO_x emissions for 2022 by SNAP code scaled from NAEI 2021

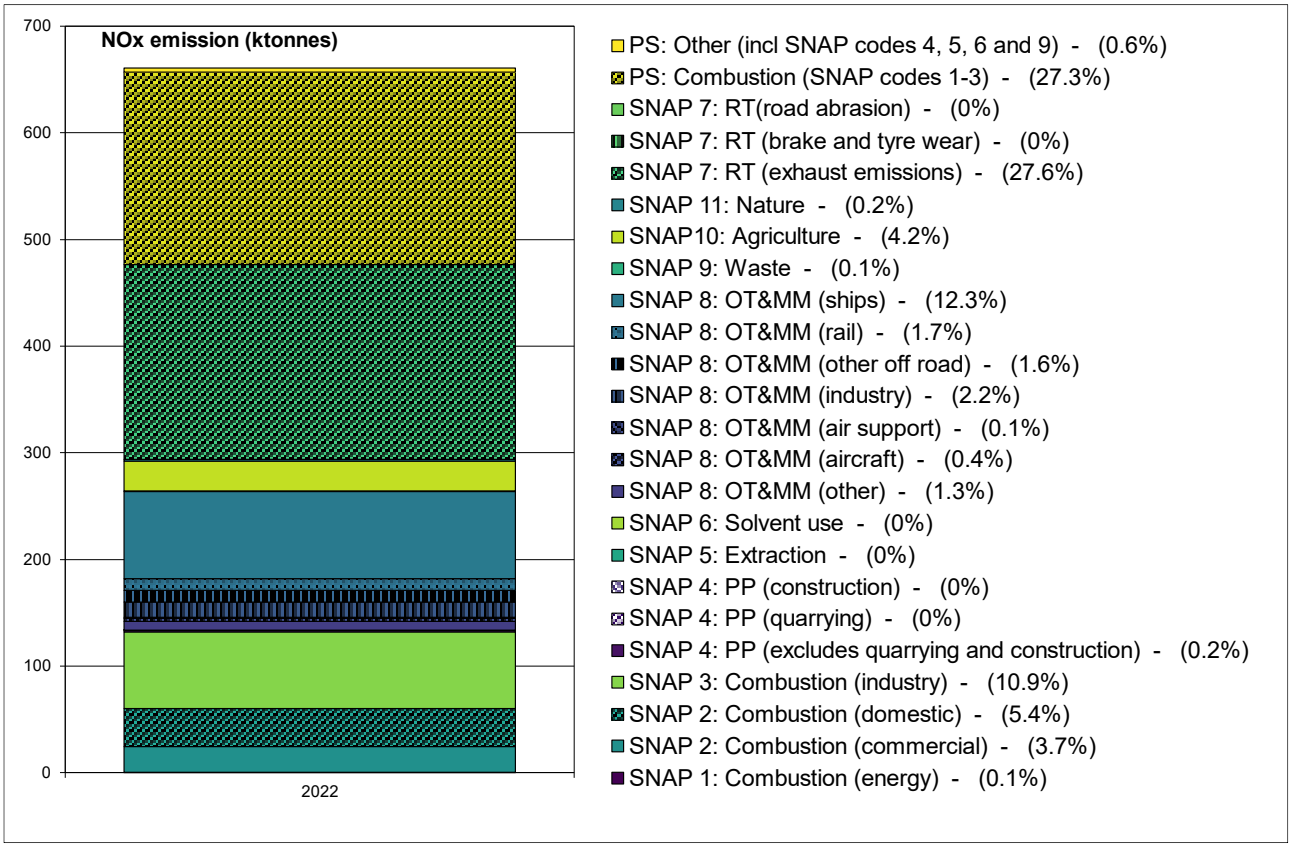

Table 3.2 - Description of SNAP sector coding

Short code	Description
SNAP 1: Combustion (energy)	SNAP 1: Combustion in energy production & transformation
SNAP 2: Combustion (commercial)	SNAP 2: Combustion in Commercial, Institutional & residential & agriculture (excludes domestic)
SNAP 2: Combustion (domestic)	SNAP 2: Combustion in Commercial, Institutional & residential & agriculture (domestic only)
SNAP 3: Combustion (industry)	SNAP 3: Combustion in industry
SNAP 4: PP (excludes quarrying and construction)	SNAP 4: Production processes (excludes quarrying and construction)
SNAP 4: PP (quarrying)	SNAP 4: Production processes (quarrying)
SNAP 4: PP (construction)	SNAP 4: Production processes (construction)
SNAP 5: Extraction	SNAP 5: Extraction & distribution of fossil fuels
SNAP 6: Solvent use	SNAP 6: Solvent use
SNAP 8: OT&MM (other)	SNAP 8: Other Transport & mobile machinery (other)
SNAP 8: OT&MM (aircraft)	SNAP 8: Other Transport & mobile machinery (aircraft)
SNAP 8: OT&MM (air support)	SNAP 8: Other Transport & mobile machinery (air support)
SNAP 8: OT&MM (industry)	SNAP 8: Other Transport & mobile machinery (industry off road mobile machinery)
SNAP 8: OT&MM (other off road)	SNAP 8: Other Transport & mobile machinery (other off road mobile machinery)
SNAP 8: OT&MM (rail)	SNAP 8: Other Transport & mobile machinery (rail)
SNAP 8: OT&MM (ships)	SNAP 8: Other Transport & mobile machinery (ships)

SNAP 9: Waste	SNAP 9: Waste treatment and disposal
SNAP10: Agriculture	SNAP10: Agriculture forestry & land use change
SNAP 11: Nature	SNAP 11: Nature
SNAP 7: RT (exhaust emissions)	SNAP 7: Road transport (exhaust emissions)
SNAP 7: RT (brake and tyre wear)	SNAP 7: Road transport (brake and tyre wear)
SNAP 7: RT (road abrasion)	SNAP 7: Road transport (road abrasion)
PS: Combustion (SNAP codes 1-3)	Combustion point sources (SNAP codes 1-3)
PS: Other (incl. SNAP codes 4, 5 and 9) *	Other point sources (including SNAP codes 4, 5 and 9)

* PS stands for Point Sources. Emissions that are mapped by the NAEI as area sources are summarised using the split in the rows above, and those that are mapped as point sources are summarised using the split in the last 2 rows of Table 3.2.

3.3 NO_X modelling

3.3.1 NO_X contributions from large point sources

Point sources in the NAEI 2021 have been classified as large if they fulfil either of the following criteria:

- Annual NO_X emissions in the NAEI 2021 are greater than 500 tonnes for any given plant.
- Stack parameters are already available for any given plant in the PCM stack parameters database (described in more detail below)

Contributions to ground level annual mean NO_X concentrations from large point sources in the NAEI 2021 were estimated by modelling each source explicitly using the atmospheric dispersion model ADMS 5.2 and sequential meteorological data for 2022 from the Weather Research and Forecasting Model (WRF), as described in Appendix 4 – WRF meteorology. The WRF model is a next-generation numerical weather prediction modelling system developed by the US National Centre for Atmospheric Science (NCAR) (UCAR, 2020). This method accounts for spatial variation in meteorological parameters across the UK representing local dispersion characteristics within the PCM output. A total of 389 large point sources were modelled. Surface roughness varied at both the dispersion and meteorological sites depending on the area type as presented in Table A5.1. Concentrations were calculated for a 99 km x 99 km square composed of a regularly spaced 1 km x 1 km resolution receptor grid. Each receptor grid was centred on the point source. For each large point source information was retrieved from the PCM stack parameters database. This database has been developed over a period of time under the Modelling of Ambient Air Quality (MAAQ) contract and its predecessors. The database is updated annually as required. Data sources for this database include a survey of Part A authorisation notices held by the Environment Agency and previously collated datasets on emission release parameters from large SO_2 point sources (Abbott and Vincent, 1999). Parameters used in the modelling from the stack parameters database include:

- Stack height
- Stack diameter
- Discharge velocity
- Discharge temperature

Where release parameters were unavailable, engineering assumptions have been applied based on information available for similar plant.

The NAEI emissions for large point sources are for the year 2021; however, the year 2022 has been modelled for the assessment. The emissions estimates for 2022 have been calculated from the 2021 values. Closure of plant or activities are taken into account when deriving the source sector projection factors by subtracting the base year emissions associated with plant closure from the relevant source sector total for point sources for the NAEI base year. Any point sources in the NAEI base year that closed before the start or early in the current assessment year are removed from the modelling, based on recommendations from the NAEI team (Personal communication from Ben Pearson, 2023).

3.3.2 NO_X contributions from small point sources

Contributions from NO_X point sources in the NAEI 2021 that were not classified as large point sources (see Section 3.3.1) were modelled using the small point source model described in Appendix 3 – Small point source model. In line with the method applied for the large point sources the NAEI 2021 emissions for small point sources have been scaled to 2022 using the same source sector specific projection factors applied to the large point sources.

3.3.3 NO_X contributions from ETS point sources

The NAEI 2021 includes point source emissions estimates derived from carbon emissions data reported under the EU-Emissions Trading Scheme (ETS), most recently described in (Tsagatakis *et al.*, 2023). These point sources are referred to as ETS points in this report. These derived air quality pollutant emissions are particularly uncertain and therefore in previous assessments (e.g. (Brookes et al., 2017) emissions were capped at reporting thresholds and treated as small point sources. For the 2016 assessment (Brookes *et al.*, 2019a) the NAEI recommended treating the ETS points that have emissions greater than the large points modelling threshold as large points and not to apply a cap (Personal communication from Ben Pearson, 2023). The 2022 assessment continues this approach. Thus, based on the criteria for the treatment of large point sources described above (Section 3.3.1), 75 ETS point sources were modelled as an additional set of large point sources (using the approach described in Section 3.3.1). ETS points that were not classified as large point sources were modelled using the small points approach (described in Appendix 3 – Small point source model). In line with the method applied for the large point sources, the NAEI 2021 emissions for ETS point sources have been scaled to 2022 using the same source sector specific projection factors applied to the large point sources, as described in Section 3.3.1.

3.3.4 NO_X contribution from rural background concentrations

Rural annual mean background NO_X concentrations have been estimated using:

- NO_X measurements at 10 selected rural AURN sites.
- NO_X estimated from NO_2 measurements at 20 rural NO_2 diffusion tube sites from the UK Eutrophying and Acidifying Atmospheric Pollutants (UKEAP) Network.

Figure 3.7 shows the locations of these monitoring sites and the interpolated rural map.

Rural NO_X was estimated from rural NO_2 at diffusion tube sites by dividing by 0.7835. This factor, which is a typical NO_X/NO_2 ratio measured at rural automatic monitoring sites (Stedman *et al.*, 2003), does not vary significantly between years or across the country. Measurements have then been corrected to remove the contribution from point source and local area sources to avoid double counting these contributions later in the modelling process.
The correction procedure is as follows:

Corrected rural background ($\mu g\ m^{-3}$) = Uncorrected rural background ($\mu g\ m^{-3}$) – (A + B + C),

where: *A* is an estimate of the contribution from area source components, derived using the area source contributions from the 2021 modelling (scaled using the ratio of 2021 and 2022 emissions),

B is the sum of contributions from large point sources based on 2021 modelling,

C is the sum of contributions from small and ETS point sources based on 2021 modelling.

The correction is applied based on 2021 model results for local area and point sources because calibrated model results for these sources for 2022 are calculated later in the modelling process and rely on a calibration that requires the subtraction of the corrected rural contribution. Automatic sites, where available have been used in preference to diffusion tubes as these are considered to be more accurate. An interpolation of corrected rural measurement data by Inverse Distance Weighted (IDW) interpolation has been used to map regional background concentrations throughout the UK.

Figure 3.7 - Rural background NO_X concentrations map with monitoring sites used in the interpolation (annual mean NO_X concentrations for 2022 (µg m^{-3}, as NO_2) are shown below the site name)

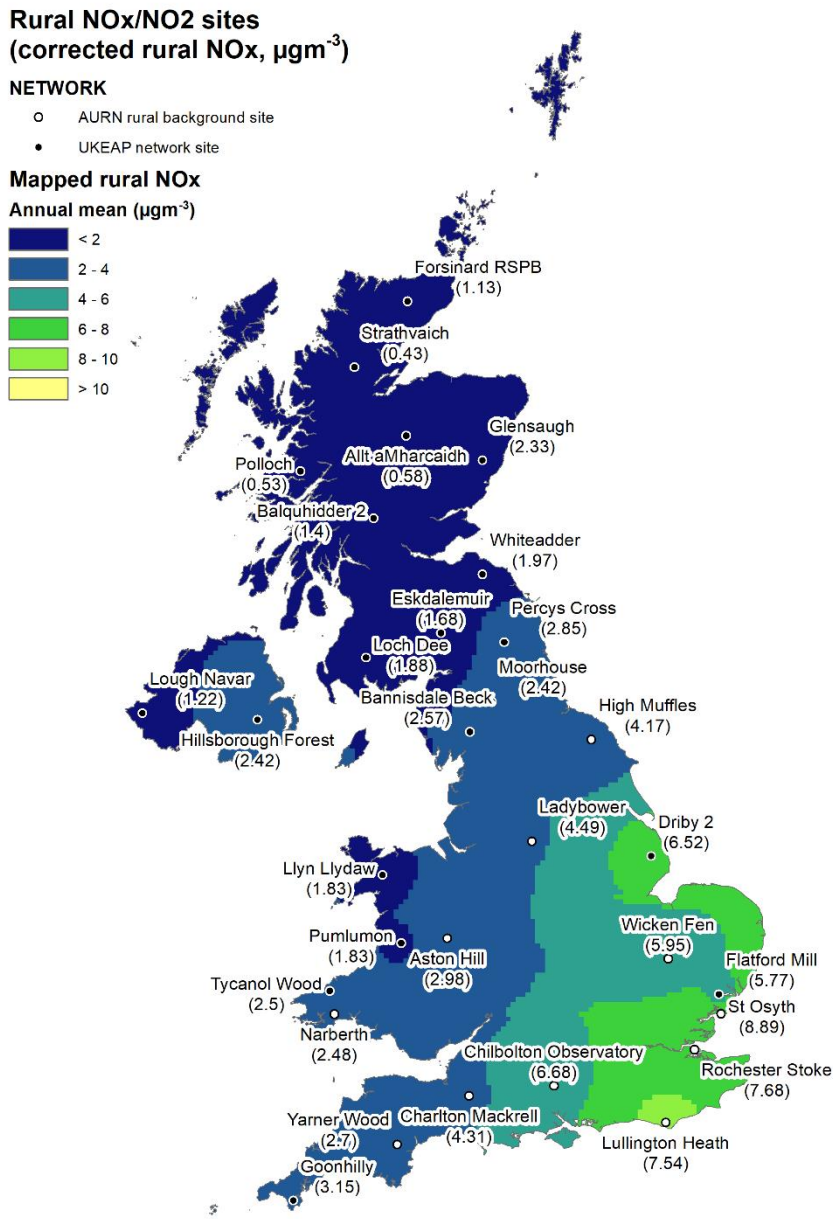

3.3.5 NO_X contributions from local area sources

In the NAEI 2021, NO_X area source emissions maps have been calculated for each source code-activity code combination using distribution grids that have been generated using appropriate surrogate statistics. These NO_X emissions grids are then added together to give SNAP code sector NO_X area source emission grids. The full method is described in (Tsagatakis *et al.*, 2023). To calculate NO_X area source emission grids for 2022 scaling factors have been used to scale 2021 emissions forwards to 2022. Emissions projections have been provided by the NAEI based on BEIS EEP 2022 energy and emissions projections (BEIS, 2022). The 2021 area source NO_X emissions have been mapped using updated distribution grids produced for the NAEI 2021 (Tsagatakis *et al.*, 2023).

The 2022 area source emissions maps have then been used to calculate uncalibrated area source concentration maps for each SNAP code sector. With the exception of SNAP sector 3 (combustion in industry), this has been done by applying an ADMS 5.2 derived dispersion kernel to the emission maps to calculate the contribution to ambient concentrations on a 1 km x 1 km receptor grid, from the area source emissions within a 33 km x 33 km square surrounding each receptor. Hourly sequential meteorological data from the WRF model in 2022 have been used to construct the dispersion kernels.

Appendix 5 – Dispersion kernels for the area source model describes these kernels in more detail and explains how they have been calculated.

Since 2011 a dispersion kernel approach including a time varying emission profile based on degree days has been applied to the SNAP 2 domestic area sources sector to weight these emissions more realistically by time of day and meteorological conditions. The approach to derive the time varying emissions profile is described in Appendix 5 – Dispersion kernels for the area source model. The temperature data for 2022 and 2021 has been compared to calculate a scaling factor to apply to SNAP 2 emissions.

A development introduced for the 2011 assessment was a revision to the methodology for treating the SNAP 3 (combustion in industry) area source component (i.e. the component of the UK SNAP 3 national total not accounted for by regulated processes). Since 2011 the small points model (described in Appendix 3 – Small point source model) has been applied to derive concentrations resulting from SNAP 3 area source emissions. By using the small points method for this sector, a more realistic release height, buoyancy and momentum of discharge is used based on the magnitude of the emission for small industrial chimneys.

Figure 3.8 shows the calibration of the area source model. The modelled concentrations from all point sources, SNAP 3 area sources and corrected rural NO_X concentrations have been subtracted from the measured annual mean NO_X concentration at background sites. This concentration is compared with the modelled area source contribution (excluding SNAP 3) to annual mean NO_X concentrations to calculate the calibration coefficients used in the area source modelling.

As part of the calibration process, emission caps have been applied to certain sectors; this is because the use of surrogate statistics for mapping area source emissions sometimes results in unrealistically large concentrations in some grid squares for a given sector. The emission caps applied are given in Table 3.3.

The modelled area source contributions for each sector except SNAP 3 were multiplied by the coefficient to calculate the calibrated area source contribution for each grid square in the country. The point source contributions, SNAP 3 area source component and regional rural concentrations were then added, resulting in a map of background annual mean NO_X concentrations.

Figure 3.8 - Calibration of area source NO_X model, 2022 (µg m^{-3}, as NO_2)

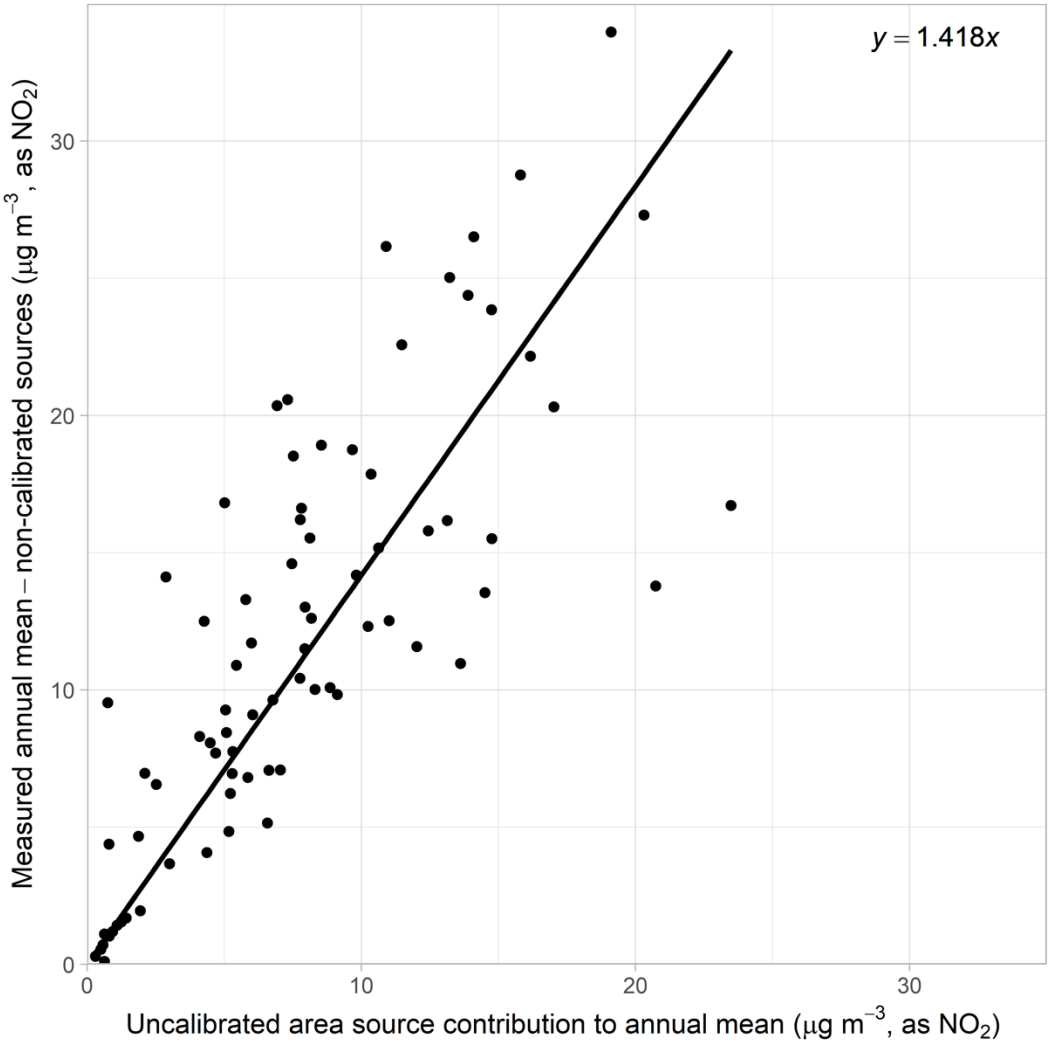

Table 3.3 - Emission caps applied to NO_X sector grids.

SNAP code	Description	Cap applied (t/a/km²)
SNAP 1 (gas production, natural gas)	Combustion in energy production & transformation	30
SNAP 8 (shipping only)	Other Transport & Mobile Machinery	100

3.3.6 NO_X Roadside concentrations

The modelled annual mean concentration of NO_X at a roadside location is made up of two parts: the background concentration (as described above) and a roadside increment:

roadside NO_X concentration = background NO_X concentration + NO_X roadside increment.

The NAEI has provided estimates of NO_X emissions for major road links in the UK for 2021 (Ingledew *et al.*, 2023) and these have been scaled to provide estimates of emissions in 2022. The emissions estimates for NO_X from road transport sources include the following assumptions:

- Department for Transport (DfT) 2022 traffic forecasts, (DfT, 2022) car sales projections including the uptake of low carbon passenger cars and LGVs with electric and hybrid electric propulsion systems, and Transport for London traffic projections for London (2023)
- Department for Transport (DfT) major road traffic counts for 2022 where available (DfT, 2022)
- NO_X emission factors from COPERT 5.4 (COPERT 5.4, 2020)

Prior to the 2020 compliance assessment, traffic speed assumptions by vehicle category were applied following categories based upon UK area type and road type taking data from DfT congestion statistics to estimate the speeds (Brown, Wakeling, Pang, & Murrells, 2018). For the 2020, 2021 and 2022 compliance assessment modelling, revised NAEI traffic speed assignments have been applied using defined urban/rural classification, A-road/motorway and speed limit. Assignments were made separately to roads in central, inner and outer London and the rest of the UK outside of London. Speed limit classification data has been assigned to OS Openroads geometry based on the length weighted median speed limit for each road link. The underlying speed limit dataset has been provided by Basemaps for Great Britain (Speed Limit Data Basemap, 2022). The vehicle speeds assigned to each category were derived from an analysis of GPS vehicle speed observations (Teletrac Navman, 2021) for England provided by DfT. The observed average speeds for England were applied across the UK. Speed limits were manually assigned to road links in Northern Ireland.

Local traffic fleet composition information was used to calculate road traffic emissions in specific areas for the first time in the 2021 assessment. This method has also been used for the 2022 assessment. Information from Automatic Number Plate Recognition has been combined with vehicle registration data in order to derive fleet composition in terms of vehicle ages and Euro standards. Emissions have been 'localised' in the following locations:

- Within the Clean Air Zone in Birmingham
- Within the Clean Air Zone in Bath
- The whole of Leeds City Council
- Within the Clean Air Zone in Bradford
- Within the Clean Air Zone in Portsmouth

The PCM Roads Kernel Model (PCM-RKM) described in Appendix 8 – The PCM Roads Kernel Model has been used to calculate the roadside increment. The PCM-RKM is based upon dispersion kernels generated by the ADMS-Roads dispersion model (v5.0). A link with measurement data is provided by using AURN measurement data to calibrate this component of the model.

Figure 3.9 shows the calibration of this model at roadside monitoring sites. In this figure, the measured roadside increment at the roadside monitoring sites is calculated as the measured concentration minus the background NO_X component, which is determined from the background NO_X concentration map described in Section 3.3.5 above. The modelled NO_X roadside increment is calculated directly using the road link emissions alone. The total modelled roadside NO_X concentration is then given from the equation above by adding the calibrated background NO_X modelled concentration to the calibrated NO_X roadside increment modelled concentration. The average distance from the kerb for the roadside and kerbside monitoring sites used to calibrate the roadside increment model is approximately 4 m. The calculated roadside concentrations are therefore representative of this distance from the kerb. Roadside concentrations for urban major road links (A-roads and motorways) only are reported and included in this report.

Figure 3.9 - Calibration of NO_X PCM RKM model, 2022 (µg m^{-3}, as NO_2)

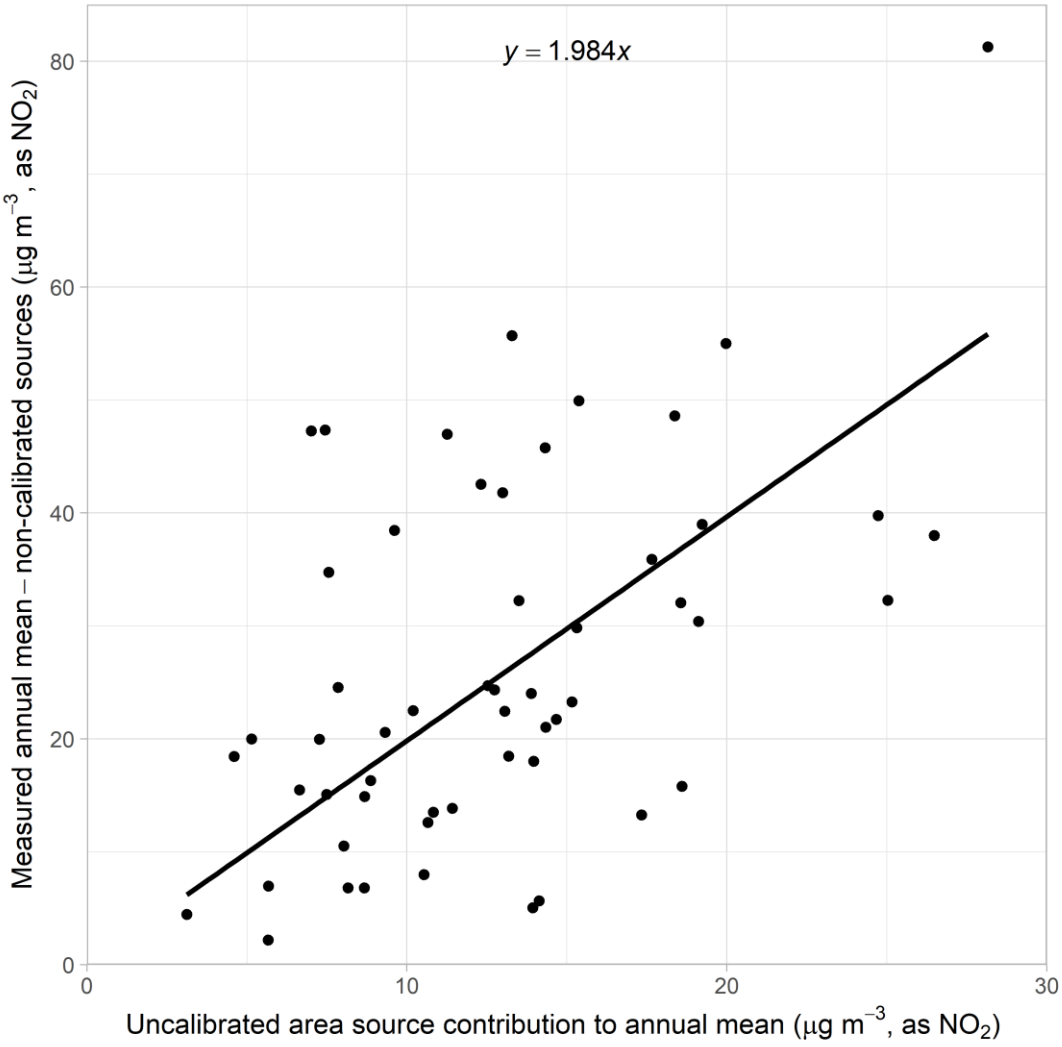

3.4 NO_2 Modelling

3.4.1 Introduction

Maps of estimated annual mean NO_2 concentrations (Figure 3.1 and Figure 3.2) have been calculated from the modelled NO_X concentrations using a calibrated version of the updated oxidant-partitioning model (Jenkin, 2004, 2012; Murrells *et al.*, 2008). This model uses representative equations to account for the chemical coupling of O_3, NO and NO_2 within the atmosphere. A key advantage of this approach for modelling NO_2 concentrations is that emission scenarios can be directly addressed by varying regional oxidant levels and/or primary NO_2 emissions.

3.4.2 The updated oxidant-partitioning model

The oxidant-partitioning model, developed by Jenkin (2004), enables NO_2 concentrations to be calculated using the following equations:

$$[NO_2] = [OX].f(NO_x) \quad (i)$$

$$[OX] = f\text{-}NO_2.[NO_x] + [OX]_B \quad (ii)$$

Where [OX] is the total oxidant (the sum of NO_2 and O_3), f-NO_2 is the primary NO_2 emission fraction (defined as the proportion of NO_X emitted directly as NO_2), $[OX]_B$ is the regional oxidant and f(NO_X) is a function, the value of which is determined by the concentration of NO_X. NO_X, NO_2, O_3 and OX are all expressed as ppb in these equations: 1 ppb of O_3 = 2 µg m^{-3}; 1 ppb of NO_2 = 1.91 µg m^{-3}. By convention when NO_X is expressed in µg m^{-3} it is expressed as "µg m^{-3} as NO_2" therefore 1 ppb of NO_X = 1.91 µg m^{-3} of NO_X as NO_2.

In Jenkin (2004), $[NO_2]/[OX]$ (i.e. $f(NO_X)$) was calculated using two equations, one of which represented background locations and the other roadside locations. Updated equations for $[NO_2]/[OX]$ were subsequently developed in Murrells et al. (2008). More recently, Jenkin, (2012) found that short term variability in NO_x concentrations is a major cause of the scatter in the relationship between $[NO_2]/[OX]$ and $[NO_x]$. The ratio of the upper to the lower quartile of hourly concentrations has been found to be a good indicator of this variability. The ratio increases with decreasing NO_x concentrations at roadside and background sites. This dependence has been used to interpolate between equations based on a constant NO_x quartile ratio. This led to two equations for calculating $[NO_2]/[OX]$, one of which represents background locations and the other roadside locations. These are the equations that are currently used in the modelling. These are an improvement over the equations presented in (Murrells *et al.*, 2008) because the background equation requires less adjustment in the background adjustment calibration and the roadside equation enables linear calibration adjustment for roadside.

Jenkin (2012) presented two equations for calculating $[NO_2]/[OX]$ as a function of $[NO_X]$ (i.e. $f(NO_X)$). These are:

- One background relationship, which has been derived using data from background sites.
- One roadside relationship, which has been derived using data from roadside sites.

The two relationships are presented in Table 3.4 below.

Table 3.4 - The two relationships in the updated oxidant-partitioning model (Jenkin, 2012)

PCM Category	Relationship (where y = $[NO_2]/[OX]$ and x = $[NO_x]$, in ppb)
Background	y = -2.5124E-13x^6 + 1.5805E-10x^5 – 4.1429E-08x^4 + 5.8239E-06x^3 – 4.8076E-04x^2 + 2.5916E-02x
Roadside	y = -2.0901E-13x^6 + 1.5001E-10x^5 – 4.2894E-08x^4 + 6.2659E-06x^3 – 5.0720E-04x^2 + 2.5322E-02x

The following sections describe the method for calculating an average regional oxidant value for the UK (Section 3.4.3), local oxidant calculations for background and roadside locations (Section 3.4.4), calculating $[NO_2]/[OX]$ in the PCM model and how the updated oxidant-partitioning model has been applied in the UK to background and roadside locations (Section 3.4.5).

3.4.3 UK regional oxidant

A fixed regional oxidant value for the whole of the UK has been used. The regional oxidant value for 2022 was calculated to be 32.1 ppb. This value was derived from an analysis of annual mean data for O_3, NO_2 and total nitrogen oxides (NO_X) at 64 AURN sites. These sites were selected using the criterion that the annual mean $[NO_X]$ in 2022 was less than or equal to 25 ppb, so that the contribution to [OX] derived from primary NO_2 was comparatively small. A constant $f\text{-}NO_2$ value of 0.093 was used to correct for the contribution from local oxidant.

3.4.4 Local oxidant calculations

Local oxidant is calculated in the updated oxidant-partitioning model as:

$$Local\ oxidant = f\text{-}NO_2.[NO_X]. \qquad (iv)$$

Where $f\text{-}NO_2$ is the fraction of NO_x emissions emitted as primary NO_2 (by volume). Therefore, to calculate local oxidant levels, the $f\text{-}NO_2$ levels from different local sources need to be understood. In general, it is possible to make a distinction between $f\text{-}NO_2$ from road traffic sources and $f\text{-}NO_2$ from non-road traffic sources. $f\text{-}NO_2$ from road traffic sources is thought to have risen during the early 2000s, although this trend displays considerable variation with location (Air Quality Expert Group (AQEG), 2007; Carslaw *et al.*, 2011). By comparison, $f\text{-}NO_2$ from non-traffic sources has remained relatively constant with time.

3.4.4.1 $f\text{-}NO_2$ for road traffic sources on individual road links

Figure 3.10 shows fleet average $f\text{-}NO_2$ projections by vehicle type for London and the rest of the UK from the NAEI.

$f\text{-}NO_2$ for all petrol vehicles is very low (less than 5%). $f\text{-}NO_2$ for diesel cars and LGVs is much greater and is expected to increase somewhat in the future. $f\text{-}NO_2$ for HGVs and buses is lower and is also expected to decline for buses, HGVs however are expected to have an increase in $f\text{-}NO_2$. $f\text{-}NO_2$ projections for London show the impact of specific measured applied to London buses and the London

low emission zone (LEZ) and ultra-low emission zone (ULEZ). An update to primary NO_2 emission factors for road vehicles[5] provides further information on *f-NO_2* values.

Figure 3.10 - Fleet average *f-NO_2* projections by vehicle type for a) London and b) rest of the UK from NAEI

a) London

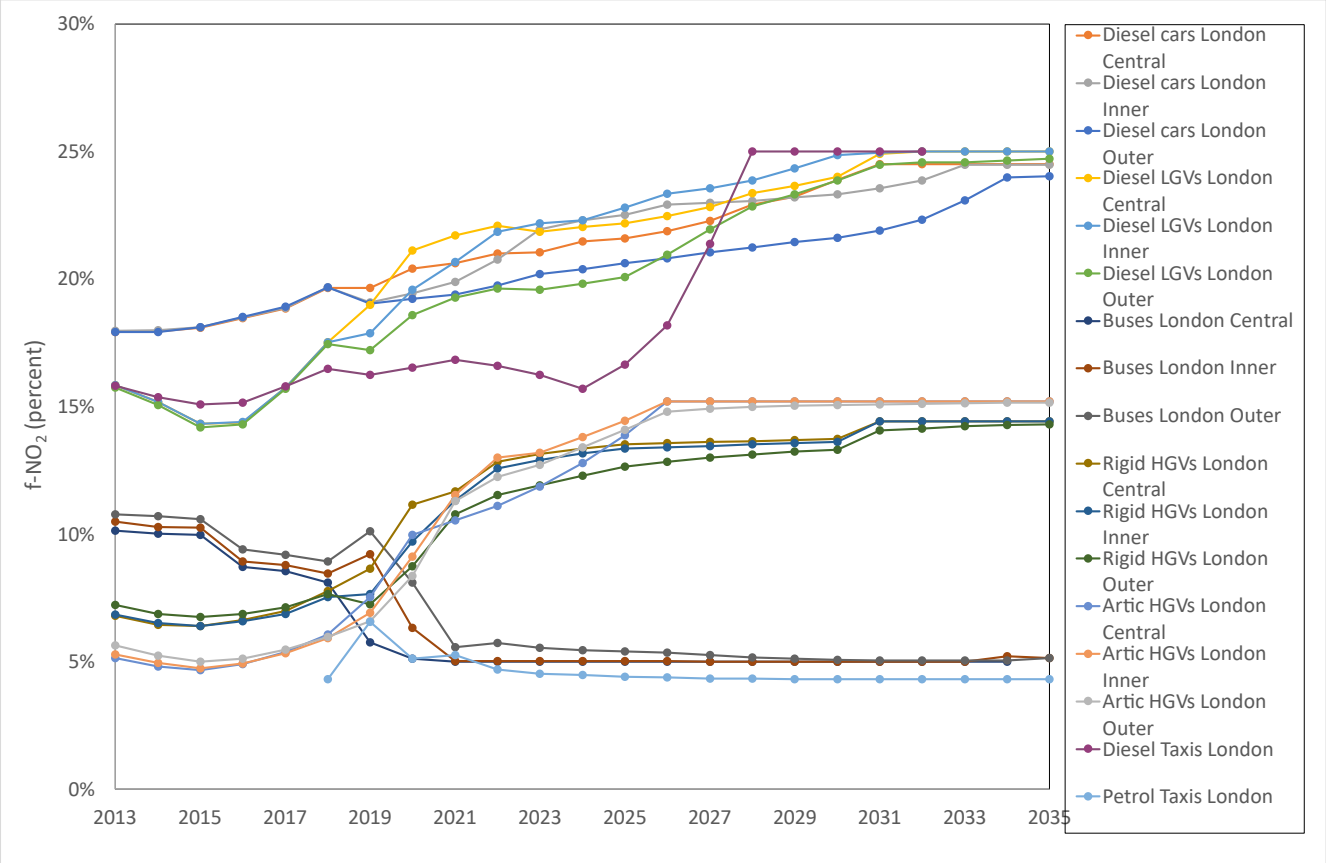

[5] https://naei.beis.gov.uk/resources/Primary%20NO2%20Emission%20Factors%20for%20Road%20Vehicles_NAEI%20Base%202023.html

b) Rest of the UK

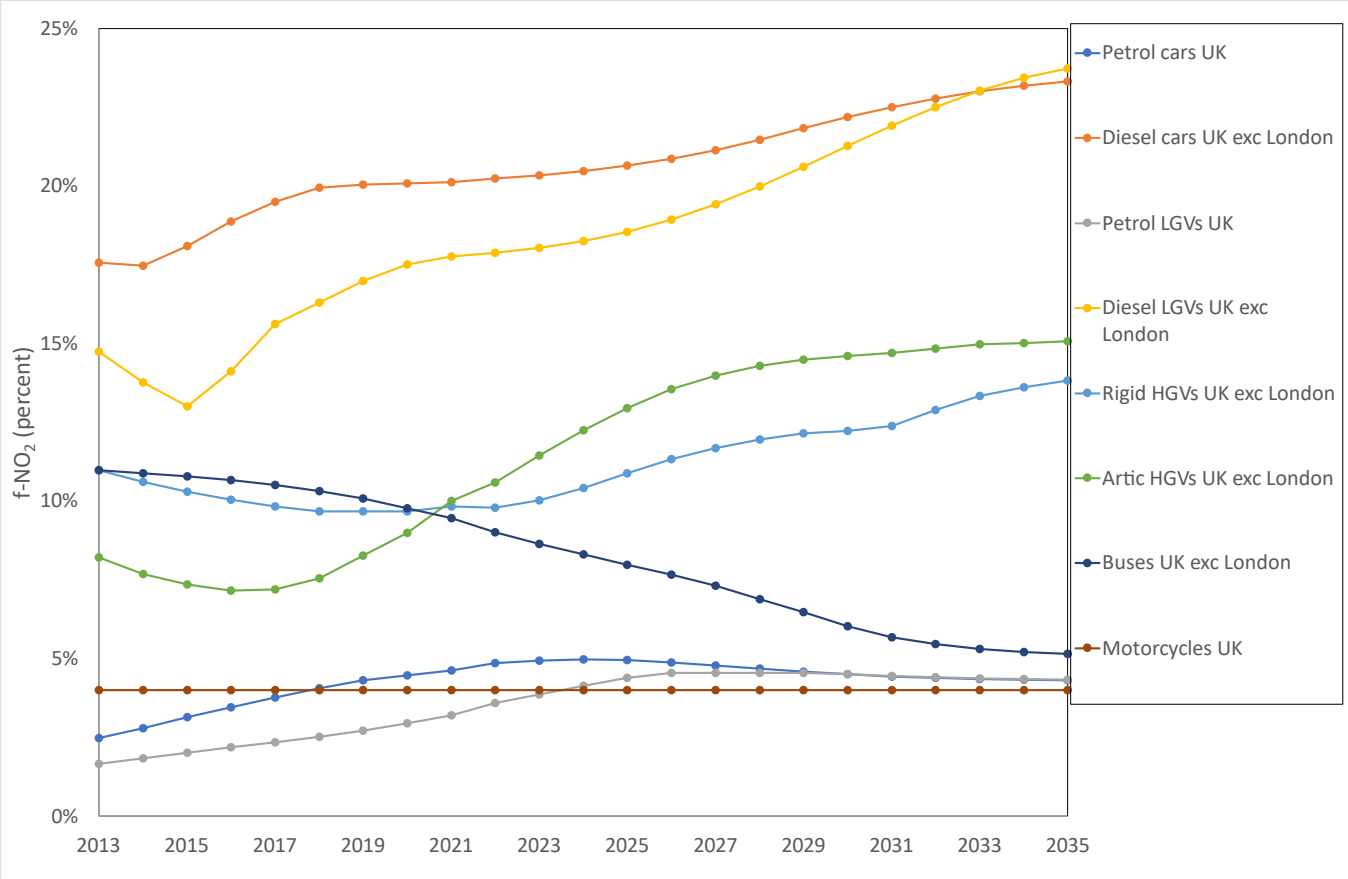

3.4.4.2 *f-NO₂* for background sources

Table 3.5 shows the *f-NO₂* values used for background sources in 2022. The non-road *f-NO₂* values used for background calculations in Table 3.5 have been taken directly from (Jenkin, 2004), as there is little evidence that this has changed significantly over the past few years. The road traffic *f-NO₂* values for background calculations have been calculated using the average of the major road link *f-NO₂* values for each area type.

Table 3.5 - Local oxidant coefficients (*f-NO₂*) for background concentrations in 2022

DfT Area type[1]	Region	Non-road *f-NO₂* for background calculations	Road *f-NO₂* for background calculations
1	Central London	0.140	0.158
2	Inner London	0.128	0.166
3	Outer London	0.093	0.167
4	Inner Conurbations	0.093	0.160
5	Outer Conurbations	0.093	0.164
6	Urban (population > 250,000)	0.093	0.165
7	Urban (population > 100,000)	0.093	0.165
8	Urban (population > 25,000)	0.093	0.166
9	Urban (population > 10,000)	0.093	0.166
10	Rural	0.093	0.167

[1] Locations in Northern Ireland have been assigned area types according to how built up the local environment is because the DfT area types map does not cover Northern Ireland. A map of the distribution of DfT area types is included in Appendix 5 – Dispersion kernels for the area source model.

3.4.4.3 Local oxidant calculations

A map of local oxidant for the background NO_2 calculations was generated by splitting the background annual mean NO_X map into its two constituent components:

- NO_X from background non-road traffic emissions (includes rural background component)
- NO_X from background road-traffic emissions

These components were multiplied by the relevant *f-NO_2* value from Table 3.5 and then added together to give a total local oxidant. Figure 3.11 shows the UK background local oxidant map for 2022.

Local oxidant on individual road links was calculated by splitting the total annual mean NO_X for the road link into its three constituent components:

- NO_X from background non-road traffic emissions (includes rural background component)
- NO_X from background road-traffic emissions
- Roadside increment NO_X concentrations from emissions on the specific road link under consideration

The background components were then multiplied by the relevant *f-NO_2* value from Table 3.5 and the roadside increment NO_X was multiplied by the specific *f-NO_2* calculated for that road link. These local oxidant values were then added together to give a total local oxidant for the road.

Figure 3.11 - Background local oxidant map for 2022 (ppb)

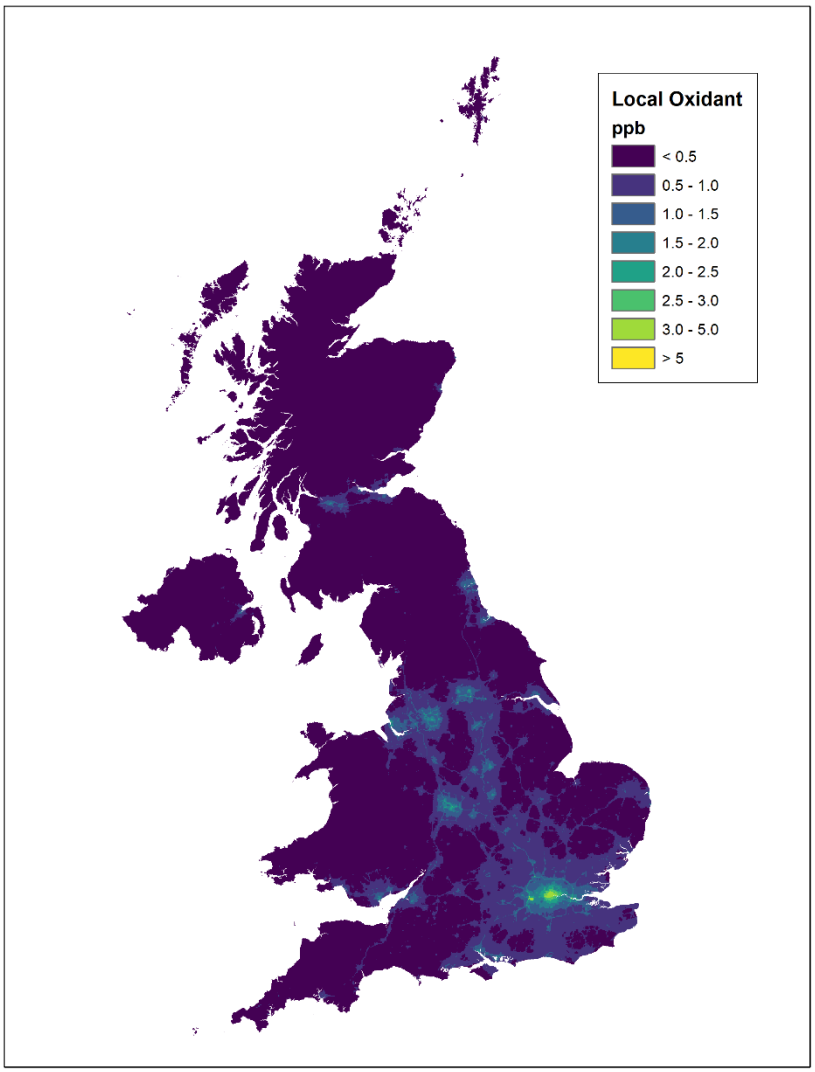

3.4.5 Calculating [NO_2]/[OX] in the PCM model

As described in Section 3.4.2, two relationships for calculating [NO_2]/[OX] have been derived in (Jenkin, 2012). The ratio of [NO_2]/[OX] has been considered separately for background and roadside locations in this analysis as there are separate relationships for these locations. Background and roadside sites tend to behave differently because of differences in the 'age' of the NO_X at these locations.

3.4.5.1 Background

For background locations, the background relationship has been calibrated using data from AURN background sites for 2022. The calibration plot for background sites is shown in Figure 3.12.

Figure 3.13 a and b show verification plots of measured NO_2 against modelled NO_2 calculated from measured NO_X using the uncalibrated background relationship and calibrated background relationship respectively. The agreement is better for the calibrated model. The background oxidant partitioning curves are only valid for annual mean NO_X concentrations up to 267.4 µg m^{-3} (as advised by (Jenkin, 2012)) hence NO_X concentrations above this value have been set to 267.4 µg m^{-3}.

Figure 3.12 - Background NO_2 calibration curve (NB verification sites are shown for reference here, but were not used in calculating the calibration), 2022

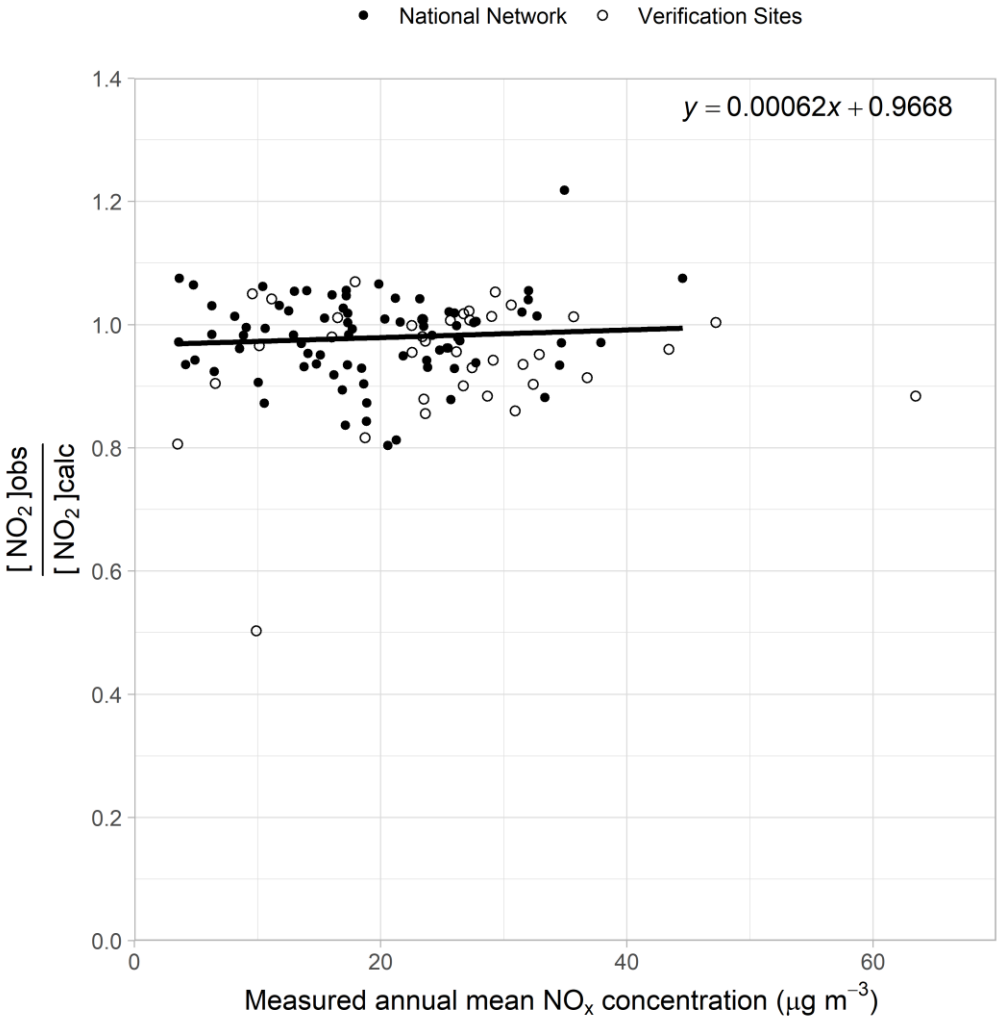

Figure 3.13 - Verification of background relationship at background locations in 2022

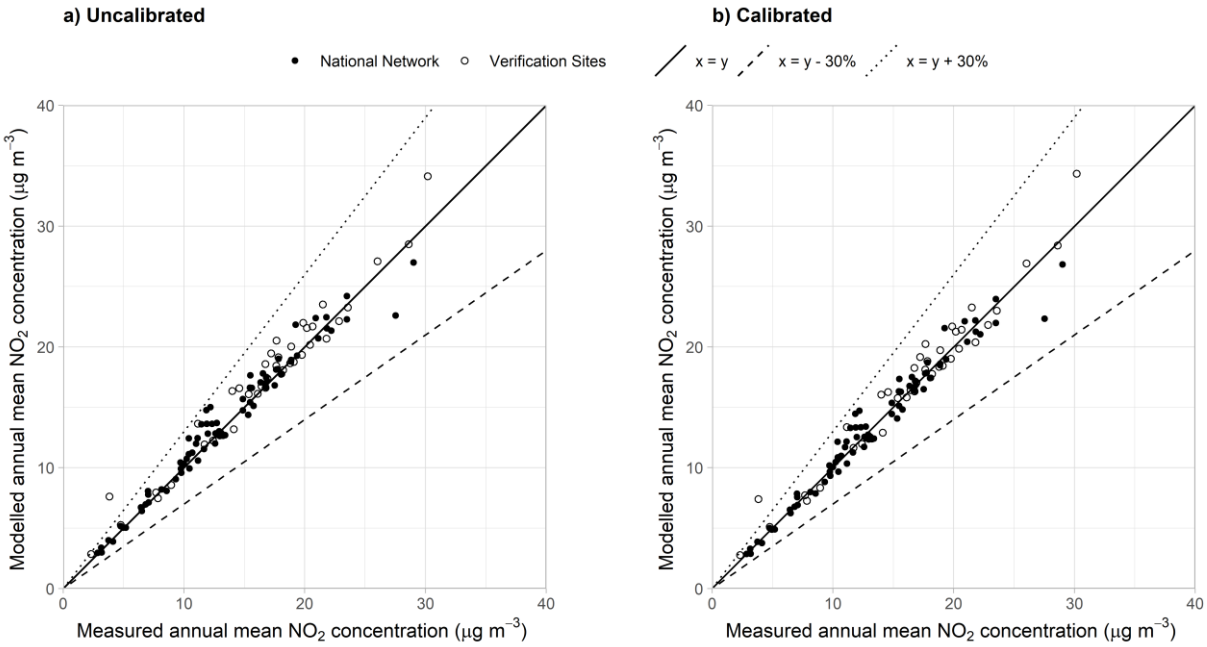

3.4.5.2 Roadside

For roadside locations, the roadside relationship has been selected and an additional calibration has been applied using data from AURN roadside sites for 2022. The model has been calibrated by plotting the ratio of measured NO_2 to modelled NO_2 as a function of NO_X for each AURN roadside sites for 2022 and then fitting a straight line through these points. Figure 3.14 shows this ratio for each site and the straight line that was fitted though the data. The verification sites are also shown on this plot for reference although they were not used to calibrate the model.

Figure 3.14 - Roadside NO_2 calibration curve (NB verification sites are shown for reference here, but were not used in calculating the calibration factors), 2022

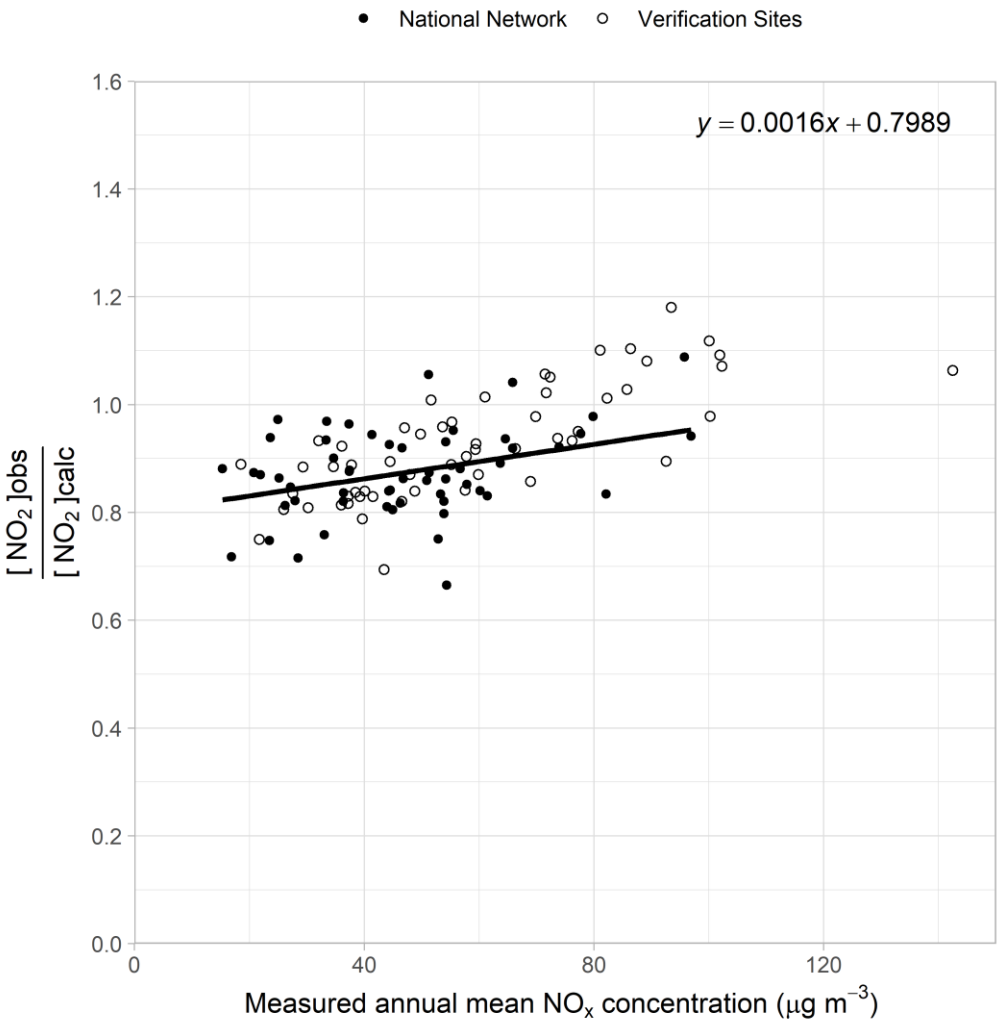

Figure 3.15a shows a verification plot of measured NO_2 against modelled NO_2 calculated from measured NO_X using the uncalibrated roadside relationship. Figure 3.15b shows the same information but using the calibrated roadside relationship. It is clear that the calibrated model provides a better fit to the monitoring data in the vicinity of the limit value of 40 µg m^{-3}. The roadside oxidant partitioning curves are only valid for annual mean NO_X concentrations up to 382 µg m^{-3} (as advised by Jenkin (2012)) hence NO_X concentrations above this value have been set to 382 µg m^{-3}.

Figure 3.15 - Verification of roadside relationship at roadside locations in 2022

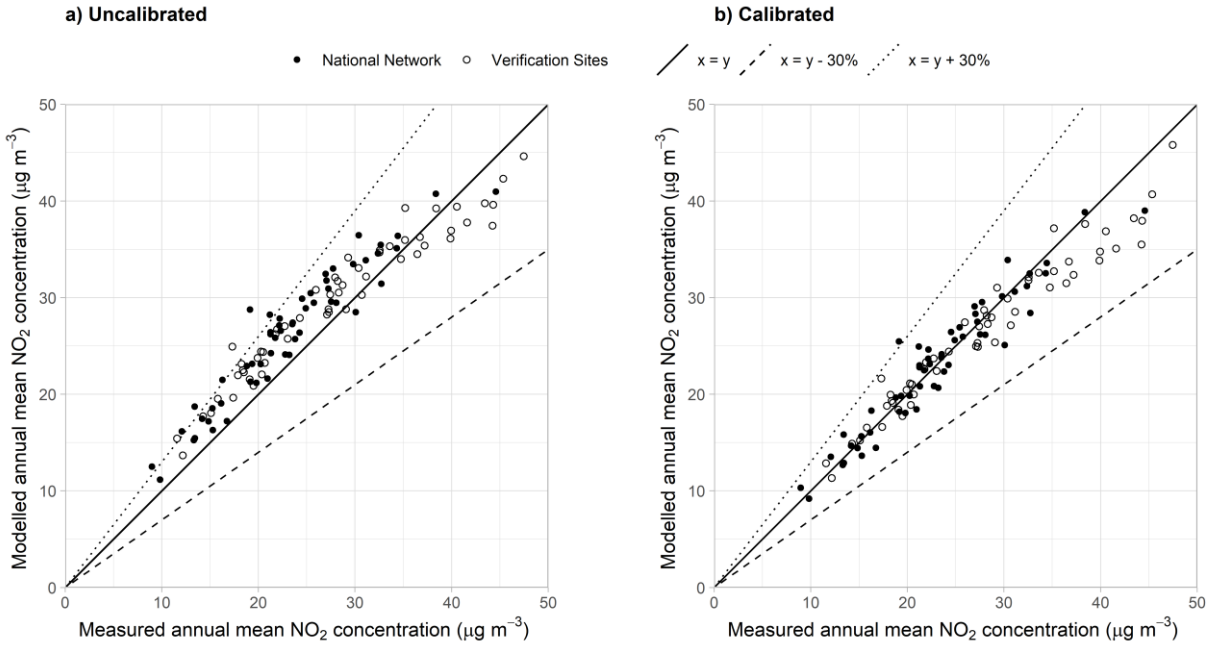

3.5 Results

3.5.1 Verification of mapped values

Figure 3.16 and Figure 3.17 show comparisons of modelled and measured annual mean NO_X and NO_2 concentration in 2022 at background monitoring site locations. Figure 3.18 and Figure 3.19 show similar comparisons for roadside sites. Both the national network sites used to calibrate the models and the verification sites are shown. National network sites that have been excluded from the model calibrations are also shown. Lines representing y = x – 30 % and y = x + 30% are also shown (this is the AQSR data quality objective for modelled annual mean NO_2 and NO_X concentrations – see Section 1.5). There is no requirement under the AQSR to report modelled annual mean NO_X concentrations for comparison with limit values for the protection of human health (the NO_X limit value for the protection of vegetation only applies in vegetation areas). However, comparisons of modelled and measured NO_X concentrations and of the modelled NO_X concentrations with the data quality objectives are presented here alongside the comparisons for NO_2. This provides an additional check on the reliability of the modelled estimates of NO_2 because the non-linear relationships between NO_X and NO_2 tend to cause modelled NO_2 concentrations to be relatively insensitive to differences between measured and modelled values of NO_X.

Summary statistics for the comparison between modelled and measured NO_X and NO_2 concentrations are listed in Table 3.6 and Table 3.7. The percentages of monitoring sites for which the modelled annual mean concentrations fall outside the data quality objectives is generally greater for NO_X than for NO_2, for the reasons discussed above.

Figure 3.16 - Verification of background annual mean NO_X model 2022

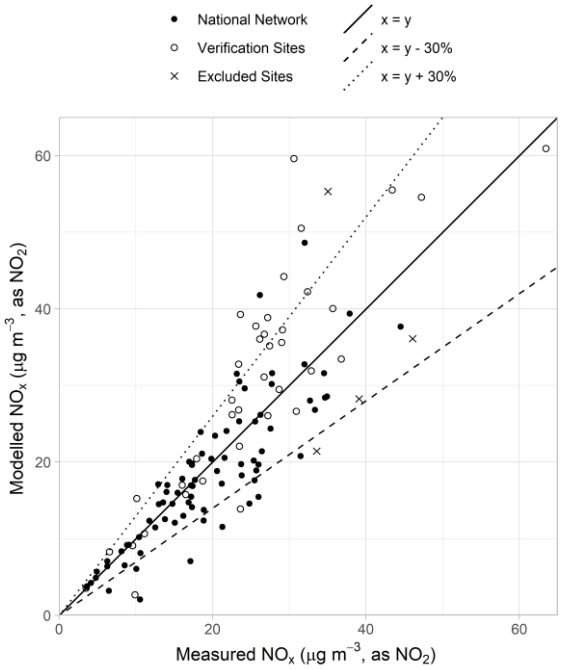

Figure 3.17 - Verification of background annual mean NO_2 model 2022

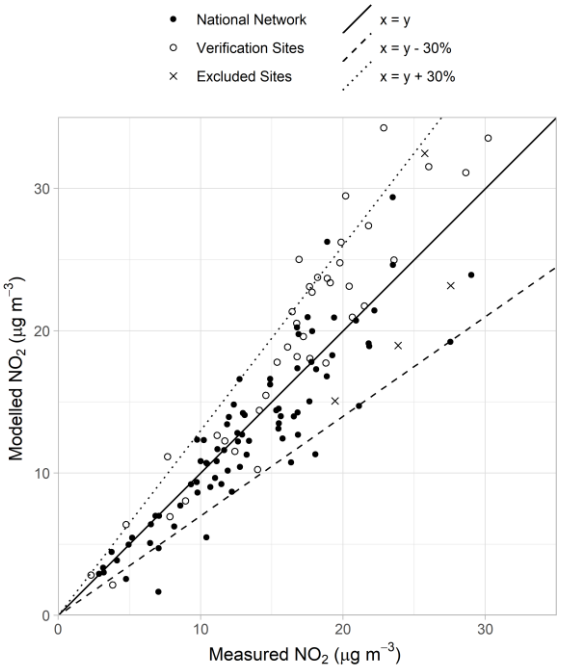

Figure 3.18 - Verification of roadside annual mean NO_X model 2022

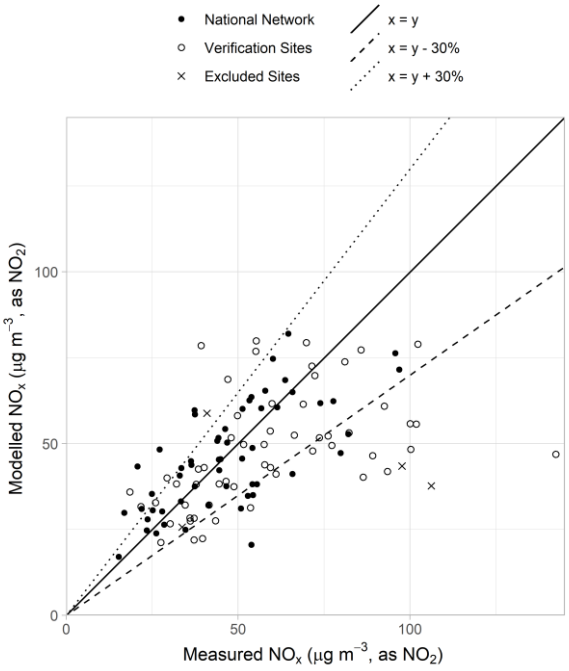

Figure 3.19 - Verification of roadside annual mean NO_2 model 2022

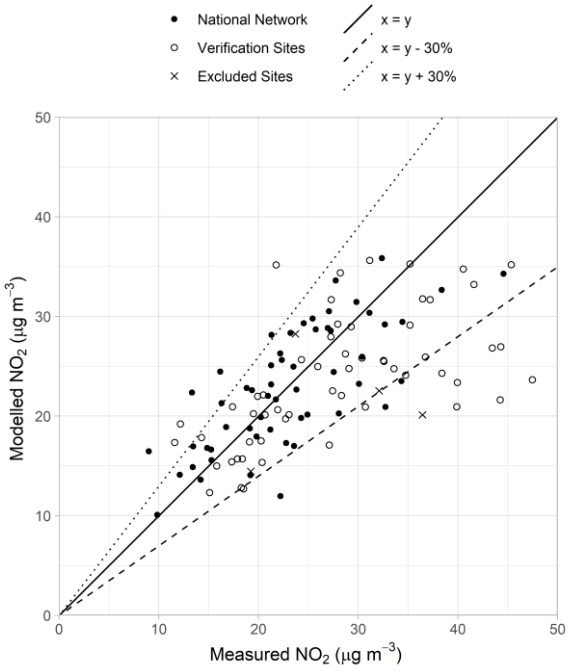

Table 3.6 - Summary statistics for comparison between modelled and measured NO_X and NO_2 concentrations at background sites (µg m^{-3}, as NO_2)

		Mean of measurements (µg m^{-3}, as NO_2)	Mean of model estimates (µg m^{-3}, as NO_2)	R^2	% outside data quality objectives	Number of sites in assessment
NO_X	National Network	19.3	18.3	0.73	17.7	79
	Verification Sites	25.5	30.3	0.75	34.2	38
NO_2	National Network	13.4	12.7	0.80	12.7	79
	Verification Sites	16.6	19.4	0.88	23.7	38

Table 3.7 - Summary statistics for comparison between modelled and measured NO_X and NO_2 concentrations at roadside sites (µg m^{-3}, as NO_2)

		Mean of measurements (µg m^{-3}, as NO_2)	Mean of model estimates (µg m^{-3}, as NO_2)	R^2	% outside data quality objectives	Number of sites in assessment
NO_X	National Network	47.1	46.0	0.5	27.3	55
	Verification Sites	59.0	48.0	0.24	42.9	56
NO_2	National Network	23.1	22.9	0.54	14.5	55
	Verification Sites	28.0	23.7	0.39	25.0	56

3.5.2 Source apportionment

Figure 3.20 and Figure 3.21 show the modelled NO_X source apportionment at AURN background and roadside sites respectively for 2022. Sites that have been excluded from the model calibration are also shown. This shows that while road transport is the dominant source at most locations, both background and roadside, contributions from other sectors such as domestic, commercial, off-road mobile machinery and industry are also significant at many sites. Contributions from aircraft and shipping are evident at some sites. No source apportionment is given for NO_2 because this is not a physically meaningful concept because of the non-linear relationship between NO_X and NO_2.

Figure 3.20 - Annual mean NO_X source apportionment at background AURN monitoring sites in 2022 (area type of each site is shown in parenthesis after its name – see Table 3.5)

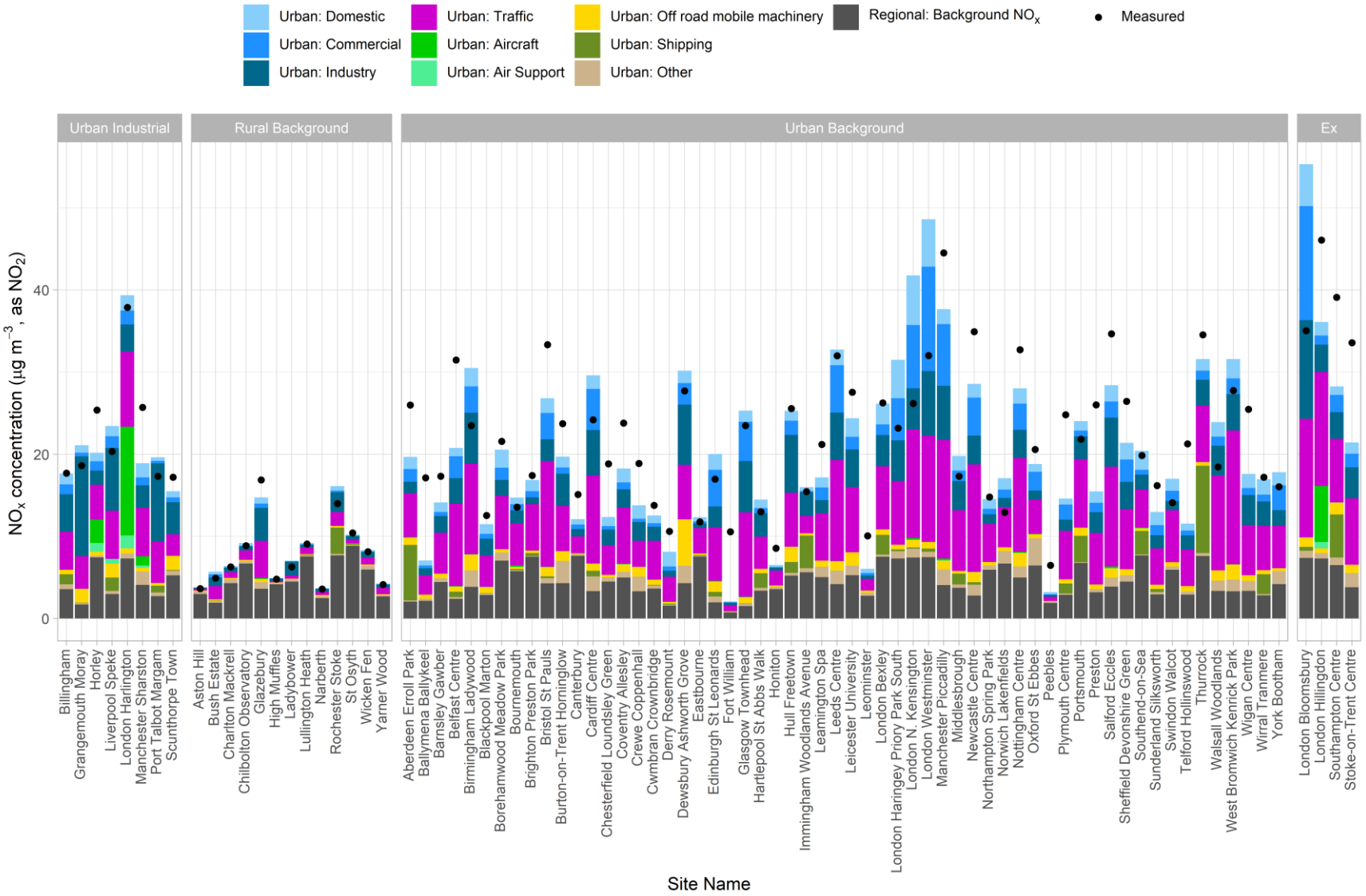

Figure 3.21 - Annual mean NO_X source apportionment at roadside AURN monitoring sites in 2022 (area type of each site is shown in parenthesis after its name – see Table 3.5)

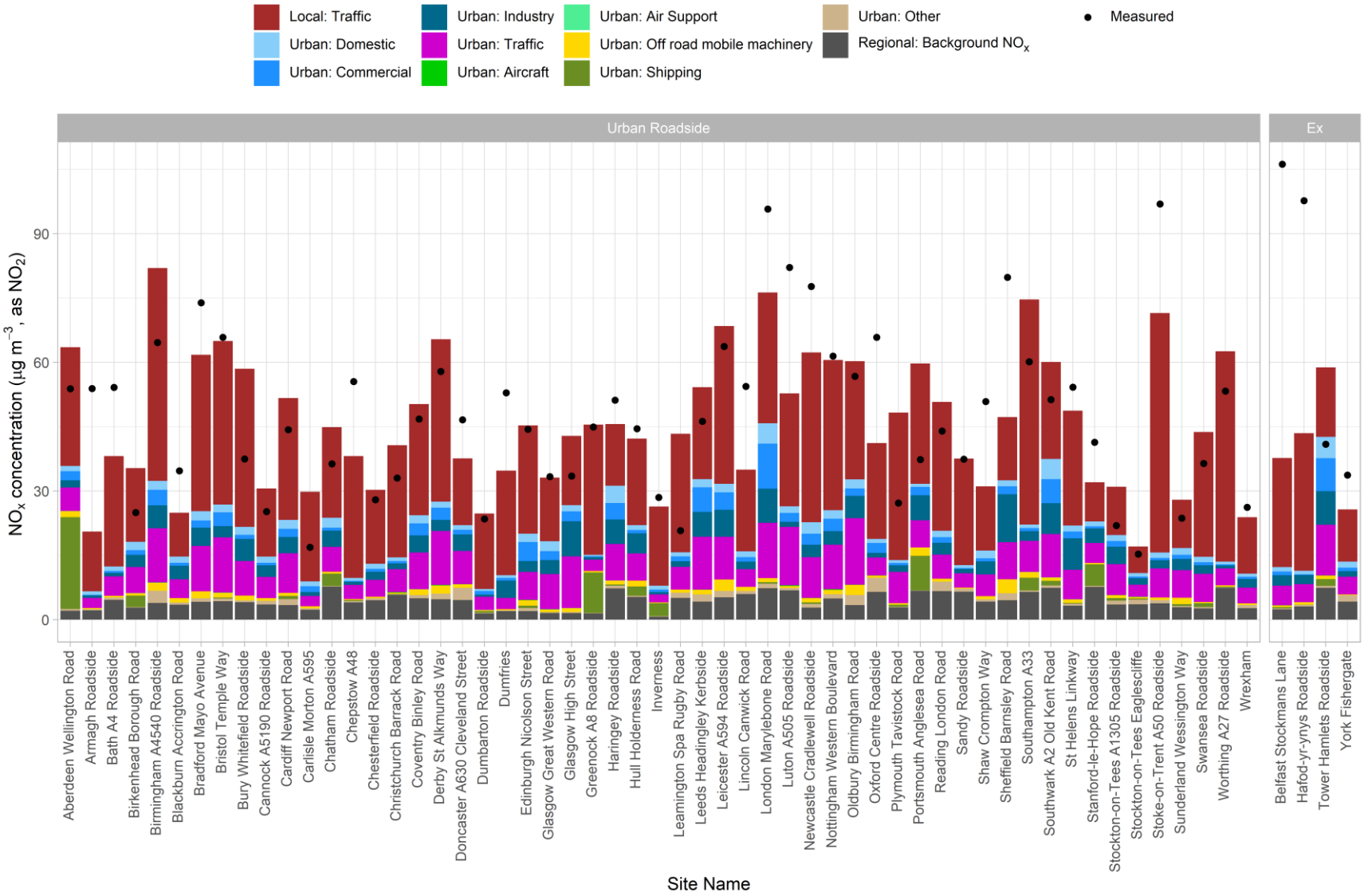

4 SO_2

4.1 Introduction

4.1.1 Limit values

Two limit values for ambient SO_2 concentrations are set out in the AQSR (*legislation.gov.uk*, 2010) for the protection of human health. These limit values have been in force since 1st January 2005 and are specified as follows:

- An hourly concentration of 350 µg m^{-3}, with 24 permitted exceedances each year
- A 24-hour mean concentration of 125 µg m^{-3}, with 3 permitted exceedances each year.

A critical level for SO_2 for the protection of vegetation has also been specified in the AQSR:

- An annual mean and winter mean concentration of 20 µg m^{-3}.

The critical level is designed to protect vegetation, so it only applies in vegetation areas as defined in the AQSR. The critical level has been in force since 2001.

4.1.2 Annual mean and winter mean modelling

A map of annual mean SO_2 concentrations for 2022 in vegetation areas has been calculated for comparison with the annual mean critical level described above; this map is shown in Figure 4.2. This map has been calculated by removing non-vegetation areas from the background SO_2 annual mean map and calculating the zonal mean of the 1 km x 1 km grid squares for a 30 km x 30 km grid so that it complies with the criteria set out in the AQSR. Mean concentrations on a 30 km x 30 km grid have been used to prevent the influence of any urban area appearing unrealistically large on adjacent vegetation areas. Thus, the modelled concentrations in vegetation areas should be representative of approximately 1000 km^2 as specified in the AQSR for monitoring sites used to assess concentrations for the vegetation critical level.

A map of winter mean SO_2 concentrations for the period October 2021 to March 2022 has also been calculated for comparison with the winter mean critical level and is shown in Figure 4.3. This map was calculated by multiplying the annual mean map for 2022 by the ratio between the average concentration measured at rural SO_2 monitoring sites during the 2021-2022 winter period and the annual concentration for 2022.

4.1.3 Modelling for comparison with the hourly and 24-hour limit values

Maps of the 99.73 percentile of the hourly mean and the 99.18 percentile of the 24-hour mean SO_2 concentrations have been calculated for 2022. They are shown in Figure 4.4 and Figure 4.5 respectively. These percentile concentrations correspond to the number of allowed exceedances of the 1-hour and 24-hour limit values for SO_2 described above.

4.1.4 Overview of the PCM model for SO_2

Figure 4.1 shows a simplified flow diagram of the PCM model for SO_2. A summary of the PCM model method, input, and assumptions for SO_2 is presented in Table 4.1.

Figure 4.1 - Flow diagram for PCM SO_2 model

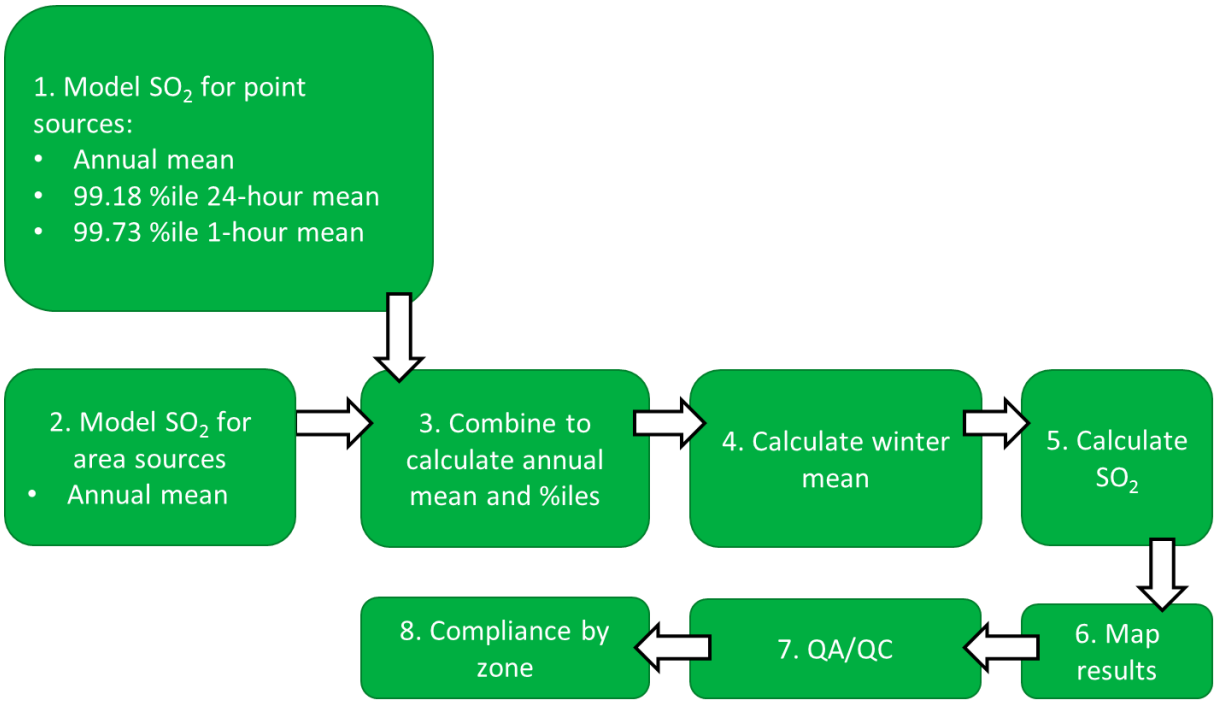

Table 4.1 - PCM model method, input and assumptions summary for SO_2

Heading	Component	Details
General	Pollutant	SO_2
	Year	2022
	Locations modelled	Background
	Metric	Annual mean Winter Mean (2021-2022) 99.18 percentile daily mean 99.73 percentile hourly mean
Input data	Emission inventory	NAEI 2021 (scaled to 2022)
	Energy projections	Energy Projections 2022
	Road traffic counts	2022 (scaled from 2021 where not available)
	Road transport activity projections	DfT (2022) car sales projections, TfL fleet projections for London (2023)
	Road transport emission factors	COPERT 5.4 (COPERT 5.4, 2020)
	Measurement data	2022
	Meteorological data	WRF (see Appendix 4 – WRF meteorology)
Model components	Regional	Constant derived from (Abbott & Vincent, 2006)
	Large point sources	384 sources modelled using ADMS 5.2
	Small point sources	PCM small points model
	ETS point sources	PCM small points model
	Large ETS point sources	80 sources modelled using ADMS 5.2
	Area sources	PCM dispersion kernels generated using ADMS 5.2. Time varying emissions for road transport and domestic sources. PCM small points model for industrial combustion emissions.
	Roadside increment	n/a

Heading	Component	Details
Calibration	Model calibrated?	No
	Number of background stations in calibration	n/a
	Number of traffic stations in calibration	n/a
Pollutant specific	Annual mean	Modelled directly
	Winter mean	Calculated from annual mean using scaling factor derived from ambient measurements at rural monitoring stations
	99.18 percentile daily mean	Maximum of values calculated by scaling and combining annual mean components or scaling and combining annual and percentile components
	99.73 percentile hourly mean	Maximum of values calculated by scaling and combining annual mean components or scaling and combining annual and percentile components

4.1.5 Outline of annual mean and winter mean modelling

The 1 km x 1 km annual mean background SO_2 concentration map has been calculated by summing the contributions from:

- Large point sources
- Small point sources
- Point sources with emissions estimates for air quality pollutants based on reported carbon emissions (ETS points)
- Local area sources
- Distant sources

The contributions from each of the above components were modelled as described in Section 4.3.1.

4.1.6 Outline of modelling for comparison with the hourly and 24-hour limit values

The 1 km x 1 km percentile SO_2 concentration maps have been calculated by combining the contributions from the same list of sources as for the annual mean modelling. Details of the method can be found in Section 4.3.2.

4.1.7 Chapter structure

This chapter describes modelling work carried out for 2022 to assess compliance with the SO_2 limit values and critical levels described above. Emission estimates for SO_2 are described in Section 4.2. Section 4.3.1 describes the SO_2 modelling methods for the annual and winter means. Section 4.3.2 describes the SO_2 modelling methods for the percentile metrics (for comparison with the hourly and 24-hour limit values). Model verification and source apportionment information are presented in Section 4.4.

Figure 4.2 - Annual mean SO_2 concentration, 2022 (µg m^{-3}) in vegetation areas

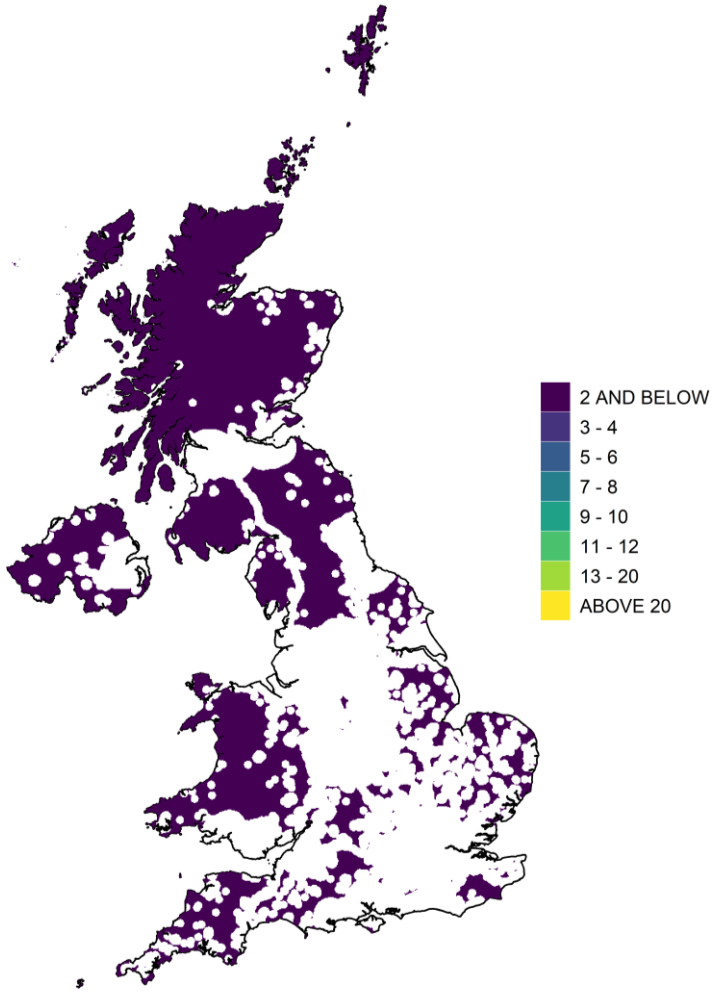

Figure 4.3 - Winter mean SO_2 concentration, 2021-2022 (µg m^{-3}) in vegetation areas

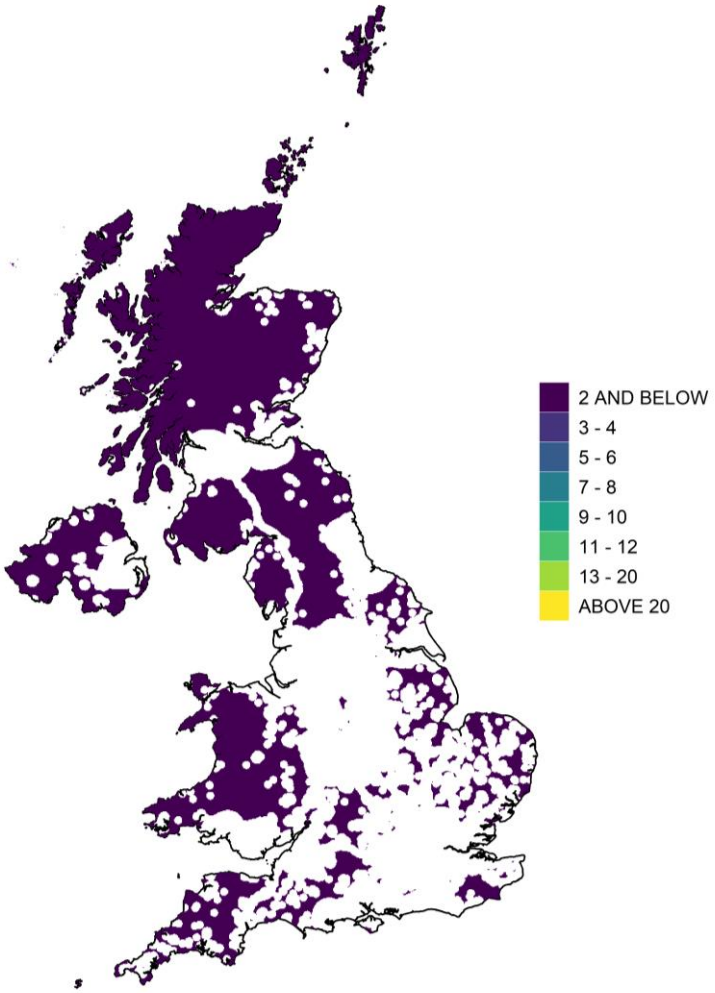

Figure 4.4 - 99.73 percentile of 1-hour mean SO_2 concentration, 2022 (µg m^{-3})

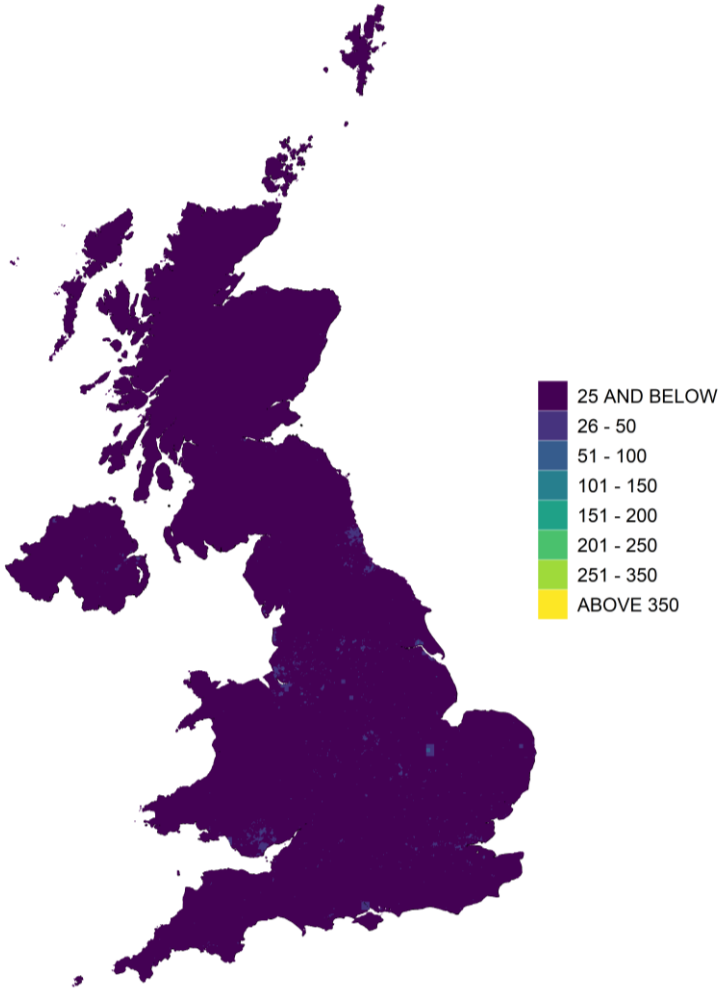

Figure 4.5 - 99.18 percentile of 24-hour mean SO_2 concentration, 2022 (µg m^{-3})

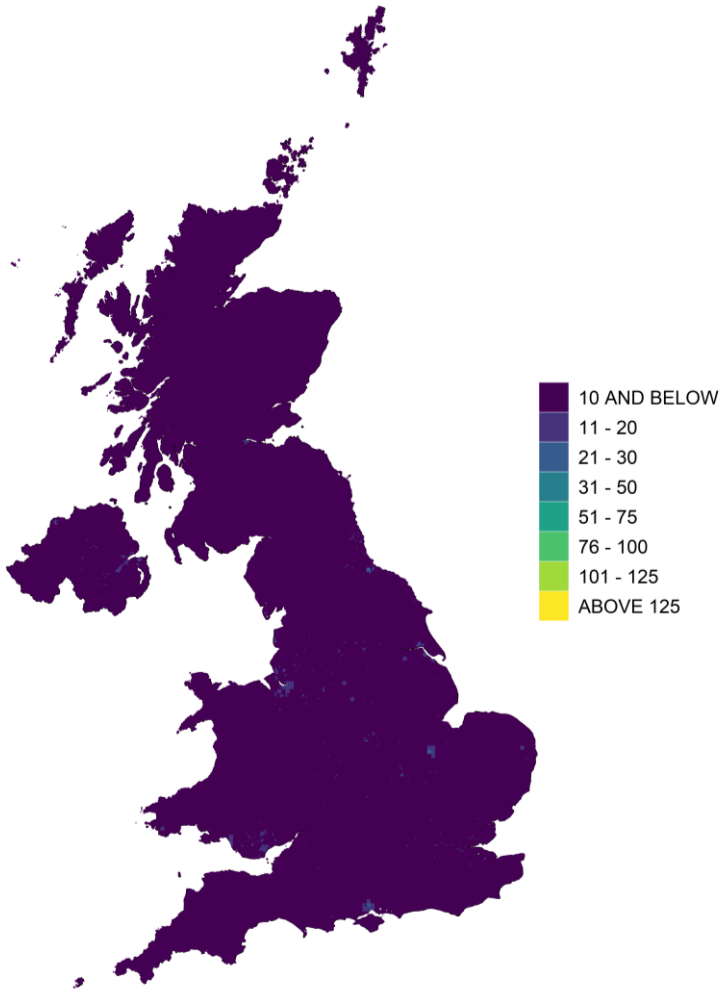

4.2 SO_2 emissions

Estimates of the emissions of SO_2 from the UK National Atmospheric Emissions Inventory 2021 (NAEI 2021) have been used in this study (Ingledew *et al.*, 2023). Emissions projections have been provided by the NAEI (Personal communication from Ben Pearson, 2023) based on BEIS EEP 2022 energy and emissions projections (BEIS, 2022). Emissions have been projected to 2022 from 2021.

Figure 4.6 shows the UK total SO_2 emissions for 2022, with the coding described in Table 3.2. The figure shows that SO_2 emissions in 2022 are dominated by three main sources:

- Combustion point sources (SNAP codes 1, 2 and 3) (40%)
- SNAP 2: Domestic combustion (20.4%)
- SNAP 3: Combustion in industry (17.6%)

Figure 4.6 - Total UK SO_2 emissions for 2022 by SNAP code scaled from NAEI 2021

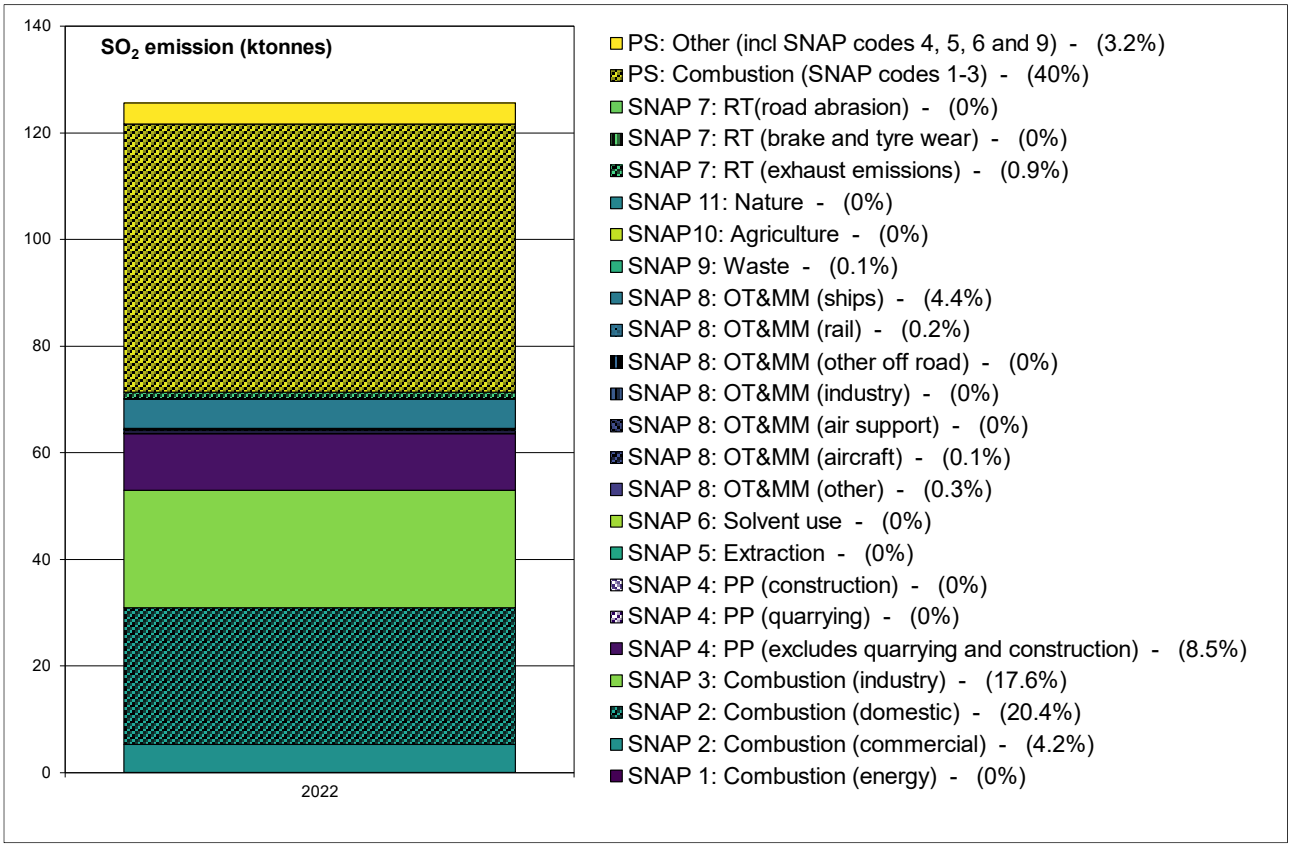

4.3 SO_2 modelling

The modelling methods for SO_2 were developed by (Abbott and Vincent, 1999, 2006). Emissions from point and area sources have been modelled separately and the results combined to produce the concentration maps.

4.3.1 Annual mean and winter mean modelling

4.3.1.1 SO_2 contributions from large and small point sources

Point sources in the NAEI 2021 have been classified as large if they fulfil either of the following criteria:

- Annual SO_2 emissions in the NAEI 2021 are greater than 500 tonnes for any given plant
- Stack parameters are already available for any given plant in the PCM stack parameters database (described in Section 3.3.1)

The contribution to ambient concentrations from large point sources were predicted using the dispersion model ADMS 5.2. Surface roughness varied at both the dispersion and meteorological sites depending on the area type as presented in Table A5.1.

Prior to 2016 the large points modelling for SO_2 used hourly emissions profiles for the power stations with the largest releases provided by the Environment Agency (England and Wales) or Scottish Power (Scotland). However, from 2016 onwards these data are not available because of changes to permit requirements under the Industrial Emissions Directive (IED, 2010). Previously (e.g. (Brookes *et al.*, 2017)) power station with large SO_2 releases for which hourly emissions profiles were not available, were modelled using time varying emissions profiles typical of electricity generation in summer and winter derived from the National Grid Seven Year Statement for 2011 (NETS, 2011). Given the lack of reported emissions profiles, these typical profiles have been applied to treat the time variation in emissions for power stations in the 2022 assessment modelling for SO_2 (Personal communication from Ben Pearson, 2023). The NAEI emissions for point sources for 2021 were scaled in order to provide values for 2022.

Concentrations resulting from emissions from other large SO_2 point sources were modelled using the projected NAEI emissions without time varying emissions. Closure of plant or activities are taken into account when deriving the source sector projection factors by subtracting the base year emissions associated with plant closure from the relevant source sector total for point sources for the NAEI base year. A total of 384 large point sources were modelled using emission release characteristics from the PCM stack parameters database.

Concentrations resulting from the projected emissions from small point sources were modelled using the small point source model described in Appendix 3 – Small point source model. In line with the method applied for the large point sources the NAEI 2021 emissions for small point sources have been scaled to 2022 using the same source sector specific projection factors applied to the large point sources. Any point sources in the NAEI base year which closed before the start or early in the current assessment year are removed from the modelling, based on recommendations from the NAEI team (Personal communication from Ben Pearson, 2023).

The NAEI 2021 includes point source emissions estimates derived from carbon emissions data reported under the EU-Emissions Trading Scheme (ETS), most recently described in (Tsagatakis *et al.*, 2023). These point sources are referred to as ETS points in this report. These derived air quality pollutant emissions are particularly uncertain and therefore in previous assessments (e.g. Brookes et al. (2017)) emissions were capped at reporting thresholds and treated as small point sources. For the 2016, 2017, 2018, 2019, 2020 and 2021 assessment (Brookes *et al.*, 2019b, 2019a, 2020, 2021; Pugsley *et al.*, 2022, 2023) the NAEI recommended treating the ETS points that have emissions greater than the large points modelling threshold as large points and not to apply a cap (Personal communication from Ben Pearson, 2023). The 2022 assessment continues this approach. Thus, based on the criteria for the treatment of large point sources described above, 80 ETS point sources were modelled as an additional set of large point sources (using the approach described above). ETS points that were not classified as large point sources were modelled using the SO_2 small points approach described above.

For the large point sources (including large ETS points), concentrations were predicted for 5 km x 5 km resolution receptor grids within a set of receptor areas (known as tiles), which together cover the UK. The size of the receptor areas was typically 100 km x 100 km, extending out to 150 km where appropriate. All sources within the receptor area and extending out 100 km from the tile border

were assumed to influence concentrations within the receptor area. Concentrations have been modelled using meteorological data for 2022 from the WRF numerical weather prediction modelling system, as described in Appendix 4 – WRF meteorology. The WRF model is a next-generation numerical weather prediction system developed by the US National Centre for Atmospheric Science (NCAR) (UCAR, 2020). This method accounts for spatial variation in meteorological parameters across the UK representing local dispersion characteristics within the PCM output. This approach ensures that the combined impact of several sources on ambient high percentile concentrations is estimated correctly. While not essential for the estimation of the annual mean, this method enables both the annual mean and high percentiles to be calculated from the same set of dispersion model calculations.

4.3.1.2 SO_2 contributions from local area sources

The 2022 area source SO_2 emissions maps have been calculated from the NAEI 2021 emissions maps following the method described in Section 3.3.5. Except for SNAP sector 3 (combustion in industry), the contribution to ambient SO_2 concentrations from area sources was calculated using a dispersion kernel approach. Concentrations are predicted for a 1 km x 1 km receptor grid, from the area source emissions within a 33 km x 33 km square surrounding each receptor. Dispersion kernels were calculated using ADMS 5.2 and hourly sequential meteorological data for 2022 from the WRF model. Modelling of the area sources is described in more detail in Appendix 5 – Dispersion kernels for the area source model.

Revised methods introduced in the 2012 compliance assessment modelling (Brookes *et al.*, 2013) for modelling the contributions to SO_2 from SNAP 2 (domestic and non-domestic combustion) and SNAP 3 (combustion in industry) area sources were used and have been described in Section 3.3.5.

The use of surrogate statistics for mapping area source emissions sometimes results in unrealistically large concentrations in some grid squares for a given sector. Emission caps have therefore been applied to certain sectors. The emission caps applied are given in Table 4.2.

Table 4.2 - Emissions caps applied to SO_2 sector grids

SNAP code	Description	Cap applied (t/a/km^2)
SNAP 8 (Shipping only)	Other Transport & Mobile Machinery	35

4.3.1.3 Deriving annual and winter mean concentration maps

The point source and area source contributions are summed without calibration, along with an estimate (0.19 µg m^{-3}) of the contribution from the long-range transport of SO_2 sources from continental European sources to derive the annual mean concentration. The long-range transport contribution was derived by a linear least-squares fit between the measured and modelled concentrations (Abbott and Vincent, 2006). The model is not calibrated for SO_2 because modelled values provide a reasonably good fit to measured concentrations and to avoid the risk of overfitting for the high percentile metrics.

The map of winter mean SO_2 concentrations was derived from the annual mean map by multiplying with a factor of 1.0497, which is the ratio between the average concentration measured at rural SO_2 monitoring sites during the 2021-2022 winter periods and annual concentration for 2022.

4.3.2 Modelling percentile concentrations for comparison with the 1-hour and 24-hour limit values

The methodology to produce the percentile maps is based on research on combining concentrations arising from area and industrial sources undertaken for the Environment Agency (Abbott and Vincent, 2006). This methodology aims to derive an estimate of the percentile concentrations at locations distant from the industrial sources. A weighted regression analysis was carried out by Abbott and Vincent, assuming that the variance of the residuals was proportional to the modelled concentration.

The regression model was of the form:

$$c_{measured} = \max \begin{bmatrix} Ac_{modelled\_industrial,\%ile} + 2(c_{modelled\_area} + c_{long\_range})_{annual} \\ 2Ac_{modelled\_industrial,annual} + k(c_{modelled\_area} + c_{long\_range})_{annual} \end{bmatrix}$$

The constant A was obtained from the regression analysis. The background multiplier factor, k, was derived from monitoring data. The factor "2", used to scale the $(c_{modelled\_area} + c_{long\_range})_{annual}$ and $c_{modelled\_industrial,annual}$ components, has been shown to be a robust factor that allows short-term average concentrations to be estimated from modelled annual mean concentrations arising from non-industrial

or industrial sources (Abbott, Stedman and Bower, 2005). Table 4.3 presents the *A* and *k* factors used in the derivation of the maps.

Table 4.3 - Factors for percentile models

Metric	Constant (*A*)	Background multiplier factor (*k*)	C_{long_range}
99.73 percentile of 1-hour values	1.09	10.1	0.19
99.18 percentile of 24-hour values	1.23	3.3	0.19

The justification for treating industrial point sources and area emissions separately is because peaks in high percentile modelled contributions from point sources may not coincide with peaks in high percentile background concentrations – a problem that is more pronounced in emissions from large industrial point sources because the meteorological conditions that give rise to high concentrations from tall stacks can be very different from those that produce high concentrations from emissions at low level.

An alternative method was used to derive the high percentile concentrations in Northern Ireland. This was required because area sources, predominately emissions from domestic solid and liquid fuel use, make a more significant contribution to observed high percentile concentrations in Northern Ireland than in the rest of the United Kingdom. Additionally, the smaller number of point sources in Northern Ireland means that these sources make a much smaller contribution to the observed high percentile concentrations.

Maps of high percentile concentrations in Northern Ireland have been calculated from the mapped annual mean SO_2 concentrations using a linear least-squares fit between measured annual mean and measured high percentile concentrations in Northern Ireland over the period from 2008 to 2022 at AURN National Network and Ricardo Calibration Club monitoring sites. Over ten years of data have been used to enable the calculation of robust estimates. Figure 4.7 and Figure 4.8 show the relationship between the annual mean and the 99.73 percentile of 1-hour mean values and the 99.18 percentile of 24-hour mean values at the sampling sites in Northern Ireland.

The equations used to derive the high percentile maps are:

Predicted 99.73%ile in Northern Ireland = 8.5779 × Modelled Annual Mean + 1.4799 µg m^{-3}, and

Predicted 99.18%ile in Northern Ireland = 4.2558 × Modelled Annual Mean + 0 µg m^{-3}.

Figure 4.7 - Relationship between mean concentration and 99.73 percentile of 1 hour concentrations at sampling sites in Northern Ireland, 2008-2022

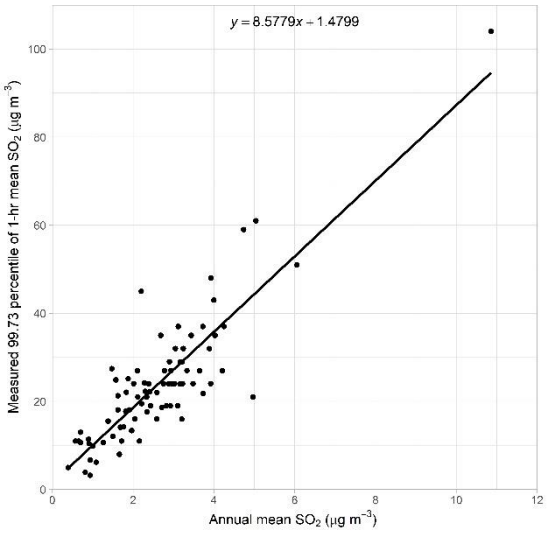

Figure 4.8 - Relationship between mean concentration and 99.18 percentile of 24-hour concentrations at sampling sites in Northern Ireland, 2008-2022

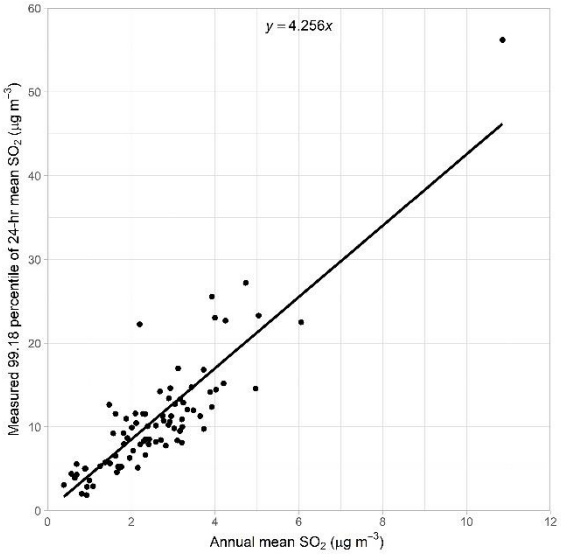

4.4 Results

4.4.1 Verification of mapped

Figure 4.9, Figure 4.10 and Figure 4.11 show comparisons of modelled and measured annual mean, 99.73 percentile of 1-hour mean and 99.18 percentile of 24-hour mean SO_2 concentrations in 2022 at monitoring site locations in the UK. Both the national network sites and the verification sites are shown. Lines representing y = x – 30 % and y = x + 30% or y = x – 50 % and y = x + 50% are also shown (the AQSR data quality objective for modelled annual mean and percentile SO_2 concentrations respectively – see Section 1.5). The 'National Network Sites' include AURN sites and (for annual means only) Acid Gases and Aerosols Monitoring Network (AGANet) sites. 'Verification sites' include ad-hoc monitoring sites and Ricardo Calibration Club monitoring sites. A complete list of the AURN sites used is presented in Data flow C of the e-Reporting submission for 2022 (*UK-Air*, 2023). Details of other verification sites are presented in Table A1.2 of Appendix 1 - Monitoring sites used to verify the mapped estimates which also includes sites maintained by Hanson Building Products Ltd.

Figure 4.9 – Verification plot for 2022 annual mean SO2 concentrations

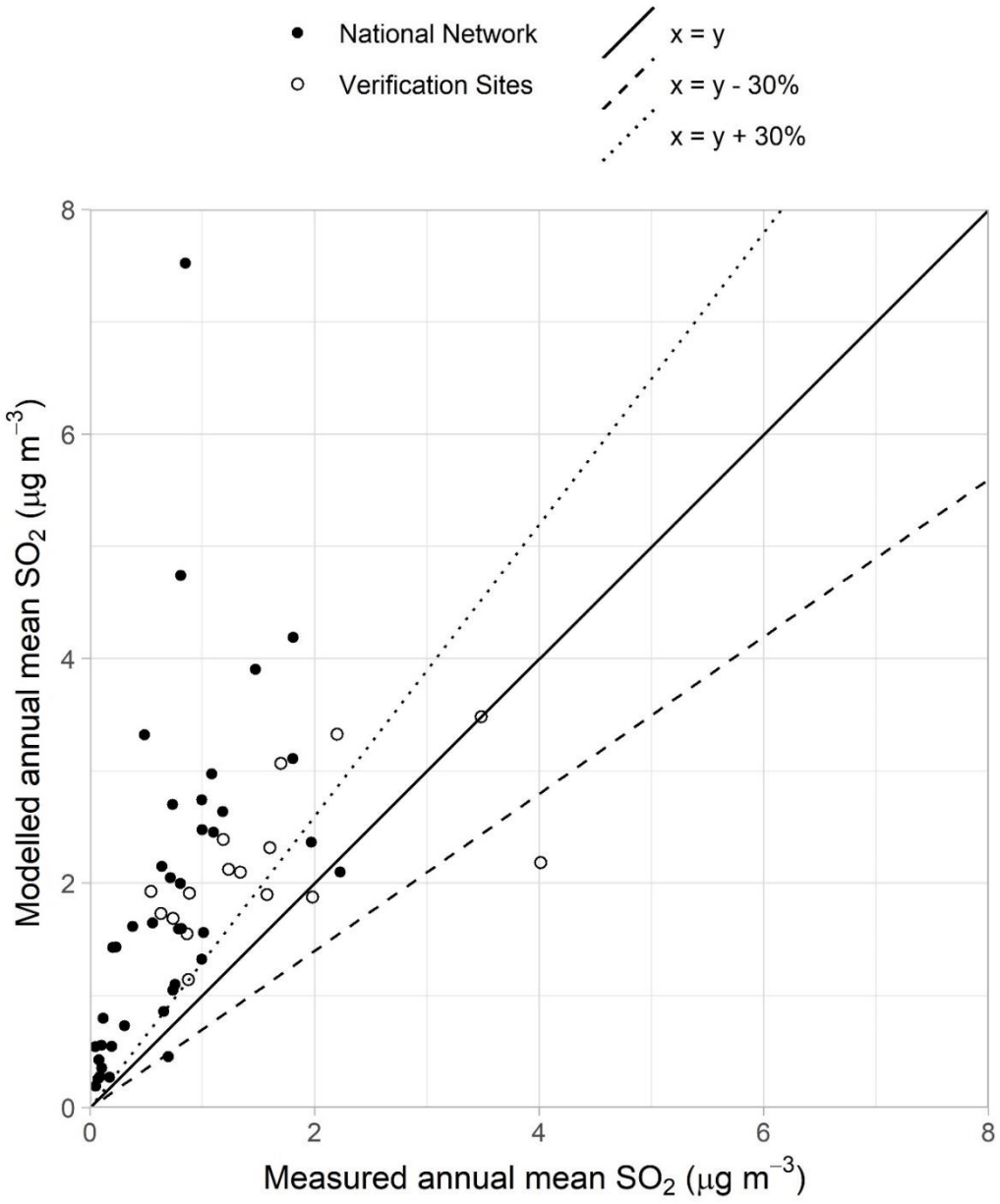

Figure 4.10 - Verification plot for 2022 99.73 percentile of 1-hour mean SO2 concentrations

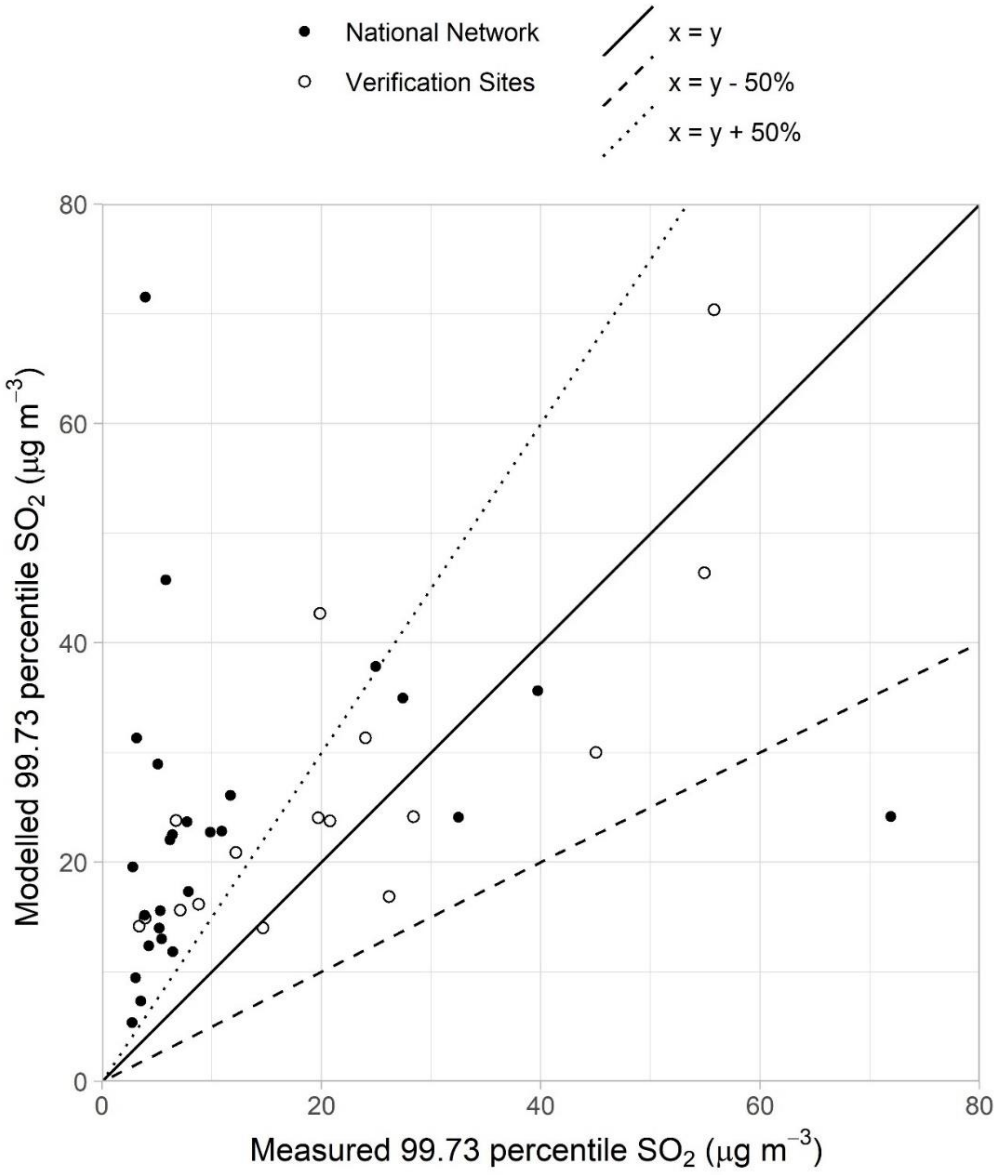

Figure 4.11 - Verification plot for 2022 99.18 percentile of 24-hour mean SO2 concentrations

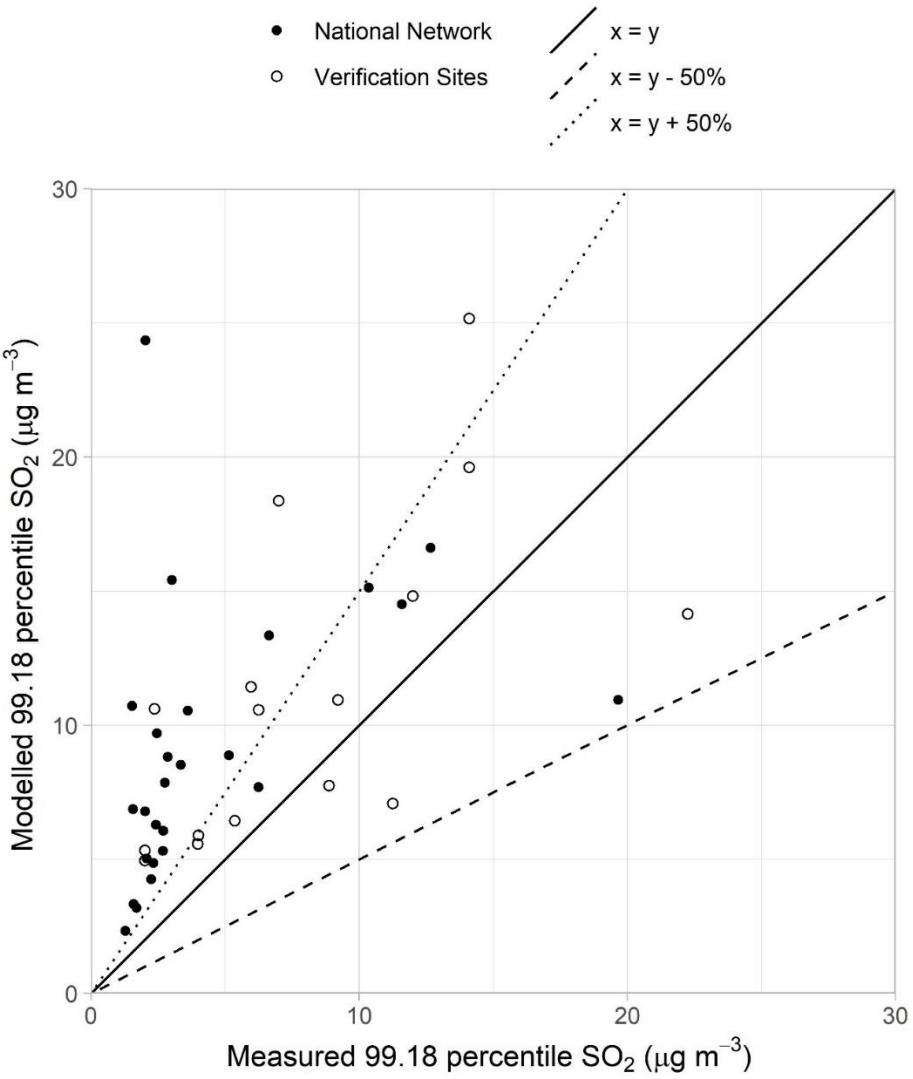

Summary statistics comparing modelled and measured SO_2 concentrations for annual mean, 99.73 percentile of hourly values and 99.18 percentile are listed in Table 4.4, Table 4.5 and Table 4.6, respectively.

Overall the models tend to overpredict the measured concentration metrics at the majority of the monitoring sites. For the National Network (comprising sites belonging to the combined the AURN and AGANet networks) the measured annual average concentration over all these sites (0.79 µg m^{-3}) did not compare favourably with the modelled concentrations predicted at the same sites (2.03 µg m^{-3}). Only about 15% of the sites fell within the DQO. Reasons for poor performance may include very local emission sources not adequately represented in the emission inventory. However, despite the poor agreement, it should be noted that both the measurements and modelled estimates are significantly below the limit values for all metrics. Note that the 1 km x 1 km grid annual mean map is not compared directly with the annual mean limit value; the zonal mean of the 1 km x 1 km grid squares in vegetation areas has been calculated for a 30 km x 30 km grid, as discussed above.

For the 99.73 percentile of 1-hour mean concentrations and the 99.18 percentile of 24-hour mean concentrations there is again reasonable agreement between measured and modelled means at the AURN sites and verification sites. Due to the more generous data quality objectives for the short-term percentile concentrations, fewer sites, as expected, will fall outside the DQO limits.

Table 4.4 - Summary statistics for comparison between modelled and measured annual mean concentrations of SO_2 at background sites

	Mean of measurements ($\mu g\ m^{-3}$)	Mean of model estimates ($\mu g\ m^{-3}$)	R^2	% of sites outside DQO of ±30%	Number of sites in assessment
National Network[a]	0.72	1.85	0.31	95%	40
Verification Sites	1.55	2.17	0.35	81%	16

a includes measurement data from sites in Defra's AURN and AGANet

Table 4.5 - Summary statistics for comparison between modelled and measured 99.73 percentile of 1-hour mean concentrations of SO_2 at background sites

	Mean of measurements ($\mu g\ m^{-3}$)	Mean of model estimates ($\mu g\ m^{-3}$)	R^2	% of sites outside DQO of ±50%	Number of sites in assessment
National Network[b]	12.23	23.66	0.04	88%	26
Verification Sites	21.96	26.83	0.64	44%	16

b includes measurement data from sites in Defra's AURN only

Table 4.6 - Summary statistics for comparison between modelled and measured 99.18 percentile of 24-hour mean concentrations of SO_2 at background sites

	Mean of measurements ($\mu g\ m^{-3}$)	Mean of model estimates ($\mu g\ m^{-3}$)	R^2	% of sites outside DQO of ±50%	Number of sites in assessment
National Network[c]	4.48	9.13	0.18	81%	26
Verification Sites	8.17	11.17	0.38	44%	16

c includes measurement data from sites in Defra's AURN only

4.4.2 Source apportionment

Figure 4.12 shows the source apportionment for modelled annual mean concentrations of SO_2 at AURN monitoring sites for 2022. Measured annual mean concentrations at each site are shown for reference. The figure shows that annual mean SO_2 concentrations at most sites are dominated by contributions from industrial emissions treated as either point sources or area sources. Some sites also have significant contributions from shipping and domestic sources of emissions.

Figure 4.12 - Annual mean SO_2 source apportionment at AURN monitoring sites in 2022 (the area type of each site is shown in parenthesis after its name – see Table 3.5)

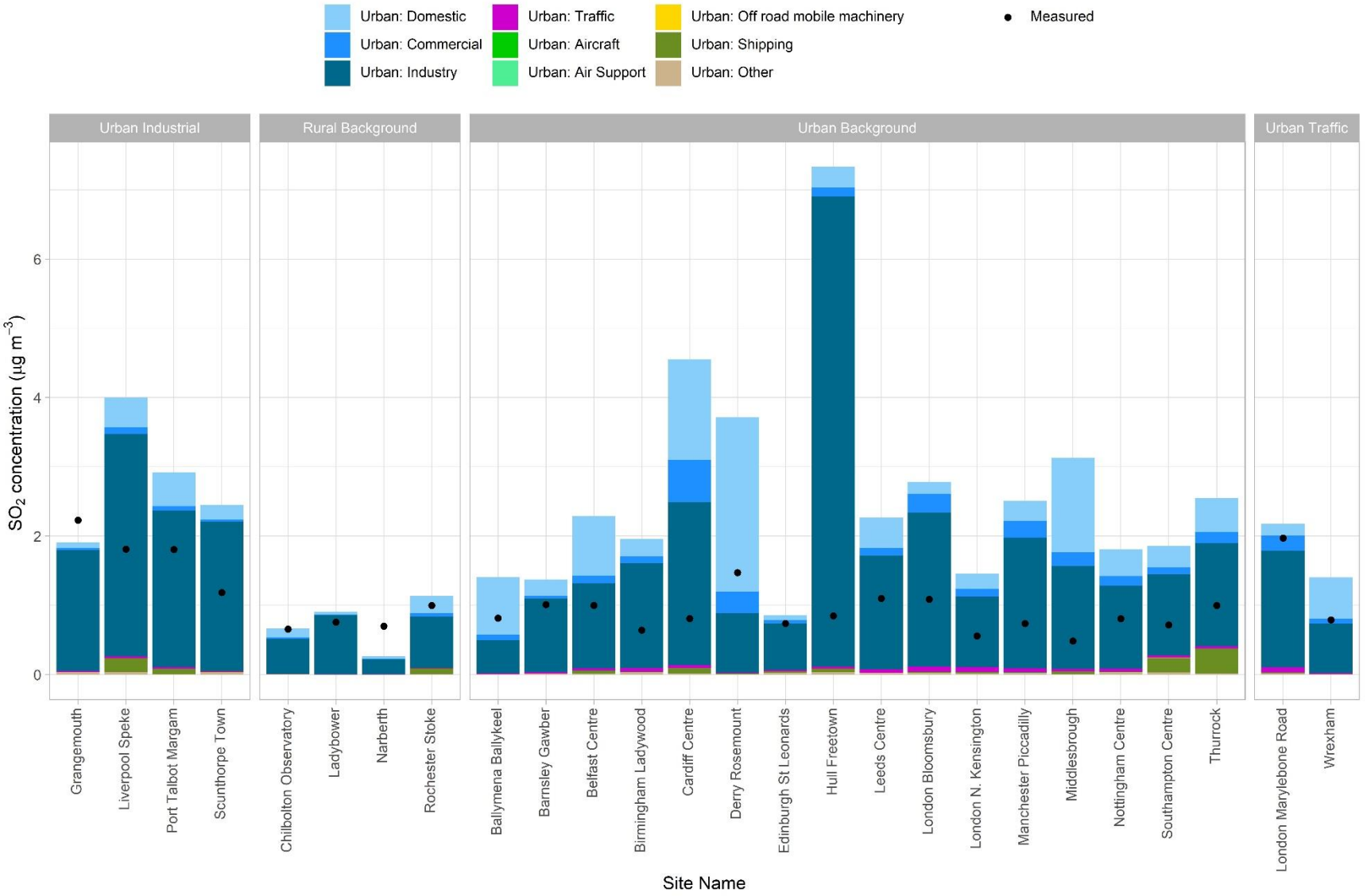

5 PM_{10}

5.1 Introduction

5.1.1 Limit values

Two limit values for ambient PM_{10} concentrations are set out in the AQSR (*legislation.gov.uk*, 2010). These have been specified for the protection of human health and came into force from 01/01/2005. These limit values are:

- An annual mean concentration of 40 µg m^{-3}.
- A 24-hour mean concentration of 50 µg m^{-3}, with 35 permitted exceedances each year

Results of the assessment in terms of comparisons of the modelled concentrations with the annual mean and 24-hour mean limit values for PM_{10} have been reported in e-Reporting Data flow G which is published on UK-Air (UK-Air, 2023).

5.1.2 Annual mean model

Maps of annual mean PM_{10} in 2022 at background and roadside locations are shown in Figure 5.1 and Figure 5.2. These maps have been calibrated using PM_{10} measurements within the national network for which co-located $PM_{2.5}$ measurements are also available. The models for PM_{10} and $PM_{2.5}$ are designed to be fully consistent. Each component is either derived from emission estimates for PM_{10} or $PM_{2.5}$ or the contributions to the fine and coarse particle size fractions are estimated separately. This enables us to carry out an additional sense check that the calibration parameters for the two pollutants are reasonably consistent. Measurements from national network sites without collocated $PM_{2.5}$ measurements have been used as an additional verification dataset (and similarly $PM_{2.5}$ sites without PM_{10} have been used as an additional verification dataset for $PM_{2.5}$). Measurements from gravimetric instruments within the national network and from non-national network sites have also been used to verify the mapped estimates. Appropriate scaling factors have been applied prior to comparison where required.

A detailed description of the Pollution Climate Mapping (PCM) models for PM in 2004 has been provided by (Stedman et al., 2007)). The methods used to derive the maps for 2022 are largely the same as was adopted for the 2021 maps described in (Pugsley *et al.*, 2023)

Figure 5.1 - Annual mean background PM_{10} concentration, 2022 (µg m^{-3}, gravimetric)

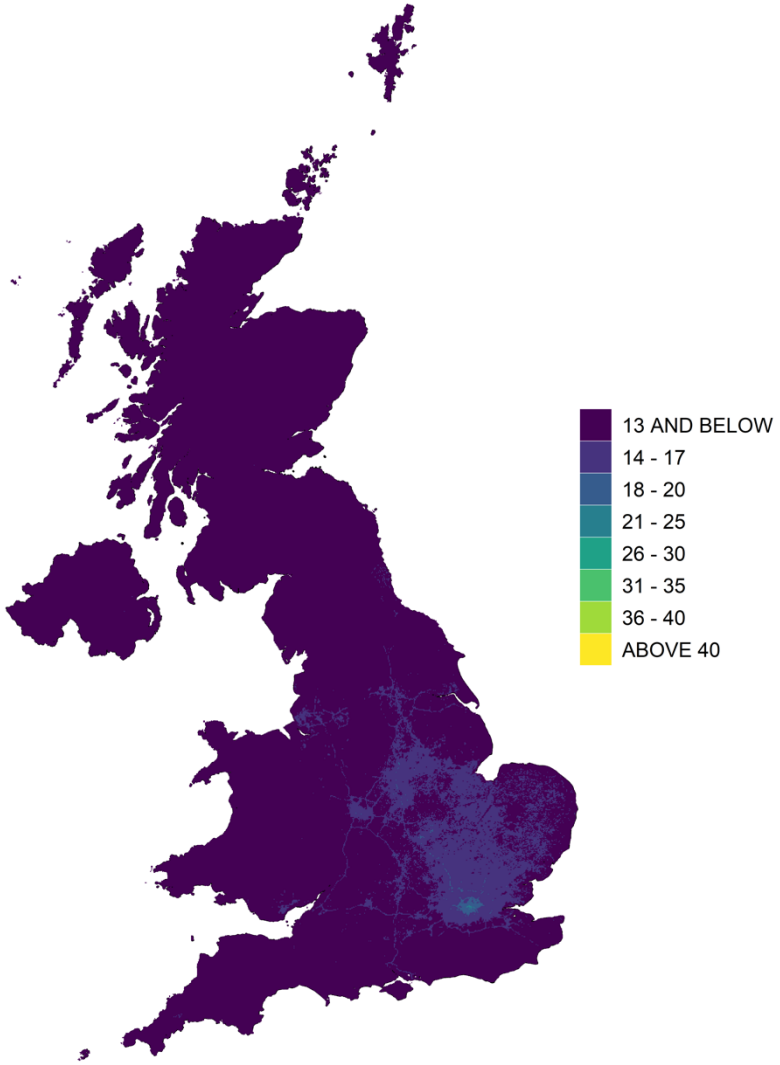

Figure 5.2 - Urban major roads, annual mean roadside PM_{10} concentration, 2022 (µg m^{-3}, gravimetric)

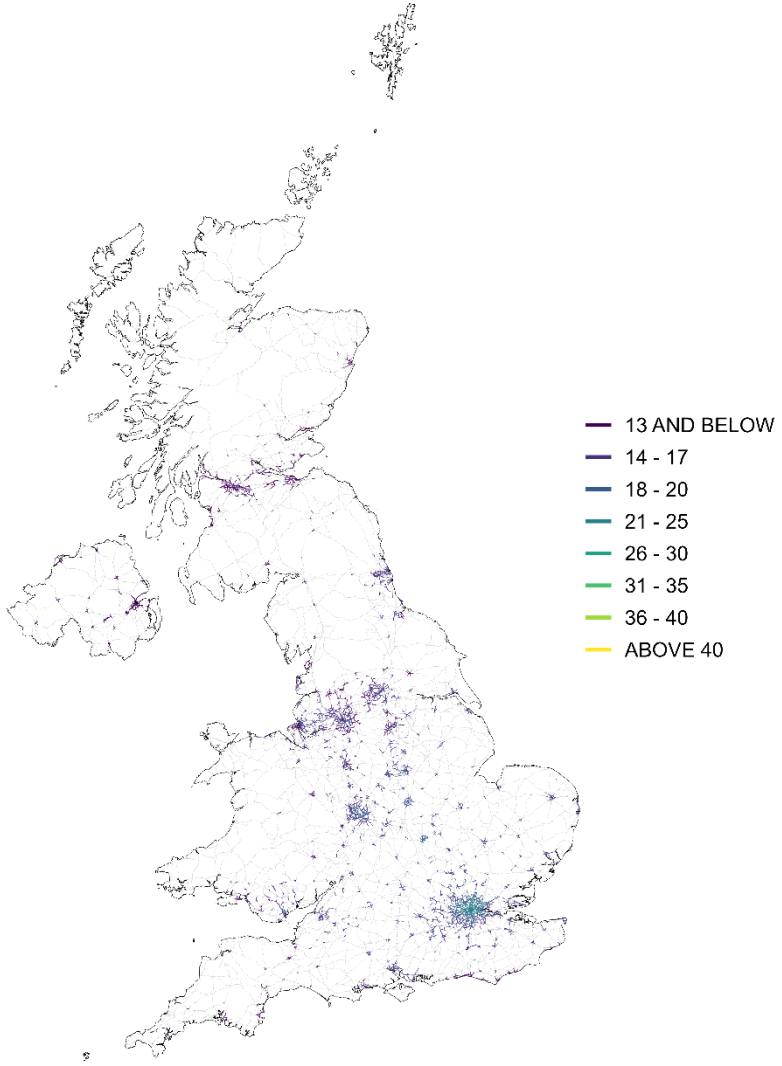

5.1.3 Overview of the PCM model for PM_{10}

Figure 5.3 shows a simplified flow diagram of the PCM model for PM_{10}. A summary of the PCM model method, input, and assumptions for PM_{10} is presented in Table 5.1.

Figure 5.3 - Flow diagram for PCM PM_{10} model

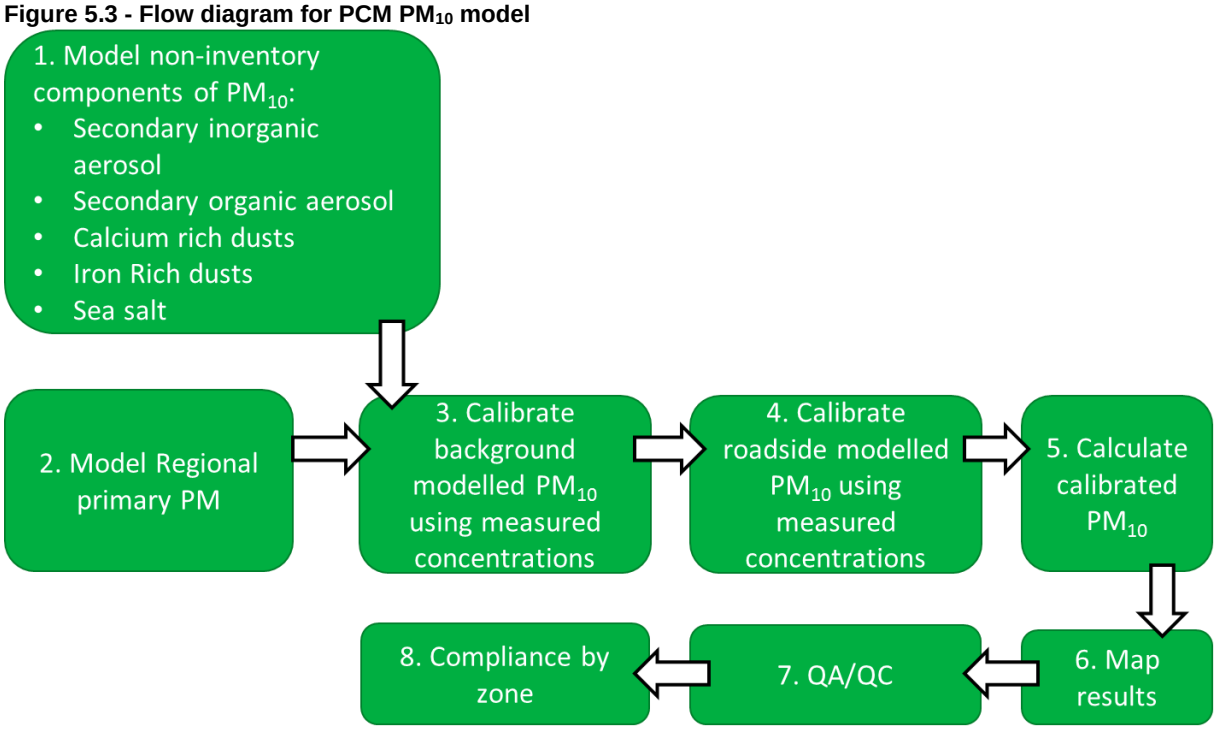

Table 5.1 - PCM model method, input and assumptions summary for PM_{10}

Heading	Component	Details
General	Pollutant	PM_{10}
	Year	2022
	Locations modelled	Background and traffic locations
	Metric	Annual mean
Input data	Emission inventory	NAEI 2021 (scaled to 2022)
	Energy projections	Energy Projections 2022
	Road traffic counts	2022 (scaled from 2021 where not available)
	Road transport activity projections	DfT (2022) car sales projections, TfL fleet projections for London (2023)
	Road transport emission factors	COPERT 5.4 (COPERT 5.4, 2020)
	Measurement data	2022
	Meteorological data	WRF (see Appendix 4 – WRF meteorology)
Model components	Regional	See details under “pollutant specific” heading
	Large point sources	404 sources modelled using ADMS 5.2
	Small point sources	PCM small points model
	ETS point sources	PCM small points model
	Large ETS point sources	85 sources modelled using ADMS 5.2
	Area sources	PCM dispersion kernels generated using ADMS 5.2. Time varying emissions for road transport and domestic sources. PCM small points model for industrial combustion emissions.

Heading	Component	Details
	Roadside increment	PCM Roads Kernel Model using ADMS-Roads 5.0
Calibration	Model calibrated?	Yes
	Number of background stations in calibration	50 (stations with both PM_{10} and $PM_{2.5}$)
	Number of traffic stations in calibration	16 (stations with both PM_{10} and $PM_{2.5}$)
Pollutant specific	Secondary inorganic aerosol	Interpolated from SO_4, NO_3 and NH_4 measurements at a network of 28 rural stations, scaling factors applied for size fraction, bound water and counterions
	Secondary organic aerosol	Results from the NAME model for 2008
	Regional primary particles	Calculated using the TRACK receptor oriented, Lagrangian statistical model
	Regional calcium rich dusts from re-suspension of soils	Modelled using information on land cover (bare soil, root and cereal crops) and dispersion kernel incorporating emissions and dispersion processes
	Regional iron rich dusts from re-suspension	Assigned a constant value of 0.5 µg m^{-3}
	Iron rich dusts from re-suspension due to vehicle activity	Modelled using information on vehicle movements on major roads (HDV) and dispersion kernel incorporating emissions and dispersion processes
	Sea Salt	Interpolated measurements of Cl, scaling factor applied for sea water composition
	Residual	A value assigned based on best fit to PM_{10} and $PM_{2.5}$ measurements: zero, no residual required

5.1.4 Outline of the annual mean model

The maps of annual mean background PM_{10} concentrations have been calculated by summing contributions from different sources:

- Secondary inorganic aerosol (sulphate, nitrate and ammonium, formed in the atmosphere by chemical reactions from gaseous species (SO_2, NO_x and NH_3)
- Secondary organic aerosol (non-volatile organic molecules formed in the atmosphere from volatile organic compounds by chemical oxidation reactions)
- Large point sources of primary particles
- Small point sources of primary particles
- Point sources with emissions estimates for air quality pollutants based on reported carbon emissions (ETS points)
- Regional primary particles
- Area sources related to domestic combustion
- Area sources related to combustion in industry
- Area sources related to road traffic
- Other area sources
- Regional calcium rich dusts from re-suspension of soils
- Regional iron rich dusts from re-suspension
- Iron rich dusts from re-suspension due to vehicle activity
- Sea salt
- Residual (zero)

The concentrations of many of these components have been estimated separately for the fine and coarse fraction. This enables a consistent method to be adopted for estimation of PM_{10} (the sum of the fine and coarse fractions) and $PM_{2.5}$ (fine fractions only). These component pieces are aggregated to a single 1 km x 1 km background PM_{10} grid. An additional roadside increment is added for roadside locations.

The results from the annual mean model can be directly compared with the annual mean limit value in order to carry out the air quality assessment.

5.1.5 Compliance assessment modelling for the 24-hour limit value

24-hour mean concentrations have not been explicitly modelled for comparison with the 24-hour limit value. An annual mean concentration of 31.5 µg m^{-3}, gravimetric has been taken to be equivalent to 35 days with 24-hour mean concentrations greater than 50 µg m^{-3} gravimetric (the 24-hour limit value) for 2022. A modelled annual mean concentration of greater than this value has been taken to indicate a modelled exceedance of the 24-hour mean limit value. This approach was initially proposed by (Stedman, Bush, *et al.*, 2001) who recommended a value of 31.5 µg m^{-3} based on an analysis of monitoring data for the period 1992 to 1999. An analysis of monitoring data (Brookes *et al.*, 2011) showed that the value of 31.5 µg m^{-3} was still valid up to and including 2010. An analysis of monitoring data for 2022 shown in Figure 5.4 showed that this value is appropriate for 2022.

Figure 5.4 - The relationship between the 90th percentile of 24-hour mean PM_{10} concentration and annual mean concentration (µg m^{-3}) for 2022

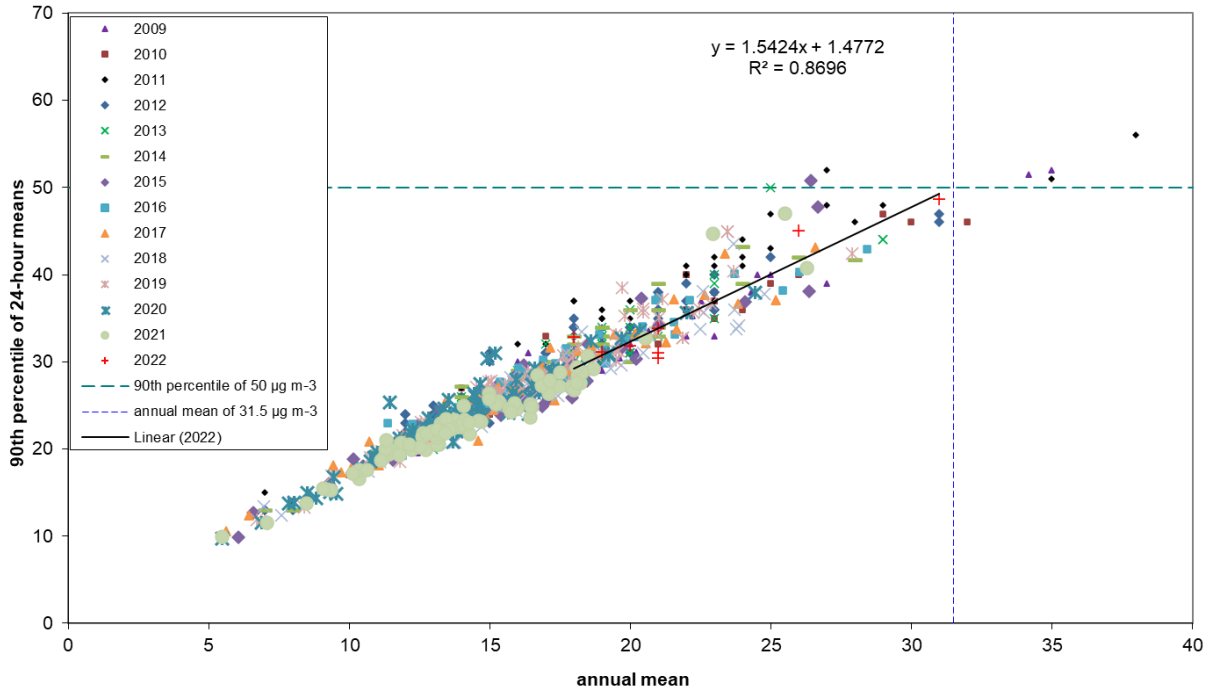

5.1.6 Chapter structure

This chapter describes modelling work carried out for 2022 to assess compliance with the PM_{10} limit values described above. Emission estimates for primary PM are described in Section 5.2, Section 5.3 describes the PM_{10} modelling methods, the modelling results are presented in Section 5.4.The methods used to subtract the contribution from natural sources (sea salt) and the results of this subtraction are presented in Section 5.5.

5.2 PM_{10} emissions

Estimates of the emissions of primary PM from the UK National Atmospheric Emission Inventory 2021 (NAEI 2021) have been used in this study (Ingledew *et al.*, 2023). Emissions projections have been provided by the NAEI (Personal communication from Ben Pearson, 2023) based on BEIS EEP 2022 energy and emissions projections (BEIS, 2022). Emissions have been projected to 2022 from 2021.

Figure 5.5 shows UK total PM_{10} emissions for 2022, with the coding described in Table 3.2. Figure 5.5 shows that PM_{10} emissions in 2022 include contributions from a wide range of different source sectors. The figure shows that PM_{10} emissions in 2022 the largest contributions are from three sources:

- SNAP 4: Production processes - construction (20.7%)
- SNAP 2: Domestic combustion (16.6%)
- SNAP 3: Industrial combustion (11.5%)

The methods used to calculate ambient concentrations from the estimates of primary PM emissions are described below for point, area, road link and regional sources.

Figure 5.5 - Total UK PM_{10} emissions for 2022 by SNAP code scaled from NAEI 2021

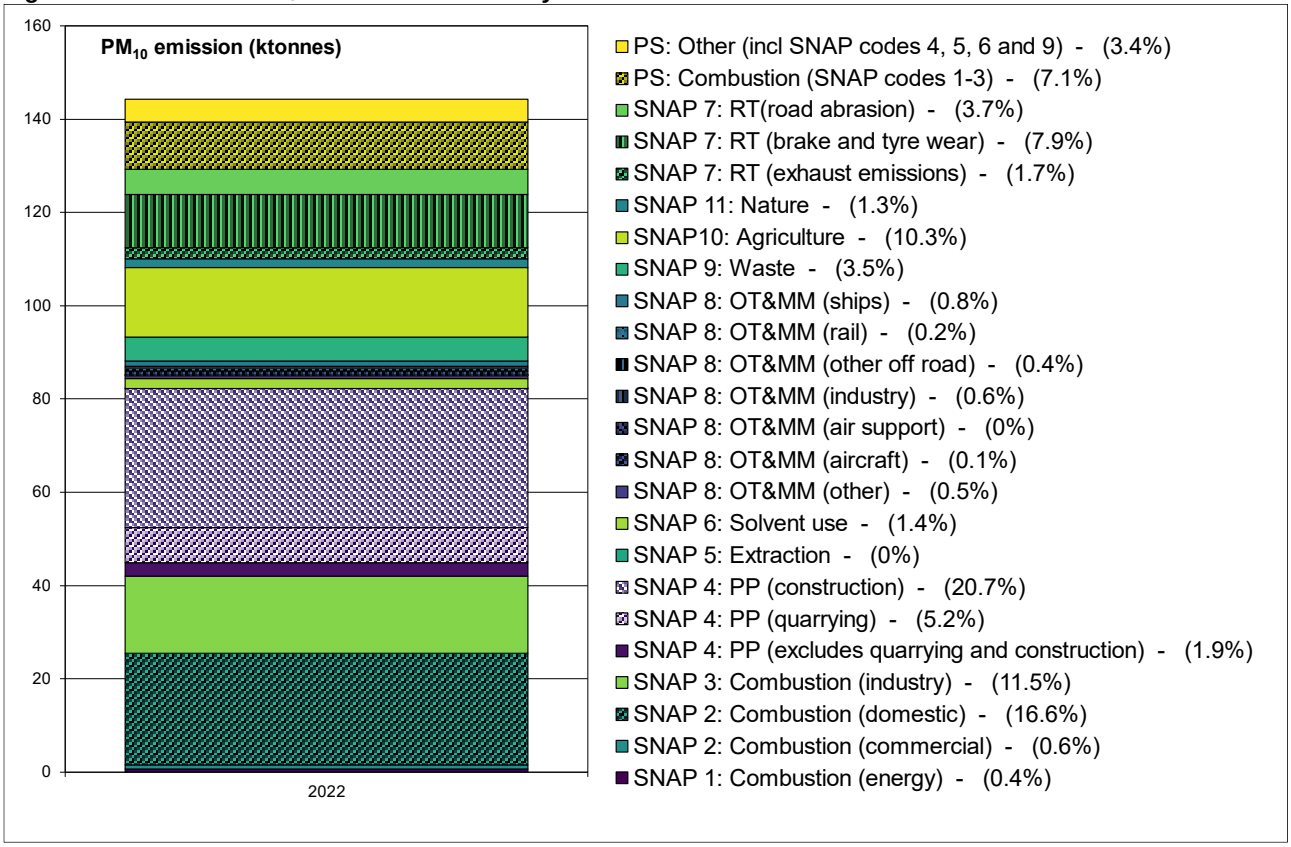

5.3 PM_{10} modelling

5.3.1 Contributions from secondary inorganic aerosol

Maps of secondary inorganic aerosol (SIA) concentrations across the UK have been calculated from rural measurements of sulphate, nitrate and ammonium concentrations by interpolation, followed by the application of scaling factors derived from mass closure modelling. Monthly measurements are available for 28 rural monitoring sites within the UKEAP AGANet and NAMN networks for 2022 (some sites were excluded due to low data capture). The measurement method used within the AGANet was changed at the beginning of 2016. This revised method typically results in higher measured concentrations of sulphate and nitrate (Tang *et al.*, 2015). Concentration surfaces on a 5 km x 5 km grid were calculated from the measurement data using inverse distance weighting (IDW).

These secondary components were then split into fine and coarse using coefficients derived with reference to the detailed PM sampling carried out during the PUMA campaign at the University of

Birmingham urban background monitoring site in June and July 1999 (Harrison and Yin, 2006) and summarised by Kent, Grice, Stedman, Bush, et al. (2007). Fine PM is used to describe $PM_{2.5}$ and coarse PM is used to describe $PM_{2.5-10}$ in this report.

The secondary components were also scaled according to 'bound water' associated with the mass of water embedded within the particles (Air Quality Expert Group (AQEG), 2005). Particle bound water is associated with the hygroscopic anions (Harrison and Yin, 2006). Therefore, a particle bound water scaling factor of 1.279 has been applied to the SIA components to account for the additional mass of water associated with the particulate matter (see Table 5.2). The factor for coarse mode nitrate is higher as this includes the mass of the counter-ion (sodium or calcium).

The split between coarse and fine nitrate was revised for the 2006 modelling assessment with reference to measurement data from the TRAMAQ (Abdalmogith, Harrison and Derwent, 2006) and Birmingham (Harrison and Yin, 2006) studies. The revised method has also been used in this assessment. The split between fine and coarse PM is simple to interpret for most PM constituents but is more complex for nitrate PM because there are two modes. The fine nitrate mode consists of ammonium nitrate, which is volatile, and is all in the fine $PM_{2.5}$ fraction. The coarse mode consists of sodium nitrate, which is split half and half between fine $PM_{2.5}$ and coarse $PM_{2.5-10}$ fractions (Abdalmogith, Harrison and Derwent, 2006). Measurement data from the Birmingham study (Harrison and Yin, 2006) shows that the fine $PM_{2.5}$ nitrate to coarse $PM_{2.5-10}$ ratio was 3.5:1. Thus the fine mode nitrate to coarse mode nitrate ratio was 1.25:1. The factors for nitrate in Table 5.2 have been derived from a combination of this factor of 1.25 and the half and half split of the coarse mode nitrate into the fine $PM_{2.5}$ and coarse $PM_{2.5-10}$ fractions.

Table 5.2 - Scaling factors for size fraction, bound water and counter ion mass for secondary inorganic and organic aerosol

Pollutant	Size fraction	Scaling factor for size fraction	Scaling factor for bound water and counter-ion mass
SO_4	Fine	0.94	1.279
	Coarse	0.06	1.279
NO_3	Fine mode	0.556	1.279
	Coarse mode fine	0.222	1.60
	Coarse mode coarse	0.222	1.60
NH_4	Fine	0.97	1.279
	Coarse	0.03	1.279
SOA	Fine	1.00	1.0
	Coarse	0.0	1.0

5.3.2 Contributions from secondary organic aerosol

Estimates of annual mean secondary organic aerosol (SOA) concentrations in 2008 from the NAME Model on a 20 km x 20 km grid across the UK have been provided by Redlington and Derwent (2013). SOA concentrations are assumed to have remained at 2008 levels in 2022 and this is reasonable because the majority (about 80% as a population-weighted mean) of the SOA is from biogenic sources. NAME is a Lagrangian dispersion model that simulates the dispersion, chemistry and deposition processes occurring in the atmosphere, utilising three dimensional meteorological fields from the Met Office Unified Model (Redlington *et al.*, 2009). The chemistry scheme includes the formation of anthropogenic and biogenic SOA, details of the scheme can be found in Redlington and Derwent (2013). The SOA component has been assumed to fall within the $PM_{2.5}$ fraction.

5.3.3 Contributions from large and small point sources

Contributions to ground level annual mean primary PM concentrations from large point sources (those with annual emission greater than 200 tonnes, or for which emission release characteristics are known) in the NAEI 2021 have been estimated by modelling each source explicitly using the atmospheric dispersion model ADMS 5.2. Concentrations have been modelled using meteorological data for 2022 from the WRF numerical weather prediction modelling system, as described in Appendix 4 – WRF meteorology. The WRF model is a next-generation numerical weather prediction system developed by the US National Centre for Atmospheric Science (NCAR) (UCAR, 2020). This method accounts for spatial variation in meteorological parameters across the UK representing local

dispersion characteristics within the PCM output. Hourly sequential meteorological data for 2022 from WRF was applied. Surface roughness varied at both the dispersion and meteorological sites depending on the area type as presented in Table A5.1. Concentrations were calculated for a 99 km x 99 km square composed of a regularly spaced 1 km x 1 km resolution receptor grid. Each receptor grid was centred on the point source. Point sources were modelled using emission release characteristics from the PCM stack parameters database (described in Section 3.3.1). The NAEI emissions for point sources for 2021 were scaled in order to provide values for 2022.

Contributions from PM point sources with less than 200 tonnes per annum release and for which emission characteristics were not known were modelled using the 'small points' model originally described by (Stedman *et al.*, 2005) and summarised in Appendix 3 – Small point source model. This model consists of separate 'in-square' and 'out-of-square' components, in which concentrations are estimated using dispersion kernels, which have been calculated by using ADMS to model the dispersion of unit emissions from a central source to a grid of receptors at a spatial resolution of 1 km x 1 km squares. In line with the method applied for the large point sources the NAEI 2021 emissions for small point sources of PM have been scaled to 2022 using the same source sector specific projection factors applied to the large point sources.

The NAEI 2021 includes point source emissions estimates derived from carbon emissions data reported under the EU-Emissions Trading Scheme (ETS), most recently described in Tsagatakis et al. (2022). These point sources are referred to as ETS points in this report. These derived air quality pollutant emissions are particularly uncertain and therefore in previous assessments (e.g. Brookes et al. (2017)) emissions were capped at reporting thresholds and treated as small point sources. For the 2016 assessment (Brookes *et al.*, 2019a) the NAEI recommended treating the ETS points that have emissions greater than the large points modelling threshold as large points and not to apply a cap (Personal communication from Ben Pearson, 2023). The 2022 assessment continues this approach. Thus, based on the criteria for the treatment of large point sources described above, ETS point sources were modelled as an additional set of large point sources (using the approach described above). ETS points that were not classified as large point sources were modelled using the PM_{10} small points approach described above.

5.3.4 Contributions from distant sources of primary particles

Contributions from long-range transport of primary particles on a 20 km x 20 km grid have been estimated using the TRACK receptor oriented, Lagrangian statistical model (Lee *et al.*, 2000). Emissions of primary PM_{10} were taken from the NAEI for UK sources and from EMEP (WebDab data, http://www.ceip.at/) for sources in the rest of Europe. Primary PM_{10} was modelled as an inert tracer. All sources within 10 km of the receptor point were excluded from the TRACK model to allow the area source model and the point source model to be nested within this long-range transport model without duplicating source contributions. Scaling factors were applied to calculate emission values applicable to 2022 from 2021 estimates for the UK and from 2020 estimates for the rest of Europe. The 2021 to 2022 factors were derived from the NAEI emissions projections (Personal communication from Ben Pearson, 2023). The 2020 to 2021 factors were derived from the activity scaling factors calculated by (Pugsley et al., 2023).

5.3.5 Iron and calcium rich dusts

5.3.5.1 Introduction

The NAEI does not explicitly include estimates of the emissions of iron or calcium rich dusts. Various process-based or more empirically based methods have therefore been applied to estimate the contribution of these dusts to ambient PM_{10} concentrations across the UK for sources not included in the NAEI.

The contributions have been split into three categories:

- Regional calcium rich dusts from re-suspension of soils
- Regional iron rich dusts from re-suspension
- Iron rich dusts from re-suspension due to vehicle activity

A method for estimating the mass of iron (Fe) and calcium (Ca) rich dusts was included in the modelling method for PM_{10} for the first time in 2006. The PCM models were revised for 2008 to incorporate a more process-based modelling approach for regional calcium rich dusts from re-suspension of soils and iron rich dusts from re-suspension due to vehicle activity. The revised models developed from those proposed by (Abbott, 2008) were also used for this 2022 assessment. The

method for regional iron rich dusts remains largely unchanged and is based on a more empirical approach.

The starting point for the assessment of iron and calcium rich dusts is the measurements of a range of PM components including Fe and Ca reported by (Harrison and Yin, 2006) for three monitoring sites in the Birmingham area. Measurements were made and urban background site (BCCS) from May 2004 to May 2005, an urban roadside site (BROS) from May 2005 to November 2005 and at a rural site about 20 km from the city (CPSS) from November 2005 to May 2006. Measurements were not made at the different sites simultaneously, but the measurement periods were sufficiently long that they can be used to provide reasonable estimates of the urban and roadside increments of various PM components. The measurement data for Fe and Ca are summarised in Table 5.3.

Table 5.3 - Measured concentration of iron and calcium and derived estimates of iron and calcium rich dusts (µg m^{-3})

	CPSS (rural)	BCCS (urban)	Conversion factor	Rural x factor	Urban increment x factor
Fe fine	0.06	0.10	9.0	0.54	0.36
Fe coarse	0.14	0.24	9.0	1.26	0.89
Ca fine	0.03	0.09	4.3	0.13	0.26
Ca coarse	0.12	0.30	4.3	0.52	0.77

Table 5.3 also includes the conversion factors suggested by Harrison et al. (2006) for use within their pragmatic mass closure model. This factor converts the mass of elemental Fe to iron related dusts and the mass of elemental Ca to calcium related dusts. The urban increment in the table has been calculated by subtracting the data for CPSS from that for the urban BCCS site. It is clear that there is an urban increment for both fine and coarse iron and calcium rich dusts. Measurement data for the BROS roadside site indicates that there is a roadside increment on top of the urban increment for Fe but not for Ca. Thus, it is reasonable to assume that the urban increment for iron rich dusts is associated with emissions generated by road traffic but that the urban increment for calcium rich dusts is associated with urban emissions that are not related to traffic activity.

5.3.5.2 Regional calcium rich dusts

The regional concentration of Ca rich dusts was assumed to be a constant value across the UK in the 2006 and 2007 assessments (Kent and Stedman, 2007; Grice *et al.*, 2009). Abbott (2008) developed a method to estimate the ambient concentration of Ca rich PM_{10} dusts resulting from the re-suspension of soils in rural areas. The starting points for this method are the proportion of bare soil, root crops and cereal crops in 1 km x 1 km grid squares across the UK within the Land Cover Map 2000 (2009). The concentration of Ca rich dusts cannot be calculated using the standard approach of using an estimate of the annual emissions and an air dispersion model. This is because the rate of re-suspension and the atmospheric dispersion of these emissions are both dependant on the meteorological conditions. The emission rate will be higher when the wind is stronger, but the dispersion of these emissions will also be more efficient under these conditions.

The method presented by Abbott (2008) makes use of combined emission and dispersion kernels for cereal and root crop fields and for bare soils. Concentrations were calculated for each hour of the year based on hourly sequential meteorological data from twelve sites throughout the UK for 1999. This year was selected because the data were readily available.

The method of Abbott (2008) has been adapted for use within the PCM models by using an inverse distance weighted average of the results from the different kernels for each receptor location. This revised method avoids the discontinuities caused by the use of a simpler nearest meteorological site to the receptor method used in the original work.

Figure 5.6a shows the results for regional Ca rich dusts. The highest concentrations are predicted to be in eastern areas where bare soils, root and arable crops are more common and there is less rainfall. A maximum value for this component has been set as 5 µg m^{-3} within the map. This value has been chosen as an estimate of the maximum likely concentration for a grid square average based on a comparison of this map with available PM_{10} measurements in the locations with the highest predicted contributions.

5.3.5.3 Urban calcium rich dusts

Prior to 2016 an empirical method was used to estimate the urban increment for Ca rich dusts (Brookes *et al.*, 2017). The NAEI for 2021 that has been used for the 2022 air quality assessment modelling includes a revised method for estimating emissions of PM from construction, first introduced in the NAEI for 2016, that results in an increase in the estimate of emissions from this source. The emissions estimates for this source have been multiplied by a factor of 0.6667 in order to achieve mass closure and provide a consistent calibration of the models for PM_{10} and $PM_{2.5}$. This revision means that urban calcium rich dusts are now accounted for within the dispersion modelling and a separate empirically modelled contribution from re-suspension of soils due to urban activity is no longer required.

5.3.5.4 Regional iron rich dusts

A constant value for the regional contribution to Fe rich dusts of 0.5 µg m^{-3} has been applied across the UK. This residual value has been chosen to provide the best fit to the measurements from the Birmingham study (Harrison and Yin, 2006) and available urban background particulate Fe measurements once the estimated contribution from re-suspension due to vehicle movements has been taken into account. Figure 5.6b shows this constant contribution across the UK.

5.3.5.5 Iron rich dusts from re-suspension associated with vehicle movements

The assessments for 2006 and 2007 used an empirical method for the Fe rich dusts associated with re-suspension from vehicle movements based on the use of vehicle km statistics for 1 km x 1 km squares (Grice *et al.*, 2009). Abbott (2008) developed a more process-based approach to estimating this contribution, which takes vehicle km statistics for heavy-duty vehicles (heavy good vehicles and buses) as its starting point. The re-suspension contribution associated with light duty vehicles is expected to be minor compared with that from heavy duty vehicles. These estimates are likely to be subject to greater uncertainty than the estimates for re-suspension from soils because there is little information on the availability of material on road surfaces to be re-suspended.

Abbott (2008) calculated two sets of combined emission and dispersion kernels for each of the 12 meteorological stations for 1999: one to represent rural conditions and one to represent urban conditions. The estimated re-suspension rate was considerably higher for rural conditions due to the higher speeds assumed. These two sets of kernels were then used to calculate the contribution to PM_{10} concentrations according to the proportion of urban and rural land cover in each 1 km x 1 km grid square. A detailed examination of the results from this assessment has shown that the concentrations in urban areas were largely driven by the small proportion of rural land cover in these urban areas. The urban kernels have therefore been chosen to apply to all roads within the PCM model.

Figure 5.6c shows the results for Fe rich dusts from vehicle movements. The highest concentrations are associated with the roads with the highest flows of heavy-duty vehicles. A maximum value for this component has been set as 2.5 µg m^{-3} within the map. This value has been chosen as an estimate of the maximum likely concentration for a grid square average based on a comparison of this map with available PM_{10} measurements in the locations with the highest predicted contributions.

An indication that the method is providing reasonable estimates of the total of Fe rich dusts is provided by Figure 5.7, which shows a comparison of modelled annual mean Fe (the sum of regional and vehicle related Fe) with ambient Fe measurements at non-industrial and non-roadside sites for 2022 from the national metals monitoring network. The modelled estimates are clearly of the correct magnitude and provide a reasonable description of the rural to urban gradients.

Figure 5.6

a) Contribution to PM_{10} from regional Ca rich dusts associated with re-suspension from soils (μg m^{-3})

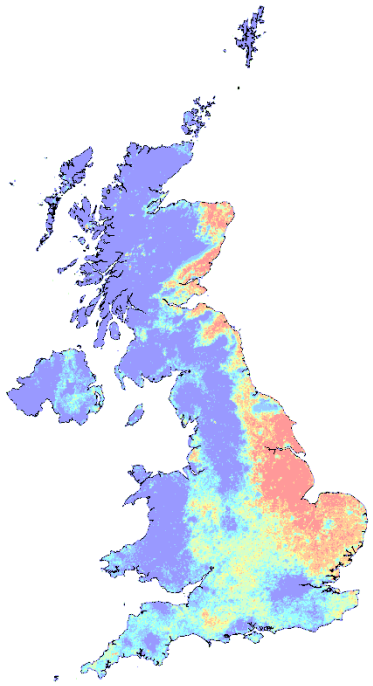

b) Contribution to PM_{10} from regional Fe rich dusts (μg m^{-3})

c) Contribution to PM_{10} from Fe rich dusts associated with vehicle movements (μg m^{-3})

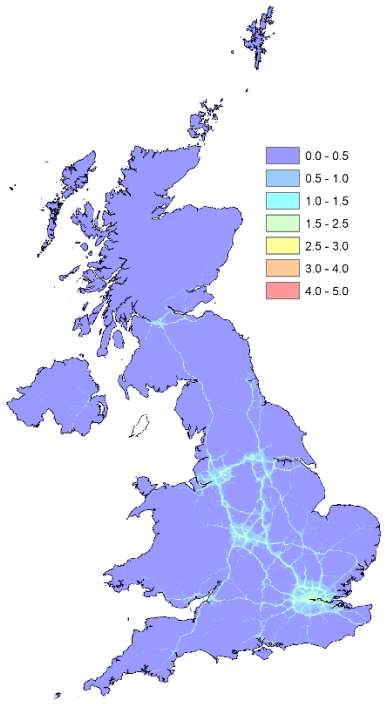

Figure 5.7 - Comparison of modelled and measured annual mean elemental Fe concentrations 2022 (µg m^{-3})

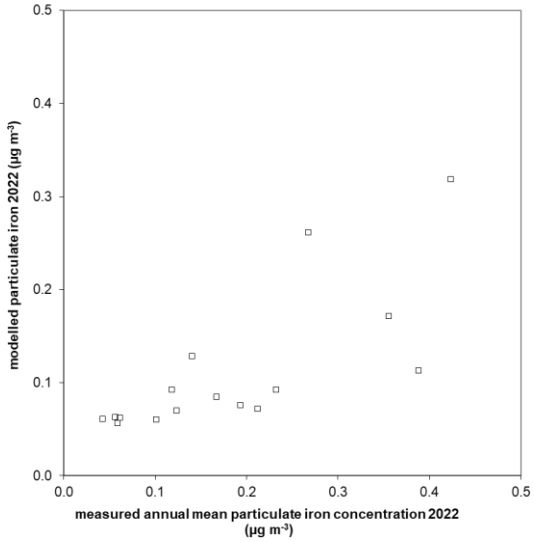

5.3.5.6 Application to the mapping of heavy metal concentrations

Abbott (2008) also suggested a method for estimating the contributions to the ambient concentrations of heavy metals from soil and vehicle related re-suspension processes. Section 10.3 on the modelling of heavy metal concentrations describe how the maps of PM mass from rural re-suspension of soils and re-suspension associated with vehicle movements have been used to estimate the contributions to the ambient concentration of heavy metals using a combination of information on the heavy metal content of soils and enhancement factors.

5.3.6 Sea salt

The contribution to ambient PM from sea salt has been derived directly from measurements of particulate chloride from sites within the UKEAP AGANet for 2022. Data from a network of 28 rural sites were interpolated using inverse distance weighting onto a 5 km x 5 km grid. A scaling factor of 1.648 was applied to convert elemental chloride mass to sodium chloride mass. 73% of the sea salt mass was assumed to be in the coarse fraction and 27% in the fine fraction. This split was derived from measurement data presented by (Airborne Particles Expert Group (APEG), 1999) and Harrison and Yin (2006).

The use of chloride is potentially subject to both positive and negative artefacts. Sea salt is not the only source of particulate chloride in the atmosphere. HCl is emitted from coal burning but reductions in coal use and flue gas abatement are likely to have reduced atmospheric HCl and ammonium chloride concentrations considerably. There will also be loss of chloride from marine aerosol due to reactions with nitric acid. The resulting sodium nitrate PM has been considered to be of anthropogenic origin and the contribution to PM mass from this sodium nitrate is explicitly included in the modelled concentrations presented. If sodium were used as the marker for sea salt rather than chloride, then this sodium nitrate would tend to be included in the natural component.

In addition to selecting chloride as the marker for sea salt, the analysis was simplified by assuming that the sea salt consists of sodium chloride only. Thus, the measured chloride concentration has been scaled by a factor of 1.648. An alternative approach would be to scale by 1.809 to take account of the full composition of sea salt. The composition of sea salt is dominated by chloride and sodium. Other components contributing more than 1% by mass are sulphate, magnesium, calcium and potassium. Sulphate is already explicitly included in the modelled concentrations and a sea salt correction has not been applied to the measured concentrations used in the PCM model. Adding a further sea salt sulphate component would lead to double counting. The other components (magnesium, calcium and potassium) have, in effect, been treated as sodium by the use of a scaling factor of 1.648. The ratio of (chloride + sodium) to chloride in sea salt is 1.552, while the ratio of (chloride + sodium + magnesium + calcium + potassium) to chloride is 1.658. Thus, the simplification of sea salt as pure sodium chloride has not had a large impact on the total mass assumed apart from

the contribution from sea salt sulphate, which, as a simplification, has been included with the rest of the sulphate as anthropogenic.

5.3.7 Contributions from area sources

Figure 5.8 shows the calibration of the area source model. The modelling method makes use of an ADMS derived dispersion kernel to calculate the contribution to ambient concentrations at a central receptor location from area source emissions within a 33 km x 33 km square surrounding each receptor. Hourly sequential meteorological data from WRF in 2022 was used to construct the dispersion kernels, as described in Appendix 5 – Dispersion kernels for the area source model. A total of 50 background monitoring sites within the national network had sufficient data capture for PM_{10} and $PM_{2.5}$ in 2022 to be used to calibrate the model. Only sites with valid data for PM_{10} and $PM_{2.5}$ have been used to calibrate the PM_{10} and $PM_{2.5}$ models, as described in Section 5.1.

Revised methods introduced in the 2011 assessment (Brookes *et al.*, 2012) for modelling the contributions to PM_{10} from SNAP 2 (domestic and non-domestic combustion) and SNAP 3 (combustion in industry) area sources were used and have been described in Section 3.4.5.

The methods used to estimate the spatial distribution of emissions from domestic wood combustion were revised for the NAEI 2015 to incorporate new information from a survey of domestic wood use (BEIS, 2016). The revised spatial distribution places a larger proportion of these emissions in large urban areas than in previous assessments. The activity estimates used to derive the estimates of emissions from domestic wood combustion have been revised downwards, resulting is a lower estimate of emissions in the NAEI 2021 and the NAEI 2020 than in the NAEI 2019. The larger estimate of domestic emissions in the NAEI 2019 provided a better agreement of the dispersion model results with ambient measurements for PM_{10} and $PM_{2.5}$ than the lower estimates from the NAEI 2021 and NAEI 2020 A combination of the spatial distribution from the NAEI 2021 and the application of a scaling factor of 2.3333 to the domestic combustion emissions total was found to provide the best agreement with measurements and calibration coefficients for PM_{10} and $PM_{2.5}$ close to unity.

The NAEI for 2021 that has been used for the 2022 air quality assessment modelling includes a method for estimating emissions of PM from construction that was first introduced in the NAEI for 2016, which has resulted in an increase in the estimate of emissions from this source. The emissions estimates for this source have been multiplied by a factor of 0.6667 in order to achieve mass closure and provide a consistent calibration of the models for PM_{10} and $PM_{2.5}$. This revision means that urban calcium rich dusts are now accounted for within the dispersion modelling and a separate empirically modelled contribution from re-suspension of soils due to urban activity is no longer required.

As part of the calibration process emission caps have been applied to certain sectors; this is because the use of surrogate statistics for mapping area source emissions sometimes results in unrealistically large concentrations in some grid squares for a given sector. The emission caps applied are given in Table 5.4.

With the exception of area sources associated with SNAP sector 3 (combustion in industry), the area source model has been calibrated using ambient PM monitoring data from the UK national networks. The modelled large point and small point source, SIA, SOA, iron and calcium rich dust, long range transport primary PM, sea salt and the residual concentrations have been subtracted from the measured annual mean PM concentration at background sites and compared with the modelled area source contribution to annual mean PM concentration. A residual concentration of zero was found to provide the best fit to the monitoring data for both PM_{10} and $PM_{2.5}$ in 2022.

The modelled area source contribution (excluding SNAP 3) was multiplied by the relevant empirical coefficient to calculate the calibrated area source contribution for each grid square in the country. The area source contribution was then added to the contributions from SNAP 3 area sources, secondary organic and inorganic particles, from small and large point sources, from regional primary particles, from sea salt, from calcium and iron rich dusts and the residual, resulting in a map of background annual mean gravimetric PM_{10} concentrations.

Figure 5.8 - Calibration of PM_{10} area source model 2022 (µg m^{-3}, gravimetric)

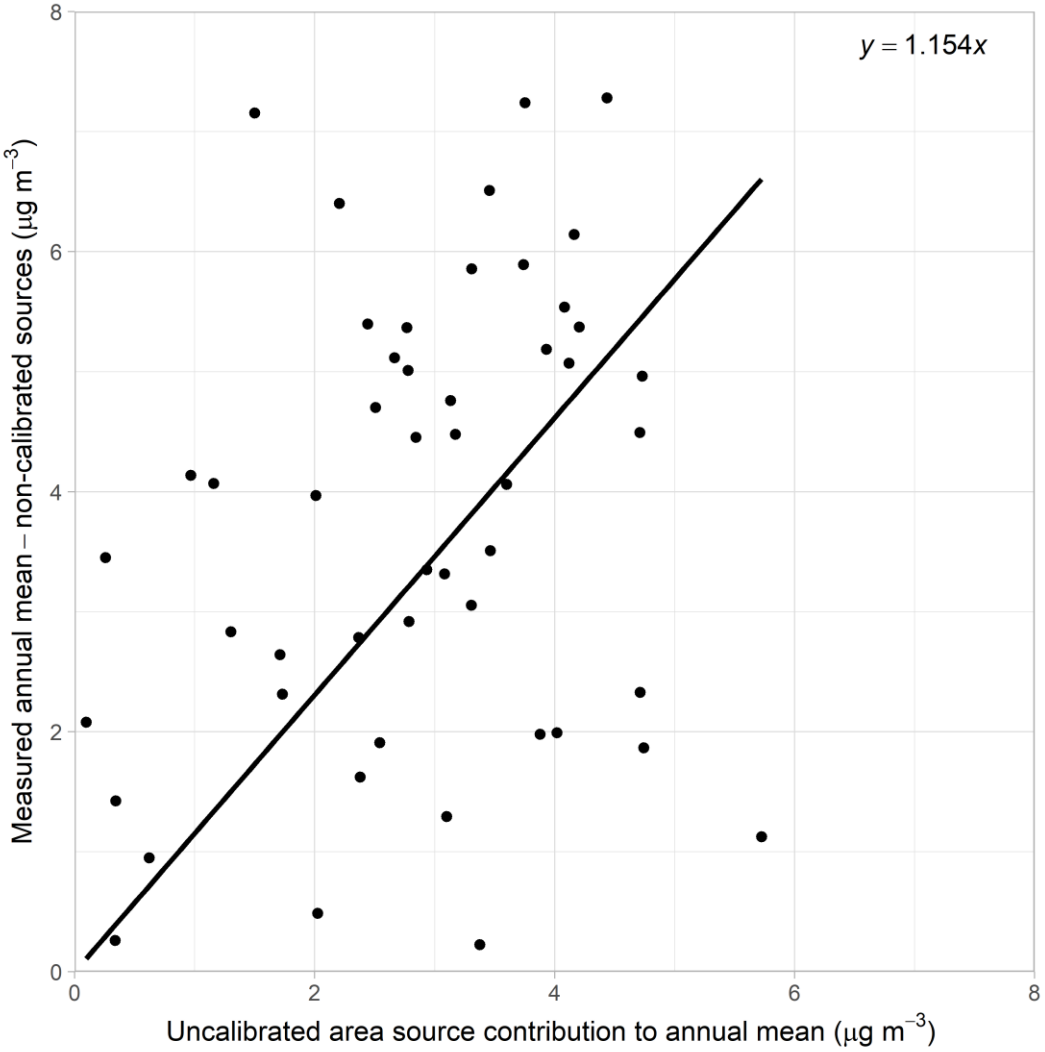

Table 5.4 - Emission caps applied to PM_{10} sector grids

SNAP code	Description	Cap applied (t/a/km²)
SNAP 4 (Production process)	Stockpiles	15

5.3.8 Roadside concentrations

The modelled annual mean concentration of PM_{10} at a roadside location is made up of two parts: the background concentration (as described above) and a roadside increment:

roadside PM_{10} concentration = background PM_{10} concentration + PM_{10} roadside increment.

The NAEI has provided estimates of PM_{10} emissions for major road links in the UK for 2022 (Ingledew *et al.*, 2023). The roadside increment model for PM_{10} has been calibrated using data from monitoring sites with valid data for both PM_{10} and $PM_{2.5}$. The PCM Roads Kernel Model (PCM-RKM) described in Appendix 8 – The PCM Roads Kernel Model has been used to calculate the roadside increment. The PCM-RKM is based upon dispersion kernels generated by the ADMS-Roads dispersion model (v5.0) and represents a more process-based approach than the previous empirical method. It provides a more robust assessment, whilst retaining the link with measurement data provided using AURN measurement data to calibrate this component of the model. Figure 5.9 shows the calibration of this model at roadside monitoring sites. Roadside concentrations for urban major road links (A-roads and motorways) only are reported and included in this report.

Figure 5.9 - Calibration of PM_{10} PCM-RKM model 2022 (µg m^{-3}, gravimetric)

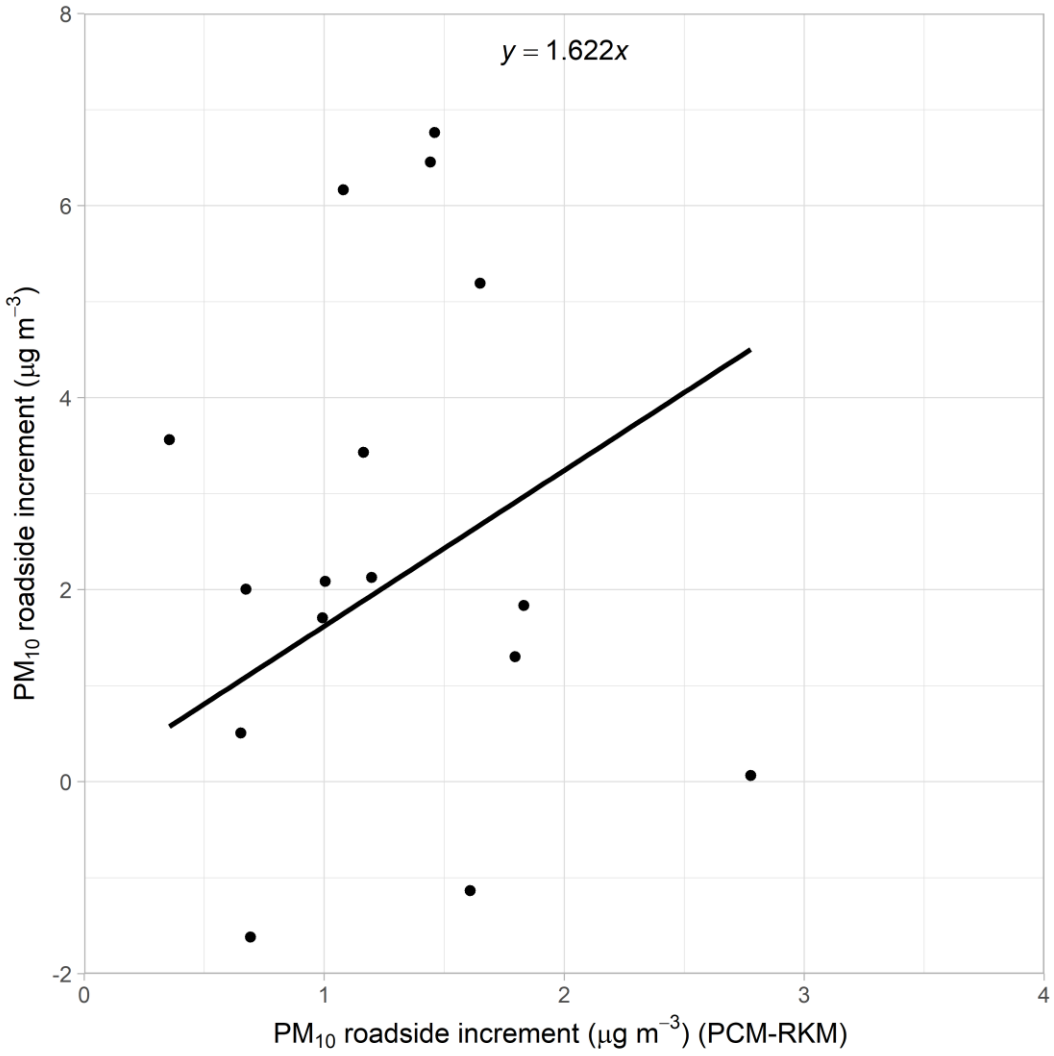

5.4 Results

5.4.1 Verification of mapped values

Figure 5.10 and Figure 5.11 show comparisons of modelled and measured annual mean PM_{10} concentration at background and roadside monitoring site locations. Lines representing y = x – 50 % and y = x + 50% are also shown because 50% is the AQSR data quality objective for modelled annual mean PM_{10} concentrations – see Section 1.5. Summary statistics for the comparison between modelled and measured PM_{10} concentrations are presented in Table 5.5 and Table 5.6.

Four categories of monitoring sites are shown in the graphs. There are some sites in the national network at which only PM_{10} or $PM_{2.5}$ are measured, but not both. These are shown as PM_{10} only sites in the graphs. Sites excluded from the calibration are also shown. TEOM PM_{10} data adjusted using the VCM model (http://www.volatile-correction-model.info/), are available for some verification sites.

The agreement between the measurement data and the modelled values is generally good.

Figure 5.10 - Verification of background annual mean PM_{10} model 2022

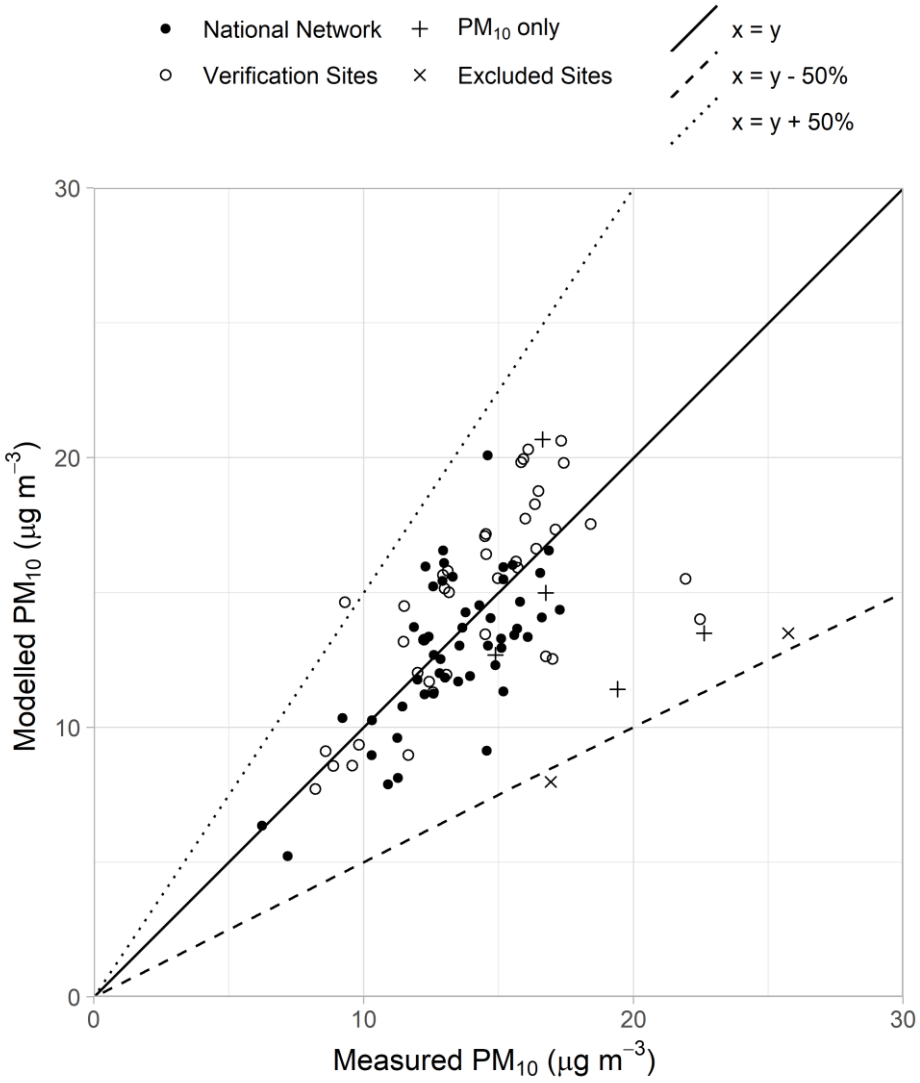

Figure 5.11 - Verification of roadside annual mean PM_{10} model 2022

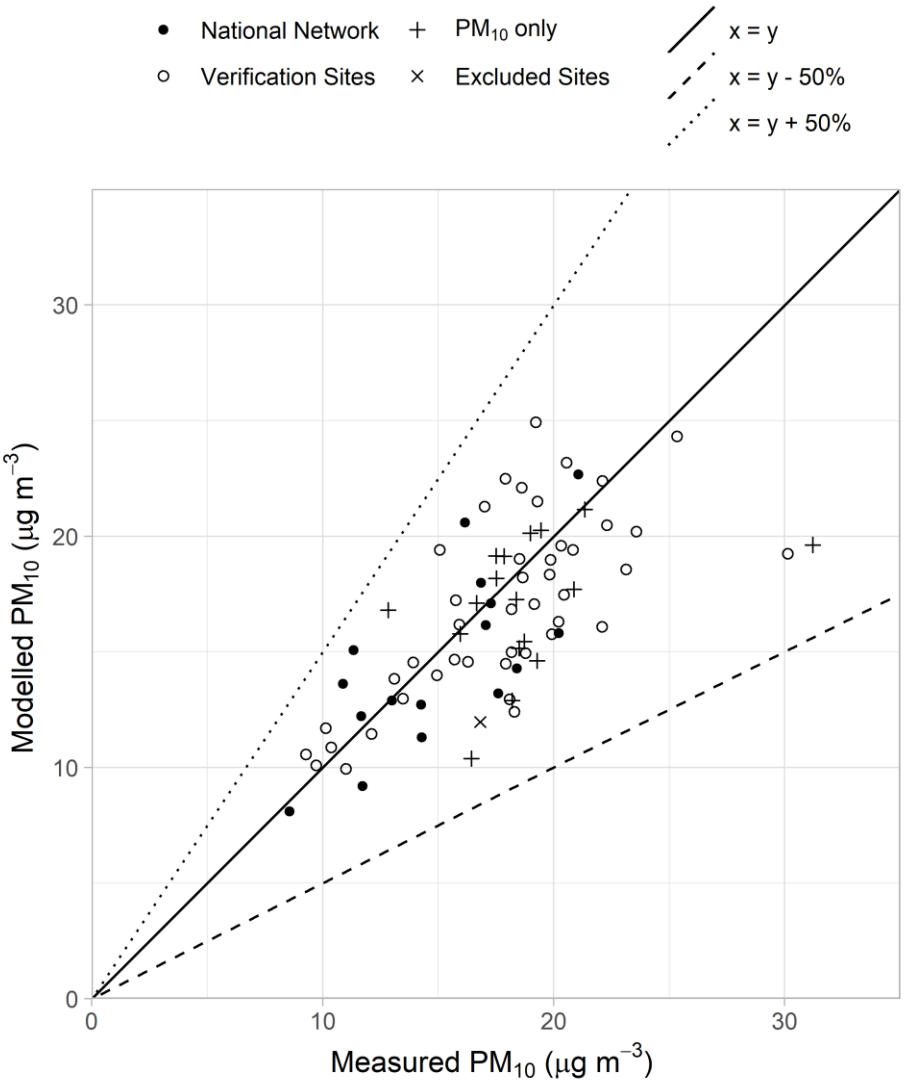

Table 5.5 - Summary statistics for comparison between gravimetric modelled and measured concentrations of PM_{10} at background sites

	Mean of measurements (µg m^{-3}, grav)	Mean of model estimates (µg m^{-3}, grav)	R^2	% outside data quality objectives	Number of sites
National network Calibration	13.4	12.9	0.46	0	50
National network PM10 only sites	19.0	13.5	0.01	14	7
Verification sites	14.2	14.6	0.45	2	41

Table 5.6 - Summary statistics for comparison between gravimetric modelled and measured concentrations of PM_{10} at roadside sites

	Mean of measurements ($\mu g\ m^{-3}$, grav)	Mean of model estimates ($\mu g\ m^{-3}$, grav)	R^2	% outside data quality objectives	Number of sites
National network Calibration	15.0	14.6	0.52	0	16
National network PM10 only sites	18.7	16.8	0.15	0	18
Verification sites	17.8	16.9	0.50	0	44

5.4.2 PM_{10} source apportionment at monitoring sites

Figure 5.12 and Figure 5.13 show the modelled annual mean PM_{10} source apportionment for 2022 at national network background and roadside monitoring sites respectively. The measured concentration at each site is also shown for reference.

At background locations, the contributions from non-emissions inventory sources (i.e. regional background sources and urban dusts), dominate with a particularly large contribution from secondary inorganic aerosols. The smaller contribution from urban background emissions sources is dominated in most locations by domestic, traffic (exhaust emissions, brake and tyre wear and road abrasion) and industry.

At roadside locations the source apportionment follows a very similar pattern to background locations, except that there is an extra local road traffic component composed of local exhaust emissions and local brake and tyre wear and local road abrasion emissions. Depending on the magnitude of the local traffic emissions, local traffic emissions can contribute up to about 4 $\mu g\ m^{-3}$ of PM_{10} at the roadside monitoring sites.

Figure 5.12 - Annual mean PM_{10} source apportionment at background national network monitoring sites in 2022

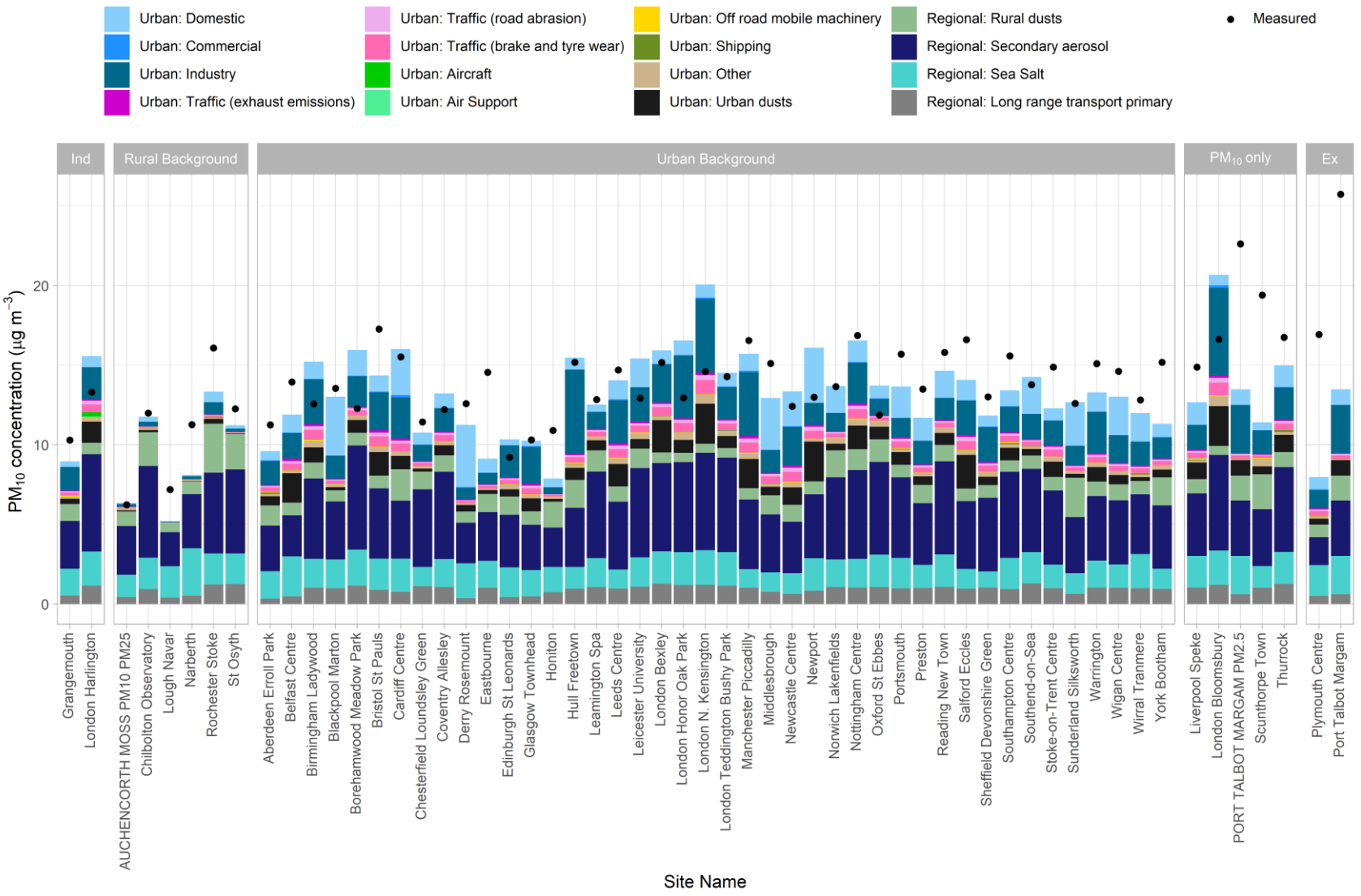

Figure 5.13 - Annual mean PM_{10} source apportionment at national network roadside monitoring sites in 2022

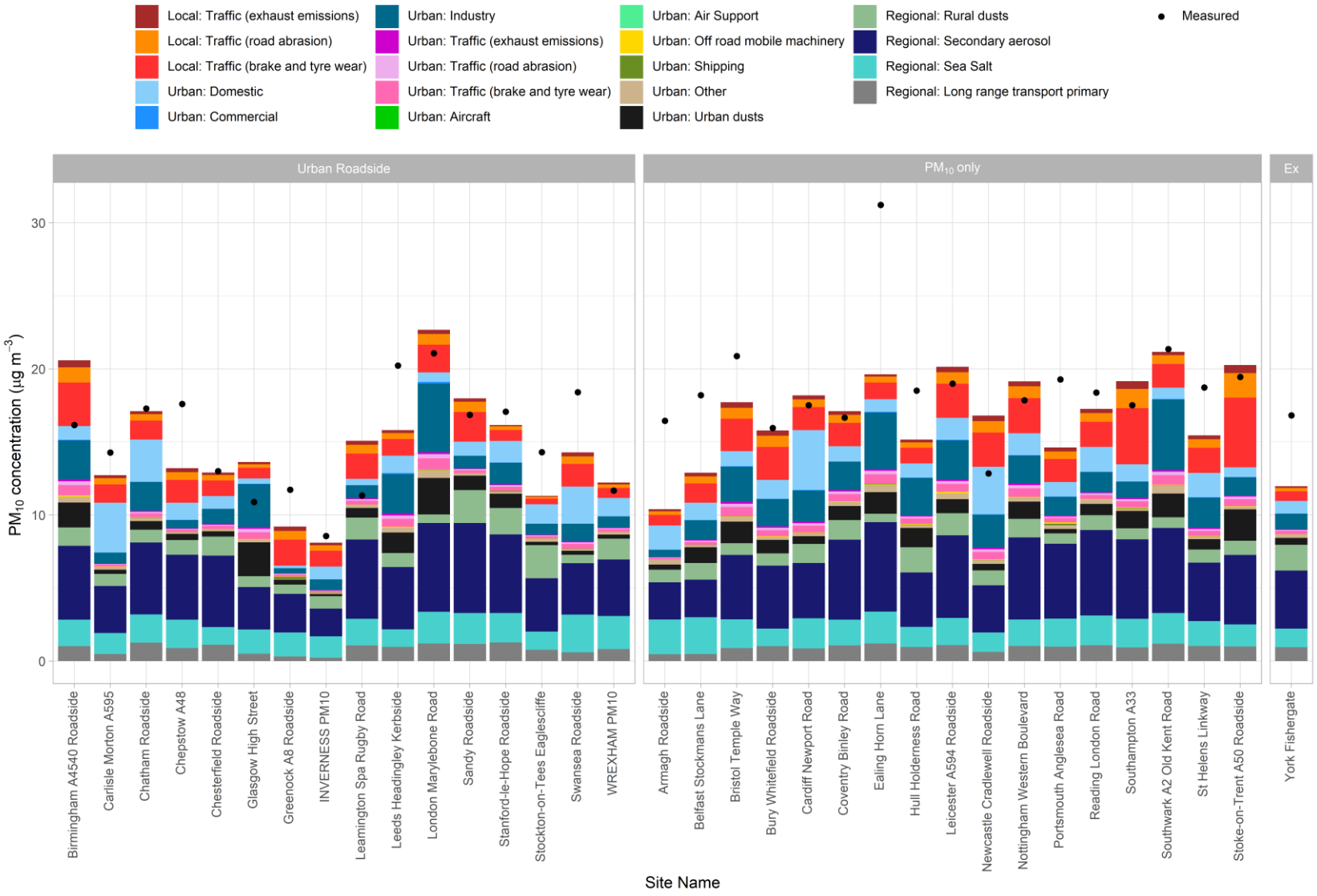

5.5 Subtraction of sea salt component

5.5.1 Introduction

The AQSR requires attribution exceedances of limit values due to natural sources when reporting the results of air quality assessments when these occur. The definition of natural sources in the AQSR includes sea spray. An assessment of concentrations with the contribution from natural sources subtracted is provided in e-Reporting Data flow G published on UK-Air (*UK-Air*, 2023) for locations with measured or modelled exceedances of the limit values. Where exceedances are attributed to natural sources, subtraction is a requirement of the AQSR.

5.5.2 Map of annual mean sea salt PM_{10}

The method used to estimate the sea salt contribution to annual mean PM_{10} concentrations across the UK has been described in Section 5.3.6. The map of annual mean sea salt PM_{10} can be used to subtract this contribution directly from measured or modelled annual mean concentrations. The uncertainties associated with estimating the sea salt contribution to annual mean PM_{10} from measurements of particulate chloride have been discussed in Section 5.3.6. It is recognised that the interpolated map of sea salt concentrations will not capture the steep gradients in sea salt concentration very close to the coast. Thus, the analysis presented may underestimate the sea salt contribution to exceedances in coastal areas.

5.5.3 Method for the 24-hour limit value

A method has also been developed to estimate the contribution from sea salt to exceedances of the 24-hour limit value for PM_{10} of no more than 35 days with concentration greater than 50 µg m^{-3}. This method has been described in detail by (Defra, 2009). This method makes use of the relationship between the number of days with concentrations greater than 50 µg m^{-3} and annual mean concentrations described by (Stedman, Bush, *et al.*, 2001). There is some scatter around the best-fit line of the relationship shown in Figure 5.4. Using the best-fit line relationship within the annual method for subtracting sea salt has been considered appropriate since this should give the best central estimate of the sea salt contribution.

An estimate of the number of days with a PM_{10} concentration greater than 50 µg m^{-3} associated with the contribution to annual mean concentration from sea salt has been calculated by applying the relationship of (Stedman, Bush, *et al.*, 2001) in the vicinity of the limit value. This has been done by calculating the difference between the number of days corresponding to 31.5 µg m^{-3} minus half the sea salt concentration and the number of days corresponding to 31.5 µg m^{-3} plus half the sea salt concentration.

Daily chloride measurements are available for two sites in the south east of the UK. These measurements can be used to calculate a daily sea salt subtraction for PM_{10} monitoring data. This method is not applicable to model results and will be less reliable for sites not in the south east of the UK. For these reasons the method based on annual mean sea salt concentrations has been used across the UK as described above. (Defra, 2009) have provided a comparison of the annual and daily methods for the years 2005, 2006 and 2007 which shows that the agreement between the methods is reasonably good.

5.5.4 Results

There were no reported exceedances of the 24-hour or annual mean limit values for PM_{10} in 2022.

6 $PM_{2.5}$

6.1 Introduction

6.1.1 Limit and Target values

The AQSR (*legislation.gov.uk*, 2010) includes a target value (TV) for annual mean $PM_{2.5}$ which came into force from 01/01/2010. This target value is:

- An annual mean concentration of 25 µg m^{-3}.

A limit value was also set for ambient $PM_{2.5}$ concentrations and came into force on 01/01/2015:

- An annual mean concentration of 25 µg m^{-3}.

A revised limit value (*legislation.gov.uk*, 2020) came into force on 01/01/2020 of:

- An annual mean concentration of 20 µg m^{-3}.

There were no measured or modelled exceedances of the annual mean target value or limit value for $PM_{2.5}$ in 2022.

An exposure reduction target and an exposure concentration obligation have also been set for $PM_{2.5}$.

Results of the assessment in terms of comparisons of the modelled concentrations with the annual mean limit and target values for $PM_{2.5}$ have been reported in e-Reporting Data flow G published on UK-Air (*UK-Air*, 2023).

6.1.2 Annual mean model

Maps of annual mean $PM_{2.5}$ in 2022 at background and roadside locations are shown in Figure 6.1 and Figure 6.2.

Full details of the models used to calculate concentrations of PM_{10} and $PM_{2.5}$ are provided in Section 5. The maps have been calibrated using measurements within the national network for which co-located PM_{10} measurements are also available. The models for PM_{10} and $PM_{2.5}$ are designed to be fully consistent, with each component either derived from emission estimates for PM_{10} or $PM_{2.5}$, or the contributions to the fine and coarse particle size fractions are estimated separately. This enables us to carry out an additional sense check that the calibration parameters for the two pollutants are reasonably consistent. Measurements from national network sites without collocated PM_{10} instruments have been used as an additional verification dataset.

The concentrations of many of the modelled components have been estimated separately for the fine and coarse fraction. This enables a consistent method to be adopted for estimation of PM_{10} (the sum of the fine and coarse fractions) and $PM_{2.5}$ (fine fractions only). The mass fractions of each component assigned to $PM_{2.5}$ are listed in Section 6.3.1. The component pieces are then aggregated to a single 1 km x 1 km background $PM_{2.5}$ grid. An additional roadside increment is added for roadside locations.

The results from the annual mean model can be directly compared with the annual mean target and limit values in order to carry out the air quality assessment.

Figure 6.1 - Annual mean background $PM_{2.5}$ concentration, 2022 (µg m^{-3}, gravimetric)

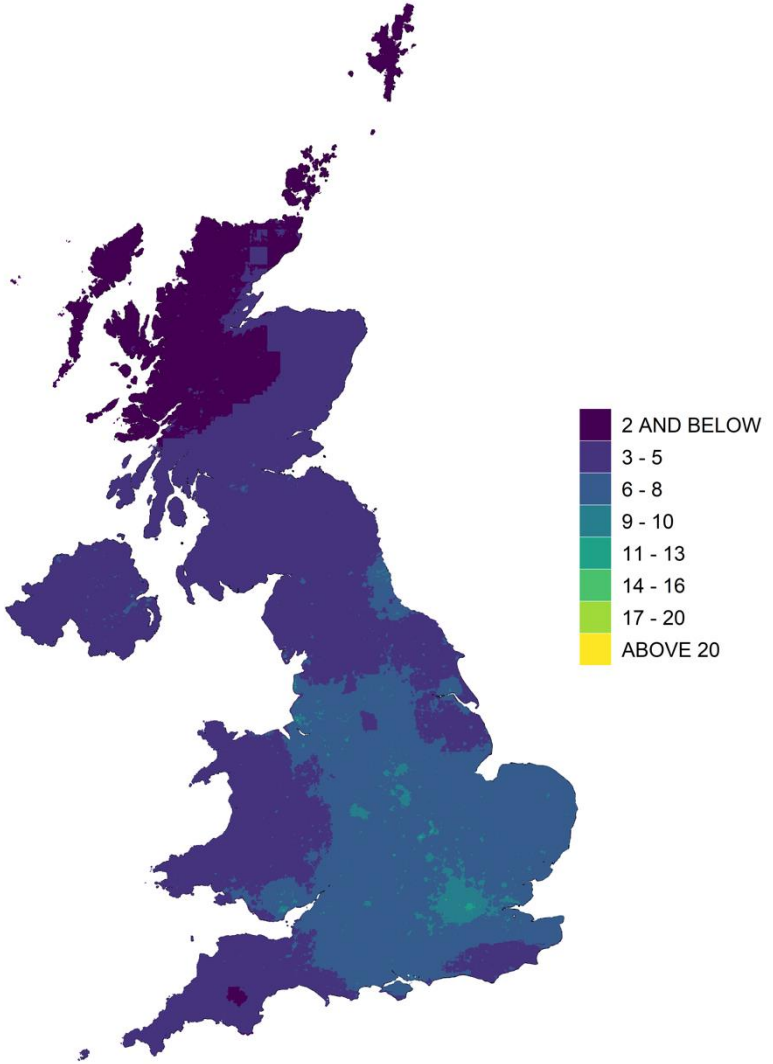

Figure 6.2 - Urban major roads, annual mean roadside $PM_{2.5}$ concentration, 2022 (µg m^{-3}, gravimetric)

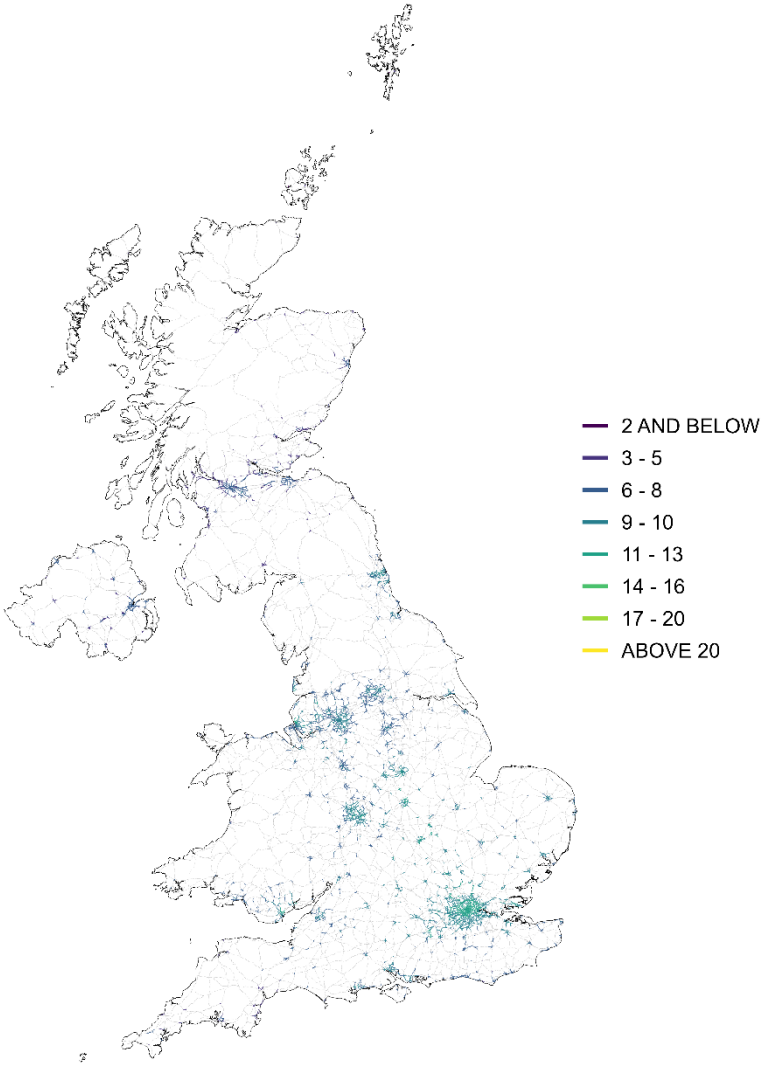

6.1.3 Overview of the PCM model for $PM_{2.5}$

Figure 6.3 shows a simplified flow diagram of the PCM model for $PM_{2.5}$. A summary of the PCM model method, input, and assumptions for $PM_{2.5}$ is presented in Table 6.1.

Figure 6.3 - Flow diagram for PCM $PM_{2.5}$ model

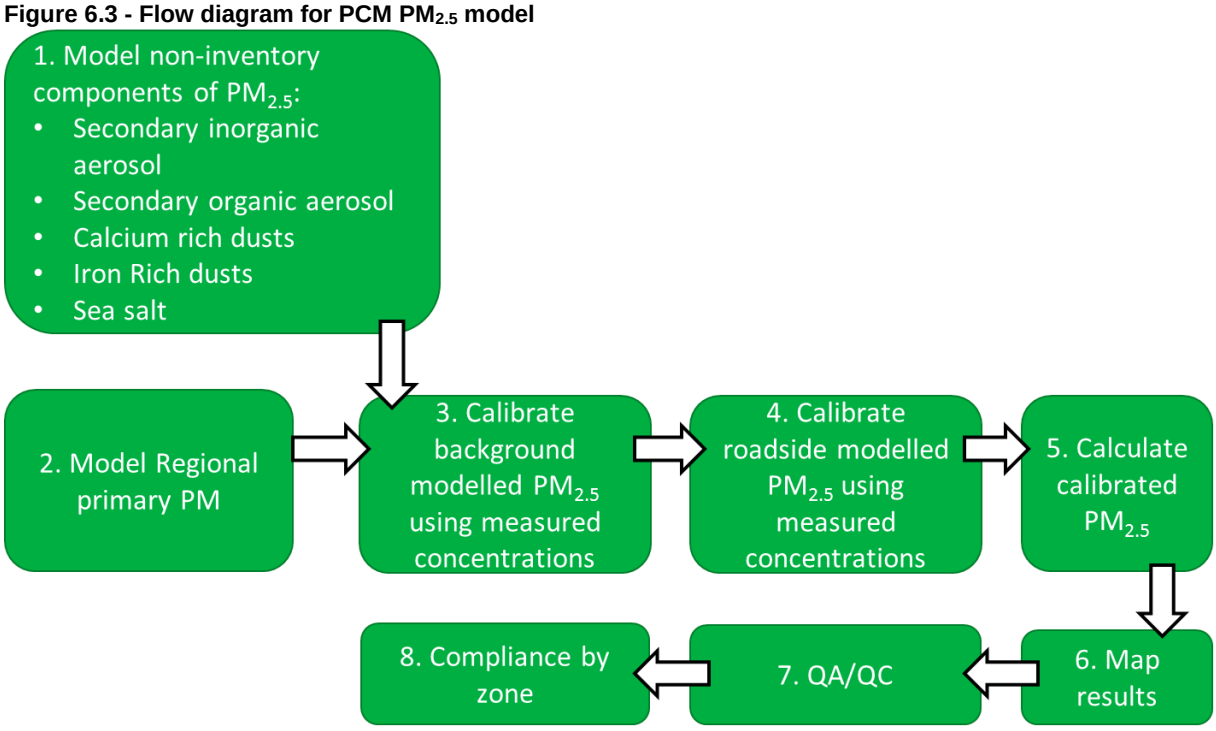

Table 6.1 - PCM model method, input and assumptions summary for $PM_{2.5}$

Heading	Component	Details
General	Pollutant	$PM_{2.5}$
	Year	2022
	Locations modelled	Background and traffic locations
	Metric	Annual mean
Input data	Emission inventory	NAEI 2021 (scaled to 2022)
	Energy projections	Energy Projections 2022
	Road traffic counts	2022 (scaled from 2021 where not available)
	Road transport activity projections	DfT (2022) car sales projections, TfL fleet projections for London (2023)
	Road transport emission factors	COPERT 5.4 (COPERT 5.4, 2020)
	Measurement data	2022
	Meteorological data	WRF (see Appendix 4 – WRF meteorology)
Model components	Regional	See details under “pollutant specific” heading
	Large point sources	404 sources modelled using ADMS 5.2
	Small point sources	PCM small points model
	ETS point sources	PCM small points model
	Large ETS point sources	85 sources modelled using ADMS 5.2
	Area sources	PCM dispersion kernels generated using ADMS 5.2. Time varying emissions for road transport and domestic sources. PCM small points model for industrial combustion emissions.
	Roadside increment	PCM Roads Kernel Model using ADMS-Roads 5.0

Heading	Component	Details
Calibration	Model calibrated?	Yes
	Number of background stations in calibration	50 (stations with both PM_{10} and $PM_{2.5}$)
	Number of traffic stations in calibration	16 (stations with both PM_{10} and $PM_{2.5}$)
Pollutant specific	Secondary inorganic aerosol	Interpolated from SO_4, NO_3 and NH_4 measurements at 28 rural stations, scaling factors applied for size fraction, bound water and counterions
	Secondary organic aerosol	Results from the NAME model for 2008
	Regional primary particles	Calculated using the TRACK receptor oriented, Lagrangian statistical model
	Regional calcium rich dusts from re-suspension of soils	Modelled using information on land cover (bare soil, root and cereal crops) and dispersion kernel incorporating emissions and dispersion processes
	Regional iron rich dusts from re-suspension	Assigned a constant value of zero
	Iron rich dusts from re-suspension due to vehicle activity	Modelled using information on vehicle movements on major roads (HDV) and dispersion kernel incorporating emissions and dispersion processes
	Sea Salt	Interpolated measurements of Cl, scaling factor applied for sea water composition
	Residual	A value assigned based on best fit to PM_{10} and $PM_{2.5}$ measurements: zero, no residual required

6.1.4 Chapter Structure

This chapter describes modelling work carried out for 2022 to assess compliance with the $PM_{2.5}$ limit and target values described above. Emission estimates for primary PM are described in Section 6.2, Section 6.3 describes the $PM_{2.5}$ modelling methods. The modelling results in terms of verification and source apportionment are presented in Section 6.4. The methods used to subtract the contribution from natural sources (sea salt) and the results of this subtraction are presented in Section 6.5. The method used to calculate the average exposure indicator (AEI) for annual mean $PM_{2.5}$ and an assessment of compliance with the exposure concentration obligation is presented in Section 6.6.

6.2 $PM_{2.5}$ emissions

Estimates of the emissions of primary PM from the UK National Atmospheric Emission Inventory 2021 (NAEI 2021) have been used in this study (Ingledew *et al.*, 2023). Emissions projections have been provided by the NAEI (Personal communication from Ben Pearson, 2023) based on BEIS EEP 2022 energy and emissions projections (BEIS, 2022). Emissions have been projected to 2022 from 2021.

Figure 6.4 shows UK total $PM_{2.5}$ emissions for 2022, with the coding described in Table 3.2. The figure shows that $PM_{2.5}$ emissions in 2022 include contributions from a wide range of different source sectors. The figure shows that $PM_{2.5}$ emissions in 2022 are dominated by two main sources:

- SNAP 2: Domestic combustion (28.1%)
- SNAP 3: Industrial combustion (19.3%).

The methods used to calculate ambient concentrations from the estimates of primary PM emissions are described below for point, area, road link and regional sources.

Figure 6.4 - Total UK $PM_{2.5}$ emissions for 2022 by SNAP code scaled from NAEI 2021

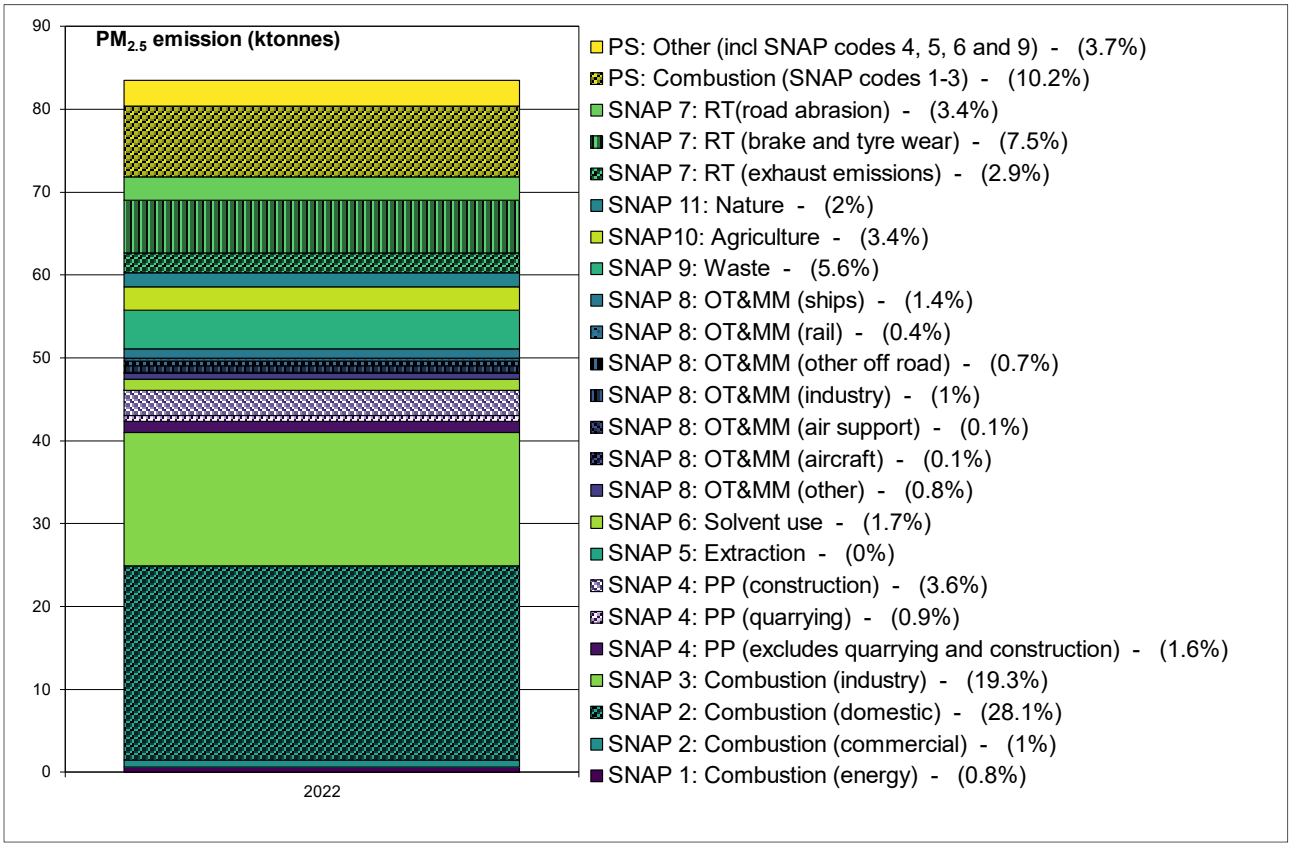

6.3 $PM_{2.5}$ modelling

6.3.1 $PM_{2.5}$ mass fractions

The proportions of the PM mass for each component assigned to the $PM_{2.5}$ fraction within the PCM models are listed in Table 6.2. The proportions for secondary inorganic aerosols have been derived as described in Section 5.3.1. The proportions for local point and area sources are based on the NAEI emission inventories for $PM_{2.5}$ and PM_{10} (Ingledew *et al.*, 2023). The NAEI $PM_{2.5}$ emission inventory has been derived from the PM_{10} emission inventory by the application of estimates of the mass fraction represented by $PM_{2.5}$ for different sources and fuels. Overall, the UK total mass emissions for $PM_{2.5}$ for 2022 were about 58% of the value for PM_{10}. The proportions for calcium and iron rich dusts have been derived with reference to the monitoring data presented in Section 5.3.5 and to provide good fit to the available co-located $PM_{2.5}$ and PM_{10} measurements. The proportions for calcium and iron rich dusts were updated for 2017 and subsequent years in order to account for the revised method for measurement of SIA (Tang *et al.*, 2015) and revised spatial distribution of emissions from domestic wood combustion to provide a consistent calibration for PM_{10} and $PM_{2.5}$. The proportion for sea salt has been derived as described in Section 5.3.6.The proportion for secondary organic aerosol, has been set at 1.0 for $PM_{2.5}$ so as to provide best fit to the available measurements.

Table 6.2 - The proportion of PM mass assigned to the $PM_{2.5}$ and $PM_{2.5-10}$ size fractions

Component	Fine fraction ($PM_{2.5}$)	Coarse fraction ($PM_{2.5-10}$)
SO_4	0.94	0.06
NO_3	0.556 (fine mode), 0.222 (coarse mode)	- (fine mode), 0.222 (coarse mode)
NH_4	0.97	0.03
SOA	1.00	-
Large point sources of primary particles	$PM_{2.5}$ emission inventory*	PM_{10} emission inventory
Small point sources of primary particles	$PM_{2.5}$ emission inventory*	PM_{10} emission inventory
Regional primary particles	$PM_{2.5}$ emission inventory*	PM_{10} emission inventory
Area sources of primary particles	$PM_{2.5}$ emission inventory*	PM_{10} emission inventory
Rural calcium rich dusts from re-suspension of soils	0.1	0.9
Regional iron rich dusts from re-suspension	0	1.0
Iron rich dusts from re-suspension due to vehicle activity	0.1	0.9
Sea salt	0.27	0.73
Residual	n/a	n/a

* The NAEI $PM_{2.5}$ emission inventory has been derived from the PM_{10} emission inventory by the application of estimates of the mass fraction represented by $PM_{2.5}$ for different sources and fuels.

6.3.2 Contributions from large and small point sources

The contributions from large and small point sources have been calculated in the same way as for the PM_{10} model described in Section 5.3.3.

6.3.3 Contributions from area sources

Figure 6.5 shows the calibration of the area source model for $PM_{2.5}$. The calibration coefficient for $PM_{2.5}$ is very similar to the calibration coefficient for PM_{10}. Small differences are considered to be well within the uncertainty of the PM_{10} and $PM_{2.5}$ measurements and the $PM_{2.5}$ mass fractions within the emission inventory. A reasonably good agreement between the calibration coefficients for area sources is one of the criteria for the choice of mass fraction parameters for $PM_{2.5}$ within the PCM model.

As part of the calibration process emission caps have been applied to certain sectors; this is because the use of surrogate statistics for mapping area source emissions sometimes results in unrealistically large concentrations in some grid squares for a given sector. The emission caps applied are given in Table 6.3.

Figure 6.5 - Calibration of $PM_{2.5}$ area source model 2022 (µg m^{-3}, gravimetric)

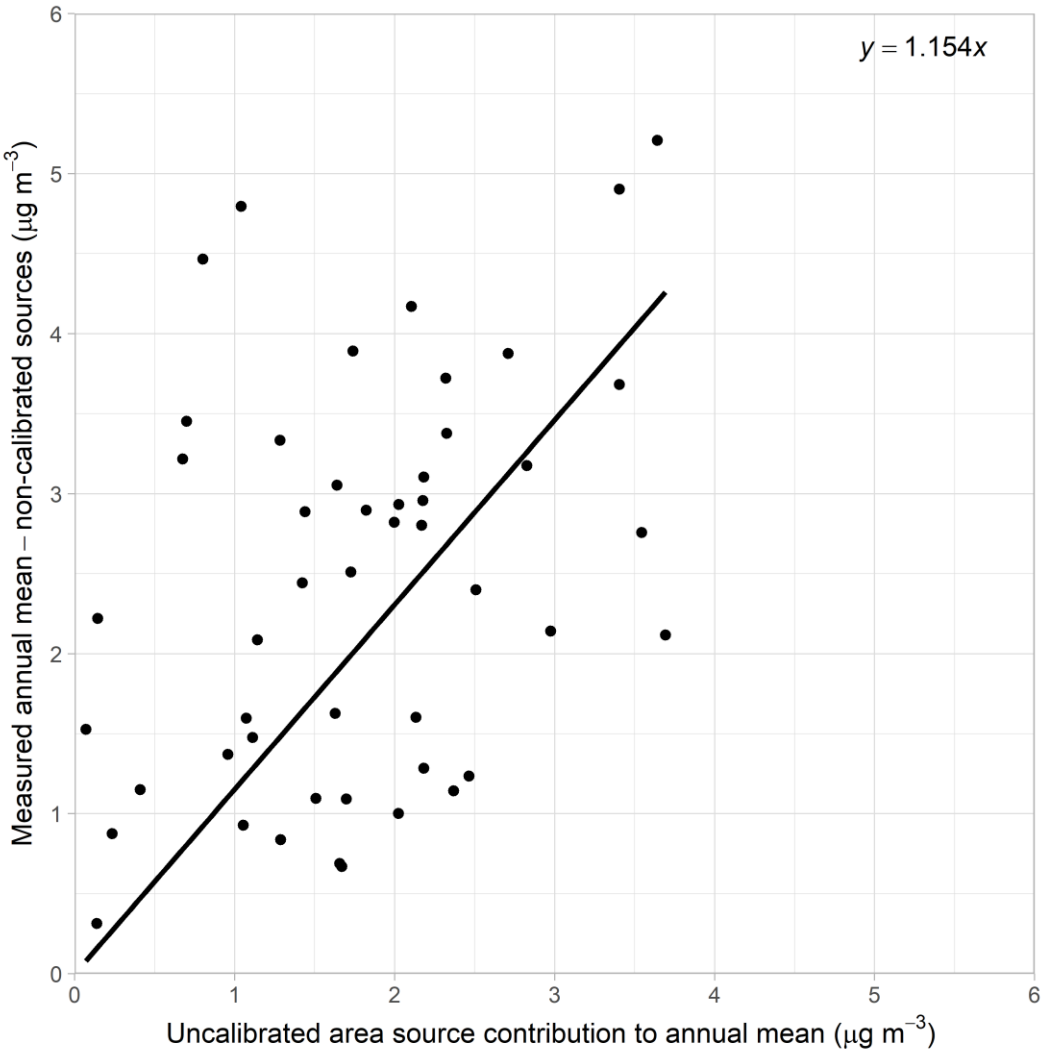

Table 6.3 - Emission caps applied to $PM_{2.5}$ sector grids

SNAP code	Description	Cap applied (t/a/km^2)
SNAP 8 (Industrial off-road mobile machinery)	Industrial off-road mobile machinery_Gas oil	2.3
SNAP 8 (Other Transport & mobile machinery)	Shipping	5
SNAP 4 (Production process)	Stockpiles	9

6.3.4 Roadside concentrations

Figure 6.6 shows the calibration of the roadside increment model for annual mean $PM_{2.5}$ concentrations.

Figure 6.6 - Calibration of $PM_{2.5}$ roadside increment model 2022 (µg m^{-3}, gravimetric)

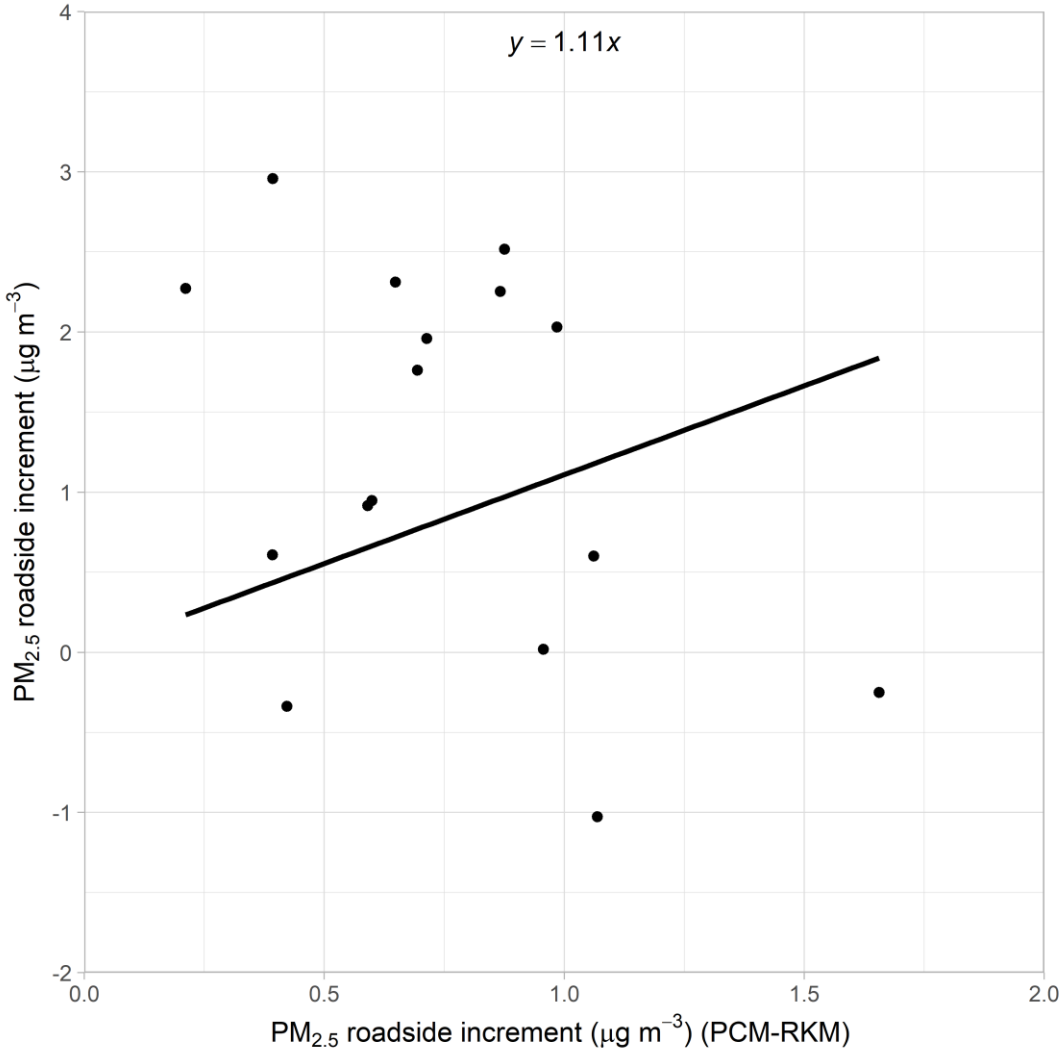

6.4 Results

6.4.1 Verification of mapped concentrations

Figure 6.7 and Figure 6.8 show comparisons of modelled and measured annual mean $PM_{2.5}$ concentrations in 2022 at background and roadside monitoring site locations. Lines representing y = x – 50 % and y = x + 50% are also shown because 50% is the AQSR data quality objective for modelled annual mean $PM_{2.5}$ concentrations – see Section 1.5.

Summary statistics for the comparison between modelled and measured $PM_{2.5}$ concentrations are presented in Table 6.4 and Table 6.5. There are three categories of monitoring sites within the tables. This is because there are some sites in the national network at which only PM_{10} or $PM_{2.5}$, but not both are measured. National network sites that have not been included in the calibrations are also shown in the graphs. The agreement between the measurement data and the modelled values is generally good.

Figure 6.7 - Verification of background annual mean $PM_{2.5}$ model 2022

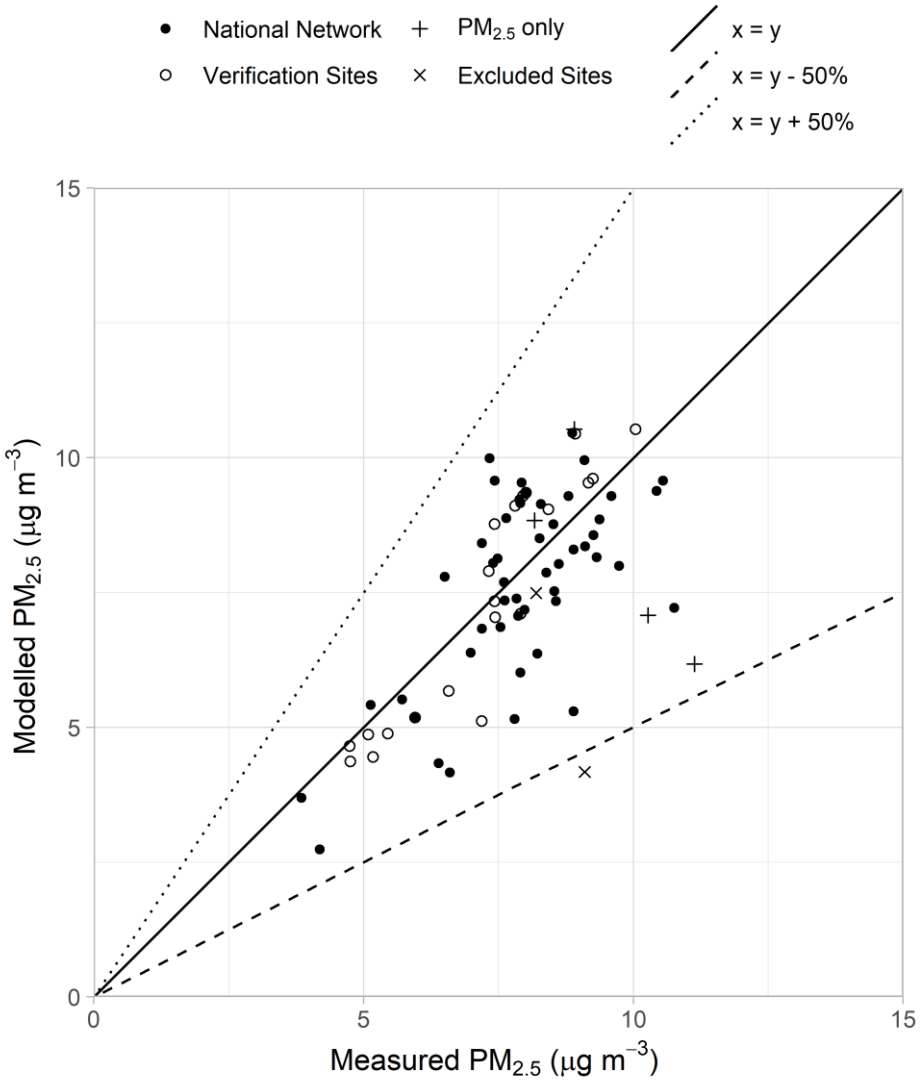

Figure 6.8 - Verification of roadside annual mean $PM_{2.5}$ model 2022

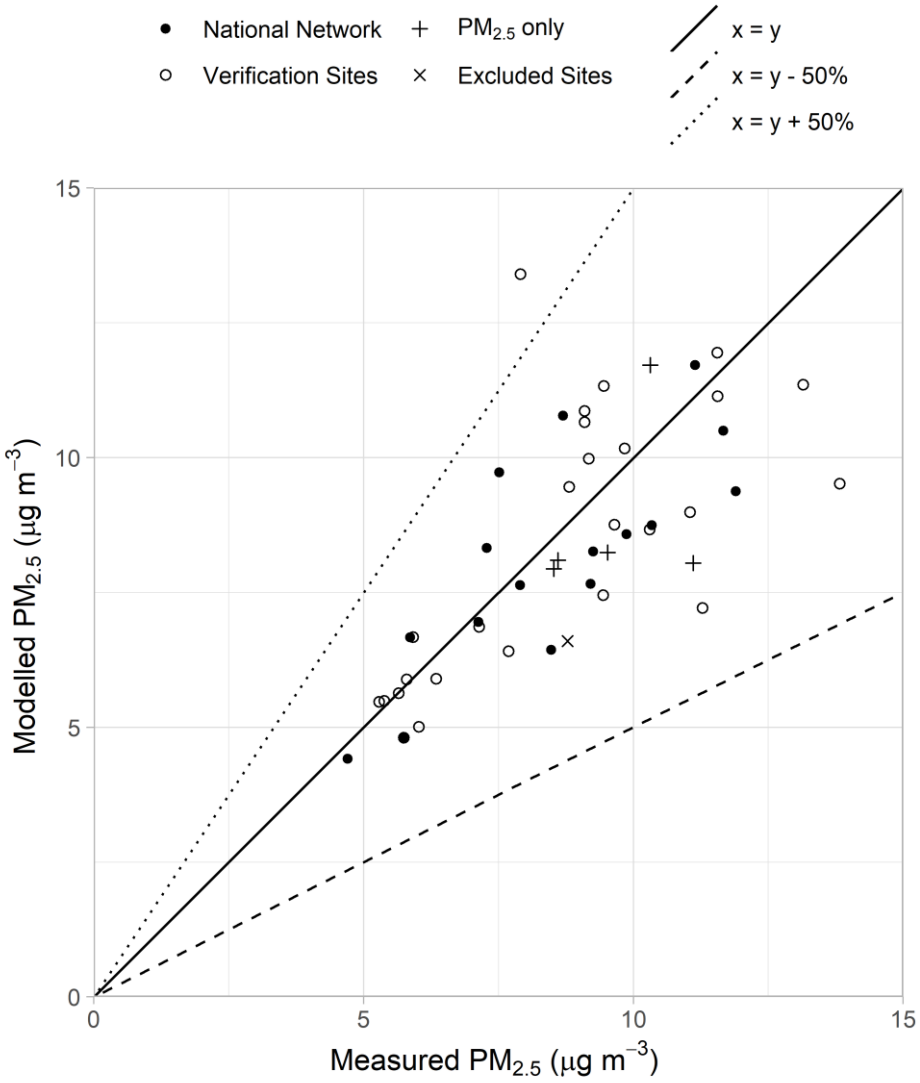

Table 6.4 - Summary statistics for comparison between gravimetric modelled and measured concentrations of $PM_{2.5}$ at background sites

	Mean of measurements (µg m^{-3}, grav)	Mean of model estimates (µg m^{-3}, grav)	R^2	% outside data quality objectives	Number of sites
National network (Calibration)	7.9	7.6	0.43	0	50
National network PM2.5 only sites	9.3	7.4	0.14	17	6
Verification sites	7.3	7.5	0.85	0	20

Table 6.5 - Summary statistics for comparison between gravimetric modelled and measured concentrations of $PM_{2.5}$ at roadside sites

	Mean of measurements ($\mu g\ m^{-3}$, grav)	Mean of model estimates ($\mu g\ m^{-3}$, grav)	R^2	% outside data quality objectives	Number of sites
National network Calibration	8.5	8.2	0.60	0	16
National Network PM2.5 only sites	9.5	8.4	0.21	0	6
Verification sites	8.8	8.6	0.46	4	25

6.4.2 $PM_{2.5}$ source apportionment at monitoring sites

Figure 6.9 and Figure 6.10 show the modelled annual mean $PM_{2.5}$ source apportionment for 2022 at national network background and roadside monitoring sites respectively. The measured concentration at each site is also shown for reference.

At background locations, the contributions from non-emissions inventory sources (i.e. regional background sources and urban dusts) dominate with a particularly large contribution from secondary inorganic aerosols. The smaller contribution from urban background emissions sources are dominated in most locations by domestic, traffic and industry.

At roadside locations the source apportionments follow a very similar pattern to background locations, except that there is an extra local road traffic component composed of local exhaust emissions, local brake and tyre wear emissions and local road abrasion emissions.

Overall regional secondary PM make a proportionally larger contribution to the total mass for $PM_{2.5}$ than for PM_{10}.

Figure 6.9 - Annual mean $PM_{2.5}$ source apportionment at background national network monitoring sites 2022

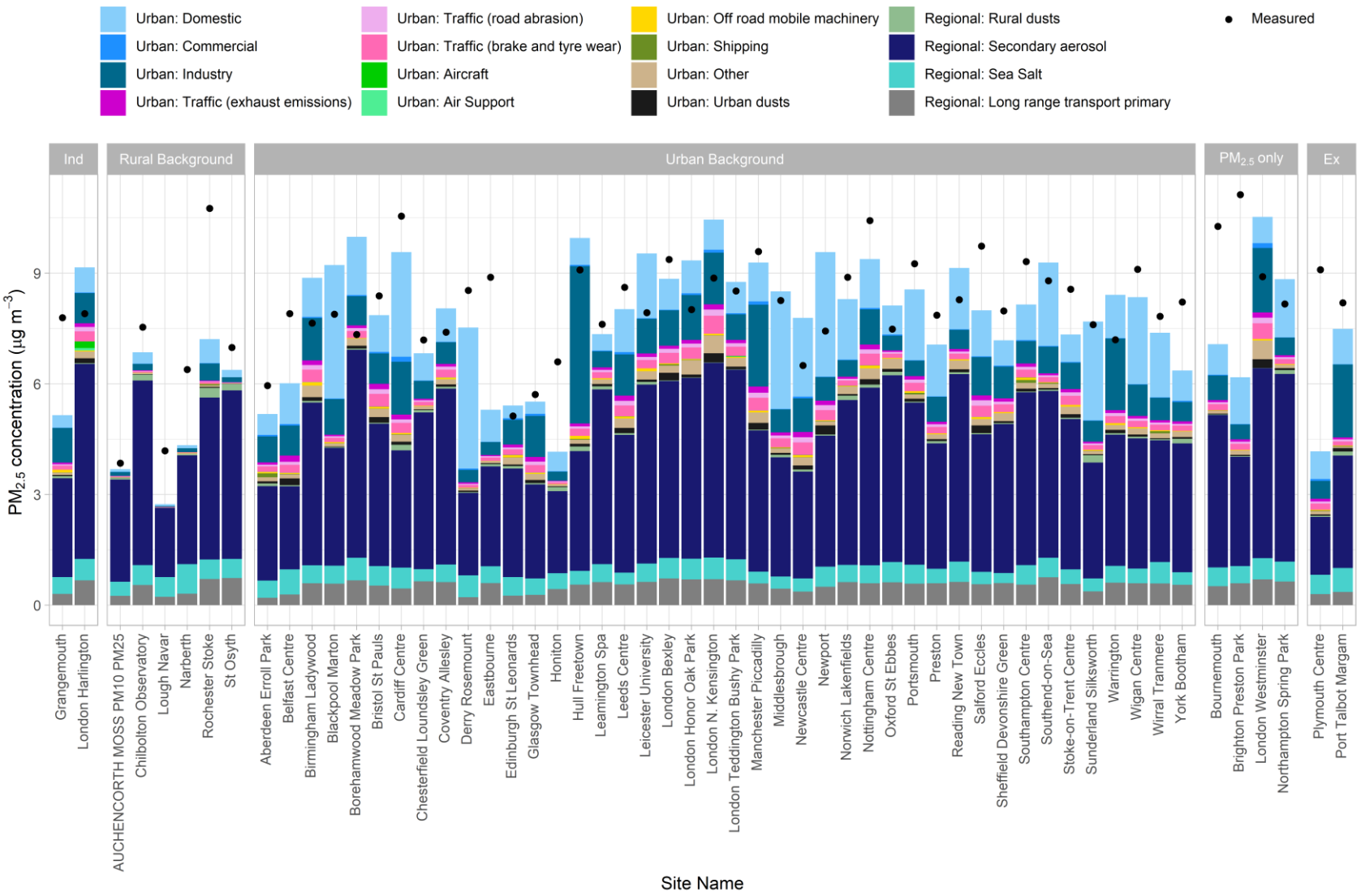

Figure 6.10 - Annual mean $PM_{2.5}$ source apportionment at roadside national network monitoring sites 2022

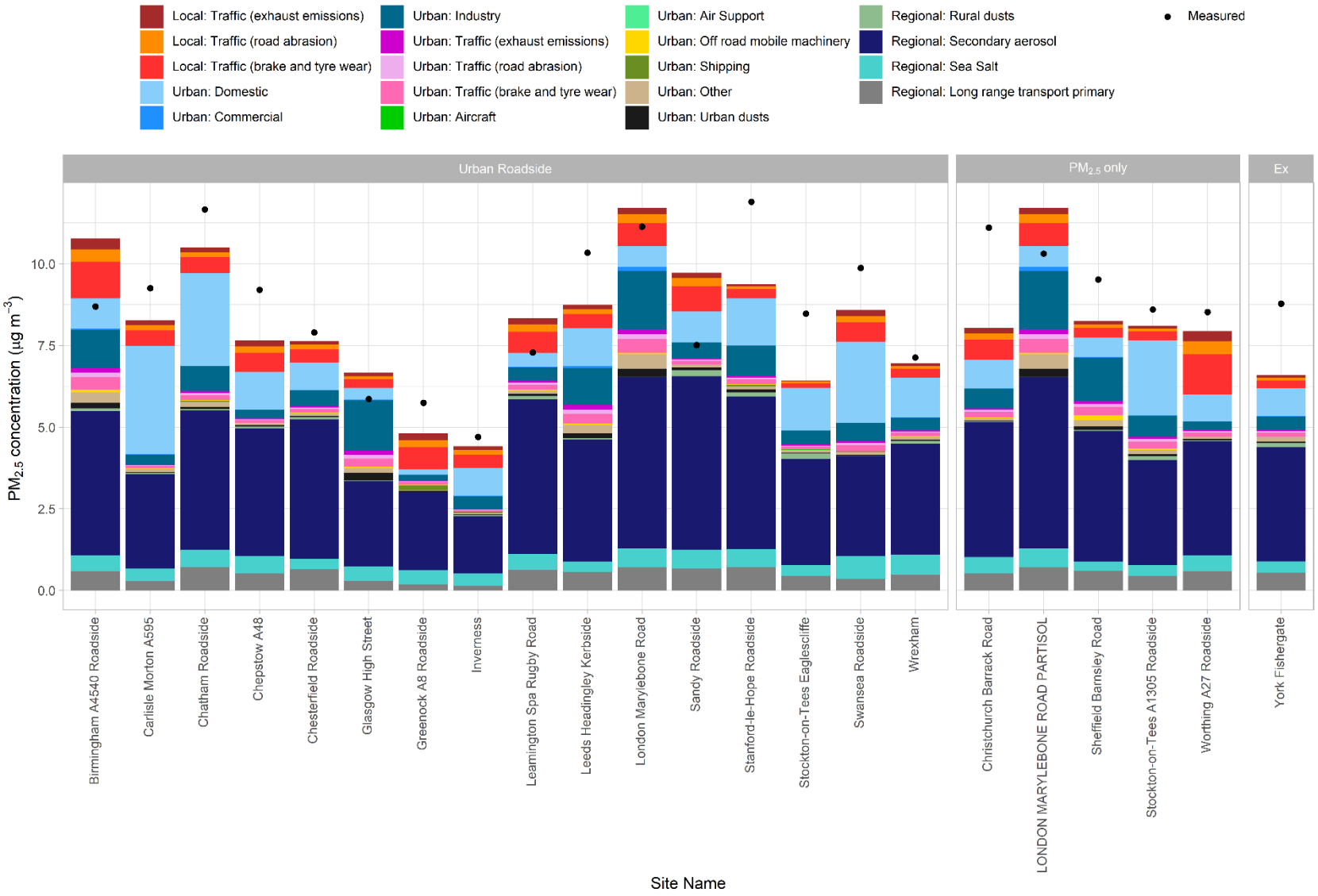

6.5 Subtraction of sea salt component

6.5.1 Introduction

The AQSR requires attribution exceedances of limit values due to natural sources when reporting the results of air quality assessments when these occur. The definition of natural sources in this directive includes sea spray. An assessment of concentrations with the contribution from natural sources subtracted is provided in e-Reporting Data flow G published on UK-Air (*UK-Air*, 2023) for locations with measured or modelled exceedances of the limit values. Where exceedances are attributed to natural sources, subtraction is a requirement of the Directive.

6.5.2 Map of annual mean sea salt $PM_{2.5}$

The method used to estimate the sea salt contribution to annual mean $PM_{2.5}$ concentrations across the UK has been described in Section 5.3.6. The map of annual mean sea salt $PM_{2.5}$ can be used to subtract this contribution directly from measured or modelled annual mean concentrations. The uncertainties associated with estimating the sea salt contribution to annual mean $PM_{2.5}$ from measurements of particulate chloride have been discussed in Section 5.3.6. It is recognised that the interpolated map of sea salt concentrations will not capture the steep gradients in sea salt concentration very close to the coast. Thus, the analysis presented may underestimate the sea salt contribution to exceedances in coastal areas.

6.5.3 Results

There were no measured or modelled exceedances of the annual mean target value, Stage 1 limit value for $PM_{2.5}$ in 2022. Therefore, there was no requirement to subtract the natural contribution.

6.6 Average Exposure Indicator

An exposure reduction target (ERT) and an exposure concentration obligation (ECO) for $PM_{2.5}$ have been set within the AQSR. Both environmental objectives are based on the value calculated for the average exposure indicator (AEI). The AEI is calculated as the three-year average of annual mean measurements at urban background and suburban background monitoring sites (listed in Appendix 7 – Monitoring stations used in $PM_{2.5}$ AEI calculation) across the country.

The AEI for the reference year 2022 has been calculated from measurements made during the years 2020, 2021 and 2022. The method used to calculate the AEI for the 2022 reference year is the same as was used for the previous assessments (Brookes *et al.*, 2012, 2013, 2015, 2016, 2017, 2019b, 2019a, 2020, 2021; Pugsley *et al.*, 2022, 2023). An assessment of compliance with the ECO is also presented in this section.

The AEI for the UK has been calculated using the method set out in guidance received for comment from the Commission on 3rd August 2012. This guidance was entitled “Procedures for Determining a National Average Exposure Indicator, for Assessment of a National Exposure Reduction Target, Requirements for Quality Assurance/Quality Control, and Requirements for the Estimation of their Measurement Uncertainties”. The guidance sets out recommended processes but recognises that Member States may adopt other procedures, and it confirms the order of the calculation method for this three-year average. An average is calculated across all of the sites for each year and the three-year average is then calculated from the values calculated for each year. The guidance also proposes a method for weighting the averages for each year according to the data capture achieved.

A total of 36 urban background and suburban background sites were included in the calculation for the 2022 assessment. The calculation is based on the following excerpt from the AQUILA guidance.

$$AEI(p) = \frac{\sum_{i=1}^{n}(\overline{x_i} d_i)}{\sum_{i=1}^{n}(d_i)}$$

$$\overline{x_i} = \frac{\sum_{j=1}^{k}(x_{ij})}{k}$$

Where: d_i is the data capture at the i^{th} station, for all stations where $d_i \geq 75\%$, $\overline{x_i}$ is the annual mean concentration in the year p at station i with the total of n stations, X_{ij} is the daily or hourly average

concentration measured at station *i* during every valid sampling day or hour *j*, and *k* is the number of valid sampling days or hours during the year at that site.

$$AEI = \frac{\sum_p AEI(p)}{3}$$

It is expected that there will have been forced changes in site selection and equipment types between 2010 and 2022 which will impact on the uncertainty of the calculation.

The years 2020, 2021 and 2022 were used for the calculation, with means of 8.0, 7.9 and 8.3 µg m^{-3} respectively.

The mean of these three values (rounded to integer) is 8 µg m^{-3}. This is the AEI for the reference year of 2022. This value is compliant with the ECO of 20 µg m^{-3} to be achieved by 2015 set within the AQSR.

The baseline AEI (based upon the years 2009, 2010, 2011) determined the National Exposure Reduction Target (NERT), to be achieved by 2020. With a value of 13 µg m^{-3} as the baseline AEI, the AQSR required the UK to reduce the AEI by 15% from this value of 13 µg m^{-3} in the three-year average for the reference year 2020. This was achieved in 2020 and the AEI for the reference year of 2022 remains below this value.

7 Benzene

7.1 Introduction

7.1.1 Limit values

A single limit value for ambient benzene concentrations is set out in the Air Quality Directive Standards Regulations (AQSR) (*legislation.gov.uk*, 2010). This limit value has been specified for the protection of human health and came into force on 01/01/2010. The limit value is an annual mean concentration of 5 µg m^{-3}.

Modelled and measured benzene concentrations for 2022 were below the limit value for all zones.

7.1.2 Annual mean model

Maps of annual mean benzene concentrations at background and roadside locations in 2022 are presented in Figure 7.2 and Figure 7.3 respectively.

Benzene concentrations have been calculated using a similar approach to that adopted for NO_X although a different approach has been adopted for the modelling of fugitive and process emissions from point sources.

7.1.3 Overview of the PCM model for benzene

Figure 7.1 shows a simplified flow diagram of the PCM model for benzene. A summary of the PCM model method, input and assumptions for benzene is presented in Table 7.1.

Figure 7.1 - Flow diagram for PCM benzene model

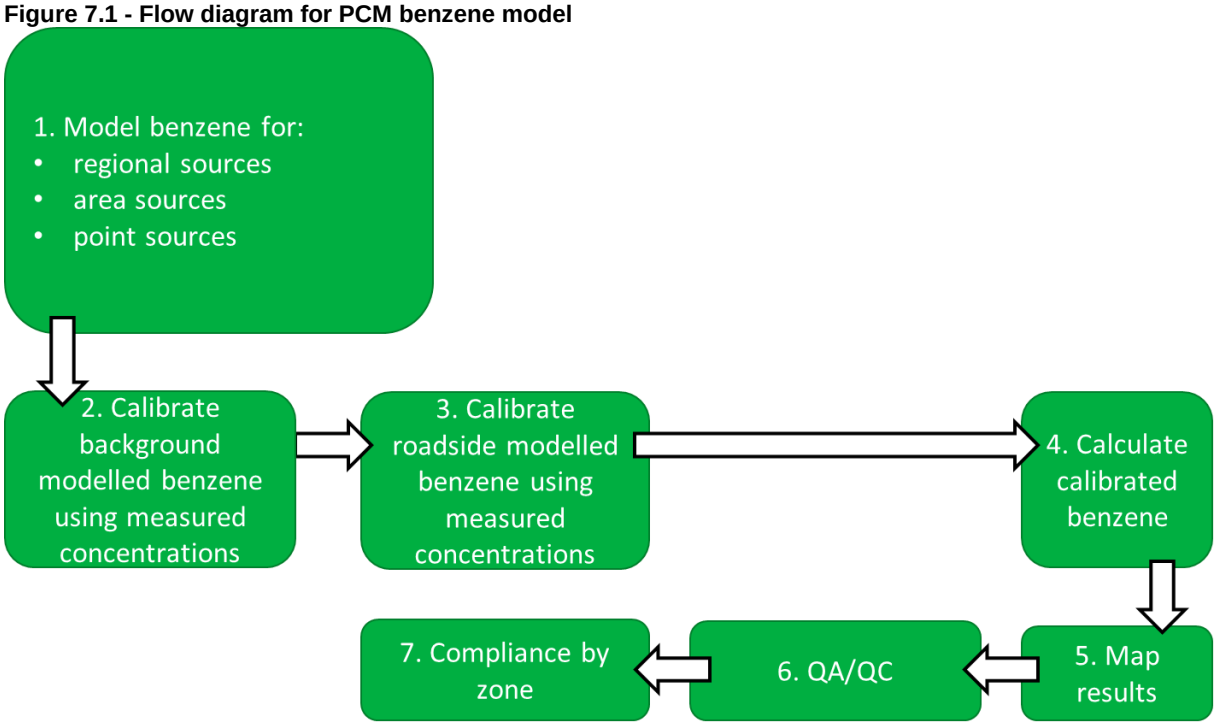

Table 7.1 – PCM model method, input and assumptions summary for benzene

Heading	Component	Details
General	Pollutant	Benzene
	Year	2022
	Locations modelled	Background and traffic locations
	Metric	Annual mean
Input data	Emission inventory	NAEI 2021 (scaled to 2022)
	Energy projections	Energy Projections 2022

Heading	Component	Details
	Road traffic counts	2021 (scaled to 2022)
	Road transport activity projections	DfT (2022) car sales projections, TfL traffic projections for London (2023)
	Road transport emission factors	COPERT 5.4 (COPERT 5.4, 2020)
	Measurement data	2022
	Meteorological data	WRF (see Appendix 4 – WRF meteorology)
Model components	Regional	Interpolated from rural NOx measurements adjusted for local contribution, scaled using measured benzene and NOx at Chilbolton
	Combustion point sources	5 sources modelled using ADMS 5.2
	Fugitive and process point sources	PCM fugitive and process points model for benzene
	ETS point sources	PCM fugitive and process points model for benzene
	Large ETS point sources	19 sources modelled using ADMS 5.2
	Area sources	PCM dispersion kernels generated using ADMS 5.2. Time varying emissions for road transport and domestic sources. PCM small points model for industrial combustion emissions.
	Roadside increment	PCM Roads Kernel Model using ADMS-Roads 5.0
Calibration	Model calibrated?	Yes
	Number of background stations in calibration	18
	Number of traffic stations in calibration	7
Pollutant specific	n/a	n/a

7.1.4 Outline of the annual mean model for benzene

The map of annual mean background benzene concentrations includes contributions from:

- Distant sources (characterised by an estimate of rural background concentration)
- Combustion point sources
- Fugitive and process point sources
- Point sources with emissions estimates for air quality pollutants based on reported carbon emissions (ETS points)
- Local area sources

The area source model has been calibrated using measurements from the national monitoring networks. At locations close to urban roads an additional roadside contribution was added to account for contributions to total benzene from road traffic sources.

7.1.5 Chapter structure

This chapter describes modelling work carried out for 2022 to assess compliance with the benzene annual mean limit value described above. Emission estimates for benzene are described in Section 7.2, Section 7.3 describes the benzene modelling methods, and the modelling results in terms of verification and source apportionment are presented in Section 7.4.

Figure 7.2 - Annual mean background benzene concentration, 2022 (µg m^{-3})

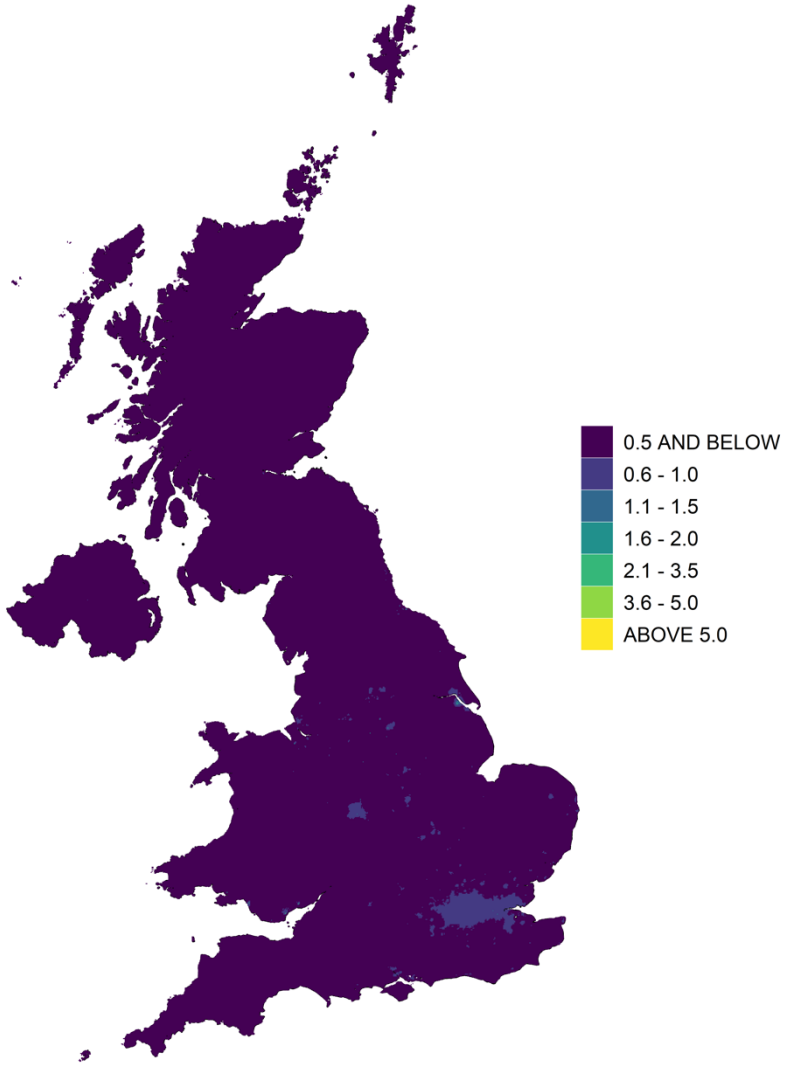

Figure 7.3 - Urban major roads, annual mean roadside benzene concentration, 2022 (µg m^{-3})

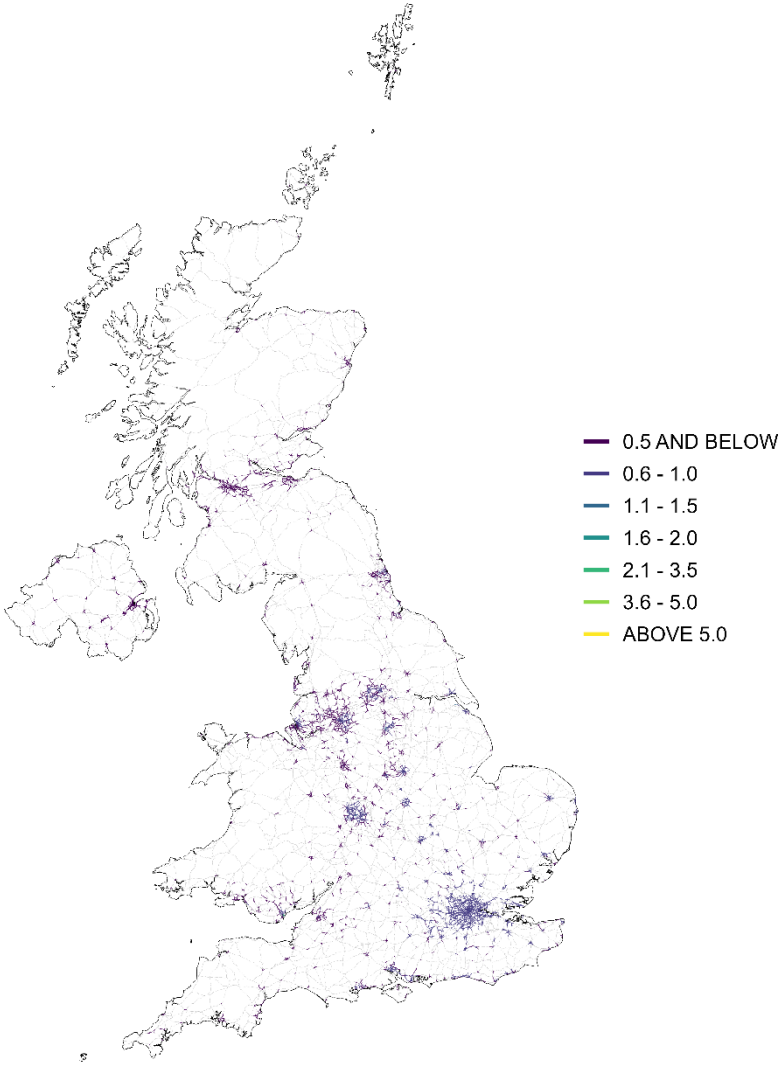

7.2 Benzene emissions

Estimates of the emissions of benzene from the UK National Atmospheric Emission Inventory 2021 (NAEI 2021) have been used in this study (Ingledew *et al.*, 2023). Emissions projections have been provided by the NAEI (Personal communication from Ben Pearson, 2023) based on BEIS EEP 2022 energy and emissions projections (BEIS, 2022). Emissions have been projected to 2022 from 2021.

Figure 7.4 shows the UK total benzene emissions for 2022, with the coding described in Table 3.2. The emissions include contributions from a variety of source sectors. The figure shows that benzene emissions in 2022 are dominated by one main source, SNAP 2 - domestic combustion (37.1%).

Figure 7.4 - Total UK benzene emissions for 2022 by SNAP code scaled from NAEI 2021

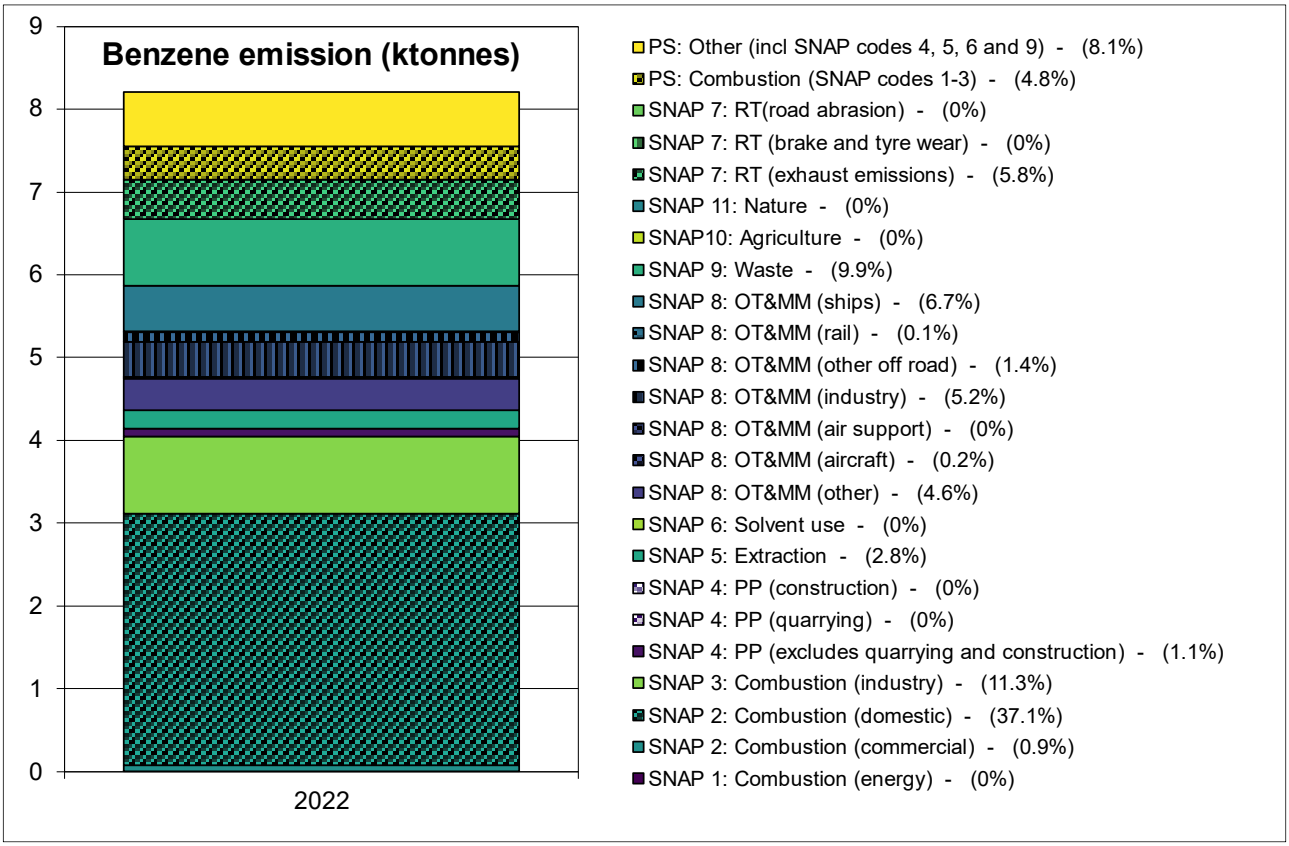

7.3 Benzene modelling

7.3.1 Contributions from large point sources

Following a similar methodology as for NO_x, benzene point sources in the NAEI 2021 have been classified as large if they fulfil any of the following criteria:

- Annual benzene emissions in the NAEI 2021 are greater than 5 tonnes for any given plant.
- Stack parameters are already available for any given plant in the PCM stack parameters database (described in more detail in Section 3.3.1).
- Emissions are not associated with fugitive releases.

Contributions to ground level annual mean benzene concentrations from large point sources in the NAEI 2021 were estimated by modelling each source explicitly using the atmospheric dispersion model ADMS 5.2 and sequential meteorological data for 2022 from the WRF numerical weather prediction modelling system, as described in Appendix 4 – WRF meteorology. The WRF model is a next-generation numerical weather prediction system developed by the US National Centre for Atmospheric Science (NCAR) (UCAR, 2020). This method accounts for spatial variation in meteorological parameters across the UK representing local dispersion characteristics within the PCM output. A total of 5 point sources were modelled as large point sources. Surface roughness varied at

both the dispersion and meteorological sites depending on the area type as presented in Table A5.1. Concentrations were calculated for a 99 km x 99 km square composed of a regularly spaced 1 km x 1 km resolution receptor grid. Each receptor grid was centred on the point source. For each large point source information was retrieved from the PCM stack parameters database.

The NAEI emissions for combustion point sources are for the year 2021; however, the year 2022 has been modelled for the assessment. The NAEI emissions for point sources for 2021 were therefore scaled to provide values for 2022.

The NAEI 2021 includes point source emissions estimates derived from carbon emissions data reported under the EU-Emissions Trading Scheme (ETS), most recently described in (Tsagatakis et al., 2022). These point sources are referred to as ETS points in this report. These derived air quality pollutant emissions are particularly uncertain and therefore in previous assessments (e.g. (Brookes *et al.*, 2017)) emissions were capped at reporting thresholds and treated as small point sources. For the 2016, 2017, 2018, 2019, 2020 and 2021 assessments (Brookes *et al.*, 2019b, 2019a, 2020, 2021; Pugsley *et al.*, 2022, 2023) the NAEI recommended treating the ETS points that have emissions greater than the large points modelling threshold as large points and not to apply a cap (Personal communication from Ben Pearson, 2023). The 2022 assessment continues this approach. Thus, based on the criteria for the treatment of large point sources described above, 19 ETS point sources were modelled as an additional set of large point sources (using the approach described above). ETS points that were not classified as large point sources were modelled using the benzene fugitive and small points approach described next.

7.3.2 Contributions from fugitive and small point sources

In line with the method applied for the large point sources the NAEI 2021 emissions for fugitive and small point sources have been scaled to 2022 using the same source sector specific projection factors applied to the large point sources.

The contributions to ambient concentrations from fugitive and small point sources were modelled using a small points modelling approach adapted specifically for fugitive and small point sources of benzene. The emissions from these sources are not generally as well characterised in terms of exact location and release parameters as emissions from large combustion related sources. Separate models are used for the concentration in the 1 km x 1 km grid square that includes the source (the 'in-square' concentration) and the concentration in surrounding grid squares (the 'out-square' concentration). The 'out-square' concentration has been estimated using a dispersion kernel similar to the one used for area sources of benzene. Hourly sequential meteorological data from the WRF model in 2022 has been used to construct the dispersion kernels. The 'in square' concentration has been estimated by assuming a volume source of dimensions 200 m x 200 m x 30 m in the centre of the square with the concentration estimated as the average across receptors excluding those inside the central 800 m x 800 m of the 1000 m x 1000 m grid square. These parameters have been chosen to provide the best fit to the range and maximum of available monitoring data in the vicinity of refineries (Grice *et al.*, 2009).

7.3.3 Contributions from rural background concentrations

Regional rural benzene concentrations were estimated from the map of rural NO_x concentration described in Section 3.3.4. The rural NO_x map was scaled using the ratio of averaged measured annual mean benzene and NO_X concentrations at the rural Chilbolton monitoring site across the last five period (2018 to 2022). This resulted in a value of 0.046921 for 2022. This is the method that was followed in 2019, 2020 and 2021 (Brookes *et al.*, 2021; Pugsley *et al.*, 2022, 2023). However, previous to this an alternative method was followed, where the ratio was based on annual mean benzene and NOx for the current modelling year only. The method change was implemented to reduce sensitivity of this component to a single year of measurements at a single site. Chilbolton has been the only rural background site in recent years providing sufficient data for both NOx and benzene, and in 2020 and 2021 the data capture was low at this site. In 2019 benzene measurements were higher than previous years, more consistent with benzene measurements at urban background locations in the network. Therefore this new method was adapted. The use of a five year average ensured that the ratio used was more consistent with previous assessments. This approach will be kept under review to ensure it remains appropriate for the future.

7.3.4 Contributions from area sources

The 2022 area source benzene emissions maps have been calculated from the NAEI 2021 emissions maps following the method applied for NO_X, described in Section 3.3.5. An ADMS derived dispersion kernel has been used to calculate the contribution to ambient concentrations at a central receptor location from the area source emissions (excluding SNAP 3) within a 33 km x 33 km square surrounding each receptor. Hourly sequential meteorological data from WRF in 2022 has been used to construct the dispersion kernels, as described in Appendix 5 – Dispersion kernels for the area source model.

Revised methods introduced in the 2011 assessment (Brookes *et al.*, 2012) for modelling the contributions to benzene from SNAP 2 (domestic and non-domestic combustion) and SNAP 3 (combustion in industry) area sources were used and have been described in Section 3.3.5.

The calibration coefficient for the area source model is derived by linear regression of a corrected measured annual mean background benzene concentration versus the modelled uncalibrated area source contribution. The measurements were derived from one site within the national automatic hydrocarbon network (London Eltham) and 17 non-automatic hydrocarbon sites. The corrected background concentration is derived by subtraction of the modelled contributions from SNAP 3 area sources, point sources and estimated rural benzene from the measured annual mean concentration at automatic and non-automatic pumped tube background monitoring sites. Figure 7.5 shows the calibration of the area source model. The modelled area source contribution (excluding SNAP 3) was multiplied by the background calibration coefficient to calculate the calibrated area source contribution for each grid square in the country. The SNAP 3 area source contribution, point source contributions and regional rural concentration were then added, resulting in a map of total background annual mean benzene concentrations.

Figure 7.5 - Calibration of area source benzene model, 2022 (µg m^{-3})

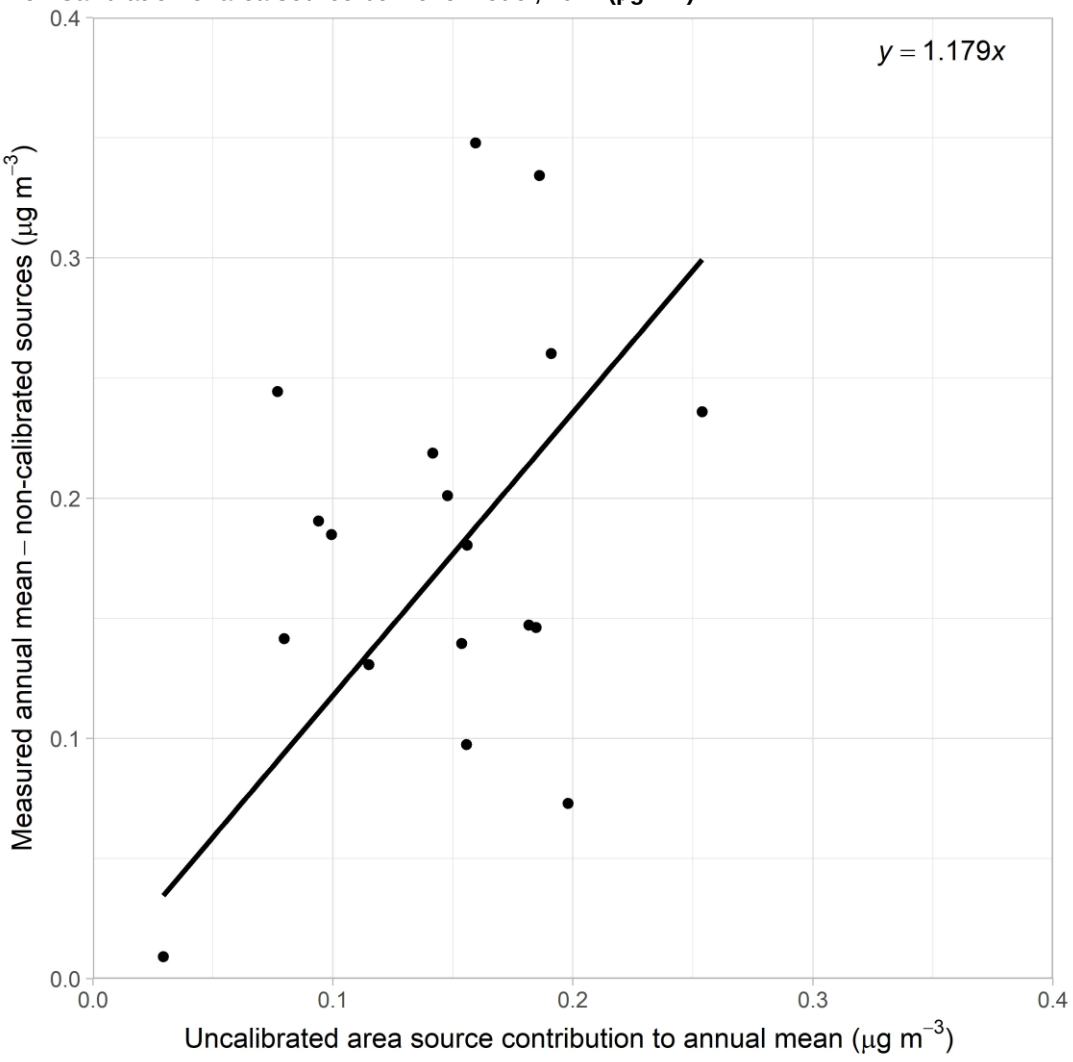

7.3.5 Roadside concentrations

Roadside annual mean concentrations of benzene for 2022 have been modelled using a similar method to the NO_X modelling described in Section 3.3.6. The NAEI provides estimates of benzene emissions for major road links in the UK for 2021 (Ingledew *et al.*, 2023) and these have been scaled to provide estimates of emissions in 2022. The projections for benzene road transport emissions include the inputs and assumptions summarised in Table 7.1.

The PCM Roads Kernel Model (PCM-RKM) described in Appendix 8 – The PCM Roads Kernel Model has been used to calculate the roadside increment. The PCM-RKM is based upon dispersion kernels generated by the ADMS-Roads dispersion model (v5.0) and represents a more process-based approach than the previous empirical method. It provides a more robust assessment, whilst retaining the link with measurement data provided using measurement data to calibrate this component of the model. Figure 7.6 shows the calibration of this model at roadside monitoring sites. Roadside concentrations for urban major road links (A-roads and motorways) only are reported to the EU and included in this report.

Measurements from seven non-automatic hydrocarbon sites were used to calibrate the roadside model.

Figure 7.6 - Calibration of benzene roadside increment model, 2022 (µg m^{-3})

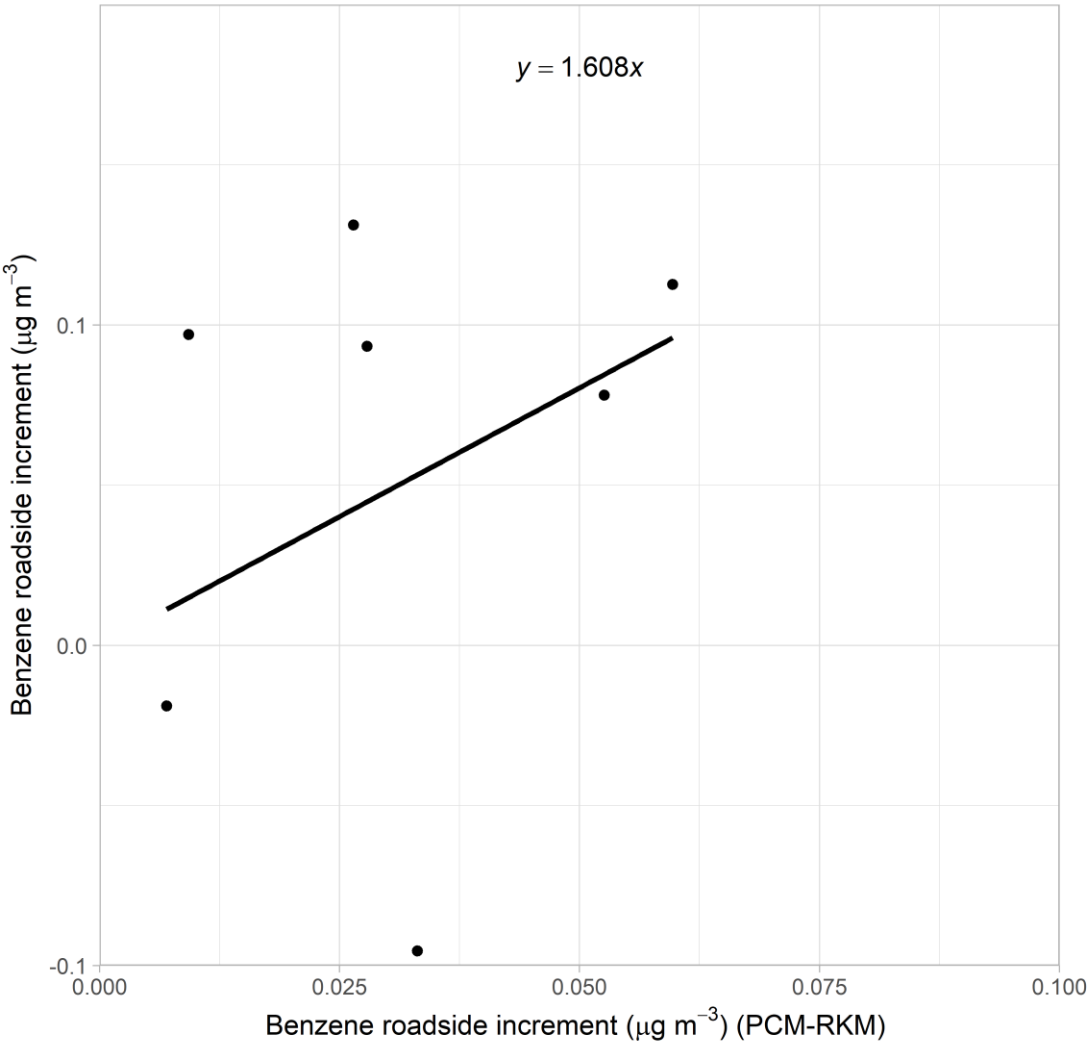

7.4 Results

7.4.1 Verification of mapped values

Figure 7.7 and Figure 7.8 show comparisons of the modelled and measured annual mean benzene concentrations for background and roadside locations. Lines showing y = x – 50% and y = x + 50% are included in these charts (the data quality objective for modelled benzene concentrations specified by the AQSR – see Section 1.5).

One monitoring site that was not included in the calibration are included in Figure 7.7. Summary statistics for the comparison between modelled and measured benzene concentrations are listed in Table 7.2 and Table 7.3.

Figure 7.7 - Verification of background annual mean benzene model 2022

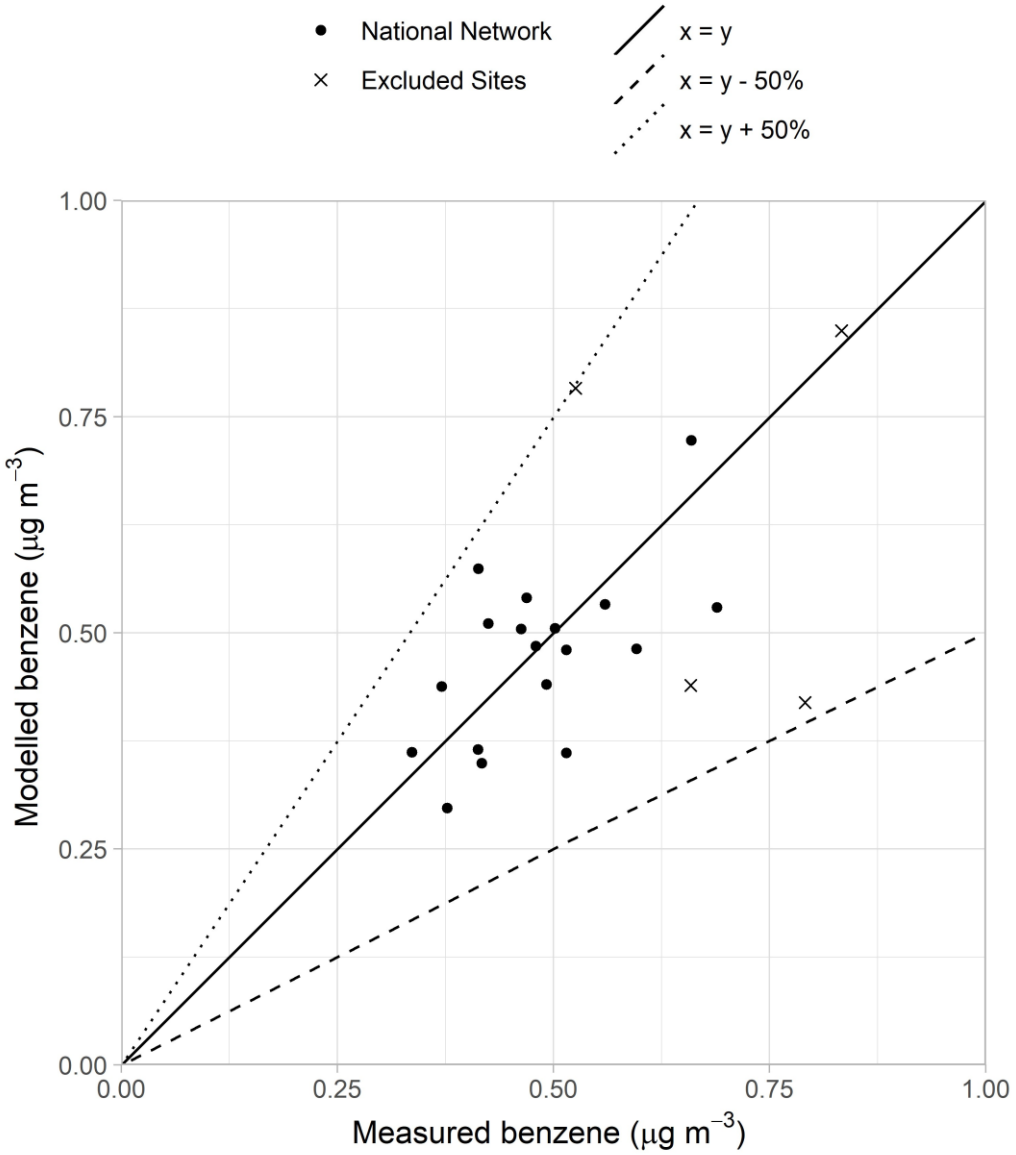

Figure 7.8 - Verification of roadside annual mean benzene model 2022

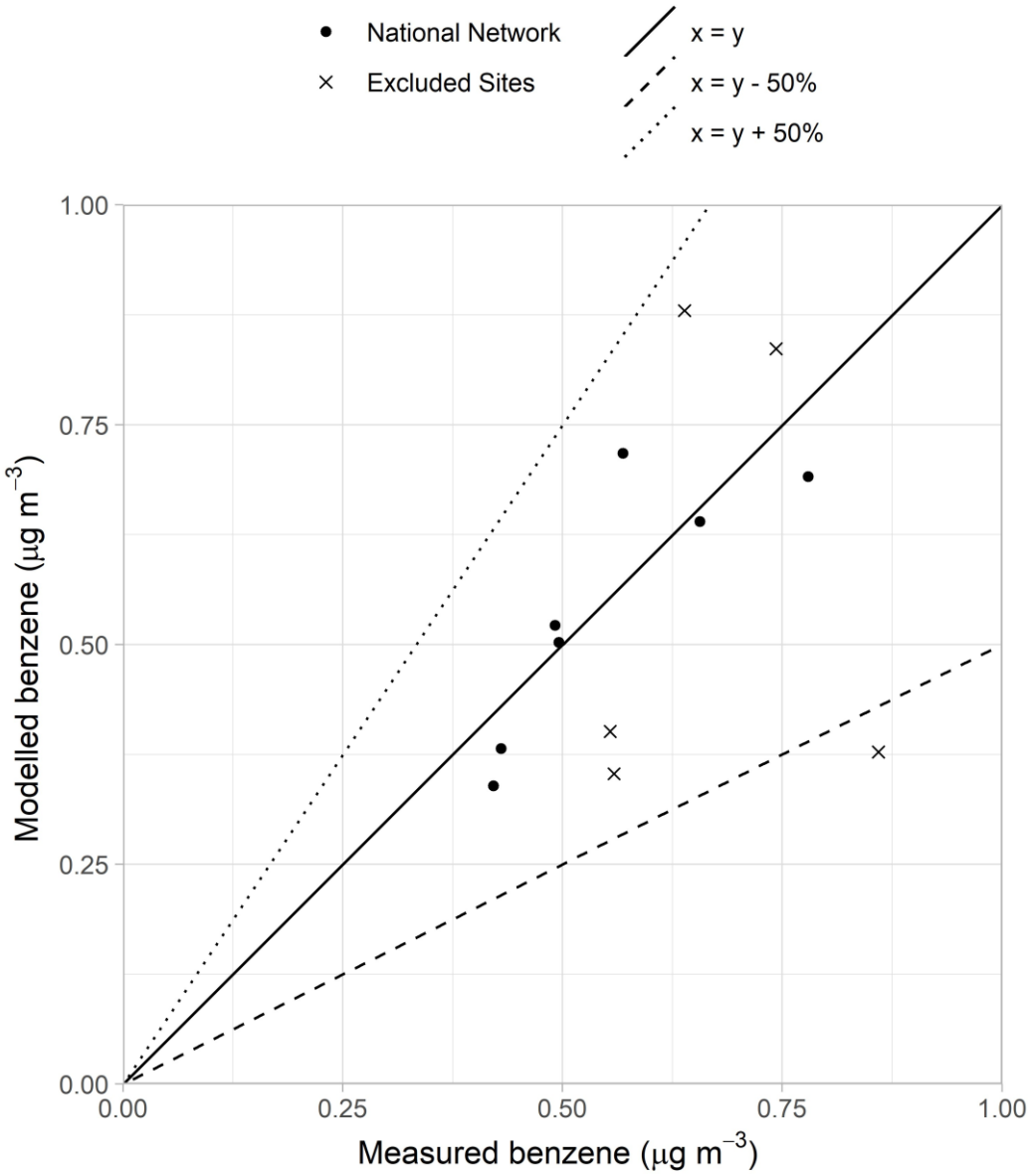

Table 7.2 - Summary statistics for comparison between modelled and measured benzene concentrations at background sites (µg m^{-3})

	Mean of measurements (µg m^{-3})	Mean of modelled (µg m^{-3})	R^2	% outside data quality objectives	Number of sites
National Network Sites	0.48	0.47	0.38	0	18

Table 7.3 - Summary statistics for comparison between modelled and measured benzene concentrations at roadside sites (µg m^{-3})

	Mean of measurements (µg m^{-3})	Mean of modelled (µg m^{-3})	R^2	% outside data quality objectives	Number of sites
National Network Sites	0.55	0.49	0.66	0	7

7.4.2 Benzene source apportionment at monitoring sites

Figure 7.9 and Figure 7.10 show the modelled annual mean benzene source apportionment for 2022 at background and roadside monitoring sites, respectively. The measured concentration at each site is also shown for reference. The regional background is an important component in the source apportionment for the majority of background monitoring sites. Contributions from domestic and industry sources are also important for many sites classified as urban and suburban background. The roadside source apportionment in Figure 7.10 shows that local traffic sources contribute up to 0.1 µg m^{-3} of benzene at these roadside sites, with the exception of London Marylebone Road where local traffic sources contribute 0.2 µg m^{-3} of benzene.

Figure 7.9 - Annual mean benzene source apportionment at background monitoring sites in 2022 (the area type of each site is shown in parenthesis after its name)

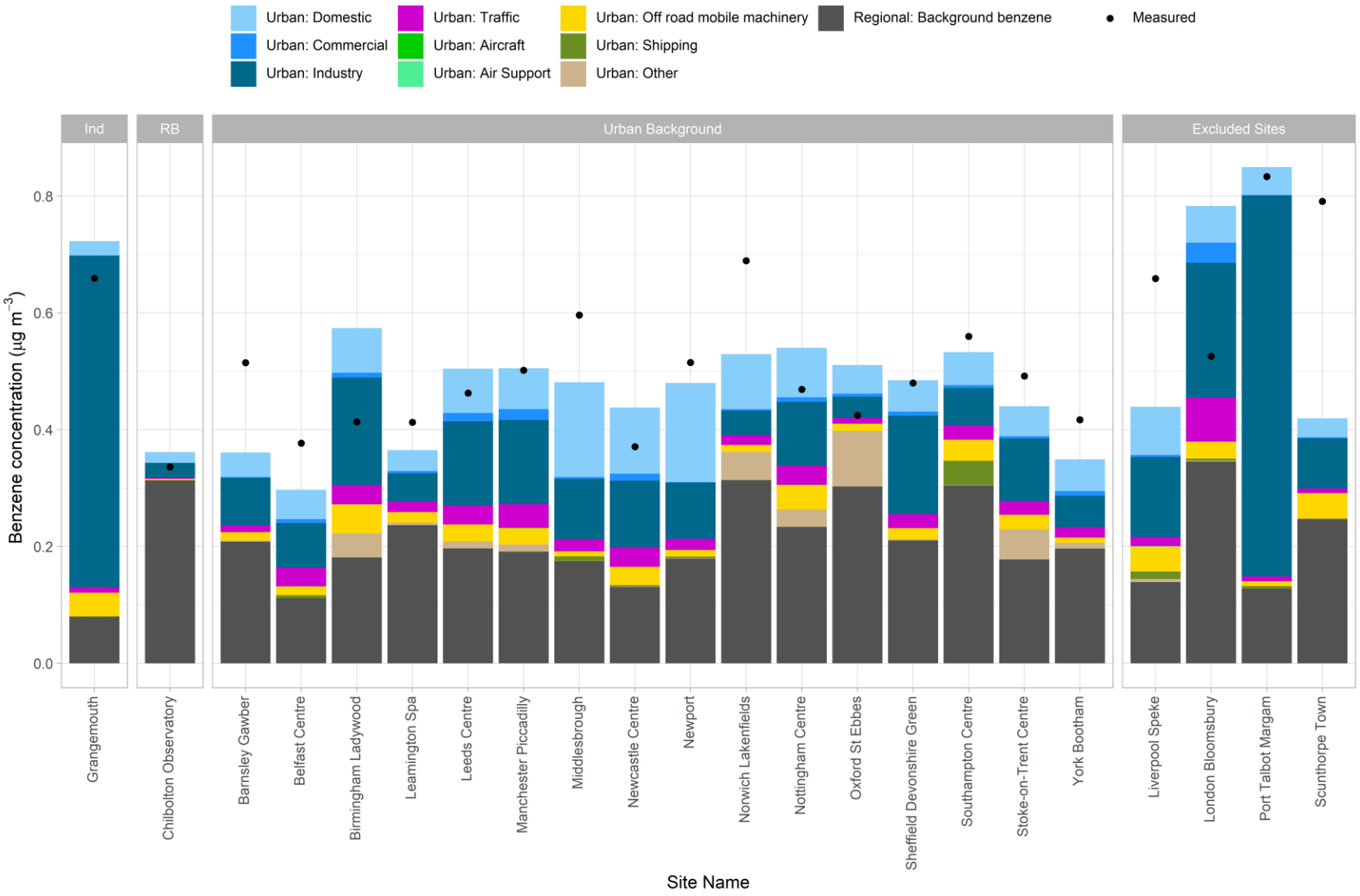

Figure 7.10 - Annual mean benzene source apportionment at roadside monitoring sites in 2022 (the area type of each site is shown in parenthesis after its name)

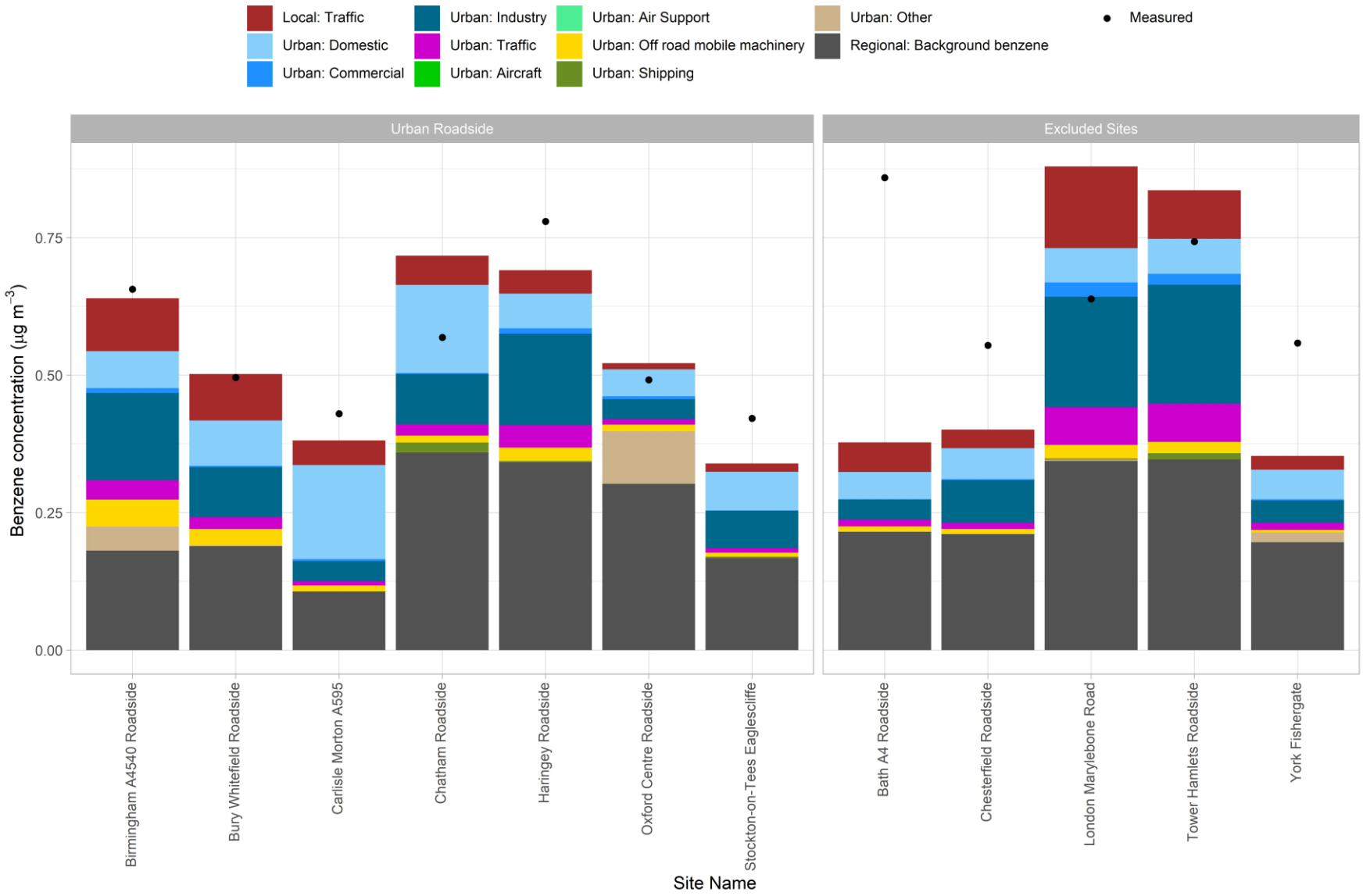

8 CO

8.1 Introduction

8.1.1 Limit values

A single limit value for ambient CO concentrations is set out in the AQSR (*legislation.gov.uk*, 2010). This limit value has been specified for the protection of human health. The limit value is a maximum daily 8-hour mean concentration of 10 mg m^{-3}.

8.1.2 Objective Estimation

The maximum measured daily 8-hour running mean for 2022 are presented in Table 8.1 for all sites. Data capture was greater than 85% at six sites, during 2022. All values are below the lower assessment threshold of 5 mg m^{-3}.

Table 8.1 - Maximum daily 8-hour running mean (mg m^{-3}) in 2022[6]

EOI code	Site Name	Maximum daily 8-hour running mean (mg m^{-3})	Data capture (%)
GB0567A	Belfast Centre	0.82	96
GB0580A	Cardiff Centre	0.90	90
GB0839A	Edinburgh St Leonards	0.49	95
GB0584A	Leeds Centre	0.63	96
GB0682A	London Marylebone Road	1.30	78
GB0620A	London N. Kensington	1.40	88
GB0906A	Port Talbot Margam	2.20	92

The AQSR states that objective estimation may be used to assess ambient air quality at levels below the lower assessment threshold. Objective estimation has been used to conclude that concentrations were likely to have been well below the limit value for CO in all zones during 2022. This assessment has been made on the basis of the low measured concentrations and the lack of any expected large increase in future CO emissions illustrated in the following section.

8.1.3 CO emissions

Estimates of the emissions from the UK National Atmospheric Emission Inventory 2021 (NAEI 2021) have been used in this assessment (Ingledew *et al.*, 2023). Emissions projections have been provided by the NAEI (Personal communication from Ben Pearson, 2023) based on BEIS EEP 2022 energy and emissions projections (BEIS, 2022). Figure 8.1 shows the UK total CO emissions for 2022 and emissions projections for each year up to 2030 split by SNAP code, with the coding described in Table 3.2. Values for intermediate years have been interpolated in this figure.

There is a relatively small decrease in emissions in road transport exhaust emissions throughout the period. Emissions from domestic combustion are expected to remain relatively constant throughout the period. Emissions from off-road mobile machinery are expected to show a small increase. Overall, the changes in emissions shown in Figure 8.1 are relatively small when viewed in the context of the significant decreases in CO emissions from road transport, domestic combustion and combustion point sources (SNAP codes 1-3) from 1990 to 2020 present in the NAEI 2021 (Ingledew *et al.*, 2023), which led to a reduction in total UK emissions of CO over this period of 79%.

[6] Values have been presented to 2 significant figures to illustrate the dynamic range of the data.

Figure 8.1 - Total UK CO emissions for 2021 and emissions projections up to 2040 by SNAP code from NAEI 2021

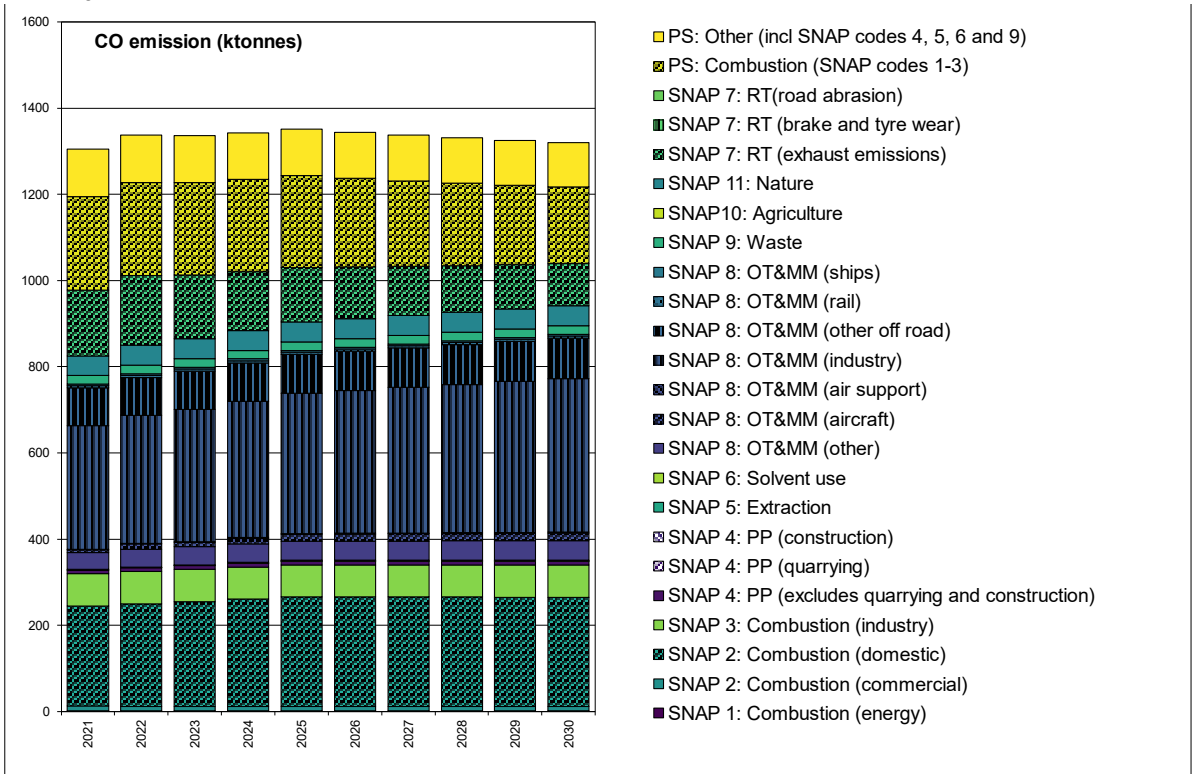

9 Ozone

9.1 Introduction

9.1.1 Target values and long-term objectives

Two target values (TV) for ambient ozone concentrations are set out in the AQSR (*legislation.gov.uk*, 2010), these are:

- A maximum daily 8-hour mean concentration of 120 µg m^{-3}, not to be exceeded on more than 25 days per calendar year averaged over three years
- AOT40[7] (calculated from 1-hour values) of 18000 µg m^{-3}.h May to July averaged over five years

The TVs have been specified for the protection of human health and the protection of vegetation respectively, both came into force from 01/01/2010.

Two long term objectives (LTO) for ambient ozone concentrations are also set out in the AQSR, these are:

- A maximum daily 8-hour mean concentration of 120 µg m^{-3} within a calendar year
- AOT40 (calculated from 1-hour values) of 6000 µg m^{-3}.h May to July

The LTOs have been specified for the protection of human health and the protection of vegetation respectively. The date for compliance with the LTOs has not been defined.

Results of the assessment in terms of comparisons of the modelled concentrations with the TVs and LTOs by zone have been reported in e-Reporting Data flow G published on UK-Air (*UK-Air*, 2023).

9.1.2 Ozone modelling

An empirical mapping approach has been used for predicting ozone concentrations in 2022; this follows recommendations originally made by (Bush and Targa, 2005) in a study comparing the relative performance of the available techniques for modelling ozone within the UK.

The empirical approach draws upon measurements from the monitoring stations in the AURN during 2022 to produce functions describing ground-level ozone based on interpolated rural measurements of the ozone metrics corrected for local emissions of NO_X. These functions predict ozone levels at a resolution of 1 km x 1 km and the methods are briefly described in the following sections. Full details can be sourced from the cited references.

The methods used here are based upon those presented by (PORG (UK Photochemical Oxidants Review Group), 1998; NEGTAP, 2001; Coyle *et al.*, 2002; Murrells *et al.*, 2011). (Murrells *et al.*, 2011) suggested that the observed dependence of the AOT40 metric on altitude, previously attributed to differences in surface deposition and reactions with local NO with altitude, was largely explained by the proximity of monitoring stations to urban areas. The 2022 assessment of the TV and LTO for AOT40, takes on the recommendations of (Murrells *et al.*, 2011) and does not include an altitude correction and thus avoids double counting the NO_X urban decrement.

9.1.3 Overview of the PCM model for ozone

Figure 9.1 shows a simplified flow diagram of the PCM model for ozone. A summary of the PCM model method, input and assumptions for ozone is presented in Table 9.1.

9.1.4 Chapter structure

This chapter describes modelling work carried out for 2022 to assess compliance with the ozone TVs and LTOs described above. Section 9.2 describes the modelling methods and results in relation to the number of days exceeding 120 µg m^{-3} metrics. Section 9.3 describes the modelling methods and results in relation to the AOT40 metrics.

[7] The definition of ATO40 has been given in Part 1.2 of the AQSR

Figure 9.1 - Flow diagram for PCM ozone model

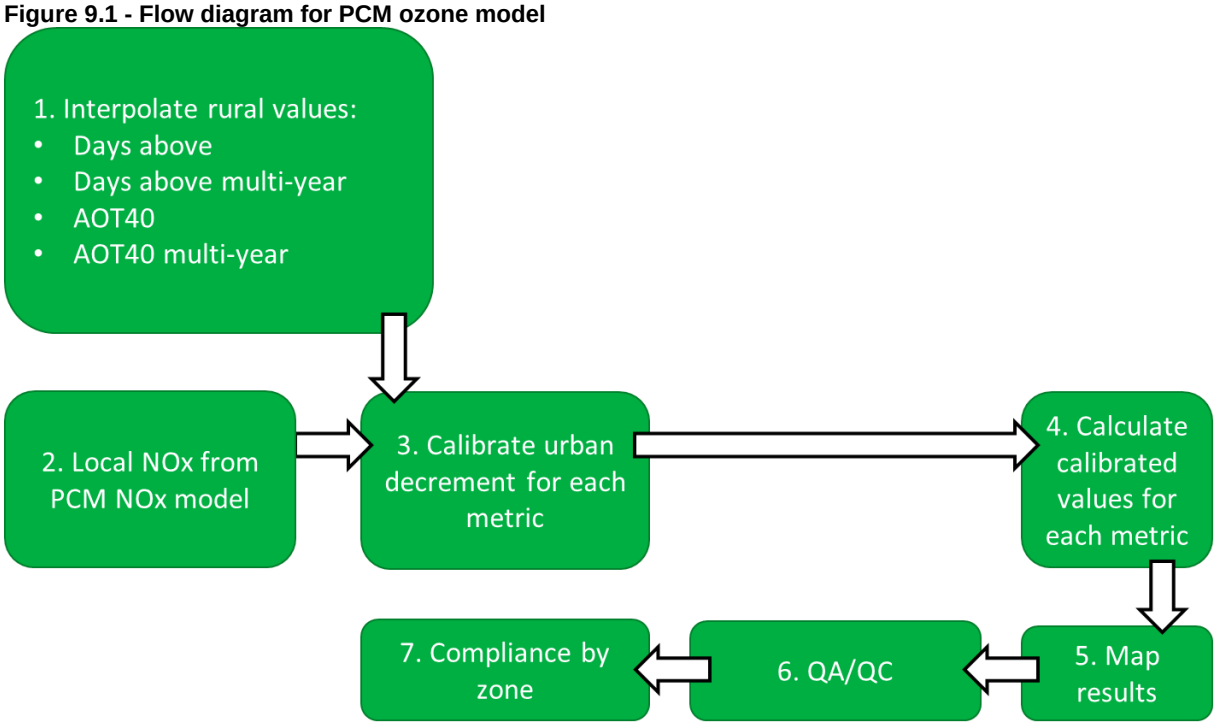

Table 9.1 - PCM model method, input and assumptions summary for ozone

Heading	Component	Details
General	Pollutant	O_3
	Year	2022, 2018-2022 mean and 2020-2022 mean
	Locations modelled	Background
	Metric	AOT40 (2022 and 2018-2022 mean), number of days with maximum 8-hour mean above 120 µg m^{-3} (2022 and 2020-2022 mean)
Input data	Emission inventory	NAEI 2021 (For NO_X)
	Energy projections	Energy Projections 2022 (For NO_X)
	Road traffic counts	2022 (scaled from 2021 where not available) (For NO_X)
	Road transport activity projections	DfT (2022) car sales projections, TfL fleet projections for London (2023) (For NOx)
	Road transport emission factors	COPERT 5.4 (COPERT 5.4, 2020) (For NO_X)
	Measurement data	2022
	Meteorological data	WRF (see Appendix 4 – WRF meteorology) (For NO_X)
Model components	Regional	Interpolated from rural ozone measurements
	Urban decrement	See details under “pollutant specific” heading
Calibration	Model calibrated?	Yes
	Number of background stations in calibration	61 (AOT40 2022), 61 (AOT40 2018-2022), 58 (days above 2022), 62 (days above 2020-2022)
	Number of traffic stations in calibration	n/a

Pollutant specific	Urban decrement	Empirical relationship between urban decrement and local NO_X contribution from PCM model results

9.2 Modelling the number of days exceeding 120 µg m^{-3} metric

9.2.1 Days greater than 120 µg m^{-3} methodology

Maps of the modelled number of days with maximum daily 8-hour mean ozone concentrations greater than 120 µg m^{-3}, for comparison with the LTO (2022) and TV (averaged 2020 to 2022) are presented in Figure 9.2 and Figure 9.3 respectively.

At rural locations in the UK exceedances of 120 µg m^{-3} as a maximum daily 8-hour mean are broadly consistent over wide spatial scales. As a result, measured exceedances from rural monitoring stations have been interpolated by Inverse Distance Weighting (IDW) throughout the whole of the UK to represent the likely exceedances of this metric in the absence of any influence from local emissions of NO_X from combustion sources.

The resultant interpolated maps, however, will overestimate exceedances in urban areas, where nitric oxide emissions from combustion sources deplete ozone concentrations. This effect has been accounted for by adding an empirically derived urban ozone decrement, expressed as a percentage. The percentage decrement is defined as follows:

% decrement = 100((measured concentrations - rural interpolated concentration)/rural interpolated concentration)*

The derivation of a coefficient relating the percentage decrement to the modelled local NO_X concentration is shown in Figure 9.4 and Figure 9.5. The local NO_X component is calculated as the sum of contributions from local point and area sources of NO_X emissions, calculated as described in Section 3.3.

Figure 9.4 shows the decrement plot for days greater than 120 µg m^{-3} in 2022 (the LTO for human health metric) and Figure 9.5 shows the decrement plot for days greater than 120 µg m^{-3} between 2020 and 2022 (the TV for human health metric). For some monitoring sites the decrement is positive, indicating that the measured number of days exceeding 120 µg m^{-3} is higher than the corresponding estimated rural value i.e. that the urban influence for these sites is not properly represented in the model. The cluster of low values close to the origin of these plots largely consists of the rural sites, at which there will be little difference between the rural estimated number of days exceeding 120 µg m^{-3} and the measured value. This helps to anchor the relationship to the origin. Percentage urban increments of -100% indicate that there were no measured exceedances of 120 µg m^{-3} at that monitoring site.

The calculated decrement is then used to correct the number of days where ozone concentrations are greater than 120 µg m^{-3} at rural sites, used for the interpolated maps:

Corrected days above 120 µg m^{-3} map = interpolated rural map + decrement

The decrement is a negative value and so reduces the concentration presented in the interpolated rural map to account for the reduction in ozone concentrations due to reaction with NO. Where the results of the expression predict a number of days less than 0.5, the predicted value is rounded to zero.

Figure 9.2 - Estimated number of days with an 8-hour mean ozone concentration above 120 µg m^{-3}, 2022

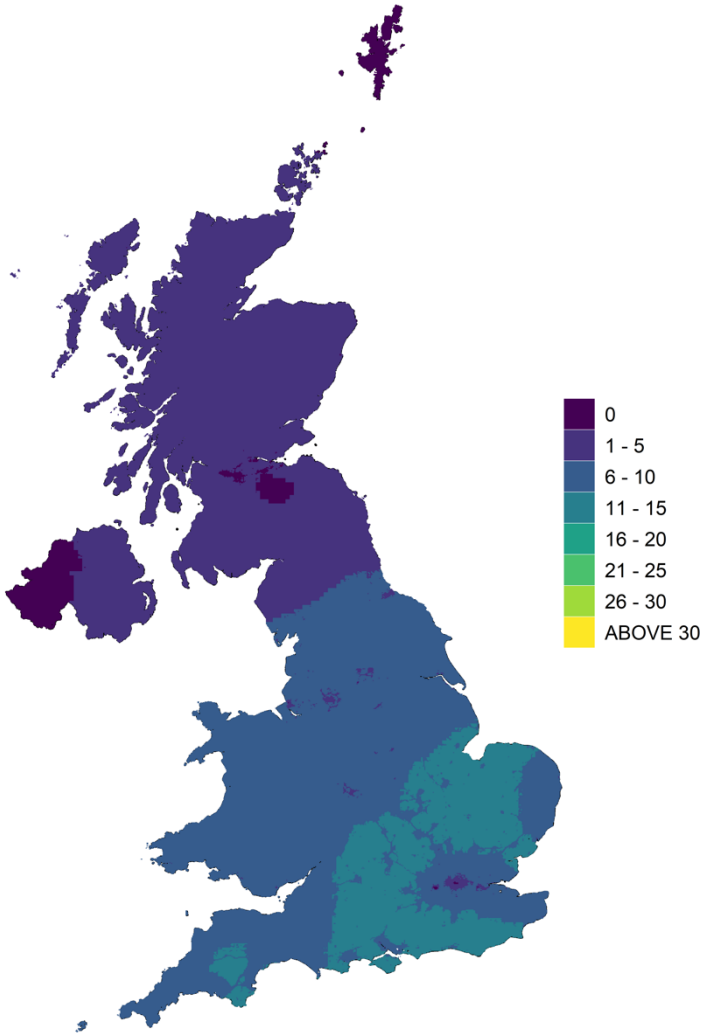

Figure 9.3 - Estimated average number of days with an 8-hour mean ozone concentration above 120 µg m^{-3}, 2020 to 2022

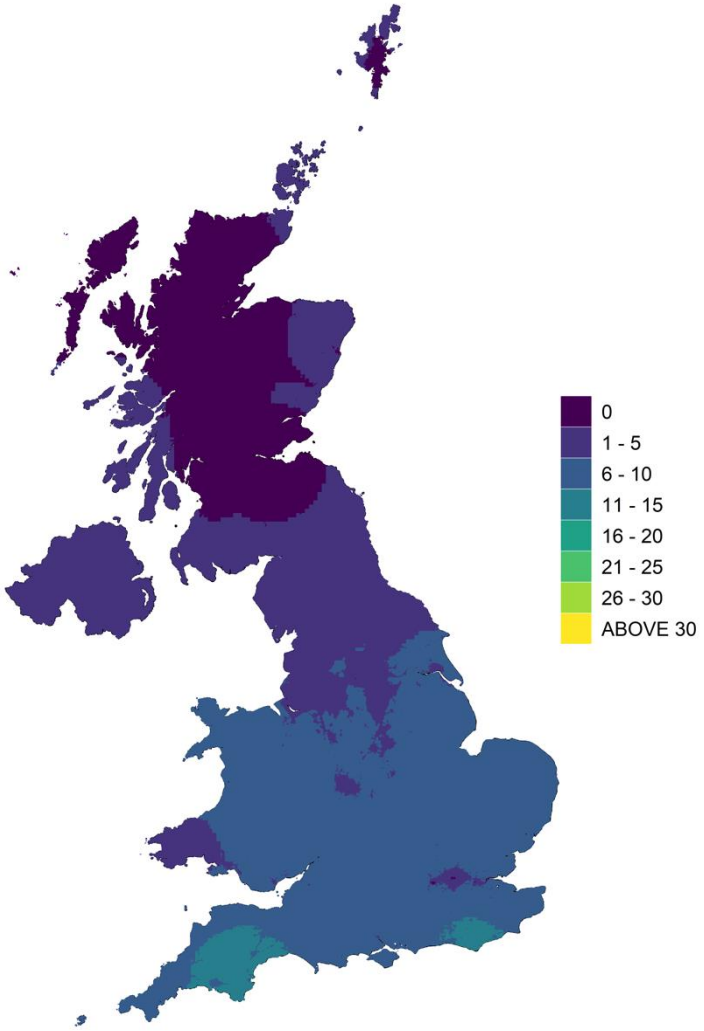

Figure 9.4 - Days greater than 120 µg m^{-3} percentage decrement in ozone concentrations, 2022

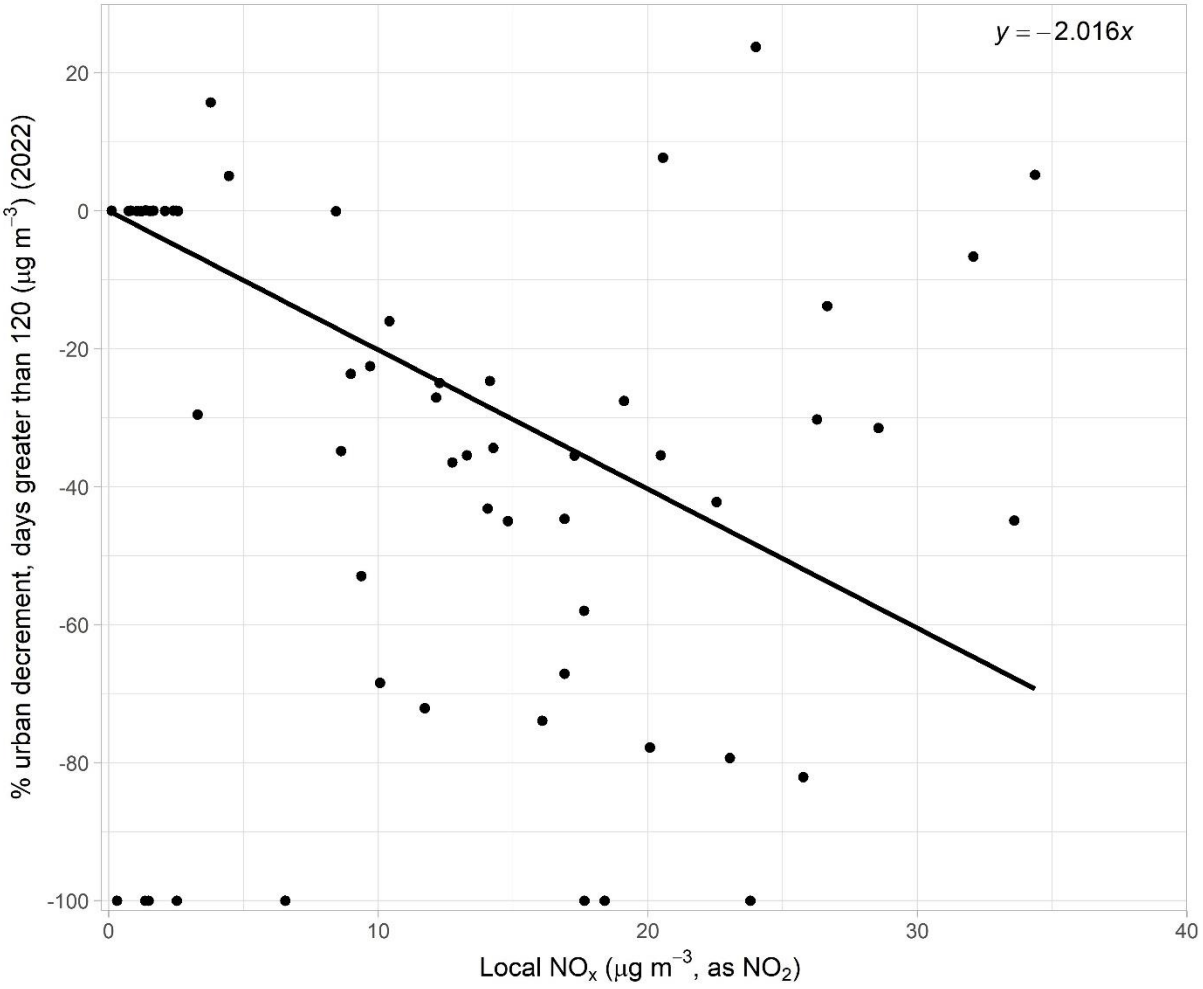

Figure 9.5 - Days greater than 120 µg m^{-3} percentage decrement in ozone concentrations, 2020-2022

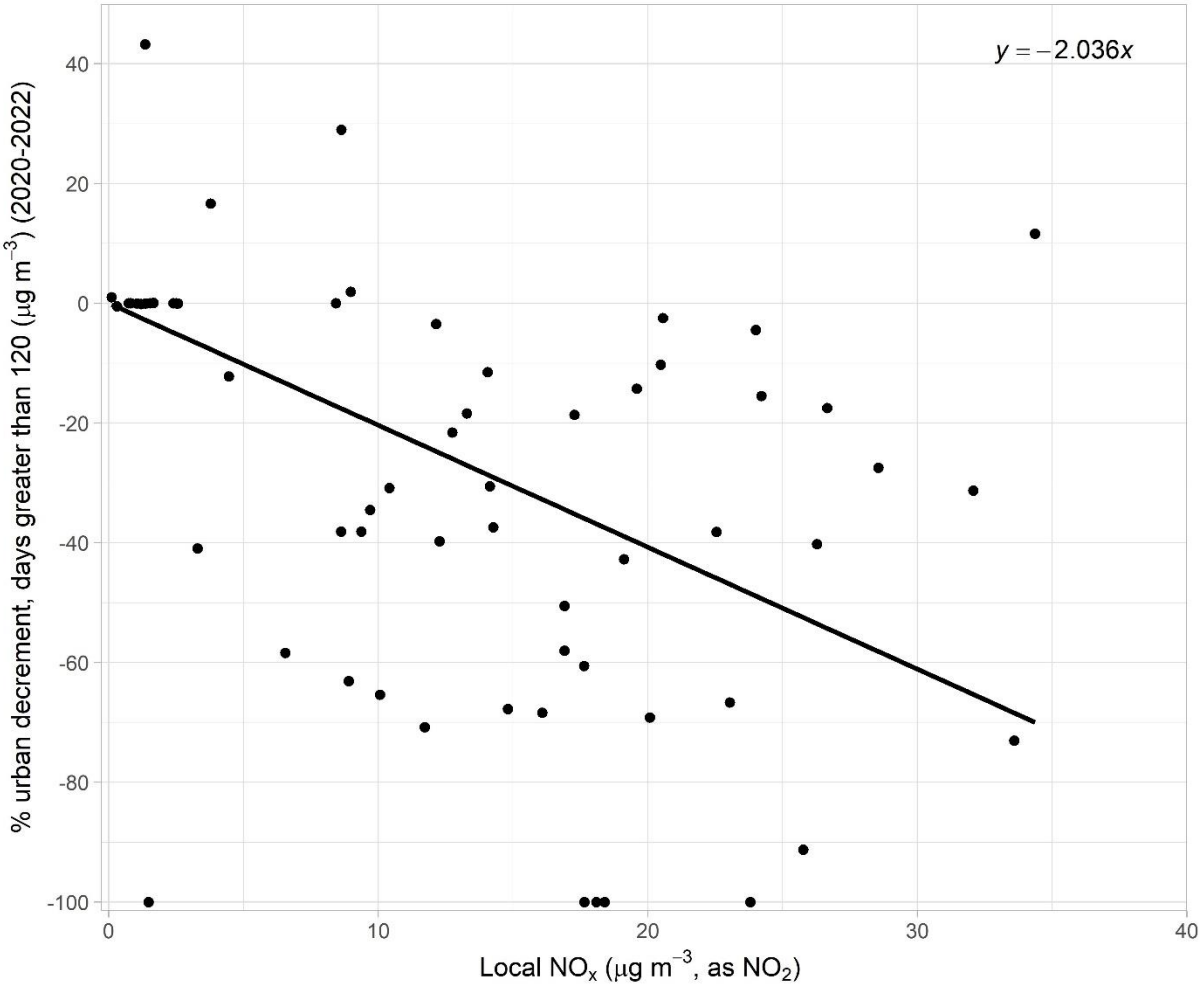

9.2.2 Verification of the number of mapped days > 120 µg m^{-3} values

Figure 9.6 and Figure 9.7 compare the number of modelled and measured days with maximum daily 8-hour mean ozone concentrations greater than 120 µg m^{-3} in 2022 and averaged 2020-2022 at background locations, respectively. Both the national network sites used to calibrate the models and the verification sites are shown. Lines representing y = x + 50 % and y = x - 50% are also shown, as this is the AQSR data quality objective for modelled ozone concentrations – see Section 1.5.

Figure 9.6 - Verification of background number of days > 120 µg m^{-3} model 2022

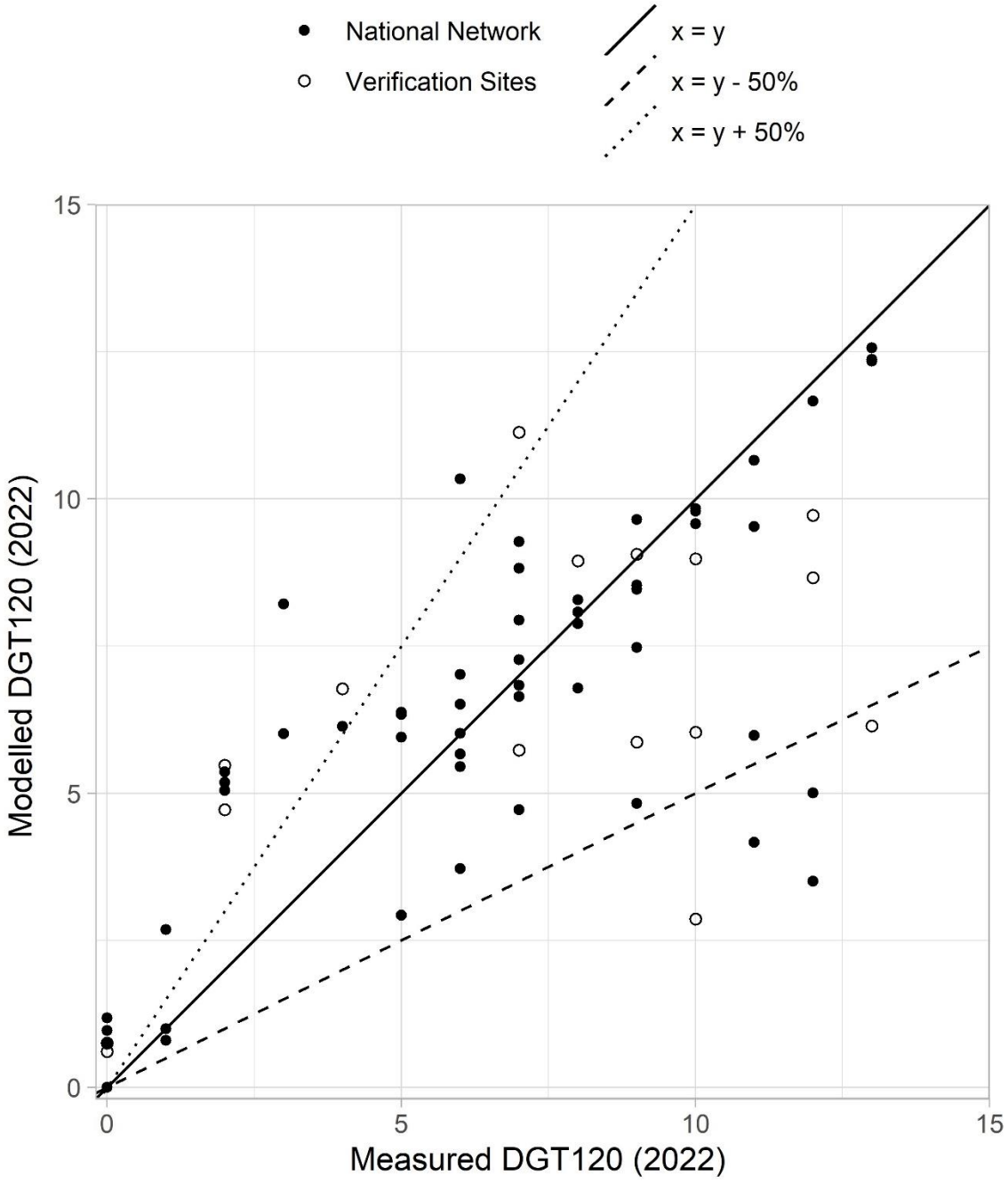

Figure 9.7 - Verification of background number of days > 120 µg m^{-3} model 2020-2022

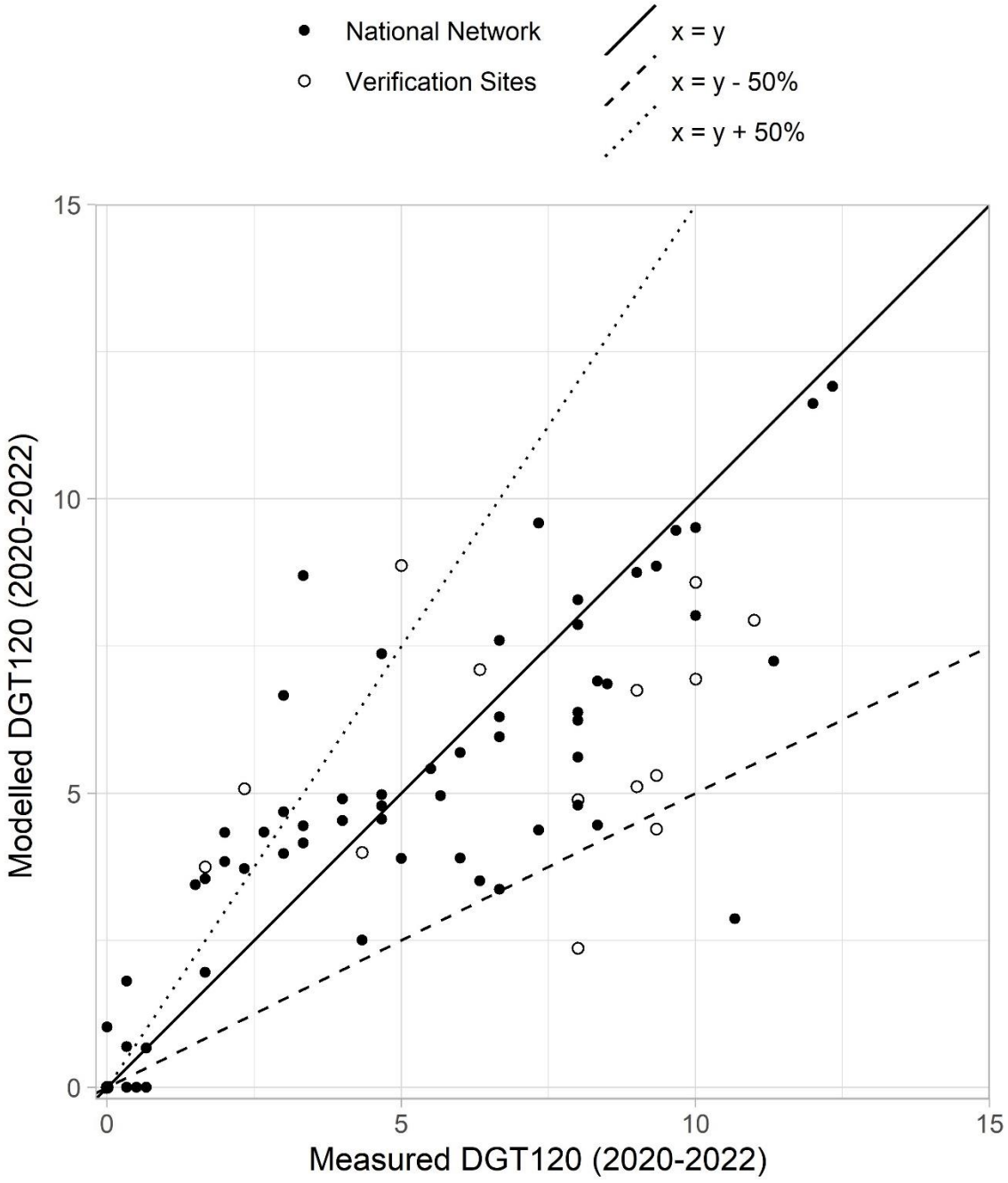

Figure 9.6, Figure 9.7 and Table 9.2 show that, on average, the agreement between model estimates and measurement is good for the number of days greater than 120 µg m^{-3} for the LTO and TV compared with measurements at verification sites. For both metrics, the agreement between model estimates and measurement is good for National network sites, which reflects that these measurements are part of the calibration process. The R^2 value for the verification sites, shown in Table 9.2 is lower for both metrics. There are few independent ozone monitoring sites available for model verification.

Table 9.2 - Summary statistics for comparison between modelled and measured number of days exceeding 120 µg m^{-3} as a maximum daily 8-hour mean

		Mean of measurements (days)	Mean of model estimates (days)	R^2	% outside DQO	No. sites
National network	2022	6.2	6.0	0.62	26%	58
Verification sites	2022	7.2	6.3	0.37	50%	16
National network	2020-2022	5.0	4.8	0.68	29%	62
Verification sites	2020-2022	6.9	5.1	0.31	33.3%	15

9.3 Modelling the AOT40 vegetation metric

9.3.1 AOT40 methodology

Maps of modelled AOT40 for comparison with the LTO (2022) and TV (averaged 2018 to 2022) are presented in Figure 9.8 and Figure 9.9 respectively.

The AOT40 vegetation metrics for 2022 and the averaged metric for 2018-2022 were calculated from measured data at rural monitoring stations in the AURN. These data were interpolated by Inverse Distance Weighting (IDW) to produce a rural map.

An urban decrement term was subsequently defined for those monitoring stations in the AURN and the rural map to correct for the depletion of ozone in areas close to sources of NO. As for the days above 120 µg m^{-3} metric, the decrement is closely related to the annual mean NO_X concentration, and has been defined in a similar fashion, using a percentage decrement in ozone concentrations associated with local NO_X concentrations.

Using the same methodology discussed in Section 9.2.1 for the days greater than 120 µg m^{-3} maps, the decrement was then used to correct the final AOT40 maps:

Corrected AOT40 map = interpolated rural map + decrement

The relationships between the decrement and modelled NO_X concentrations for 2022 and 2018-2022 averaged metrics are presented in Figure 9.10 and Figure 9.11 respectively.

Figure 9.8 - Estimated AOT40 vegetation metric, 2022 (µg m^{-3} hours)

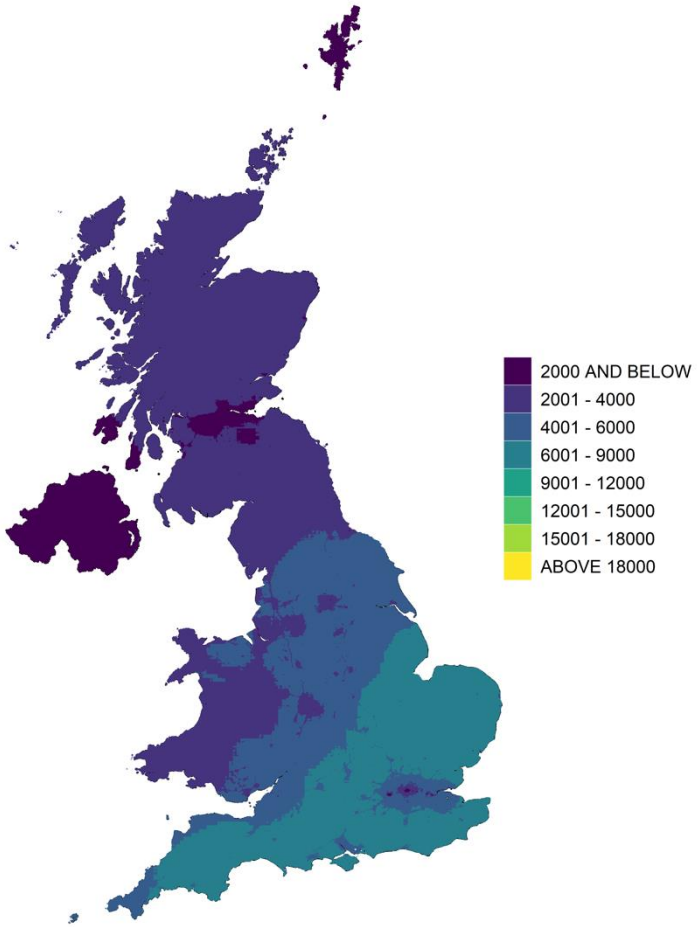

Figure 9.9 - Estimated AOT40 vegetation metric, averaged 2018-2022 (µg m^{-3} hours)

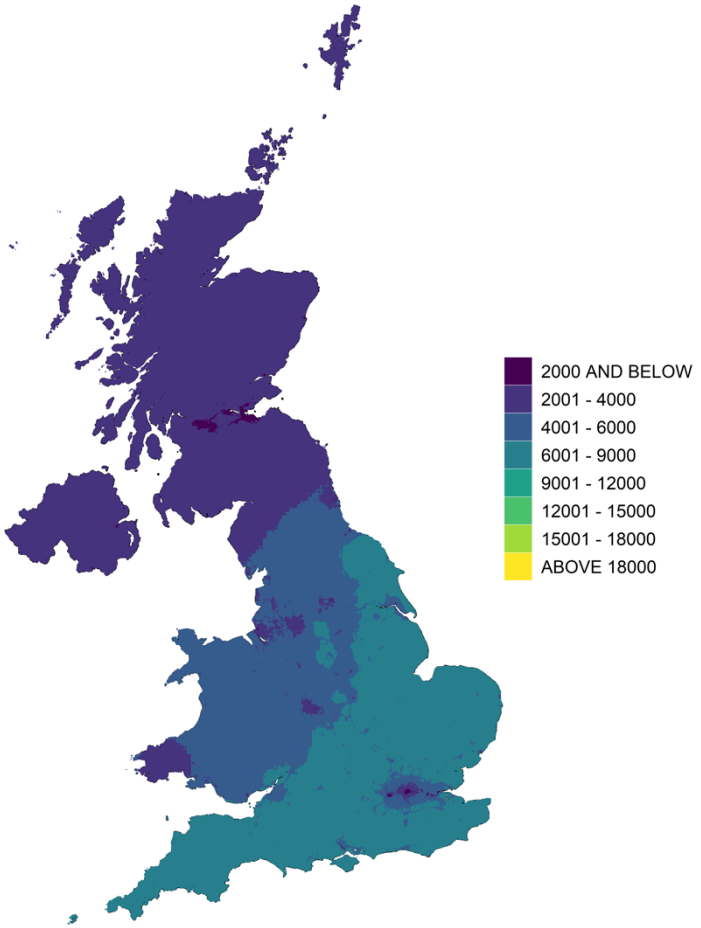

Figure 9.10 - AOT40 percentage decrement in ozone concentrations, 2022

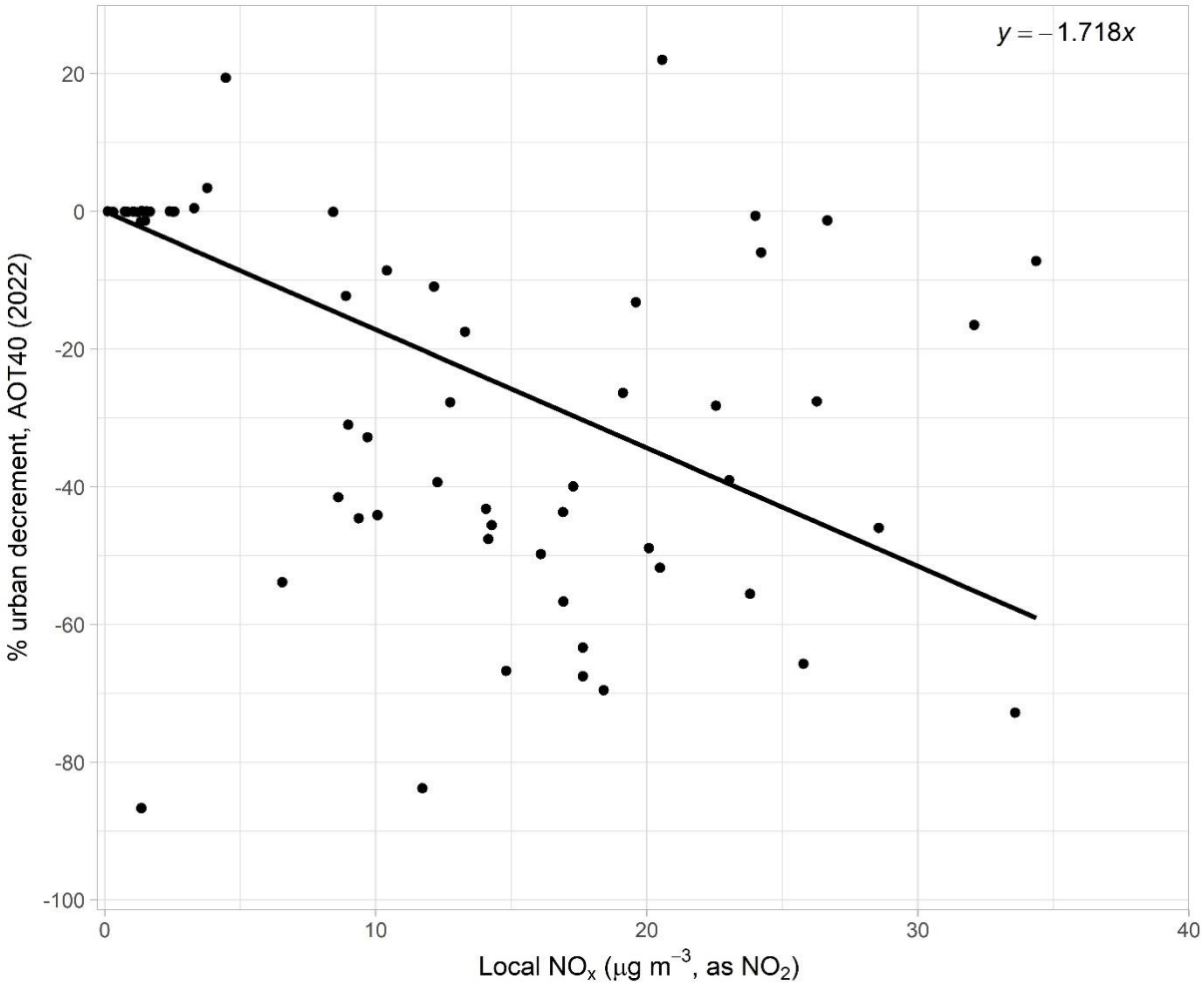

Figure 9.11 - AOT40 percentage decrement in ozone concentrations, 2018-2022

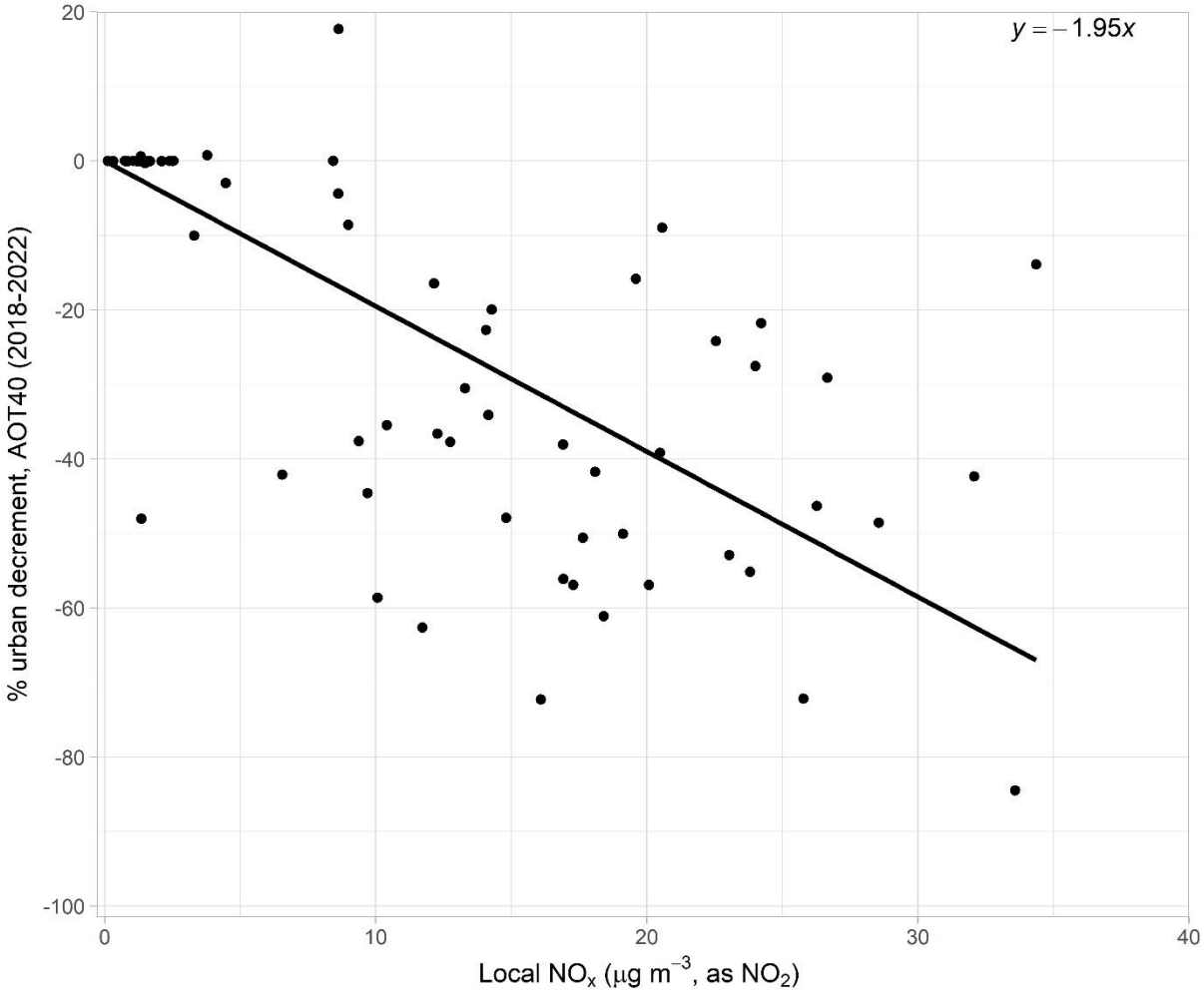

9.3.2 Verification of mapped AOT40 values

Figure 9.12 and Figure 9.13 show a comparison of modelled and measured AOT40 metrics in 2022 and averaged 2018-2022 at background locations. Both the national network sites used to calibrate the models and the verification sites are shown. Lines representing y = x + 50 % and y = x - 50% are also shown, as this is the AQSR data quality objective for modelled ozone concentrations – see Section 1.5.

Figure 9.12 - Verification of background AOT40 vegetation model, 2022

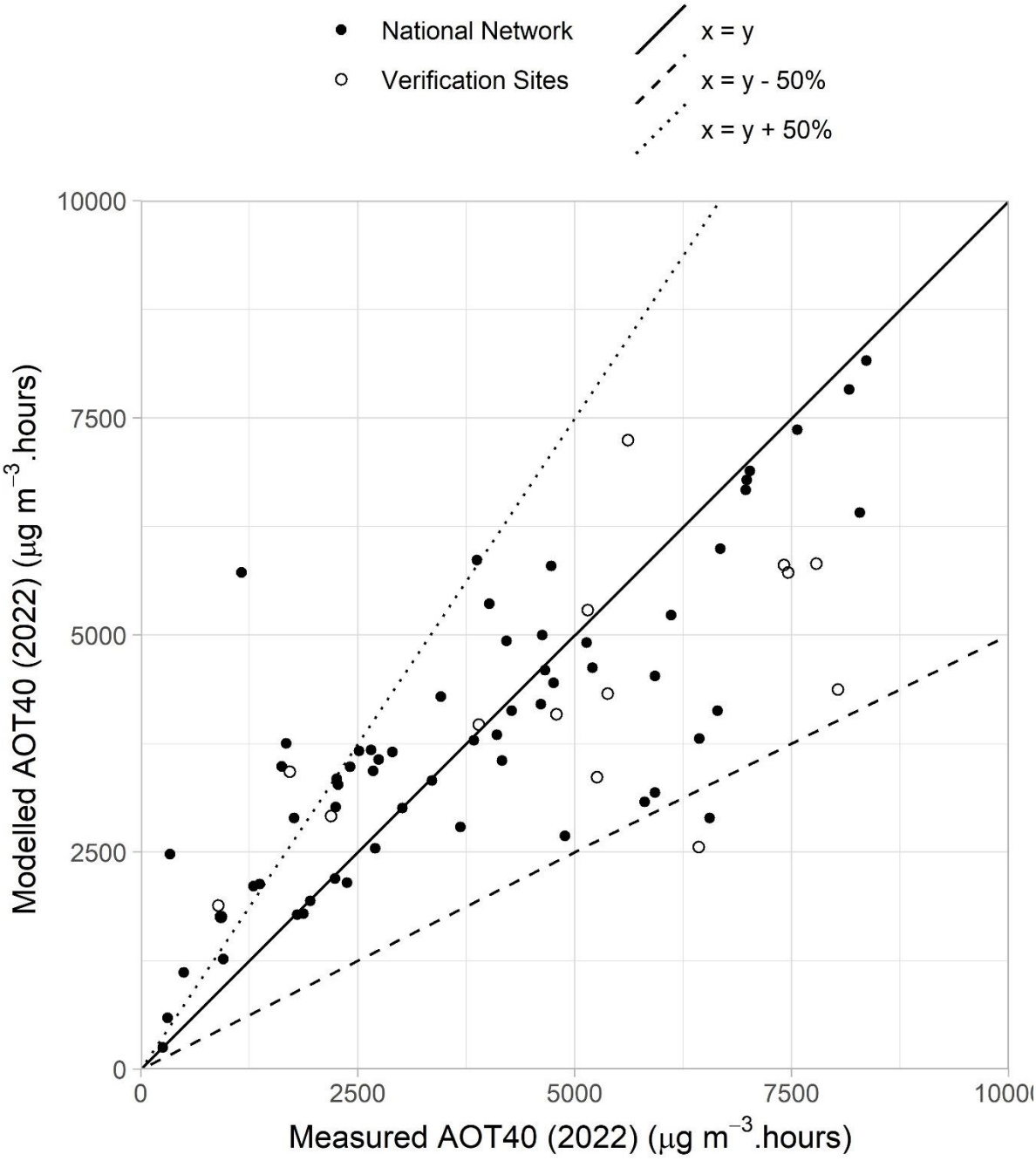

Figure 9.13 - Verification of background AOT40 vegetation model, 2018-2022

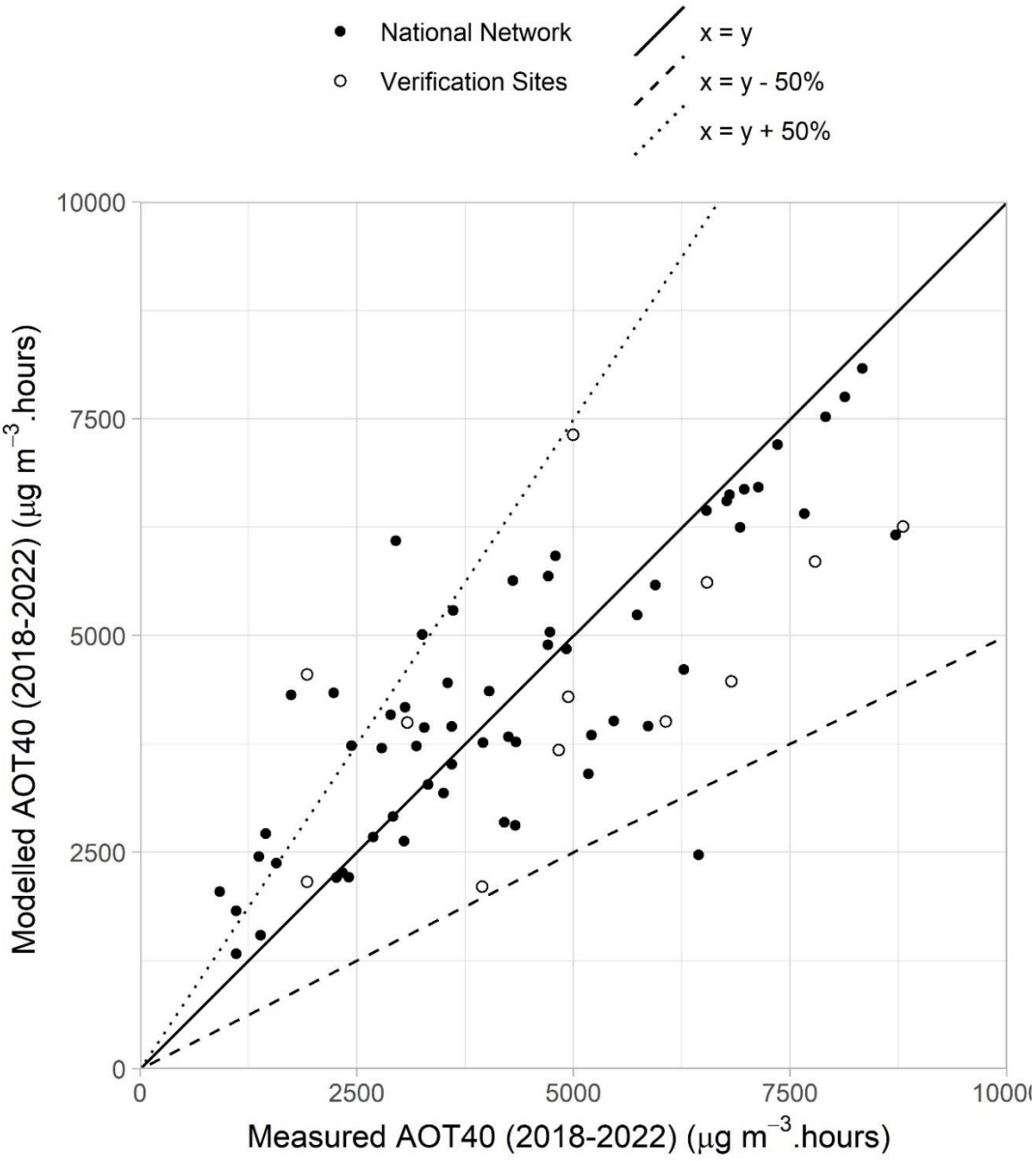

Model performance for both the LTO and TV for the AOT40 metrics is similar to that for the days greater than 120 µg m^{-3}. The R^2 values are relatively poor for the verification sites for both metrics. However, there the R^2 value is higher for the LTO and there are fewer sites outside the DQO than for the days greater than 120 µg m^{-3} for both metrics.

Table 9.3 - Summary statistics for comparison between modelled and measured AOT40 vegetation metric

		Mean of measurements (µg m^{-3} hours)	Mean of model estimates (µg m^{-3} hours)	R^2	% outside DQO	No. sites
National network	2022	3801	3883	0.63	20%	61
Verification sites	2022	4861	4170	0.49	27%	15
National network	2018-2022	4299	4346	0.66	18%	61
Verification sites	2018-2022	5138	4473	0.35	8%	12

10 Arsenic, Cadmium, Nickel and Lead

10.1 Introduction

10.1.1 Target and Limit values

A single limit value for ambient lead (Pb) concentrations is set out in the AQSR (*legislation.gov.uk*, 2010). This limit value has been specified for the protection of human health and came into force from 01/01/2005. The limit value is an annual mean concentration of 0.5 µg m^{-3}.

The target values (TV) for As, Cd and Ni included in the AQSR are listed in Table 10.1. The regulations states that all necessary measures not entailing disproportionate costs to ensure that the target values are not exceeded after the compliance date should be taken.

Table 10.1 - Target values for As, Cd, and Ni

Pollutant	Averaging period	TV (ng m^3)	Date after which the TV is not to be exceeded
As	Calendar year	6	31 December 2012
Cd	Calendar year	5	31 December 2012
Ni	Calendar year	20	31 December 2012

10.1.2 Annual mean models

Maps of annual mean As, Cd, Ni and Pb concentrations in 2022 at background locations are shown in Figure 10.2, Figure 10.3, Figure 10.4 and Figure 10.5 respectively. These maps are presented in ng m^{-3}, where 1000 ng m^{-3} = 1 µg m^{-3}.

10.1.3 Overview of the PCM models for As, Cd, Ni and Pb

Figure 10.1 shows a simplified flow diagram of the PCM models for As, Cd, Ni and Pb. A summary of the PCM model method, input and assumptions for these pollutant models is presented in Table 10.2.

Figure 10.1 - Flow diagram for PCM As, Cd, Ni and Pb models

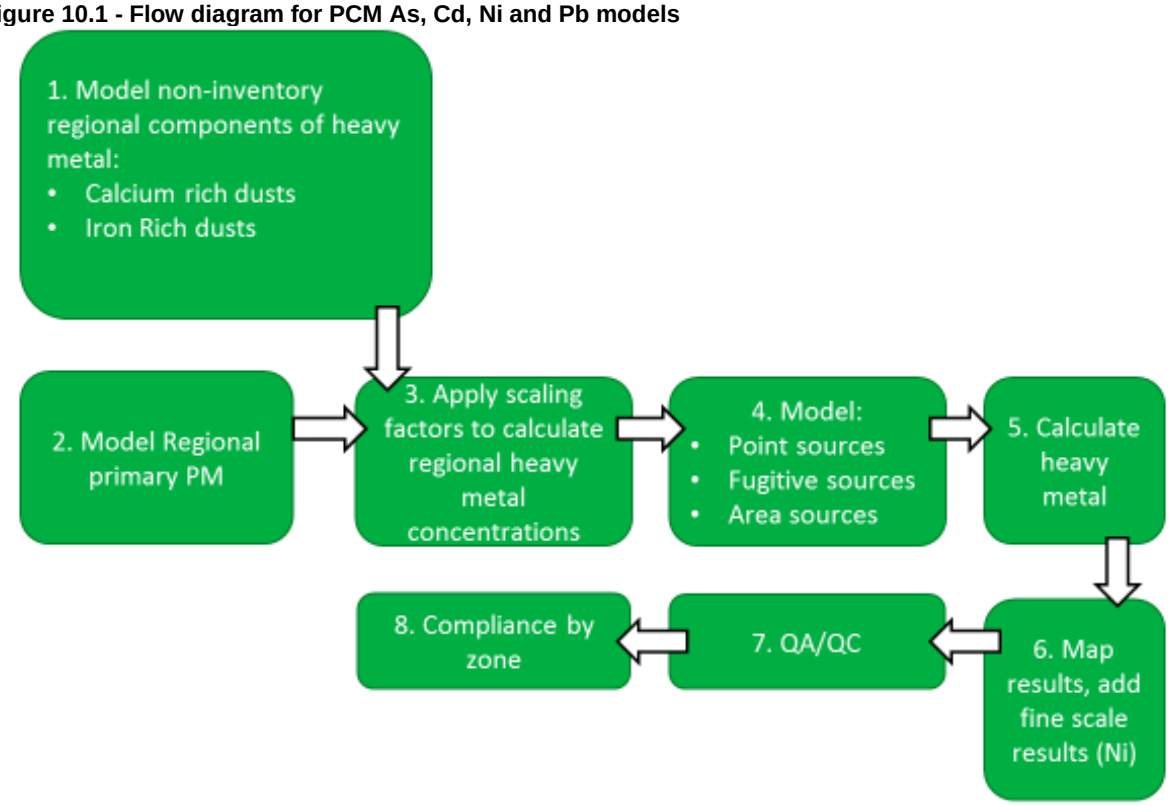

Table 10.2 - PCM model method, input and assumptions summary for As, Cd, Ni and Pb

Heading	Component	Details
General	Pollutant	As, Cd, Ni, Pb
	Year	2022
	Locations modelled	Background
	Metric	Annual mean
Input data	Emission inventory	NAEI 2021 (scaled to 2022)
	Energy projections	Energy Projections 2022
	Road traffic counts	2022 (scaled from 2021 where not available)
	Road transport activity projections	DfT (2022) car sales projections, TfL traffic fleet projections for London (2023)
	Road transport emission factors	COPERT 5.4 (COPERT 5.4, 2020)
	Measurement data	2022
	Meteorological data	WRF (see Appendix 4 – WRF meteorology)
Model components	Regional	See details under “pollutant specific” heading
	Large point sources	291 (As), 277 (Cd), 275 (Ni) and 294 (Pb) sources modelled using ADMS 5.2.
	Small point sources	PCM dispersion kernels generated using ADMS 5.2.
	Fugitive point sources	PCM dispersion kernels generated using ADMS 5.2. Fugitive emissions estimated as a proportion of reported emissions.
	ETS point sources	PCM dispersion kernels generated using ADMS 5.2.
	Large ETS point sources	62 (As), 63 (Cd), 63 (Ni) and 62 (Pb) sources modelled using ADMS 5.2.
	Area sources	PCM dispersion kernels generated using ADMS 5.2. Time varying emissions for road transport and domestic sources.
	Roadside increment	n/a
Calibration	Model calibrated?	No
	Number of background stations in calibration	n/a
	Number of traffic stations in calibration	n/a
Pollutant specific	Regional primary particles	Calculated using the TRACK receptor oriented, Lagrangian statistical model, scaled by applying heavy metal to PM_{10} emission ratio. Additional factors also applied.
	Regional dusts from re-suspension of soils	Modelled using information on land cover (bare soil, root and cereal crops) and dispersion kernel incorporating emissions and dispersion processes. Multiplied by heavy metal concentration in soil and empirical enhancement factor.
	Dusts from re-suspension due to vehicle activity	Modelled using information on vehicle movements on major roads (HDV) and dispersion kernel incorporating emissions and dispersion processes. Multiplied by heavy metal concentration in soil and empirical enhancement factor.

	Fine scale modelling (Ni only)	• Contribution of emissions from an industrial source at Pontardawe modelled at 20 m spatial resolution using local meteorological measurements. Model includes building effects and terrain. • Contribution of emissions from an industrial source in Sheffield modelled at 50 m spatial resolution using local meteorological measurements and incorporating local terrain effects.

10.1.4 Outline of the annual mean models for As, Cd, Ni and Pb

The maps of background concentrations of As, Cd, Ni and Pb have been calculated by summing contributions from different sources:

- Large point source emissions
- Small point source emissions
- Fugitive point source emissions
- Point sources with emissions estimates for air quality pollutants based on reported carbon emissions (ETS points)
- Area sources related to domestic combustion
- Area sources related to road traffic
- Other area sources
- Regional primary particles
- Re-suspension from bare soils
- Re-suspension as a result of vehicle movement

These components are aggregated to a single 1 km x 1 km background grid value for each pollutant.

10.1.5 Chapter structure

This chapter describes modelling work carried out for 2022 to assess compliance with the Pb limit value and As, Cd, and Ni target values described above. Emission estimates are described in Section 10.2, Section 10.3 describes the modelling methods, and the modelling results are presented in Section 10.4 to Section 10.7. The source apportionment of ambient concentrations is discussed in each pollutant results section and is often very different from the split for total national emissions. Ambient concentrations are influenced by the location and release characteristics of the emissions and are also influenced by sources not included in the inventory, such as re-suspension.

Figure 10.2 - Annual mean background As concentration, 2022 (ng m^{-3})

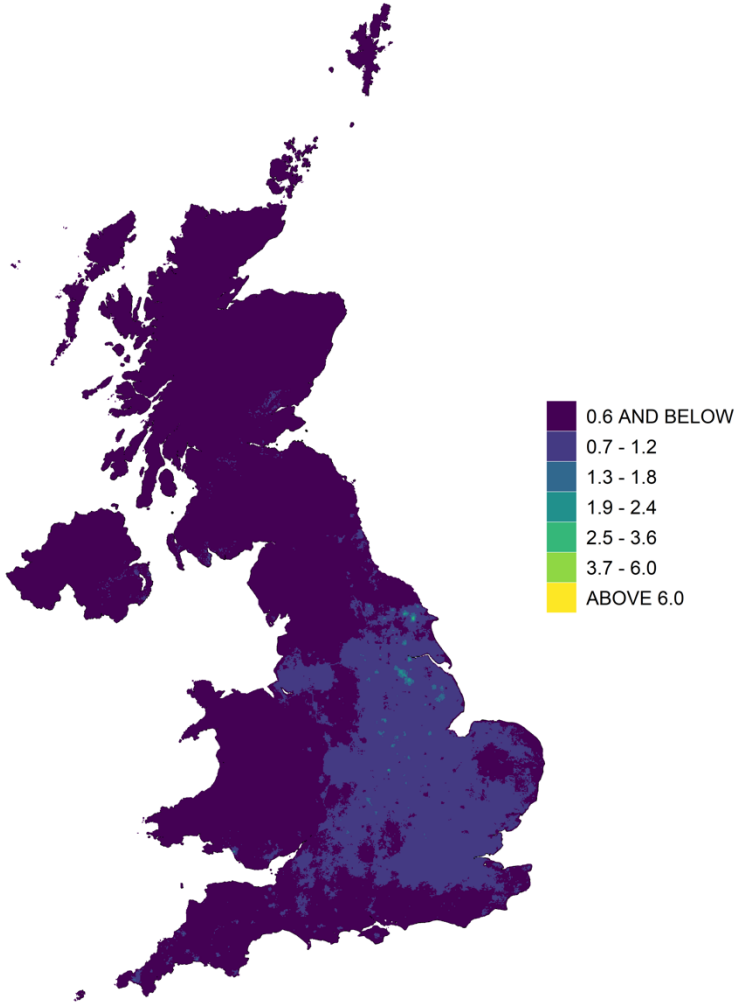

Figure 10.3 - Annual mean background Cd concentration, 2022 (ng m^{-3})

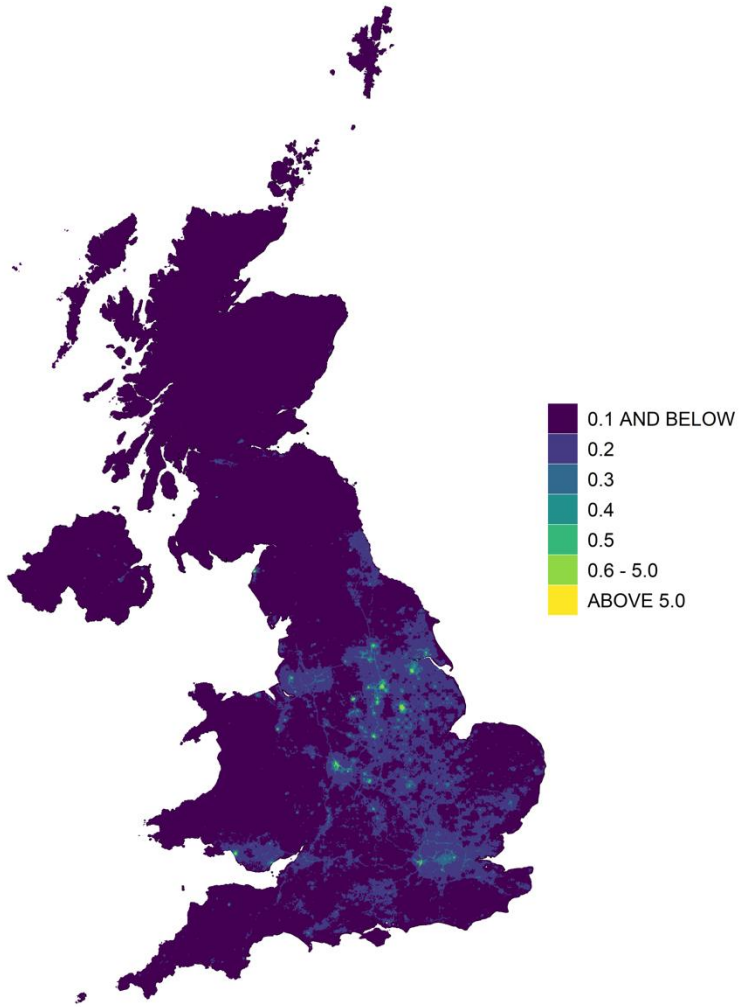

Figure 10.4 - Annual mean background Ni concentration, 2022 (ng m^{-3})

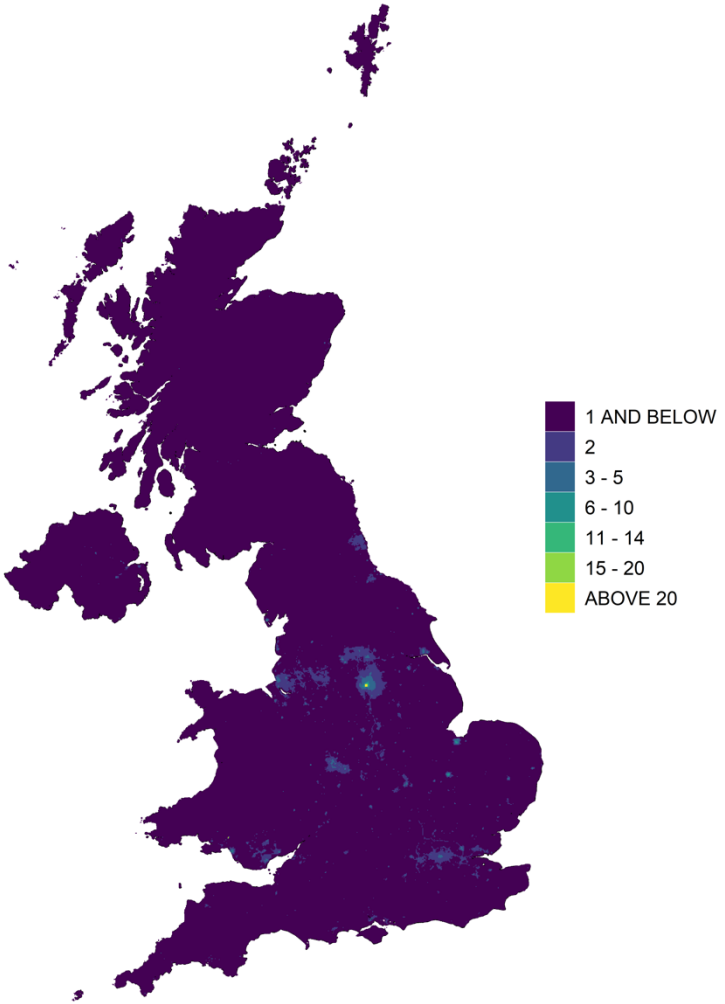

Figure 10.5 - Annual mean background Pb concentration, 2022 (µg m^{-3})

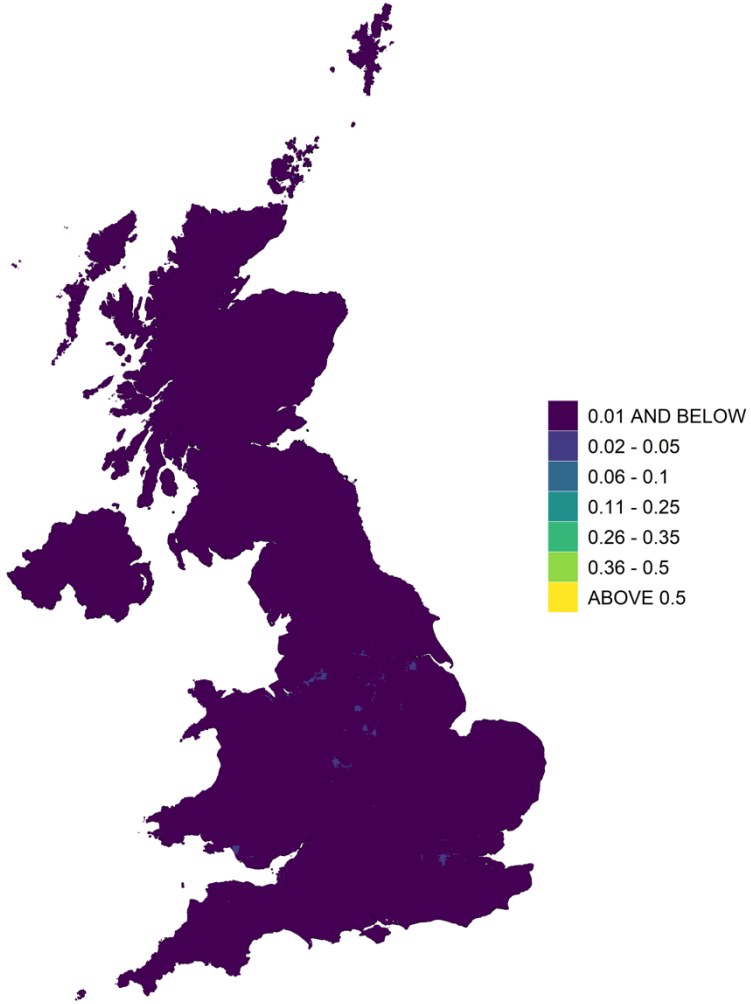

10.2 Emissions

Estimates of the emissions of Heavy Metals from the UK National Atmospheric Emissions Inventory 2021 (NAEI 2021) have been used in this study (Ingledew *et al.*, 2023). Emissions projections have been provided by the NAEI (Personal communication from Ben Pearson, 2023) based on BEIS EEP 2022 energy and emissions projections (BEIS, 2022). UK total emissions for 2022 split by SNAP code for As, Cd, Ni and Pb are shown in Figure 10.6, Figure 10.7, Figure 10.8 and Figure 10.9 respectively, with the coding described in Table 3.2.

Figure 10.6 shows that arsenic emissions in 2022 are dominated by two main sources:

- SNAP 3: Industrial combustion (68%)
- Other point sources (SNAP 4, 5, 6 and 9) (20.8%).

Emissions of arsenic are primarily from the combustion of solid fuel. The majority of emissions are estimated to be from the burning of treated wood. There are no reliable estimates of the extent of this activity, and since the emission factor for this source is also very uncertain, the total emission estimate for this source is highly uncertain.

Figure 10.7 shows that total emissions of cadmium for 2022 are dominated by four main sources:

- SNAP 3: Industrial combustion (34.1%)
- Combustion point sources (SNAP codes 1, 2 and 3) (22%)
- SNAP 2: Domestic combustion (15.8%).
- Other point sources (SNAP 4, 5, 6 and 9) (12.9%)

Figure 10.8 shows the 2022 nickel emissions are dominated by two main sources:

- SNAP 2: Domestic combustion (37.6%)
- SNAP 3: Industrial combustion (20.5%).

Nickel emissions to the atmosphere arise primarily from the combustion of liquid fuels and solid fuels derived from petroleum (petroleum coke and solid smokeless fuels).

Figure 10.9 shows that overall lead emissions for 2022 are dominated by two main sources:

- SNAP 7: Road transport (brake and tyre wear) (34.3%)
- Combustion point sources (SNAP codes 1, 2 and 3) (34%)

Lead emissions are largely from point sources, road transport brake and tyre wear, combustion in industry and solvent use (specifically Fireworks process emissions).

Figure 10.6 - Total UK As emissions for 2022 by SNAP code scaled from NAEI 2021

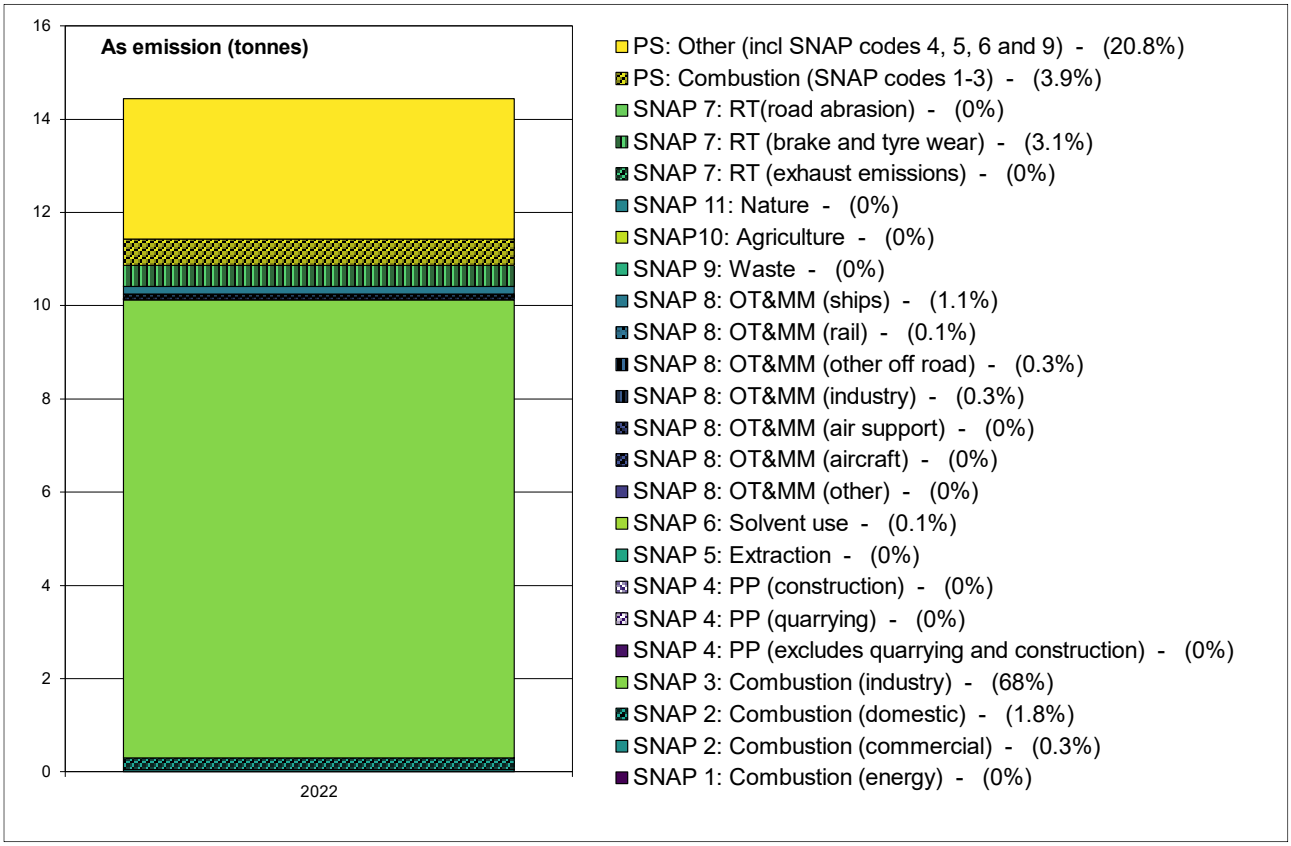

Figure 10.7 - Total UK Cd emissions for 2022 by SNAP code scaled from NAEI 2021

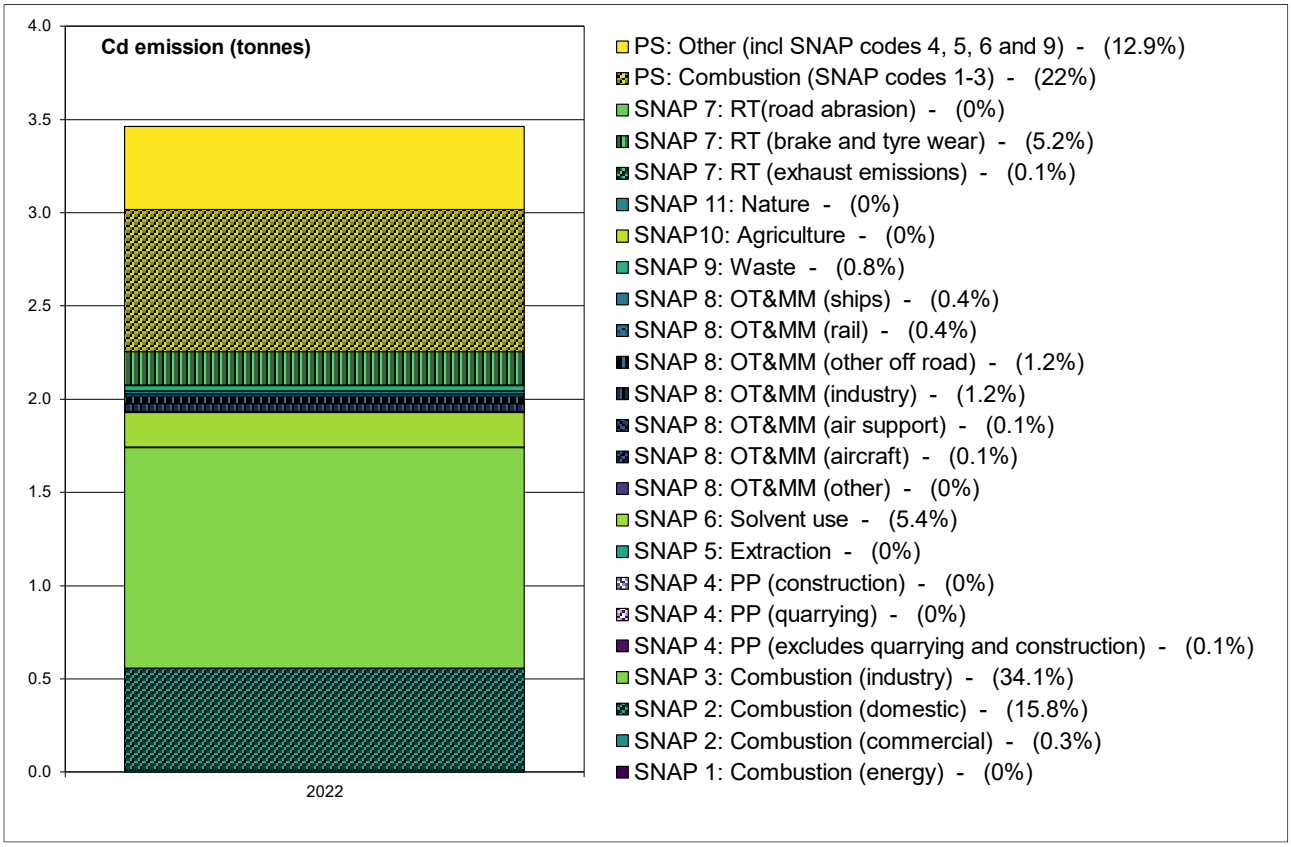

Figure 10.8 - Total UK Ni emissions for 2022 by SNAP code scaled from NAEI 2021

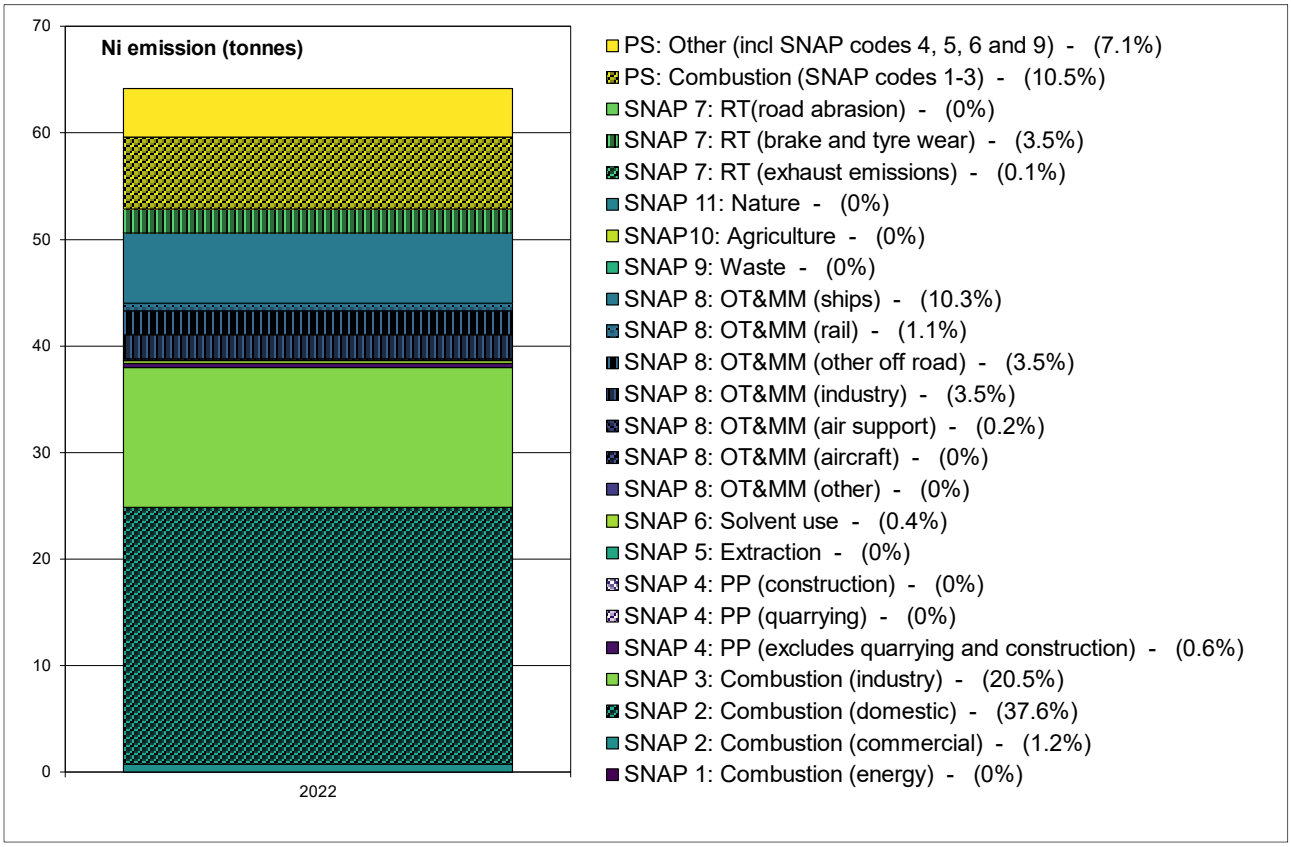

Figure 10.9 - Total UK Pb emissions for 2022 by SNAP code scaled from NAEI 2021

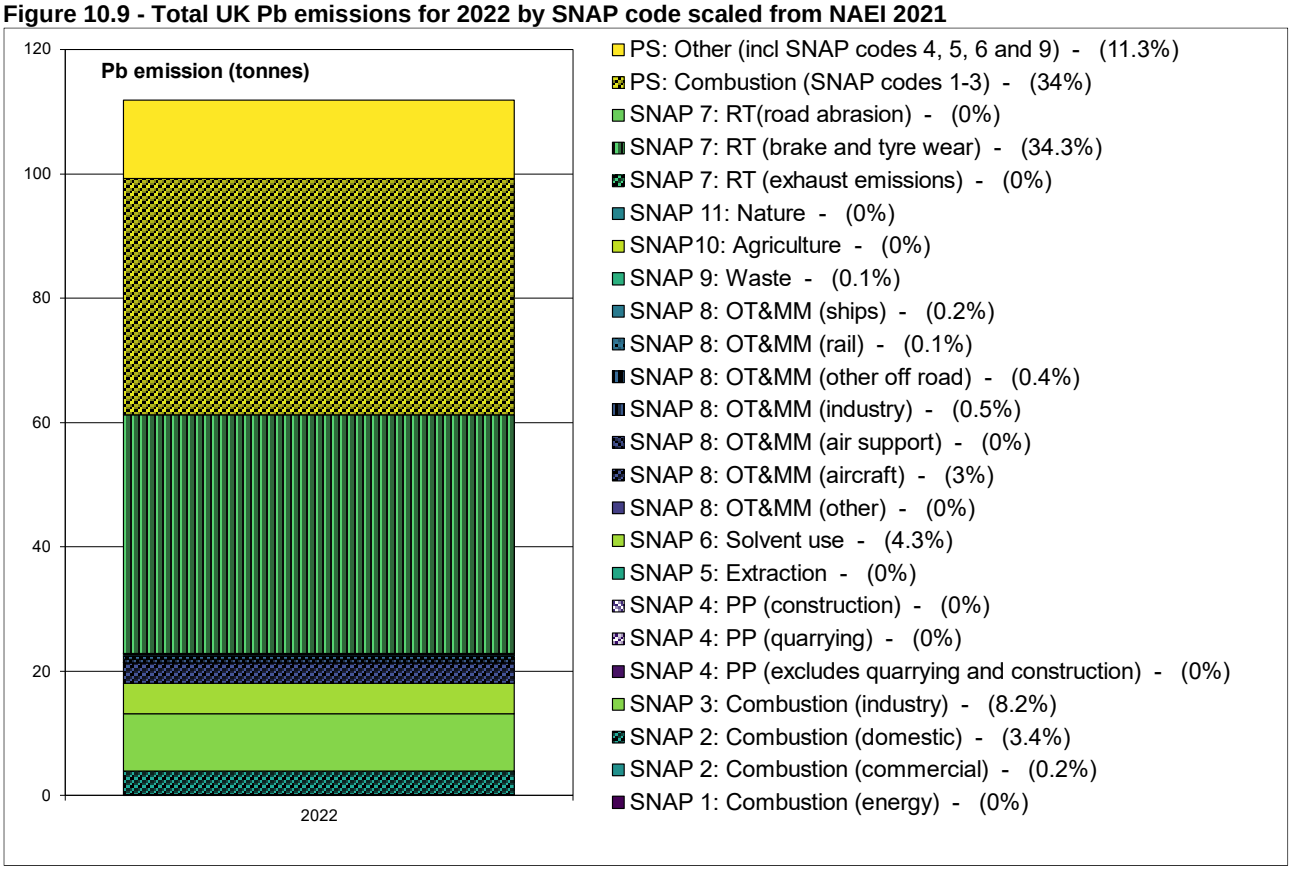

10.3 The model

10.3.1 Contribution from large point sources

Contributions to ground level annual mean heavy metal concentrations from point sources (those with annual emissions of greater than the thresholds listed by pollutant in Table 10.3, or for which emission release characteristics are known) in the NAEI 2021 were estimated by modelling each source explicitly using the atmospheric dispersion model ADMS 5.2 and sequential meteorological data for 2022 from the WRF model, as described in Appendix 4 – WRF meteorology. Concentrations were calculated for a 99 km x 99 km square composed of a regularly spaced 1 km x 1 km resolution receptor grid. Each receptor grid was centred on the point source. The total number of point sources modelled explicitly is given in Table 10.3. For each large point source information was retrieved from the PCM stack parameters database (as described in Section 3.3.1). The NAEI emissions for point sources for 2021 were scaled in order to provide values for 2022.

The Vale Clydach refinery in South Wales is located within the Pontardawe Valley a few miles from the Pontardawe Tawe Terrace monitoring station. To provide the best estimate of Ni concentrations in this area, reported 2022 emissions and updated stack parameters for this site were provided by the site operator and incorporated into the large points modelling for Ni.

A factor of 0.3 has been applied to the modelled contribution of large point sources to As concentrations, consistent with the 2013, 2014, 2015, 2016, 2017, 2018, 2019, 2020 and 2021 modelling. Factors of unity have been applied to the modelled contribution from large point sources to concentrations of Ni, Pb and Cd. Factors were chosen to provide the best agreement of total model predictions with measured heavy metal concentrations. Activity levels for combustion of coal in industry were about 50% higher in the 2012 NAEI than in the 2011 NAEI and have remained at this higher level in subsequent inventories. There has been no clear trend or change in ambient As concentrations measured in the UK over this period. A factor of less than unity was therefore required for industrial emissions of As.

The NAEI 2021 includes point source emissions estimates derived from carbon emissions data reported under the EU-Emissions Trading Scheme (ETS), most recently described in (Tsagatakis *et al.*, 2023). These point sources are referred to as ETS points in this report. These derived air quality pollutant emissions are particularly uncertain and therefore in previous assessments (e.g. (Brookes *et al.*, 2017)) emissions were capped at reporting thresholds and treated as small point sources. For the 2016, 2017, 2018, 2019, 2020 and 2021 assessments (Brookes *et al.*, 2019b, 2019a, 2020, 2021; Pugsley *et al.*, 2022, 2023) the NAEI recommended treating the ETS points that have emissions greater than the large points modelling threshold as large points and not to apply a cap (Personal communication from Ben Pearson, 2023). The 2022 assessment continues this approach. Thus, those ETS point sources of As, Cd, Ni and Pb meeting the criteria for the treatment of large point sources described above, were modelled as an additional set of large point sources (using the approach described above). The total number of ETS point sources modelled explicitly is given in Table 10.3. ETS points that were not classified as large point sources were modelled using the small and fugitive points approach described next.

10.3.2 Contributions from small point and fugitive sources

The contributions to ambient concentrations from fugitive and small point sources (those without stack parameters datasets and annual emissions less than or equal to values displayed in Table 10.3) in the NAEI 2021 were modelled using a small points model. The NAEI 2021 emissions for fugitive and small point sources have been scaled to 2022 using the same source sector specific projection factors applied to the large point sources.

The models consist of separate ‘in-square’ and ‘out-of-square’ components, in which concentrations are estimated using a point source dispersion kernel. The dispersion kernel for small points has been calculated by using the dispersion model ADMS 5.2 to model the dispersion of unit emissions from a central source to a grid of receptors at a spatial resolution of 1 km x 1 km squares with the stack characteristics as presented in Table 10.4. Hourly sequential meteorological data from the WRF model in 2022 has been used to construct the dispersion kernels. The greatest concentration would be expected close to the point of emission. The receptor for the central grid square within the dispersion kernel is, however, at exactly the same location as the point of release. The concentration at this location is therefore zero. The value for the central grid square within the dispersion kernel has therefore been assigned to be equal to the highest of the values for the adjacent grid squares.

A factor of 0.3 has been applied to the modelled contribution of small point sources to As concentrations, consistent with the 2013, 2014, 2015, 2016, 2017, 2018, 2019, 2020 and 2021 modelling and the treatment of large point sources. Factors of unity have been applied to the modelled contribution from small point sources to concentrations of Ni, Pb and Cd. Factors were chosen to provide the best agreement of total model predictions with measured heavy metal concentrations.

Table 10.3 - Thresholds to determine modelling method, and number of large point sources for 2022

Pollutant	Tonnes per year	Number of large point sources	Number of large ETS point sources
As	0.025	291	62
Cd	0.025	277	63
Ni	0.05	275	63
Pb	1.2	294	62

Table 10.4 - Stack release parameters used to characterise emissions from point sources with no available stack parameters

Variable	Parameters
Stack height	15 m
Diameter	1 m
Temperature	15˚C
Emission rate as PM_{10}	1g/s
Surface roughness at dispersion site	0.5 m
Surface roughness at met site	0.02 m

Characterising the amount of fugitive heavy metal emission from industrial plant is notoriously difficult. For the modelling of Ni concentrations, assuming a fugitive emission of 0.05 times the reported emission was found to provide the best agreement with the available measurements. For the modelling of As, a fugitive emission 0.015 times the reported emission was assumed. For the modelling of Pb, a fugitive emission 0.02 times the reported emission was assumed. For the modelling of Cd, a fugitive emission 0.0025 times the reported emission was assumed.

The emission release parameters for fugitive sources are provided in Table 10.5. Once again, the value for the central grid square within the dispersion kernel has been set to the maximum of the values in the surrounding grid squares.

Table 10.5 - Stack release parameters used to characterise fugitive emission release

Variable	Parameters
Stack height	10 m
Diameter	1 m
Temperature	15˚C
Emission rate as PM_{10}	1g/s
Surface roughness at dispersion site	0.5 m
Surface roughness at met site	0.02 m

10.3.3 Contributions from local area sources

The 2022 area source emissions maps for heavy metals have been calculated from the NAEI 2021 emissions maps following the method described in Section 3.3.5. ADMS derived dispersion kernels have been used to calculate the contribution to ambient concentrations on a 1 km x 1 km receptor grid, from the area source emissions within a 33 km x 33 km square surrounding each receptor. Hourly sequential meteorological data from the WRF model in 2022 has been used to construct the dispersion kernels, as described in Appendix 5 – Dispersion kernels for the area source model. Revised methods introduced in the 2011 assessment (Brookes *et al.*, 2012) for modelling the contributions to As, Cd, Ni and Pb from SNAP 2 (domestic and non-domestic combustion) and SNAP 3 (combustion in industry) area sources were used and have been described in Section 3.3.5.

A factor of 0.7 has been applied to the modelled contribution of domestic area sources to Ni concentrations. Factors of unity have been applied to the modelled contribution from area sources to concentrations of As, Pb and Cd, and to other area source types for Ni modelling. Factors were

chosen to provide the best agreement of total model predictions with measured heavy metal concentrations.

For certain sectors (noted within each pollutant results section below) caps have been applied to emissions based on expert judgement of the model results to address known artefacts in the area source emissions grids and to reconcile the model results with the measured data at each monitoring site.

10.3.4 Contribution from long range transport of primary particulate matter

The contribution to ambient concentrations from long range transport of heavy metals was derived from estimates of regional primary particulate matter used in the 2022 PCM model for PM_{10} mass (Section 5.3.4). The contribution of long-range transport sources to ambient heavy metal concentrations was derived by calculating a fraction of the PM mass for each heavy metal. This fraction was estimated as the ratio of the UK total emissions for each metal for each SNAP sector to the total PM_{10} emission for that sector. The following scaling factors for long range transport of primary particulate matter were then applied: 4.5 for As, 1.0 for Cd, 0.4 for Ni and 3.0 for Pb. These factors chosen to provide the best agreement of total model predictions with measured heavy metal concentrations.

10.3.5 Heavy metal contribution from re-suspension

The 2022 model for heavy metal concentrations includes a contribution to ambient concentrations from re-suspension calculated in the same way as in the 2011 models (Brookes *et al.*, 2012). The contributions from two processes have been included:

- Regional PM dusts from re-suspension of soils and
- PM dusts from re-suspension due to vehicle activity.

The heavy metal contribution from re-suspension has been calculated by using the methods suggested by (Abbott, 2008). The methods used to estimate the total PM mass from these processes are detailed in Section 5.3.5.

(Abbott, 2008) also suggested a method for estimating the contributions to the ambient concentrations of heavy metals from soil and vehicle related re-suspension processes. The maps of PM mass from re-suspension of soils and re-suspension associated with vehicle movements can be used to estimate the contributions to the ambient concentration of heavy metals using a combination of information on the heavy metal content of soils and enhancement factors.

The National Soil Inventory (http://www.landis.org.uk/data/natmap.cfm) provides a data set of As, Cd, Ni and Pb concentrations in topsoil at 5 km resolution throughout England and Wales. Measurement data on heavy metals concentration in topsoil for other areas of the UK is available from the Geochemical Atlas of Europe developed under the auspices of the Forum of European Geological Surveys (FOREGS) (http://weppi.gtk.fi/publ/foregsatlas/). These data were interpolated onto a 1 km x 1 km grid. The predicted annual PM emission rates and the contribution to atmospheric concentrations were multiplied by the topsoil concentrations to estimate the annual metal re-suspension rates and the contributions to atmospheric concentrations of the heavy metals.

There is some evidence that metal concentrations in the surface soils are higher than in the underlying topsoil. EMEP have suggested that there may be some enhancement of the metal content of the re-suspended dust because the metals may form complexes with humic matter (Abbott, 2008). (Abbott, 2008) carried out regression analyses of measured heavy metal concentrations against the combined model predictions for sites in the UK Rural Heavy Metal Network. This analysis suggested that there may be other mechanisms by which heavy metals are concentrated in the small particle fraction of soils. For example, much of the metal content may be present as the result of historical deposition of small particles or the application of sewage sludge and farmyard slurries. These materials may only be loosely bonded to the surface of the soil particles. The fine particles released by re-suspension mechanisms would therefore be likely to contain a much higher concentration of metals than the underlying topsoil. The enhancement factors listed in Table 10.6 have been chosen to provide the best agreement of total model predictions with measured heavy metal concentrations. The factors are broadly consistent with the regression coefficients determined by (Abbott, 2008).

Caps have been applied for the contribution generated from re-suspension of soil for some of the heavy metals. The values have been chosen as an estimate of the maximum likely concentration generated from this source and are also listed in Table 10.6.

Table 10.6 - Heavy metal enhancement factors used in the assessment

Pollutant	Enhancement factor	Maximum concentration (ng m^{-3})
As	12.5	3.5
Cd	25	2.5
Ni	2	5
Pb	15	5

10.4 Arsenic Results

10.4.1 Introduction

The map of modelled annual mean As concentrations is shown in Figure 10.2. There were no modelled or measured exceedances of the target value of 6 ng m^{-3} in 2022.

10.4.2 Verification of mapped concentrations

A comparison between modelled and measured annual mean As concentrations in 2022 at monitoring site locations is shown in Figure 10.10. This figure includes lines to represent the AQSR data quality objective for modelled annual mean As concentrations: y=x-60% and y=x+60% (see Section 1.5).

Summary statistics for modelled and measured As concentrations are listed in Table 10.7, including the percentage of sites at which modelled concentrations are outside of the data quality objectives (DQOs), and the total number of sites included in the analysis.

The means of measured and modelled concentrations are in reasonable agreement for all site types, with all but two sites falling within the DQOs. The agreement between measured and modelled concentrations on a site-by-site basis (quantified using R^2) is reasonably good for all site types.

It should be noted that non-emission inventory sources (such as fugitive, re-suspension and long-range transport of primary PM) result in additional uncertainty when compared with a pollutant such as NO_X, for which the source apportionment is better known.

Figure 10.10 - Verification of annual mean As across all sites.

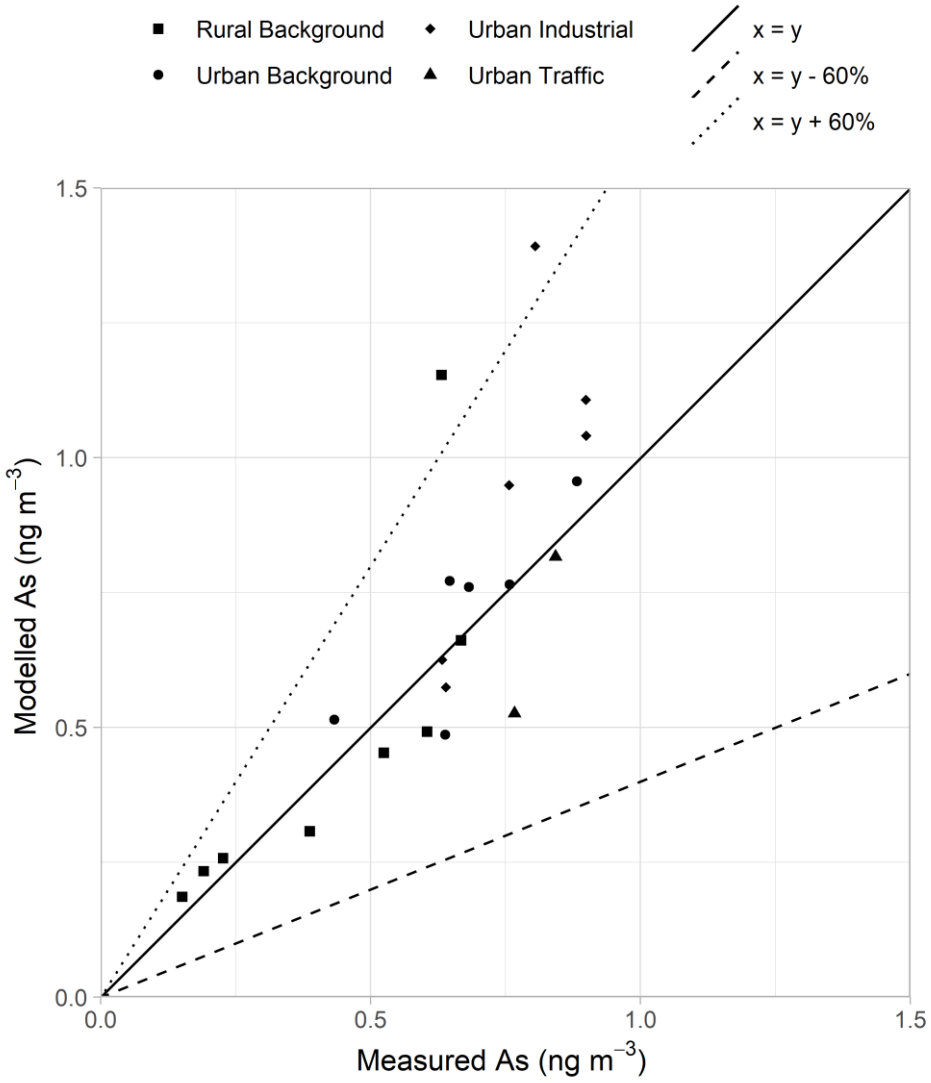

Table 10.7 - Summary statistics for comparison between modelled and measured annual mean As concentrations at different monitoring sites, 2022.

	Mean of measurements (ng/m^3)	Mean of model estimates (ng/m^3)	R^2	% of sites outside DQO of ±60%	Number of sites in assessment
Industrial sites	0.77	0.95	0.59	17%	6
Urban background sites	0.67	0.71	0.69	0%	6
Roadside sites	0.80	0.67	1.00	0%	2
Rural sites	0.42	0.47	0.62	13%	8
All	**0.62**	**0.68**	**0.66**	**9%**	**22**

10.4.3 Source apportionment

Figure 10.11 shows the modelled As contribution from different sources at monitoring site locations. Measured concentrations at the sites are also presented, giving an indication of the level of agreement between modelled and measured concentrations. This analysis suggests that the main sources of arsenic are long range transport primary, resuspension and industry.

Figure 10.11 - Annual mean As source apportionment at monitoring sites in 2022.

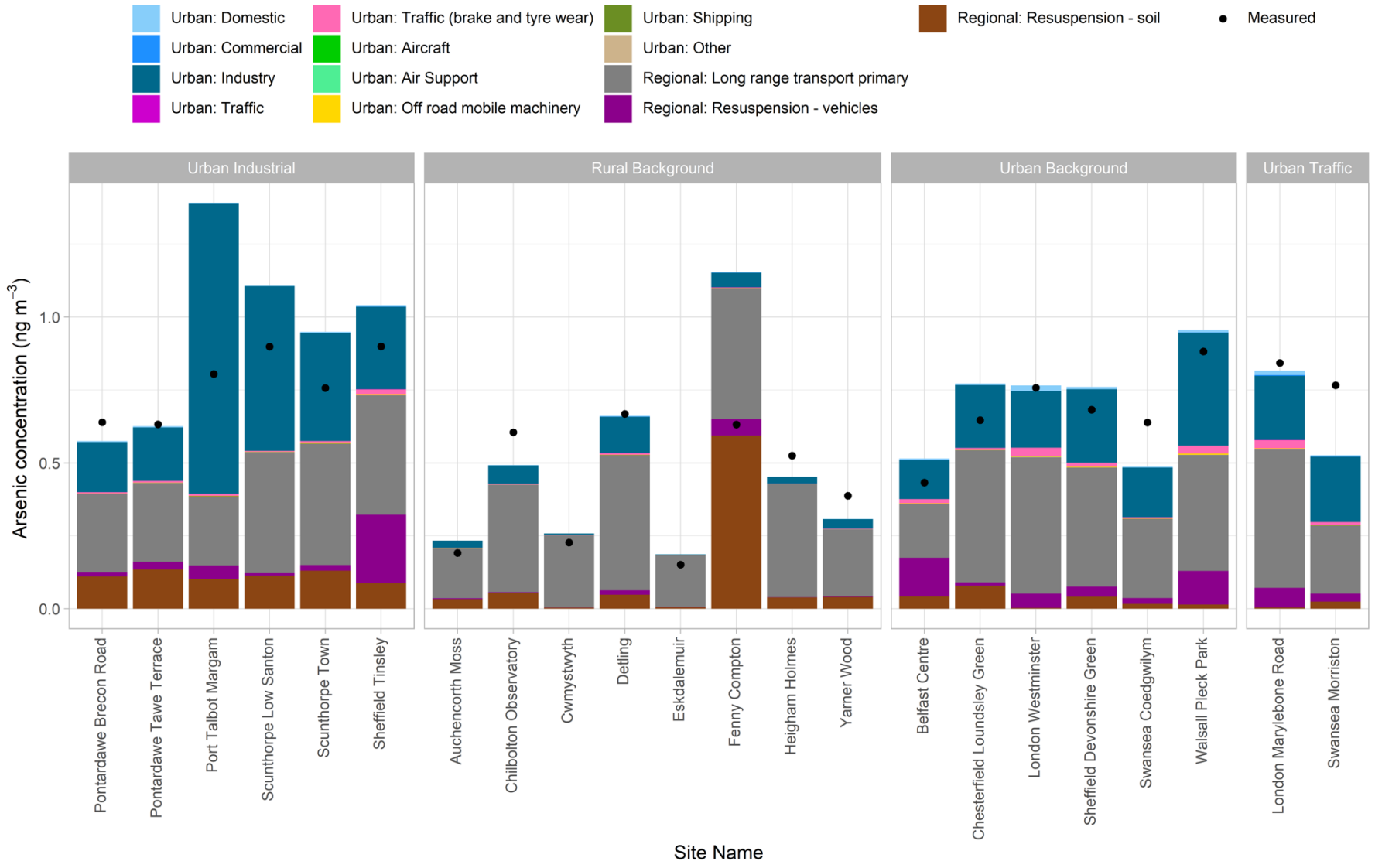

10.5 Cadmium Results

10.5.1 Introduction

The map of modelled annual mean Cd concentrations is shown in Figure 10.3. There were no modelled or measured exceedances of the target value of 5 ng m^{-3} in 2022.

10.5.2 Verification of mapped concentrations

A comparison between modelled and measured annual mean Cd concentrations in 2022 at monitoring site locations is shown in Figure 10.12. This figure includes lines to represent the AQSR data quality objective for modelled annual mean Cd concentrations: y=x-60% and y=x+60% (see Section 1.5).

Summary statistics for modelled and measured Cd concentrations are listed in Table 10.8, including the percentage of sites at which modelled concentrations are outside of the DQOs and the total number of sites included in the analysis.

The agreement between measured and modelled concentrations on a site-by-site basis (quantified using R^2) is good for rural and urban background monitoring locations, and reasonable for industrial monitoring locations.

It should be noted that non-emission inventory sources (such as fugitive, re-suspension and long-range transport of primary PM) result in additional uncertainty when compared with a pollutant such as NO_X, for which the source apportionment is better known.

Figure 10.12 - Verification of annual mean Cd across all sites.

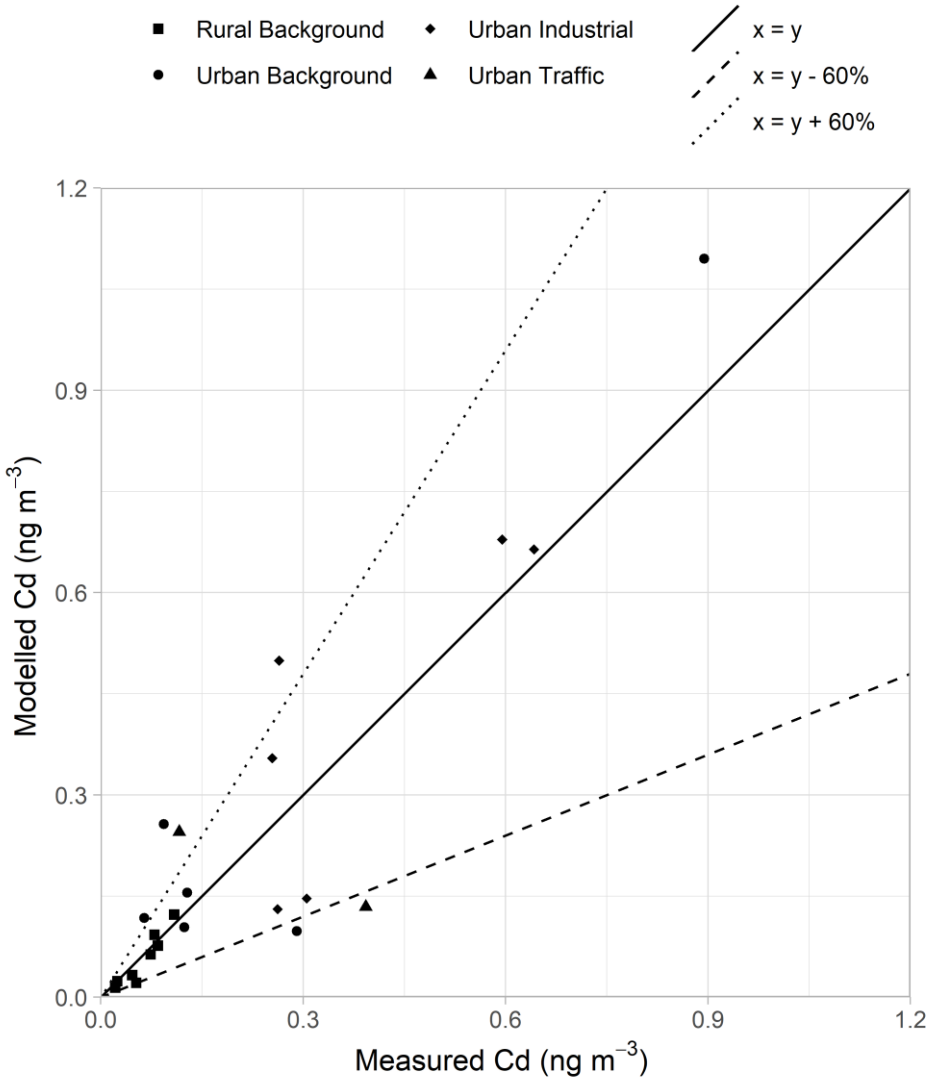

Table 10.8 - Summary statistics for comparison between modelled and measured annual mean Cd concentrations at different monitoring sites, 2022.

	Mean of measurements (ng/m^3)	Mean of model estimates (ng/m^3)	R^2	% of sites outside DQO of ±60%	Number of sites in assessment
Industrial sites	0.39	0.41	0.62	17%	6
Urban background sites	0.27	0.30	0.89	50%	6
Roadside sites	0.25	0.19	1.00	100%	2
Rural sites	0.06	0.06	0.89	0%	8
All	**0.22**	**0.23**	**0.81**	**27%**	**22**

10.5.3 Source apportionment

Figure 10.13 shows the modelled Cd contribution from different sources at monitoring site locations. Measured concentrations at the sites are also presented, giving an indication of the level of agreement between modelled and measured concentrations. This analysis suggests that at those sites where the highest concentrations are measured, the main sources of cadmium are industry, resuspension, and long-range transport primary. Industrial sites have larger quantities of emissions assigned to industry than non-industrial sites.

Figure 10.13 - Annual mean Cd source apportionment at monitoring sites in 2022.

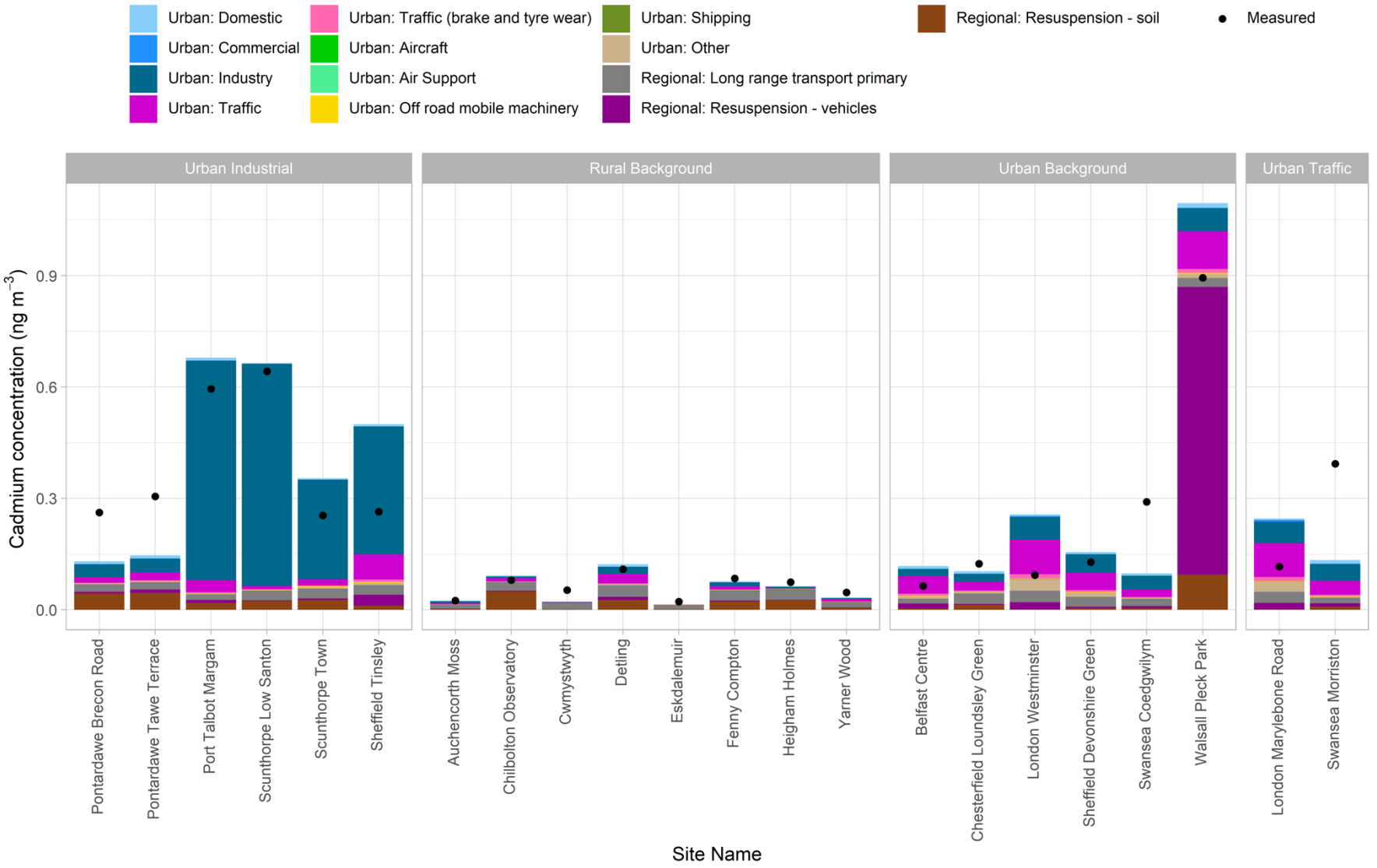

10.6 Nickel Results

10.6.1 Introduction

The method used to estimate ambient Ni concentrations across the UK is described in Section 10.3 above.

A cap of 30 t/a/km^2 also applied to shipping emissions.

The map of modelled annual mean Ni concentrations is shown in Figure 10.4. Historically there have been issues with compliance for nickel and this was the case in 2022. Detailed local modelling carried out to characterise the impact of emissions on ambient concentrations at locations associated with exceedances is discussed in Section 10.6.4.

10.6.2 Verification of mapped concentrations

A comparison between modelled and measured annual mean Ni concentrations in 2022 at monitoring site locations is shown in Figure 10.14(a) at full scale showing all sites, and (b) on an expanded scale to better show performance at lower concentrations). This figure includes lines to represent the AQSR data quality objective for modelled annual mean Ni concentrations: y=x-60% and y=x+60% (see Section 1.5).

The results for several monitoring site locations included in Figure 10.4 (Pontardawe Tawe Terrace, Sheffield Tinsley, and Sheffield Devonshire Green) are covered by more detailed local modelling assessments (see Section 10.6.4). A modelled Ni concentration of 17.1 ng m^{-3} has been reported for the 2022 compliance assessment modelling for the 1 km grid square containing the Pontardawe Tawe Terrace monitoring site, equal to the measured value for this monitoring site. For model verification the modelled value including the local detailed modelling was also 17.1 ng m^{-3} hence the modelled and measured values in Figure 10.14 for Pontardawe Tawe Terrace are equal. Modelled Ni concentrations of 17.4 ng m^{-3} and 2.9 ng m^{-3} have been reported for the 2022 compliance assessment modelling for the 1 km grid squares containing the Sheffield Tinsley and Sheffield Devonshire Green monitoring sites respectively taking into account the average (mean) of the detailed modelling results per 1 km grid square. For model verification the measured Ni concentrations at Sheffield Tinsley and Sheffield Devonshire Green are 17.3 ng m^{-3} and 2.5 ng m^{-3} respectively, while the modelled values for the 50 m grid squares containing the Sheffield monitoring sites from the local detailed modelling are 17.4 ng m^{-3} and 2.9 ng m^{-3} respectively. Hence there are small differences in the modelled and measured values in Figure 10.14 for Sheffield Tinsley and for Sheffield Devonshire Green.

Summary statistics for modelled and measured Ni concentrations are listed in Table 10.9, including the percentage of sites for which the modelled values are outside of the DQOs as well as the total number of sites included in the analysis.

The agreement between measured and modelled concentrations on a site-by-site basis are good for all monitoring sites as quantified using R^2, and poorer in terms of comparison of the measured and modelled mean concentrations where there is a tendency for the model to overestimate at lower measured concentrations. The results for the Pontardawe Tawe Terrace, Sheffield Tinsley and Sheffield Devonshire Green sites are discussed in Section 10.6.4.

It should be noted that non-emission inventory sources (such as fugitive, re-suspension and long-range transport of primary PM) result in additional uncertainty when compared with a pollutant such as NO_X, whose source apportionment is better known.

Figure 10.14 - Verification of annual mean Ni across all sites: (a) full scale showing all sites; (b) expanded scale where the results from Tawe Terrace and Sheffield Tinsley are off scale.

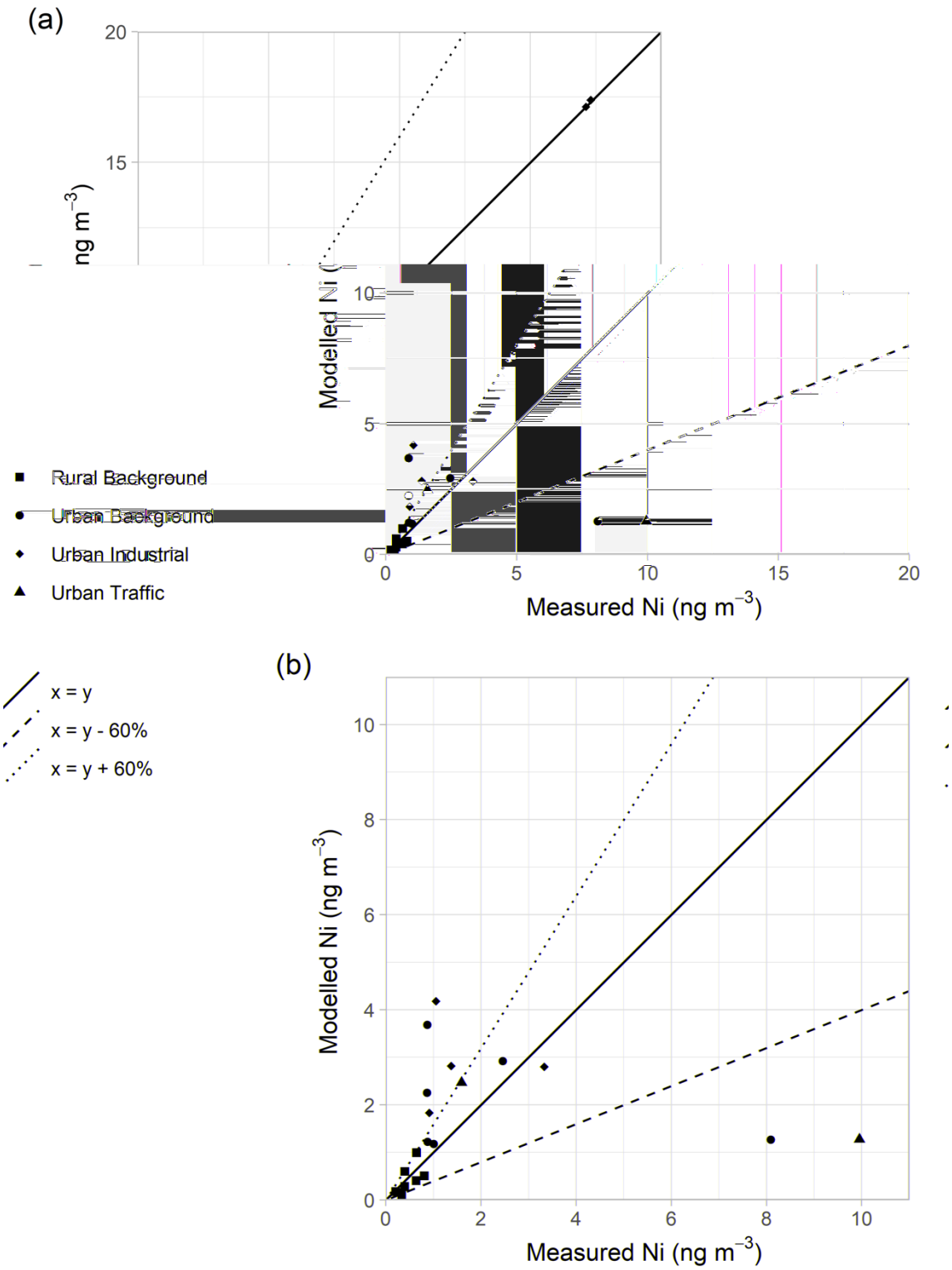

Table 10.9 - Summary statistics for comparison between modelled and measured annual mean Ni concentrations at different monitoring sites, 2022.

	Mean of measurements (ng/m^3)	Mean of model estimates (ng/m^3)	R^2	% of sites outside DQO of ±60%	Number of sites in assessment
Industrial sites	6.85	7.69	0.98	50%	6
Urban background sites	2.36	2.08	0.10	50%	6
Roadside sites	5.77	1.87	1.00	50%	2
Rural sites	0.47	0.40	0.41	13%	8
All	**3.21**	**0.26**	**0.42**	**36%**	**22**

10.6.3 Source apportionment

Figure 10.15 shows the modelled Ni contribution from different sources at monitoring site locations. Measured concentrations at the sites are also presented, giving an indication of the level of agreement between modelled and measured concentrations. This analysis suggests that the main sources of nickel are long range transport primary, industry, traffic and resuspension. Emissions from local industrial point sources are important for Pontardawe Brecon Road, Pontardawe Tawe Terrace, and Sheffield Tinsley, and this is discussed in detail in Section 10.6.4.

Figure 10.15 - Annual mean Ni source apportionment at monitoring sites in 2022

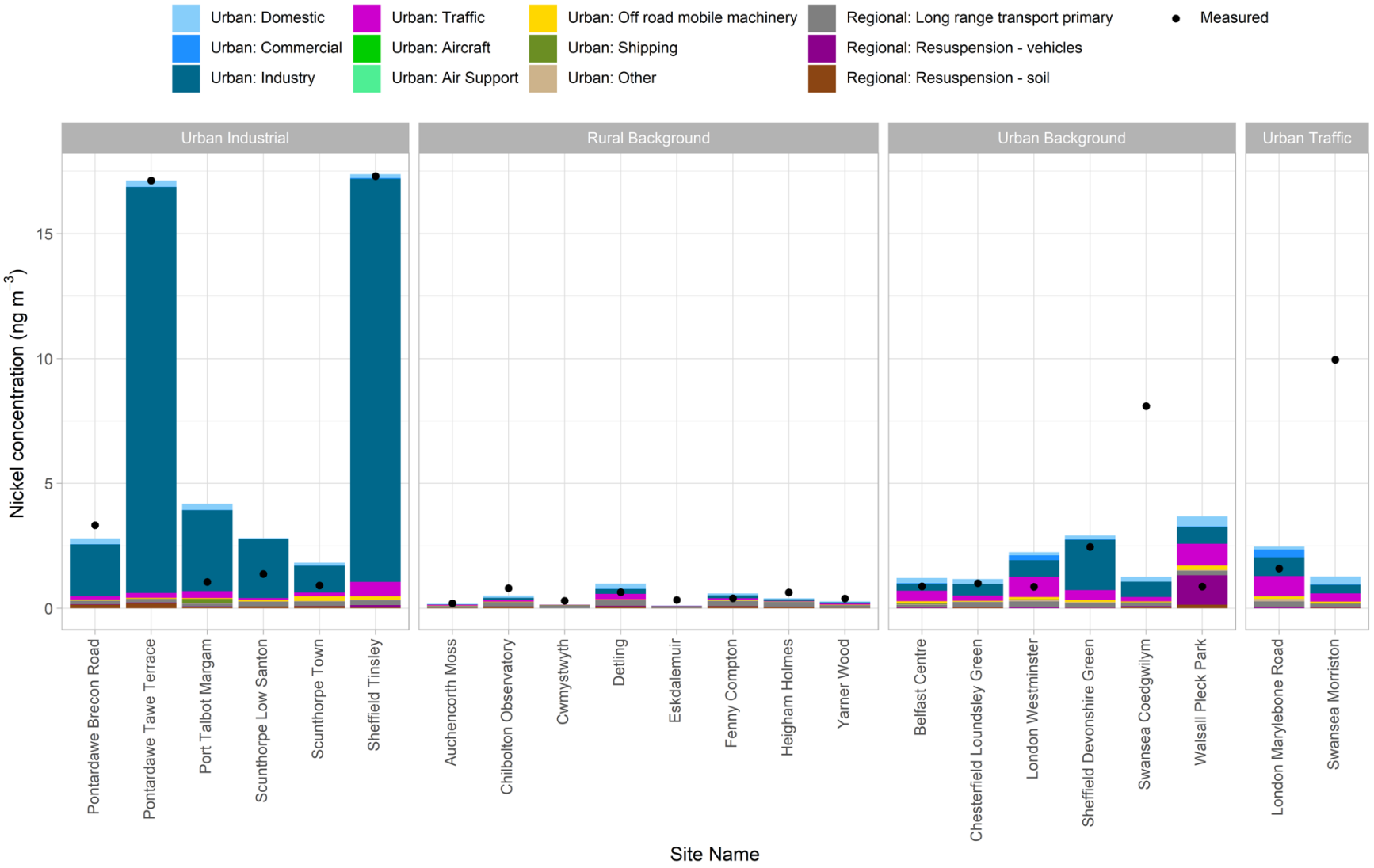

10.6.4 Detailed comparison of modelled results with the target value

10.6.4.1 Introduction

There were exceedances reported in three zones for 2022, all three exceedances are based on models (i.e. Sheffield Urban Area, South Wales and Yorkshire and Humberside). Results of the assessment in terms of comparisons of the modelled concentrations with the TV have been reported in e-Reporting Data flow G published on UK-Air (*UK-Air*, 2023). Exceedance of the Ni TV in all three zones have been reported in previous years. Swansea Urban area has been reported to be compliant with the Target Value in 2022, having been reported as non-compliant in recent years. Local monitoring and detailed modelling in the vicinity exceedances are carried out annually and inform the maximum concentration and, where applicable, area of exceedance reported in e-Reporting for each zone.

A maximum concentration of 29 ng m^{-3} for the South Wales zones was reported based on the maximum of the average (mean) of exceeding 20 m grid squares from the detailed local modelling. The value for the Swansea Urban Area zone was based on the annual mean Ni concentration measured at Pontardawe Tawe Terrace which was below the Target Value in 2022. This monitoring site is within the Swansea Urban Area zone but is very near to the boundary of the South Wales zone. The value for the South Wales zone was based on model results. Detailed modelling of the principal source of local nickel emissions for these two zones is described below in Section 10.6.4.2.

Maximum concentrations of Ni for the Sheffield Urban Area and Yorkshire and Humberside zones were reported based upon consideration of the maximum of measured concentrations within these zones, concentrations from the national modelling and detailed local modelling of the contributions of significant industrial sources within Sheffield. A maximum concentration of 253 ng m^{-3} was reported for the Sheffield zone based on the maximum of the average (mean) of exceeding 50 m grid squares from the detailed local modelling for Sheffield per 1 km grid square in the zone. Similarly, a maximum concentration of 32 ng m^{-3} was reported for the Yorkshire and Humberside zone also based on the detailed local modelling for Sheffield. Detailed modelling of the principal sources of nickel emissions for the exceedances in these zones is described below in Section 10.6.4.3.

10.6.4.2 Swansea Urban Area and South Wales Zones

Detailed dispersion modelling has been undertaken using ADMS 5.2 for the area in South Wales where exceedances of the annual mean TV of 20 ng m^{-3} have been reported in 2022. This fine-scale modelling has been used to assess the likely magnitude and spatial extent of exceedance.

Information on the Ni emissions from the principal Ni point source at Wall Colmonoy in Pontardawe were provided by the site operators. The annual Ni emission from one plant was reported by the site operator to be 71.6 kg $year^{-1}$. The modelling was undertaken and the results scaled to provide the best fit to the monitoring data at Pontardawe Tawe Terrace.

Emissions were released from thirteen emission points distributed across the site. Building effects were included in the model, and a 6 km x 6 km area was extracted from the OS Terrain 50 dataset to allow the effect of the topographical features of the valley to be included in the model. The height of the terrain was specified at the centre of each 50 m x 50 m grid square.

Table 10.10 compares measured annual mean Ni concentrations with modelled concentrations. The modelled concentrations include a component resulting from the local industrial point source in Pontardawe and a background component from the annual modelling Ni concentrations across the UK. The model reproduces the measured concentration at Pontardawe Leisure Centre and Pontardawe Brecon Road well. Agreement is also good at Pontardawe Tawe Terrace, for which the measured concentration was used to inform the scaling of emissions estimates and thus good agreement is to be expected.

Figure 10.16 shows the modelled annual mean Ni concentration on a 20 m x 20 m grid resolution resulting from the local industrial point source in Pontardawe and including a background component from the annual modelling of Ni concentrations across the UK. The Ni concentrations in Pontardawe were strongly influenced by the terrain in the area, as can be seen in Figure 10.16. The Swansea Valley runs south-west to north-east through the village of Pontardawe, where the point source is located. The distribution of the Ni concentrations in the vicinity of Pontardawe shows the channelling of the local wind flow by the Swansea Valley.

The conclusions from this dispersion modelling study are that Ni concentrations in only the South Wales zone in 2022 exceeded the Ni TV. The annual averaged measured Ni concentrations at the Tawe Terrace were shown to be lower than the target value, with this observation being confirmed by the modelled concentrations in this zone as well. However, the modelled concentrations at the North East boundary of the Wall Colomony facility were shown to be higher than the target value, resulting in an exceedance of the concentrations in this zone.

The source apportionment plot (Figure 10.15) and scatter plot (Figure 10.14) presented earlier in this section include the modelled contribution to ambient concentrations at the Pontardawe Tawe Terrace and Pontardawe Brecon Road sites from the local industrial point source.

Figure 10.16 - Modelled annual mean Ni concentration resulting from the local industrial point source in Pontardawe in 2022.

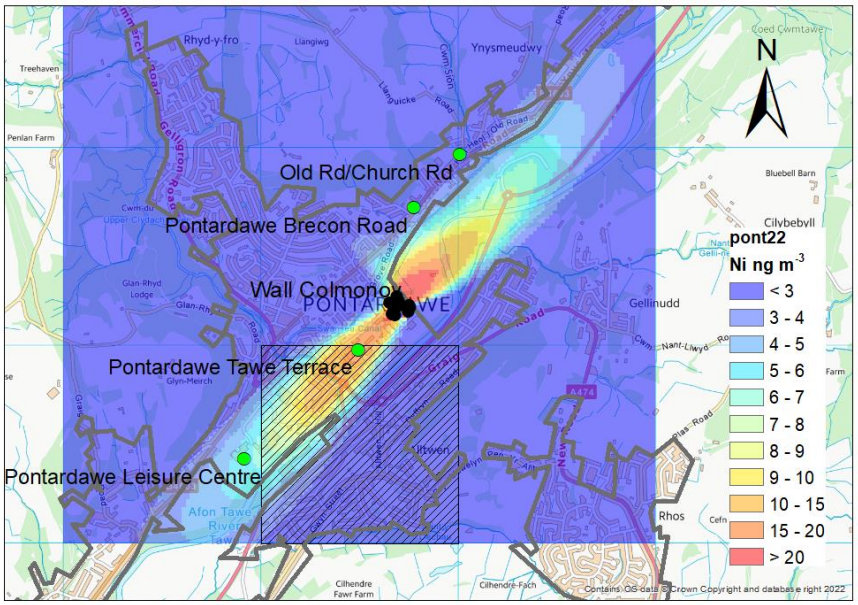

Contains Ordnance Survey data © Crown copyright and database right [2024]

Table 10.10 - Comparison of annual mean measured and modelled annual mean Ni concentrations at Pontardawe Tawe Terrace, Pontardawe Leisure Centre and Pontardawe Brecon Road in 2022.

	Measured Ni (ng m^{-3})	Modelled Ni (ng m^{-3})
Pontardawe Tawe Terrace	17.1	17.1
Pontardawe Leisure Centre*	8.0	5.6
Pontardawe Brecon Road	3.3	2.8

***** Local authority monitoring site, not part of national network, included to provide additional verification of model

10.6.4.3 Sheffield Urban Area and Yorkshire and Humberside Zones

The Sheffield Tinsley monitoring station is located in the valley of the river Don to the North East of Sheffield City Centre in the Sheffield Urban Area agglomeration zone. Exceedances of the annual mean TV of 20 ng m^{-3} have been reported in previous years: 2014 and 2016 on the basis of measurements at the Sheffield Tinsley monitoring station and 2018, 2019, 2020 and 2021 on the basis of model results. The AQSR requires that actions and measures are put in place to help meet the TV following an exceedance. Reports on Measures have been published[8] providing detail on the assessment of the exceedances reported in previous years and the actions and measures that have already been taken or are planned that will help the UK meet the Ni TV. Detailed dispersion modelling has been undertaken for the 2022 compliance assessment using ADMS 5.2 for an area in Sheffield covering the locations of the Sheffield Tinsley and Sheffield Devonshire Green monitoring stations and the principal industrial Ni sources. This fine scale modelling has been used to assess the likely magnitude and spatial extent of exceedance and takes into account work carried out for the report on measures for 2016, 2018, 2019, 2020 and 2021 for the Sheffield Urban Area agglomeration zone (Defra, 2018, 2020, 2021, 2022b, 2023a) in terms of related modelling work and high time resolution monitoring campaigns. For other sites with Ni measurements in the Yorkshire and Humberside zone

[8] https://uk-air.defra.gov.uk/library/bap-nickel-measures

(Scunthorpe Low Santon and Scunthorpe Town) there are no reported exceedances for 2022, hence the focus of the detailed modelling has been on Sheffield.

To support this detailed modelling, information on Ni emissions and release characteristics for the principal industrial Ni emission sources were provided by the Environment Agency (including data collated on sites regulated by Sheffield City Council and Rotherham Metropolitan Borough Council) and complemented by emissions data from the NAEI 2021. Emissions were released from 15 emission sources from one plant. The emissions from the plant were modelled to be released from 14 point sources and one area source. Terrain effects were included in the modelling based on OS Terrain 50.

Figure 10.17 shows the modelled annual mean Ni concentration on a 50 m x 50 m grid resolution resulting from the principal local industrial Ni source in the Sheffield area and including a background component from the annual modelling of Ni concentrations across the UK. The best representation of concentrations at the Sheffield Tinsley monitoring station was obtained as the sum of the modelled contribution from the principal local source and the background contribution. Due to the limited emissions data from the stockyards, the emission rate from this source was scaled based on the measurement data at the Tinsley monitoring station.

The conclusions from this dispersion modelling study are that Ni concentrations in both Sheffield Urban Area and Yorkshire & Humberside zones in 2022 exceeded the Ni TV.

The source apportionment plot (Figure 10.15) and scatter plot (Figure 10.14) presented earlier in this section include the modelled contribution to ambient concentrations at the Sheffield Tinsley and Sheffield Devonshire Green sites from the local industrial Ni sources in Sheffield.

Figure 10.17 - Modelled annual mean Ni concentration resulting from the local industrial sources in Sheffield Tinsley in 2022.

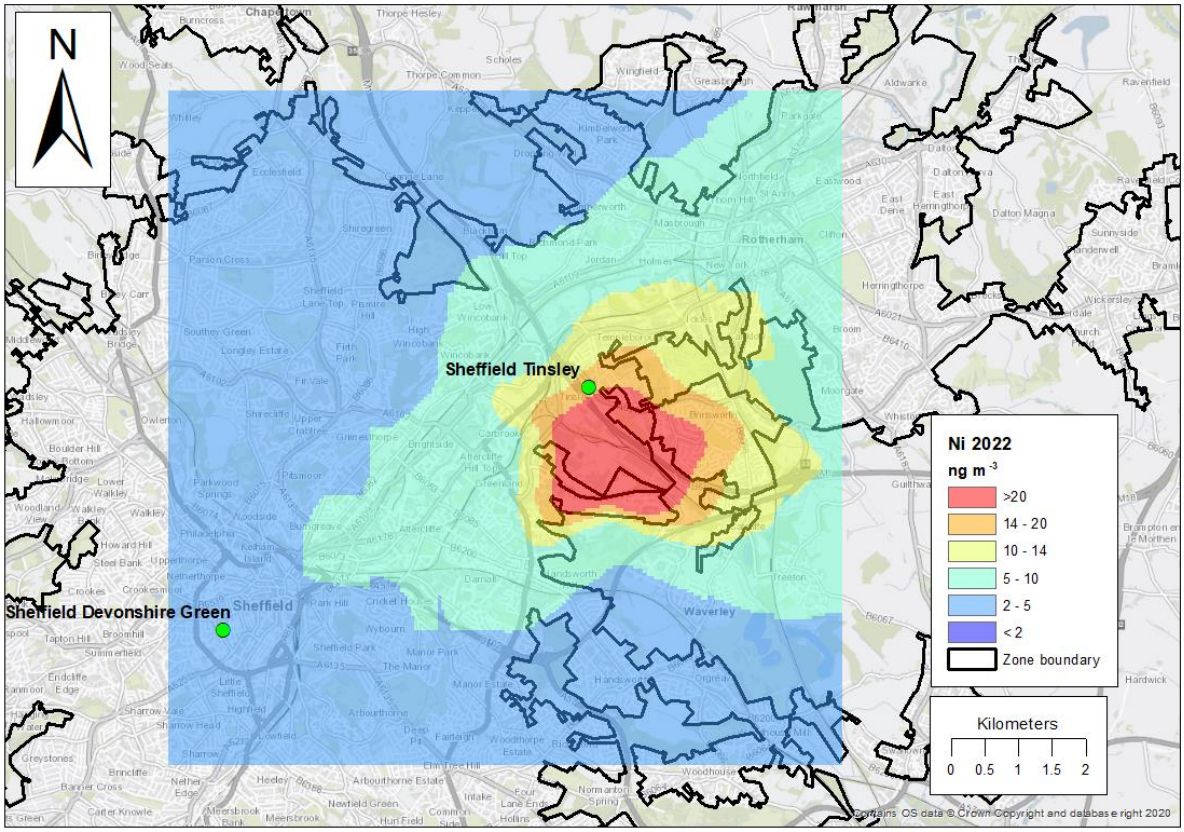

Contains Ordnance Survey data © Crown copyright and database right [2024]

10.7 Lead Results

10.7.1 Introduction

The method used to estimate the Pb ambient concentration across the UK is described in Section 10.3 above.

The map of modelled annual mean Pb concentrations is shown in Figure 10.5. There were no modelled or measured exceedances of the limit value of 0.5 µg/m^3 in 2022.

10.7.2 Verification of mapped concentrations

A comparison between modelled and measured annual mean Pb concentrations in 2022 at different monitoring site locations is shown in Figure 10.18. These figures include lines to represent the AQSR data quality objective for modelled annual mean Pb concentrations: y=x-50% and y=x+50% (see Section 1.5).

Summary statistics for modelled and measured Pb concentrations are listed in Table 10.11, including the percentage of sites at which modelled concentrations are outside of the data quality objectives (DQOs), and the total number of sites included in the analysis.

The mean and distribution (quantified using R^2) of measured and modelled concentrations agree very well for the rural monitoring sites.

It should be noted that non-emission inventory sources (such as fugitive, re-suspension and long-range transport of primary PM) result in additional uncertainty when compared with a pollutant such as NO_X, for which the source apportionment is better known.

Figure 10.18 - Verification of annual mean Pb across all sites.

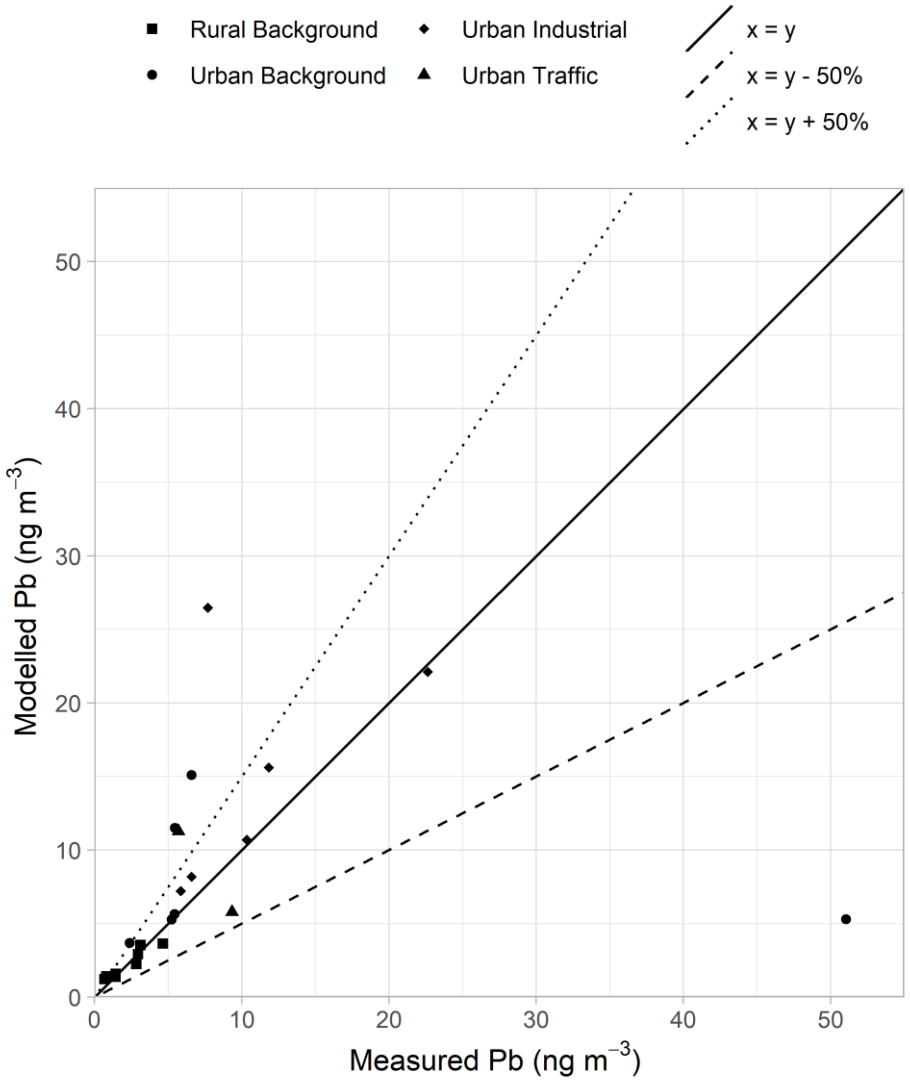

Table 10.11 - Summary statistics for comparison between modelled and measured annual mean Pb concentrations at different monitoring sites, 2022.

	Mean of measurements (ng/m^3)	Mean of model estimates (ng/m^3)	R^2	% of sites outside DQO of ±50%	Number of sites in assessment
Industrial sites	10.83	15.05	0.24	17%	6
Urban background sites	12.69	7.75	0.05	67%	6
Roadside sites	7.51	8.54	1.00	50%	2
Rural sites	2.24	2.25	0.88	25%	8
All	**7.91**	**7.81**	**0.07**	**36%**	**22**

10.7.3 Source apportionment

Figure 10.19 shows the modelled Pb contribution from different sources at monitoring locations. Measured concentrations at the sites are also presented, giving an indication of the level of agreement between modelled and measured concentrations. This analysis suggests that the main sources of lead are emissions from industrial emissions and re-suspension processes, and contributions from long range transport primary.

Figure 10.19 - Annual mean Pb source apportionment at monitoring sites in 2022.

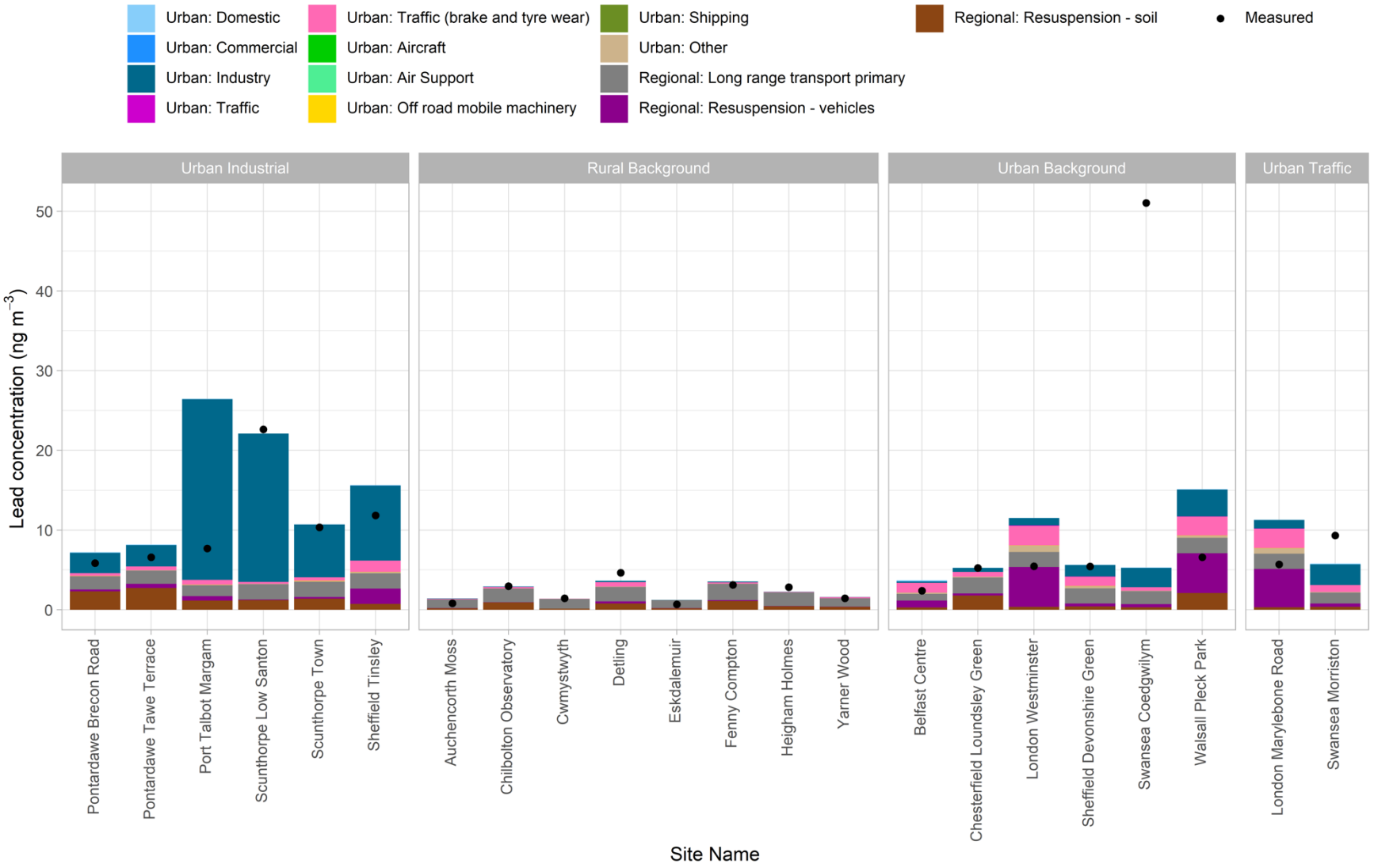

11 Benzo(a)pyrene

11.1 Introduction

11.1.1 Target values

A single target value (TV) for ambient concentrations of benzo(a)pyrene (B(a)P) is set out in AQSR (*legislation.gov.uk*, 2010). The regulations states that all necessary measures not entailing disproportionate costs to ensure that the target value is not exceeded after 31 December 2012 should be taken. The target value is an annual mean concentration of 1 ng m^{-3}.

11.1.2 Annual mean modelling

A map of annual mean B(a)P in 2022 at background locations is shown in Figure 11.2. B(a)P concentrations were modelled for 2005 by (Vincent, Bush and Coleman, 2007) to inform the UK Preliminary Assessment for AQDD4 (Bush, 2007). 2022 is the fifteenth year for which a full air quality assessment is required, and national modelling of B(a)P was undertaken to assess compliance with the target value.

The B(a)P annual mean model is calibrated based on monitoring data from the national network. Consideration has been given to the appropriate application of calibration factors in the model, and for this reason separate calibration factors have been used for the contributions from area sources in Great Britain and Northern Ireland and for coke ovens at steelworks in England and Wales. The 2022 assessment follows a similar approach to that adopted since the 2015 assessment (Brookes *et al.*, 2017), including detailed local scale modelling to improve the representation of contributions from the most dominant industrial sources for B(a)P at locations with the highest concentrations (coke ovens at steelworks in England and Wales). The calibration process is described further in Sections 11.3.2, 11.4.2 and 11.4.4.

11.1.3 Overview of the PCM model for B(a)P

Figure 11.1 shows a simplified flow diagram of the PCM model for B(a)P. A summary of the PCM model method, input, and assumptions for B(a)P is presented in Table 11.1.

Figure 11.1 - Flow diagram for PCM B(a)P model

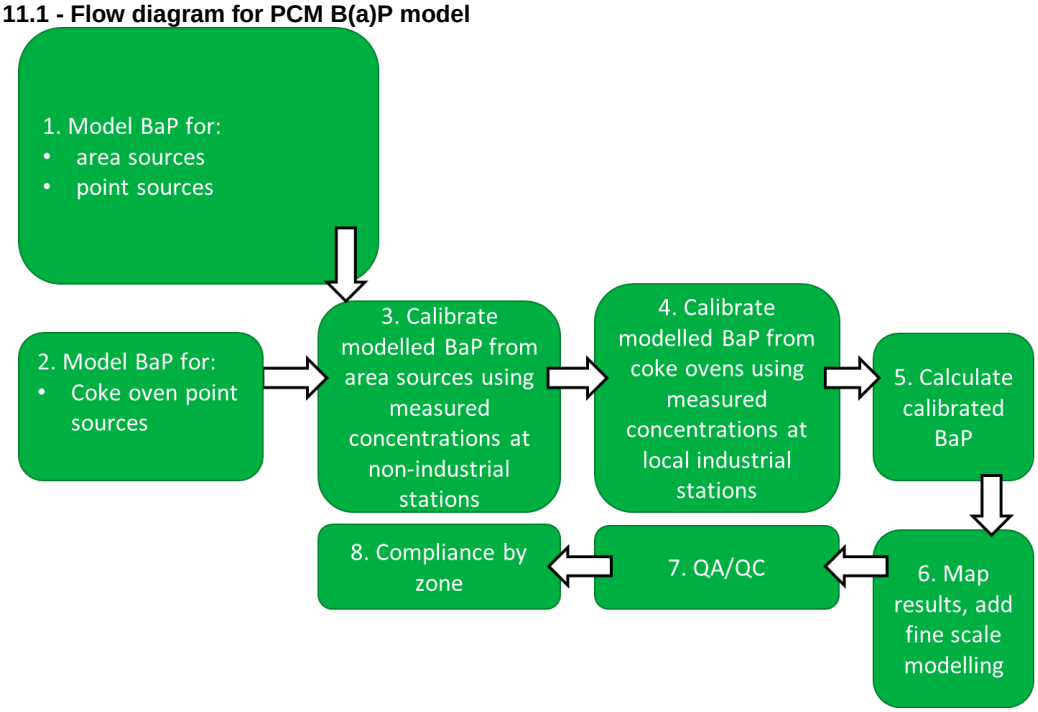

Table 11.1 - PCM model method, input and assumptions summary for B(a)P

Heading	Component	Details
General	Pollutant	BaP
	Year	2022
	Locations modelled	Background
	Metric	Annual mean
Input data	Emission inventory	NAEI 2021 (scaled to 2022) plus operator data for 2022 for integrated steelworks where available
	Energy projections	Energy Projections 2022
	Road traffic counts	2022 (scaled from 2021 where not available)
	Road transport activity projections	DfT (2022) car sales projections, TfL traffic projections for London (2023)
	Road transport emission factors	COPERT 5.4 (COPERT 5.4, 2020)
	Measurement data	2022
	Meteorological data	WRF (see Appendix 4 – WRF meteorology)
Model components	Regional	n/a
	Large point sources	164 sources modelled using ADMS 5.2
	Small point sources	PCM dispersion kernels generated using ADMS 5.2.
	ETS point sources	PCM dispersion kernels generated using ADMS 5.2.
	Large ETS point sources	132 sources modelled using ADMS 5.2
	Area sources	PCM dispersion kernels generated using ADMS 5.2. Time varying emissions for road transport and domestic sources.
	Coke ovens door emissions	Emissions from coke oven door emissions modelled using ADMS 5.2
	Coke oven bleeder emissions	Unflared coke oven bleeder releases were included for Scunthorpe using ADMS 5.2
	Roadside increment	n/a
Calibration	Model calibrated?	Yes (see Pollutant specific information)
	Number of background stations in calibration	27 background + 4 industrial
	Number of traffic stations in calibration	n/a
Pollutant specific	Fine scale modelling	Impact of emissions from coke ovens at Scunthorpe and Port Talbot modelled at 100 m spatial resolution using local meteorological data and incorporating terrain effects for Port Talbot. A contribution from unflared coke oven bleeder releases was also included at Scunthorpe. For the areas covered by the fine scale modelling, 1 km grid cells have been classified as exceeding the TV if at least nine 100 m grid squares exceed the TV or at least one square exceeds and there is population in the 1 km grid cell containing the exceeding 100m grid squares. A concentration value was defined for each 1 km grid square from the fine scale modelling from the mean of the 100 m grid squares exceeding the TV

Heading	Component	Details
		within that 1 km grid square or the mean of all 100 m grid squares for non-exceeding grid squares within the fine scale modelling domain. An exceedance was only reported if the modelled exceedance area includes locations outside of the boundary of the industrial site.
	Calibration	Separate calibration for area sources in Great Britain (24 background stations across Great Britain) and Northern Ireland (27 background stations across the UK). Separate calibration for contributions from coke ovens (local calibration using data from 2 stations in Scunthorpe and 1 station in Port Talbot with concentrations being modelled at 100 m resolution)

11.1.4 Outline of the annual mean model for B(a)P

The 1 km x 1 km annual mean background B(a)P concentration map was calculated by summing the contributions from:

- Large point sources
- Small point sources
- Point sources with emissions estimates for air quality pollutants based on reported carbon emissions (ETS points)
- Coke oven sources modelled at 100m spatial resolution.
- Local area sources

Figure 11.2 - Annual mean background B(a)P concentration, 2022 (ng m^{-3})

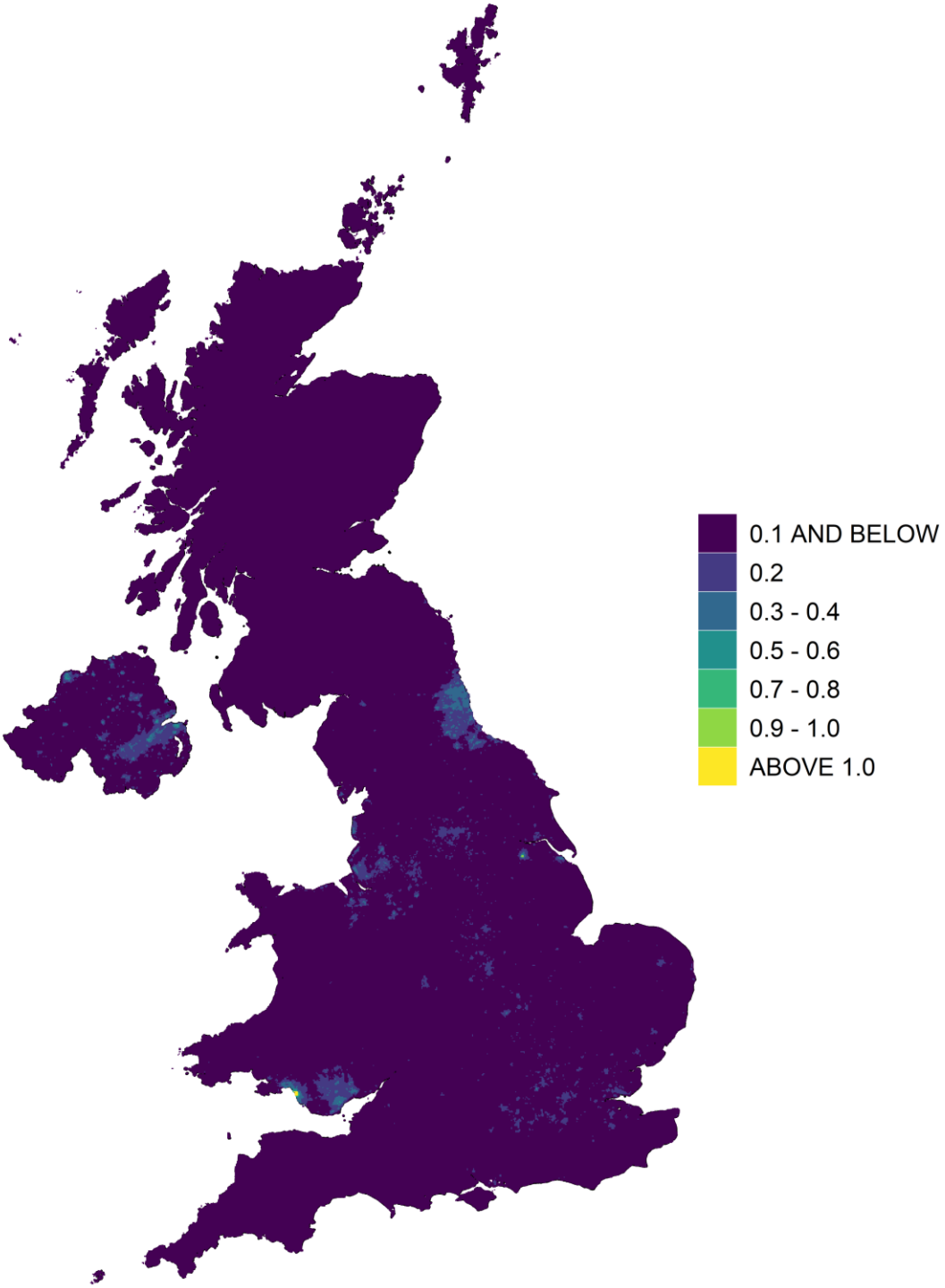

11.1.5 Chapter structure

This chapter describes modelling work carried out for 2022 to assess compliance with the B(a)P target value described above. Emissions estimates for B(a)P are described in Section 11.2. Sections 11.3 and 11.4 describes the B(a)P modelling methods for the annual mean. The modelling results are presented in Section 11.5. Detailed local scale modelling of exceedances relating to B(a)P emissions from coke ovens at steelworks in England and Wales is described in Section 11.5.3.

11.2 Emissions

B(a)P emission estimates from the UK National Atmospheric Emissions Inventory 2021 (NAEI 2021) have been used in this study (Ingledew *et al.*, 2023). Emissions projections have been provided by the NAEI (Personal communication from Ben Pearson, 2023) based on BEIS EEP 2022 energy and emissions projections (BEIS, 2022). Figure 11.3 shows UK total B(a)P emissions for 2022, with the coding described in Table 3.2.

Figure 11.3 shows that B(a)P emissions in 2022 are dominated by two main sources:

- SNAP 2: Domestic combustion (61.2%)
- SNAP 11: Nature (33%)

The emissions inventory provides maps of emissions on a 1 km x 1 km grid, which is likely to be too coarse to incorporate very local variations in emissions from sources such as domestic heating, where there may be considerable in-square variation due to differences in fuel use (Vincent and Tsagatakis, 2014). SNAP 11: 'Nature', refers to B(a)P emissions from combustion in the natural environment such as forest fires. Despite the relatively high emissions contribution from this source sector, the method for distribution of these emissions used in the NAEI ensures that natural combustion is spread evenly across the UK and does not unduly affect the modelled ambient concentrations in any particular area.

Figure 11.3 - Total UK B(a)P emissions for 2022 by SNAP code scaled from NAEI 2021

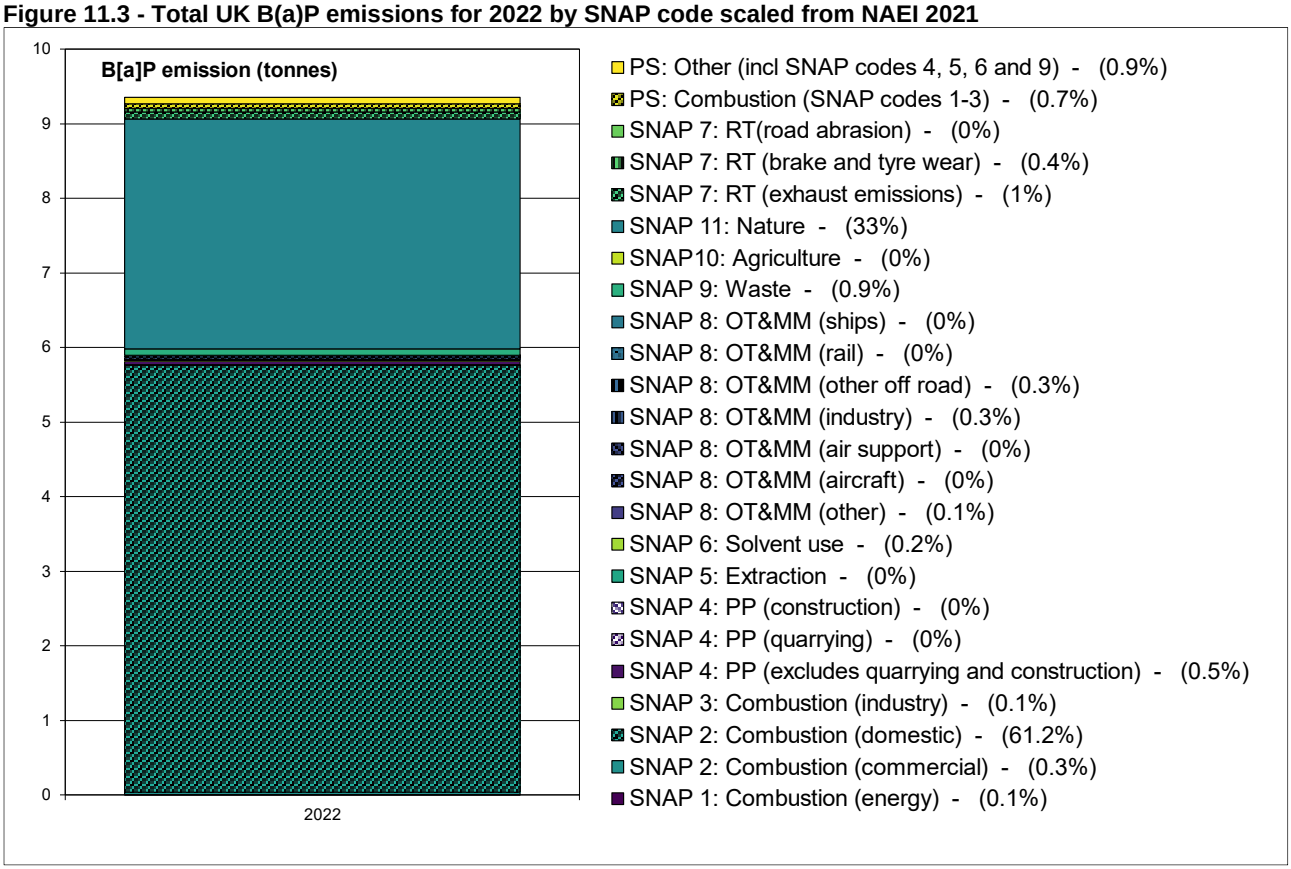

11.3 B(a)P modelling: Contributions from local area sources

11.3.1 Introduction

The 2022 area source B(a)P emissions maps have been calculated from the NAEI 2021 emissions maps following the method described in Section 3.3.5. ADMS derived dispersion kernels have been used to calculate the contribution to ambient B(a)P concentrations on a 1 km x 1 km receptor grid, from the area source emissions within a 33 km x 33 km square surrounding each receptor. Concentrations have been modelled using meteorological hourly sequential data for 2022 from the WRF numerical weather prediction modelling system, as described in Appendix 4 – WRF

meteorology. The WRF model is a next-generation numerical weather prediction system developed by the US National Centre for Atmospheric Science (NCAR) (UCAR, 2020). This method accounts for spatial variation in meteorological parameters across the UK representing local dispersion characteristics within the PCM output. Meteorological data from WRF was used to construct the dispersion kernels, as described in Appendix 5 – Dispersion kernels for the area source model.

11.3.2 Area source model calibration

Figure 11.4 shows the separate calibration of the modelled annual mean area source B(a)P contribution for locations in Great Britain and Northern Ireland applied in the 2022 assessment. The calibration coefficient for locations in Great Britain has been derived by comparing the uncalibrated modelled area source component with measured concentrations at monitoring stations in Great Britain. The calibration coefficient for locations in Northern Ireland has been derived by comparing the uncalibrated modelled area source component with measured concentrations at monitoring stations across the UK. The measured concentrations have been adjusted to represent background (non-industrial) concentrations by subtracting the uncalibrated modelled point source contribution at these locations. Those stations where the uncalibrated point source contribution was ≥ 5% were excluded from the calibration hence the adjustment to the measured concentrations is minimal. To calculate the calibrated area source contribution for each grid square in the country, the modelled area source contribution was multiplied by the relevant calibration fit coefficient.

As noted, for the 2022 assessment, a separate area source calibration has been carried out for locations in Great Britain and Northern Ireland. This approach was followed on the basis that:

- There are no measured exceedances for 2022 in Northern Ireland.
- Measured and modelled concentrations do not scale consistently between monitoring stations in Great Britain and Northern Ireland.
- Applying a separate calibration to domestic only for Northern Ireland based on Northern Ireland monitoring as per previous assessments (Walker *et al.*, 2011; Brookes *et al.*, 2012) would lead to over prediction.
- The Derry Brandywell and Ballymena Ballykeel monitoring stations remain influential in the 2022 area source calibration for Northern Ireland. Including all UK sites in the calibration for Northern Ireland moderates the influence of these stations on the calibration while providing model estimates close to the observed concentrations at Kilmakee Leisure Centre.

In common with previous assessments, the indication that a greater calibration coefficient is required on area source contributions (primarily domestic) in Northern Ireland compared to area sources overall for the UK suggests further improvements are needed for quantifying and mapping domestic combustion emissions in Northern Ireland.

Figure 11.4 indicates similar scatter in the area source calibration for 2022 as for 2021, 2020, 2019, 2018, 2017 and 2016. As part of the calibration process, emission caps have been applied to certain sectors; this is because the use of surrogate statistics for mapping area source emissions sometimes results in unrealistically large concentrations in some grid squares for a given sector. The emission caps applied are given in Table 11.2.

Table 11.2 - Emission caps applied to B(a)P sector grids

SNAP code	Description	Cap applied (kg/a/km^2)
SNAP 4 (production processes, excludes quarrying and construction)	Chemical industry – general, non-fuel bitumen use	0.66
SNAP 4 (production processes, excludes quarrying and construction)	Electric arc furnaces, Steel production (electric arc)	0.66

Figure 11.4 - Calibration of area source model for B(a)P, where the solid regression line and y_1 refer to Great Britain only, and the dashed line and y_2 refer to Great Britain and Northern Ireland.

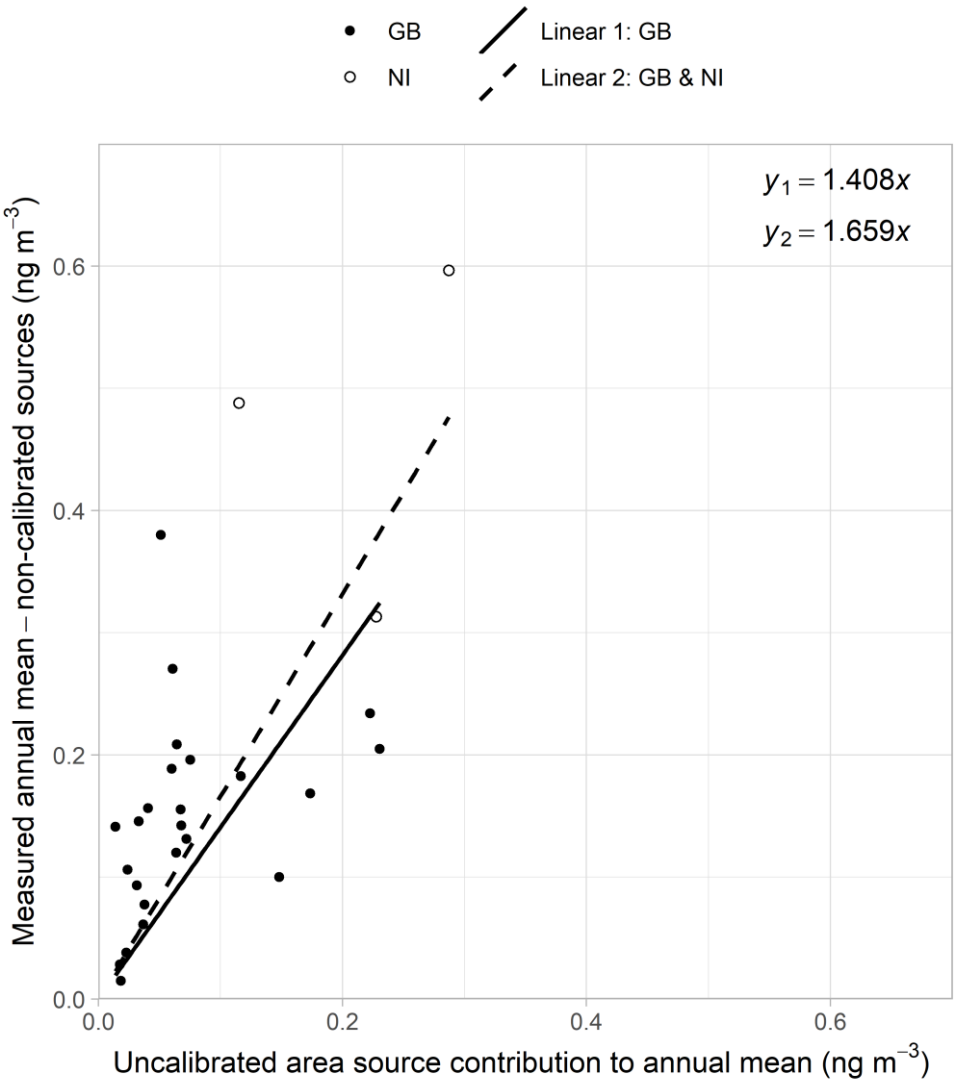

11.4 B(a)P Modelling: Contributions from large and small point sources

11.4.1 Introduction

Contributions to ground level annual mean B(a)P concentrations from large point sources (those with annual emissions greater than 0.001 tonnes, or for which emission release characteristics are known) in the NAEI 2021 have been estimated by modelling each source explicitly using the atmospheric dispersion model ADMS 5.2 and sequential meteorological data for 2022 from the WRF Model. Surface roughness varied at both the dispersion and meteorological sites depending on the area type as presented in Table A5.1. Concentrations were calculated for a 99 km x 99 km square composed of a regularly spaced 1 km x 1 km resolution receptor grid. Each receptor grid was centred on the point source.

Industrial point sources of B(a)P are either fugitive (as from coking plants) or from clearly defined stacks for other sources. The emission amount is derived either from direct measurement or by emission factors. 164 point sources from the NAEI 2021 were classified as large points sources and modelled using emissions release information retrieved from the PCM stack parameters database (described in more detail in Section 3.3.1).

The NAEI 2021 also includes point source emissions estimates derived from carbon emissions data reported under the EU-Emissions Trading Scheme (ETS) (Tsagatakis *et al.*, 2023), referred to as ETS

points in this report. These derived air quality pollutant emissions are particularly uncertain and therefore in previous assessments (e.g. (Brookes *et al.*, 2017)) emissions were capped at reporting thresholds and treated as small point sources. For the 2016, 2017, 2018, 2019, 2020 and 2021 assessments (Brookes *et al.*, 2019b, 2019a, 2020, 2021; Pugsley *et al.*, 2022, 2023) the NAEI recommended treating the ETS points that have emissions greater than the large points modelling threshold as large points and not to apply a cap (Personal communication from Ben Pearson, 2023). The 2022 assessment continues this approach. Thus, based on the criteria for the treatment of large point sources described above, 132 ETS point sources were modelled as an additional set of large point sources (using the approach described above). ETS points that were not classified as large point sources were modelled using the B(a)P small points approach.

The impact of 2 further large point sources, the emissions as the result of door leakage from the coke works at Port Talbot and Scunthorpe (which are the dominant industrial sources for B(a)P), have been modelled as line sources. The emissions from the bleeders at Scunthorpe have been modelled as point sources. The models have been run at finer spatial resolution on a regularly spaced 100 m x 100 m resolution receptor grid. The detailed local scale modelling of the 2 coke ovens is described in Section 11.4.2.

For the majority of large point sources NAEI 2021 emissions were applied with scaling using projection factors to provide emission values for 2022, as described in Section 3.3.1. For each sinter plant stack and coke oven batteries at the integrated steelworks in England and Wales, reported B(a)P emissions for the year 2022 have been acquired and applied in order to provide the best representation of contributions from the most dominant industrial sources for B(a)P at exceedance locations. The NAEI provided operator reported emissions for 2022 for the integrated steelworks at Port Talbot and Scunthorpe (Personal communication from Clare Aston, 2023).

Contributions from B(a)P point sources with less than 0.001 tonnes per year emissions and without emissions release characteristics were modelled using an area source approach. NAEI 2021 emissions for small point sources were scaled to 2022 emissions using the same source sector specific projection factors applied to the large point sources. These emissions were aggregated onto a 1 km x 1 km grid before applying an ADMS 5.2 derived dispersion kernel (for non-domestic, non-road transport) to calculate the contribution to ambient concentrations at a central receptor location from small point source emissions within a 33 km x 33 km square surrounding each receptor. The method used to generate area source dispersion kernels is described in Appendix 5 – Dispersion kernels for the area source model.

11.4.2 Coke oven door sources

Detailed dispersion modelling was undertaken to derive contributions from BaP emissions from the coke ovens in England and Wales. Each source was modelled explicitly using the atmospheric dispersion model ADMS 5.2. Hourly sequential meteorological data for 2022 from WRF was used. Surface roughness was assumed to be 0.5 m at the dispersion site for both Scunthorpe and Port Talbot. Surface roughness was assumed to be 0.1 m and 0.5 m at the meteorological sites for Scunthorpe and Port Talbot respectively. Calm conditions were treated in the dispersion modelling using the ADMS calm module at the ADMS with minimum wind speed at 10 m of 0.3 m/s and critical wind speed of 1 m/s. Concentrations were calculated for a 15 km x 15 km area for Scunthorpe and a 23 km x 23 km area for Port Talbot both composed of regularly spaced 100 m x 100 m resolution receptor grids, centred on the coke ovens. To account for the complex terrain surrounding Port Talbot the effect of the local topography has been included in the 2022 modelling, with terrain heights based upon the OS Terrain 50 dataset.

11.4.3 Coke oven bleeder sources at Scunthorpe

There were 40 unflared releases from eight bleeders reported by the operator at the Appleby coke ovens batteries at Scunthorpe during 2022. Coke ovens operate at positive pressure and flared, and unflared releases of coke oven gas can occur from these bleeders for safety reasons for short periods. These releases are in addition to the reported BaP annual emission from the normal operation of the plant.

Additional dispersion modelling was undertaken to assess the contribution of these short term releases to ambient annual average concentrations. Each release was modelled as an individual short period release of one hour duration with efflux volume flow rate equal to that recorded (i.e. raw gas volume released divided by the duration of the release), but with BaP emission rate factored by the duration of the release to ensure that the total mass released was correct. A source height of 26 m and diameter of 0.62 m was assumed for each release. The temperature of the release was assumed

to be 80°C and the molecular weight and specific heat capacity of the release was calculated from the typical composition of wet raw coke oven gas. The influence of nearby buildings on dispersion was accounted for in the dispersion model's building wake module.

Industry estimates of BaP concentration in raw coke oven gas range from negligible to the highly conservative assumption that all the BaP in the tar is volatilised and released in the gas.

Flared sources are generally not included in the modelling as flaring would destroy any BaP in the release. It should however be noted that no flaring activity from the coke ovens were reported in 2022.

The atmospheric dispersion model ADMS 5.2 was used to model both hourly and annual mean concentrations. The meteorological parameters (data and surface roughness) were the same as those assumed for Scunthorpe in the modelling of coke oven sources (Section 11.4.2)

The hourly mean concentrations were used to form monthly averages, which were compared with monthly monitoring data from the Scunthorpe Town and Scunthorpe Low Santon monitoring sites. Measurement data from Scunthorpe Town showed an elevated monthly averaged concentration of 1.5 ng/m^3 during March 2022. The modelled concentrations as the result of the operation of the coke ovens were calibrated using the best fits to the measured ambient concentrations at both Scunthorpe Town and Low Santon monitors. The modelled concentrations at Low Santon monitoring station were in better agreement than those of the Scunthorpe Town. However, the modelled concentrations fell short of predicting the peak at the Scunthorpe Town station.

The contribution to ambient annual mean concentrations from the coke oven bleeder releases were calculated for a 15 km x 15 km area composed of regularly spaced 100 m x 100 m resolution receptor grids, centred on the coke ovens.

11.4.4 Point source model calibration

In earlier assessments the modelled point source contribution (excluding coke ovens) has been calculated using a single calibration based upon monitoring data from the national network to obtain results consistent with measured concentrations. Since the 2016 assessment, the modelling and monitoring data at other industrial sites no longer supports application of a general point source calibration. With recent closures of dominant industrial sources of B(a)P there are only 2 industrial monitoring stations (Scunthorpe Low Santon and Port Talbot Margam) where the uncalibrated point source contribution is ≥ 50% of the uncalibrated modelled concentration. Thus for 2016, 2017, 2018, 2019, 2020, 2021 and 2022, only the coke ovens contribution has been calibrated, using local monitoring data and the detailed local scale modelling of these sources (described in Section 11.4.2).

There is an element of circularity involved in the calibration of both area and point sources because the calibration process for each requires the subtraction of the other to isolate the component being calibrated. An approach to minimise interdependence of the calibrations was introduced in the 2012 assessment (Brookes *et al.*, 2013) and this was carried forward into the 2022 assessment, as follows:

- The area source component is calibrated first and as discussed in Section 11.3.2 only monitoring stations where the uncalibrated point source contribution is < 5%, are included in the area source calibration. This minimises the influence of point sources on the area source calibration, since the contribution from point sources at non-industrial monitoring stations is typically very small and is guaranteed to be < 5% by this approach.
- In addition, monitoring stations where the uncalibrated point source contribution is ≥ 5%, but still relatively low (< 50%) are excluded from the model calibration completely. Data for these stations are still included in the model verification.
- Given the two conditions above, only monitoring stations where the uncalibrated point source contribution is ≥ 50% of the uncalibrated modelled concentration (area sources plus point sources) are included in the calibration of the point sources.

Since the 2016 assessment a general point source calibration is no longer applied, hence there is no potential for interdependence of the calibrations except for the locations impacted by the coke ovens. The approach remains valuable elsewhere as it ensures the monitoring stations applied in calibrations are most representative of the source sectors being calibrated.

To calibrate the coke ovens contribution, local scaling factors have been applied: 3.63 for door leakage (no scaling for bleeders was required due to negligible effect at the ambient monitoring stations, compared to 2.84 for doors and 6.95 for bleeders in 2021, respectively) at Scunthorpe and 5.24 for door leakage (compared to 2.55 for 2021) at Port Talbot. Local scaling factors were adopted because a general calibration fit would otherwise lead to over or under prediction at each location. Measured concentrations at the industrial monitoring stations were adjusted by subtracting the

calibrated modelled area source contribution and the uncalibrated contribution from other point sources (the sum of other large, small and ETS point source contributions, excluding the coke ovens) so that the measured value represented the coke ovens component only. The local scaling approach guarantees the modelled total B(a)P concentration provides a reasonable representation of the observed concentrations at these monitoring stations.

The contribution from the coke oven bleeder releases was included in the adjustment of the monitoring data prior to calculation of the calibration coefficient for the reported coke oven point source. The local scaling for Scunthorpe was derived from the Scunthorpe Town and Low Santon monitoring sites.

11.5 Results

11.5.1 Verification of mapped values

Figure 11.5 presents a comparison of modelled and measured annual mean B(a)P concentrations in 2022 at monitoring station locations differentiated by station classification. This figure includes lines to represent the data quality objective for modelled annual mean B(a)P concentrations: y=x-60% and y=x+60% (see Section 1.5).

Figure 11.5 - Verification of annual mean B(a)P across all stations

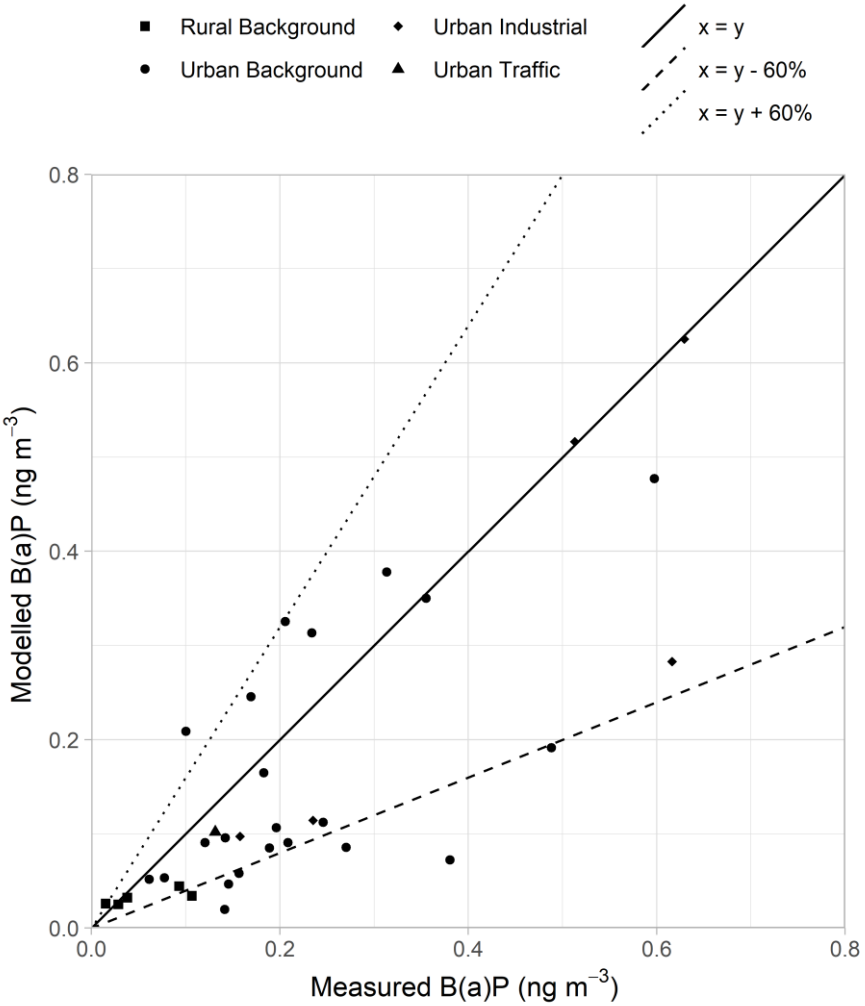

Summary statistics for modelled and measured B(a)P concentrations are listed in Table 11.3, including the percentage of stations at which modelled concentrations are outside of the data quality objectives (DQOs), and the total number of stations included in the analysis. Summary statistics from the national modelling have been calculated for rural, industrial, traffic and urban background stations.

The mean measured and modelled concentrations are in reasonable agreement for all monitoring stations, except those industrial stations not influenced by contributions from coke ovens for which the

dominant local industrial sources are no longer operating. The agreement between measured and modelled concentrations at industrial stations influenced by contributions from coke ovens is naturally better since for two of these three stations the model has been scaled to reproduce the observed concentrations. The R^2 value across all stations is generally better than that for individual station classes reflecting that overall, the model is capturing the variation in observed concentrations. R^2 is less meaningful for the individual station classes, in particular where the number of stations is low, however it does indicate that for background stations that are primarily expected to be influenced by domestic emissions, the model captures a reasonable proportion of the observed variation in concentrations. The low concentrations at rural stations are captured by the modelling.

Table 11.3 - Summary statistics for comparison between modelled and measured annual mean B(a)P concentrations at different monitoring stations, 2022

	Mean of measurements (ng/m^3)	Mean of model estimates (ng/m^3)	R^2	% of stations outside DQO of ±60%	Number of stations in assessment
Rural Background sites	0.06	0.03	0.62	0%	5
Urban Industrial sites	0.43	0.33	0.67	100%	2
Urban Background sites	0.23	0.16	0.37	68%	22
Urban Traffic sites	0.13	0.10	0	0%	1
All	**0.23**	**0.17**	**0.61**	**27%**	**33**

11.5.2 Source apportionment

A source apportionment graph is plotted in Figure 11.6 to present the B(a)P contribution from different sources at monitoring station locations. It should be noted that for industrial and background stations in the areas covered by the fine scale modelling of the coke ovens (Scunthorpe Town, Scunthorpe Low Santon, Port Talbot Margam, Swansea Cwm Level Park), described in Section 11.4.2, the modelled source apportionment includes the local modelling. The source apportionment for stations outside these areas is from the national scale modelling. Measured concentrations at the stations are also presented, giving an indication of the level of agreement between modelled and measured concentrations. Domestic combustion, at many stations, and industry, at industrial stations, are the most important sources. The contributions from other sources are much smaller.

Figure 11.6 - Annual mean B(a)P source apportionment at background national network monitoring stations in 2022 (the area type of each station is shown in parenthesis after its name)

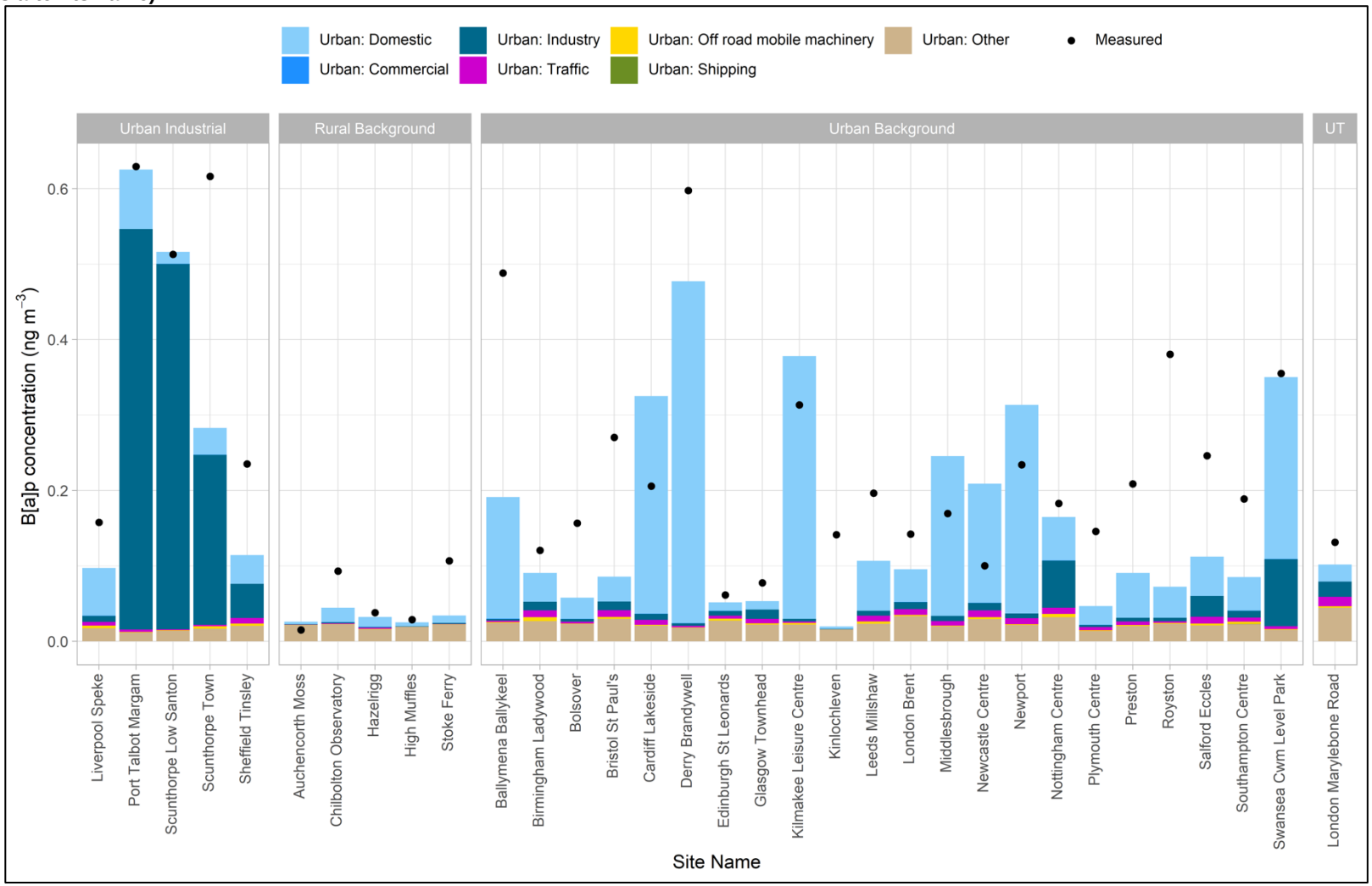

11.5.3 Detailed comparison of modelling results with the target value

Results of the assessment in terms of comparisons of the modelled concentrations with the TV have been reported in e-Reporting Data flow G (*UK-Air*, 2023). For the areas covered by the fine scale modelling, 1 km grid cells have been classified as exceeding the TV if at least nine 100 m grid squares exceed the TV or at least one 100 m square exceeds and there is population in the exceeding 1 km grid square. A concentration value was defined for each 1 km grid square from the fine scale modelling from the mean of the 100 m grid squares exceeding the TV within that 1 km grid square or the mean of all 100 m grid squares for non-exceeding grid squares within the fine scale modelling domain.

Exceedances of the 1 ng m^{-3} TV have been modelled for two zones (South Wales and Swansea Urban Area) for 2022. The following information is based on a source apportionment assessment including the fine scale modelling.

No exceedance of the TV has been modelled in the Yorkshire & Humberside zone for 2022. As the elevated ground level concentrations of BaP, from the Appleby coke ovens of the Scunthorpe steelworks, are confined to the boundary of the site.

Exceedances in 6 km^2 of the South Wales zone and 3 km^2 of the Swansea Urban Area have been modelled, associated with industrial emissions from the coke oven at the steel plant at Port Talbot.

Figure 11.7 and Figure 11.8 show the modelled annual mean B(a)P concentration at a 100 m x 100 m spatial resolution in the vicinity of the coke ovens at Scunthorpe and Port Talbot respectively. Figure 11.9 shows the complex terrain surrounding Port Talbot which has been incorporated into the 2022 modelling and influences the dispersion of emissions from the coke ovens in this location.

Figure 11.7 - Modelled total annual mean B(a)P concentration in the vicinity of the Appleby coke ovens at the Scunthorpe steelworks in 2022.

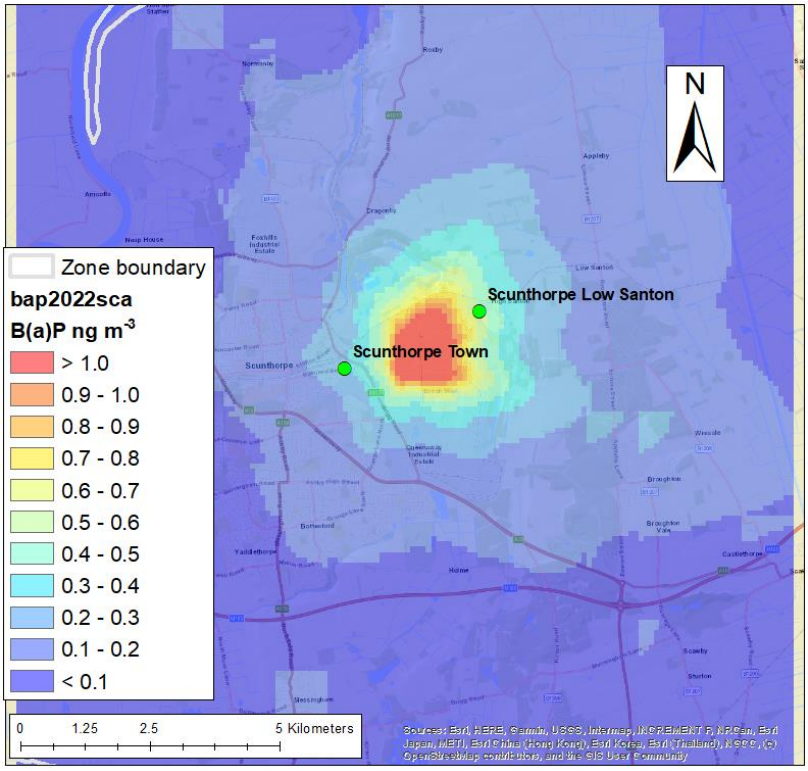

Contains Ordnance Survey data © Crown copyright and database right [2024]

Figure 11.8 - Modelled total annual mean B(a)P concentration in the vicinity of the coke ovens at the Port Talbot steelworks in 2022

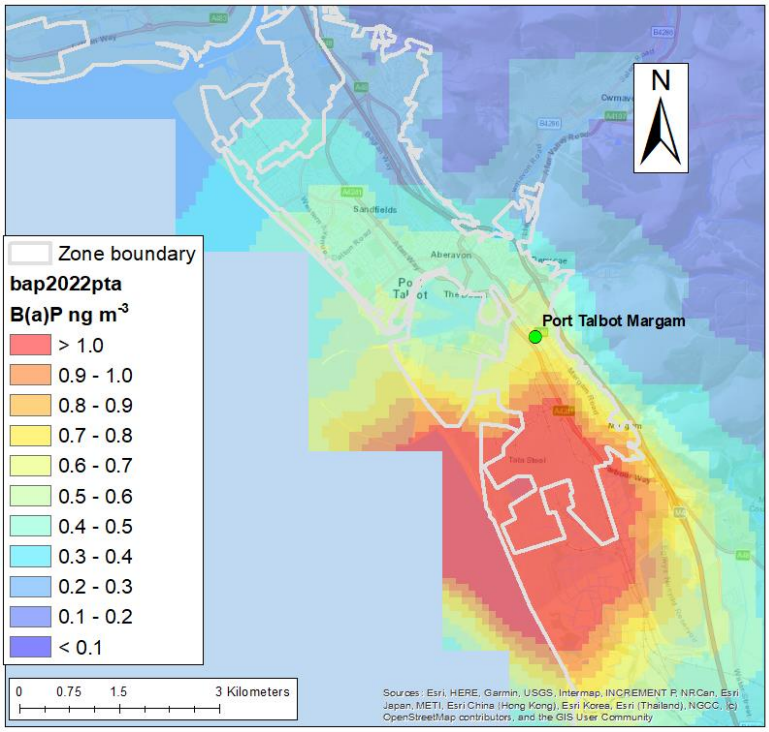

Contains Ordnance Survey data © Crown copyright and database right [2024]

Figure 11.9 - Terrain heights in the vicinity of Port Talbot

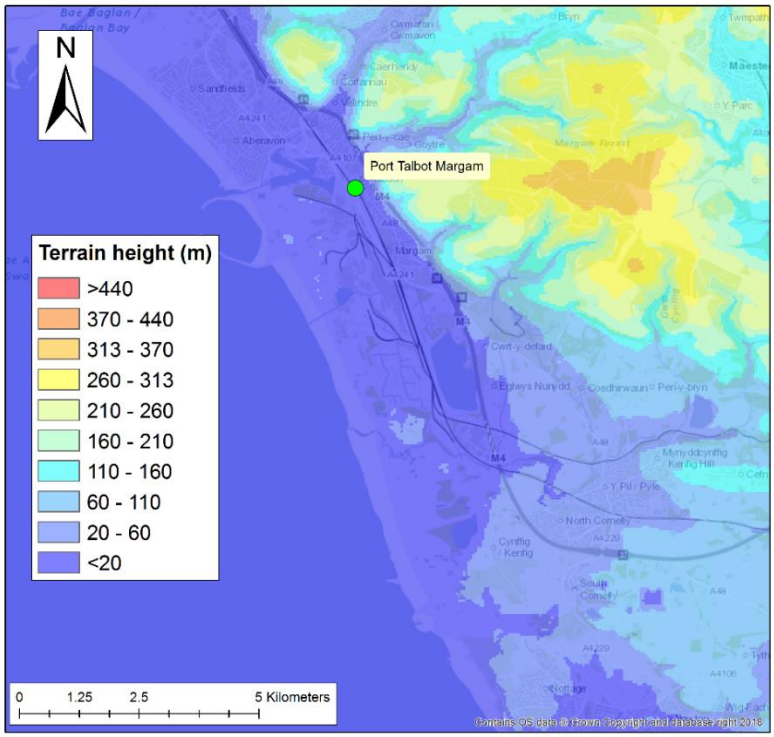

Contains Ordnance Survey data © Crown copyright and database right [2024]

12 Acknowledgements

This work was funded by the UK Department for Environment, Food and Rural Affairs, The Welsh Government, The Scottish Government and The Department of the Environment for Northern Ireland.

The authors would also like to thank: Hanson Building Products Limited for providing SO_2 measurements and INEOS for providing benzene measurements.

Detailed information and measurements for the Pontardawe Leisure Centre monitoring site was kindly provided by Neath Port Talbot County Borough Council. This monitoring site was included in the analysis for verification of the local scale modelling of Ni concentrations in Pontardawe. The authors would also like to thank the Natural Resources Wales, local authorities and plant operators for helping with the nickel emission data and release characteristics for specific plants.

The authors would like the thank providers of model input data that supported local scale modelling of B(a)P concentrations in the vicinity of the steelworks at Port Talbot and Scunthorpe. Detailed B(a)P emission data for Port Talbot and Scunthorpe were provided by the NAEI and plant operators.

13 References

Abbott, J. (2008) *Modelling re-suspended heavy metal emissions. AEA report. AEAT/ENV/R/2926 Issue 2.*

Abbott, J., Stedman, J. and Bower, J. (2005) *Review of background air-quality data and methods to combine these with process contributions: technical modelling aspects. A report produced on behalf of the Environment Agency by AEA Energy and Environment. Science Report: SC030174/SR2. Report available from: https://www.gov.uk/government/publications/review-of-background-air-quality-data-and-methods-to-combine-these-with-process-contributions*.

Abbott, J. and Vincent, K. (1999) *Annual average sulphur dioxide concentration maps derived by dispersion modelling. AEA Technology, National Environmental Technology Centre. Report AEAT – 4629. https://uk-air.defra.gov.uk/assets/documents/reports/empire/kvann1/so2ann.html*.

Abbott, J. and Vincent, K. (2006) *Annual audits of the contribution to pollutant concentrations from processes regulated by the Environment Agency: Application of method for current case. Environment Agency (Science Report: SC030172/SR3)*.

Abdalmogith, S., Harrison, R. and Derwent, R. (2006) ' Particulate sulphate and nitrate in Southern England and Northern Ireland during 2002/3 and its formation in a photochemical trajectory model.', *Science of the Total Environment*, 368, pp. 768–780.

Air Pollution in the UK 2022 (September 2023). Report for The Department for Environment, Food and Rural Affairs, Welsh Government, the Scottish Government and the Department of the Environment for Northern Ireland. https://uk-air.defra.gov.uk/library/annualreport/viewonline?year=2022_issue_1#report_pdf (2023).

Air Quality Expert Group (AQEG) (2004) *Nitrogen Dioxide in the United Kingdom. https://uk-air.defra.gov.uk/library/aqeg/publications*.

Air Quality Expert Group (AQEG) (2005) *Particulate Matter in the United Kingdom. https://uk-air.defra.gov.uk/library/aqeg/publications*.

Air Quality Expert Group (AQEG) (2007) *Trends in Primary NO2 in the United Kingdom. https://uk-air.defra.gov.uk/assets/documents/reports/aqeg/primary-no-trends.pdf*.

Airborne Particles Expert Group (APEG) (1999) *Source Apportionment of Airborne Particulate Matter in the United Kingdom. ISBN 0-7058-1771-7, https://uk-air.defra.gov.uk/library/reports?report_id=32*.

BEIS (2016) *BEIS Domestic Wood Use Survey. https://www.gov.uk/government/publications/summary-results-of-the-domestic-wood-use-survey and https://www.gov.uk/government/publications/energy-trends-march-2016-special-feature-article-summary-results-of-the-domestic-wood-use-survey*.

BEIS (2022) *Updated energy and emissions projections: 2021*, *https://www.gov.uk/government/collections/energy-and-emissions-projections#full-publication-update-history*.

Brookes, D.M. *et al.* (2011) *UK air quality modelling under the Air Quality Directive (2008/50/EC) for 2010 covering the following air quality pollutants: SO2, NOx, NO2, PM10, PM2.5, lead, benzene, CO, and ozone. Report for The Department for Environment, Food and Rural Affairs, Welsh Government, the Scottish Government and the Department of the Environment for Northern Ireland. AEA report. AEAT/ENV/R/3215 Issue 1. https://uk-air.defra.gov.uk/library/reports?report_id=697*.

Brookes, D.M. *et al.* (2012) *Technical report on UK supplementary assessment under the Air Quality Directive (2008/50/EC), the Air Quality Framework Directive (96/62/EC) and Fourth Daughter Directive (2004/107/EC) for 2011. Report for The Department for Environment, Food and Rural*

Affairs, Welsh Government, the Scottish Government and the Department of the Environment for Northern Ireland. Ricardo-AEA. Report AEAT/ENV/R/3316. https://uk-air.defra.gov.uk/library/reports?report_id=768.

Brookes, D.M. *et al.* (2013) *Technical report on UK supplementary assessment under the Air Quality Directive (2008/50/EC), the Air Quality Framework Directive (96/62/EC) and Fourth Daughter Directive (2004/107/EC) for 2012. Report for The Department for Environment, Food and Rural Affairs, Welsh Government, the Scottish Government and the Department of the Environment for Northern Ireland. Ricardo-AEA. Report Ricardo-AEA/R/3380 Issue 1.* https://uk-air.defra.gov.uk/library/reports?report_id=780.

Brookes, D.M. *et al.* (2015) *Technical report on UK supplementary assessment under the Air Quality Directive (2008/50/EC), the Air Quality Framework Directive (96/62/EC) and Fourth Daughter Directive (2004/107/EC) for 2013. Report for The Department for Environment, Food and Rural Affairs, Welsh Government, the Scottish Government and the Department of the Environment for Northern Ireland. Ricardo-AEA. Report Ricardo-AEA/R/3421 Issue 1.* https://uk-air.defra.gov.uk/library/reports?report_id=797.

Brookes, D.M. *et al.* (2016) *Technical report on UK supplementary assessment under the Air Quality Directive (2008/50/EC), the Air Quality Framework Directive (96/62/EC) and Fourth Daughter Directive (2004/107/EC) for 2014. Report for The Department for Environment, Food and Rural Affairs, Welsh Government, the Scottish Government and the Department of the Environment for Northern Ireland. Ricardo Energy & Environment. Report Ricardo Energy & Environment/R/3459.* https://uk-air.defra.gov.uk/library/reports?report_id=813.

Brookes, D.M. *et al.* (2017) *Technical report on UK supplementary assessment under the Air Quality Directive (2008/50/EC), the Air Quality Framework Directive (96/62/EC) and Fourth Daughter Directive (2004/107/EC) for 2015. Report for The Department for Environment, Food and Rural Affairs, Welsh Government, the Scottish Government and the Department of the Environment for Northern Ireland. Ricardo Energy & Environment. Report Ricardo Energy & Environment/R/3465.* https://uk-air.defra.gov.uk/library/reports?report_id=910.

Brookes, D.M. *et al.* (2019a) *Technical report on UK supplementary assessment under the Air Quality Directive (2008/50/EC), the Air Quality Framework Directive (96/62/EC) and Fourth Daughter Directive (2004/107/EC) for 2016. Report for The Department for Environment, Food and Rural Affairs, the Welsh Government, the Scottish Government and the Department of the Environment for Northern Ireland. Ricardo Energy & Environment. Report Ricardo Energy & Environment/R/3467.* https://uk-air.defra.gov.uk/library/reports?report_id=933.

Brookes, D.M. *et al.* (2019b) *Technical report on UK supplementary assessment under the Air Quality Directive (2008/50/EC), the Air Quality Framework Directive (96/62/EC) and Fourth Daughter Directive (2004/107/EC) for 2017. Report for The Department for Environment, Food and Rural Affairs, the Welsh Government, the Scottish Government and the Department of the Environment for Northern Ireland. Ricardo Energy & Environment. Report Ricardo Energy & Environment/R/3469.* https://uk-air.defra.gov.uk/library/reports?report_id=965.

Brookes, D.M. *et al.* (2020) *Technical report on UK supplementary assessment under the Air Quality Directive (2008/50/EC), the Air Quality Framework Directive (96/62/EC) and Fourth Daughter Directive (2004/107/EC) for 2018. Report for The Department for Environment, Food and Rural Affairs, the Welsh Government, the Scottish Government and the Department of the Environment for Northern Ireland. Ricardo Energy & Environment. Report Ricardo Energy & Environment/R/3469.* https://uk-air.defra.gov.uk/library/reports?report_id=993.

Brookes, D.M. *et al.* (2021) *Technical report on UK supplementary assessment under the Air Quality Directive (2008/50/EC), the Air Quality Framework Directive (96/62/EC) and Fourth Daughter Directive (2004/107/EC) for 2019. Report for The Department for Environment, Food and Rural Affairs, the Welsh Government, the Scottish Government and the Department of the Environment for Northern Ireland. Ricardo Energy & Environment. Report Ricardo Energy & Environment/R/3472* https://uk-air.defra.gov.uk/library/reports?report_id=1007.

Bush, T. (2000) *Article 5 Assessment of Nitrogen Dioxide, PM10, sulphur dioxide and lead in the UK. Report to the Department for Environment, Food and Rural Affairs, the Scottish Executive, Welsh Assembly Government and the Department of the Environment in Northern Ireland. AEA Technology, National Environmental Technology Centre. Report AEAT/R/ENV/0165.* https://uk-air.defra.gov.uk/library/reports?report_id=303.

Bush, T. (2007) *Preliminary Assessment of PAH and heavy metal levels in the UK. Report to the Department for Environment, Food and Rural Affairs, the Scottish Executive, Welsh Assembly Government and the Department of the Environment in Northern Ireland. AEA Technology, National Environmental Technology Centre. Report AEAT/R/ENV/2243.* https://uk-air.defra.gov.uk/library/reports?report_id=496.

Bush, T. *et al.* (2007) *UK and Gibraltar air quality modelling for annual reporting 2005 on ambient air quality assessment under Council Directives 96/62/EC and 2002/3/EC relating to ozone in ambient air. Report to Department for Environment, Food and Rural Affairs, the Scottish Executive, Welsh Assembly Government, the Department of the Environment in Northern Ireland and the Government of Gibraltar. AEA/ENV/R/2403.* https://uk-air.defra.gov.uk/library/reports?report_id=456.

Bush, T. and Targa, J. (2005) *Ozone Mapping Techniques for the 3rd Daughter Directive; OSRM vs Empirical modelling Comparison Report. A report to The Department for Environment, Food and Rural Affairs, Welsh Assembly Government, The Scottish Executive and the Department of the Environment for Northern Ireland. AEA Technology plc, Netcen, Harwell. Report AEAT/ENV/R/2053.*

Bush, T., Targa, J. and Stedman, J. (2006) *UK Air Quality modelling for annual reporting 2004 on ambient air quality assessment under Council Directives 96/62/EC and 2002/3/EC relating to ozone in ambient air. A report to the Department for Environment Food and Rural Affairs, Welsh Assembly Government, The Scottish Executive and the Department of the Environment for Northern Ireland. AEAT/ENV/R/2053.* https://uk-air.defra.gov.uk/library/reports?report_id=379.

CAA (2022) https://www.caa.co.uk/Data-and-analysis/UK-aviation-market/Airports/Datasets/UK-airport-data/.

Carslaw, D.C. *et al.* (2011) *Trends in NOx and NO2 emissions and ambient measurements in the UK. Version: July 2011.* https://uk-air.defra.gov.uk/library/reports?report_id=673.

Carslaw, D.C. and Ropkins, K. (2012) *"openair — An R package for air quality data analysis." Environmental Modelling & Software, 27–28(0), 52–61. ISSN 1364-8152, doi:* https://doi.org/10.1016/j.envsoft.2011.09.008.

Coleman, P. *et al.* (2001) *Assessment of Benzo[a]pyrene Atmospheric concentrations in the UK to Support the Establishment of a National PAH Objective. Report produced for the Department for Environment, Food and Rural Affairs, the National Assembly for Wales, the Scottish Executive and the Department of the Environment for Northern Ireland. AEAT/ENV/R/0620.* https://uk-air.defra.gov.uk/library/reports?report_id=24.

COPERT 5.4 (2020) https://www.emisia.com/wp-content/uploads/files/docs/COPERT_v5.4_Report.pdf.

Coyle, M. *et al.* (2002) 'Quantifying the spatial distribution of surface ozone concentration in the UK.', *Atmospheric Environment*, 36, pp. 1013–1024.

Day, T. (2006) *Degree-days: Theory and application. CIBSE. TM41.* https://www.cibse.org/Knowledge/knowledge-items/detail?id=a0q20000008I73TAAS.

Defra (2009) *UK Notification to the European Commission to secure additional time to meet the limit values for particulate matter for certain zones/agglomerations in accordance with the Council Directive 2008/50/EC on Ambient Air Quality and Cleaner Air for Europe.* https://webarchive.nationalarchives.gov.uk/20091118105042/http://www.defra.gov.uk/environment/quality/air/airquality/eu-int/eu-directives/airqual-directives/notification.htm.

Defra, R.E.& E. (2018) *Report on measures for 2016 exceedance of the Target Value for Nickel in Sheffield Urban Area agglomeration zone (UK0007).* https://uk-air.defra.gov.uk/assets/documents/reports/bap-nickel-measures/ni_sheffield_UK0007_reportonmeasures_2016.pdf.

Defra, R.E.& E. (2020) *Report on measures for 2018 exceedance of the Target Value for Nickel in Sheffield Urban Area agglomeration zone (UK0007).* https://uk-air.defra.gov.uk/assets/documents/reports/bap-nickel-measures/ni_sheffield_UK0007_reportonmeasures_2018.pdf.

Defra, R.E.& E. (2021) *Report on measures for 2019 exceedance of the Target Value for Nickel in Sheffield Urban Area agglomeration zone (UK0007).* https://uk-air.defra.gov.uk/assets/documents/reports/bap-nickel-measures/ni_sheffield_UK0007_reportonmeasures_2019.pdf.

Defra, R.E.& E. (2022) *Report on measures for 2020 exceedance of the Target Value for Nickel in Sheffield Urban Area agglomeration zone (UK0007).* https://uk-air.defra.gov.uk/assets/documents/reports/bap-nickel-measures/ni_sheffield_UK0007_reportonmeasures_2020.pdf.

Defra, R.E.& E. (2023) *Report on measures for 2021 exceedance of the Target Value for Nickel in Sheffield Urban Area agglomeration zone (UK0007).* https://uk-air.defra.gov.uk/assets/documents/reports/bap-nickel-measures/ni_sheffield_UK0007_reportonmeasures_2021.pdf.

Design Manual for Roads and Bridges (DMRB) (2005) *Volume 6, Section 1, Part 2, TD 27/05, "Cross-Sections and Headrooms", https://www.gov.uk/guidance/standards-for-highways-online-resources*.
DfT (2021) https://www.gov.uk/government/statistics/transport-use-during-the-coronavirus-covid-19-pandemic.

DfT (2022) https://roadtraffic.dft.gov.uk/downloads.

Entec (2010) *UK Ship Emissions Inventory. Retrieved from* https://uk-air.defra.gov.uk/reports/cat15/1012131459_21897_Final_Report_291110.pdf.

Environment Agency/Joint Air Quality Unit (2022) *UK Urban NO2 Network Annual Report 2021,* https://uk-air.defra.gov.uk/library/reports?report_id=1099.

GFS Forecast (2021) https://www.ncdc.noaa.gov/data-access/model-data/model-datasets/global-forcast-system-gfs.

Grice, S.E. *et al.* (2009) *UK air quality modelling for annual reporting 2007 on ambient air quality assessment under Council Directives 96/62/EC, 1999/30/EC and 2000/69/EC. Report to the Department for Environment, Food and Rural Affairs, the Scottish Executive, Welsh Assembly Government and the Department of the Environment in Northern Ireland. AEA report. AEAT/ENV/R/2656 Issue 1.* https://uk-air.defra.gov.uk/library/reports?report_id=554.

Grice, S.E., Cooke, S.L., *et al.* (2010) *UK air quality modelling for annual reporting 2008 on ambient air quality assessment under Council Directives 96/62/EC, 1999/30/EC and 2000/69/EC. Report to The Department for Environment, Food and Rural Affairs, Welsh Assembly Government, the Scottish Government and the Department of the Environment for Northern Ireland. AEA report. AEAT/ENV/R/2859 Issue 1.* https://uk-air.defra.gov.uk/library/reports?report_id=594.

Grice, S.E., Brookes, D.M., *et al.* (2010) *UK air quality modelling under the Air Quality Directive (2008/50/EC) for 2009 covering the following air quality pollutants: SO2, NOx, NO2, PM10, PM2.5, lead, benzene, CO, and ozone. Report for The Department for Environment, Food and Rural Affairs, Welsh Assembly Government, the Scottish Government and the Department of the Environment for Northern Ireland. AEA report. AEAT/ENV/R/3069 Issue 1.* https://uk-air.defra.gov.uk/library/reports?report_id=695.

Harrison, R.M. *et al.* (2006) 'Measurement and modelling of air pollution and atmospheric chemistry in the U.K. West Midlands conurbation: Overview of the PUMA consortium project. https://doi.org/10.1016/j.scitotenv.2005.08.053', *Science of the Total Environment*, 360, pp. 5–25.

Harrison, R.M. and Yin, J. (2006) *Characterisation of particulate matter in the United Kingdom. Final Project Report. University of Birmingham. CPEA 6.*

Ingledew, D. *et al.* (2023) *UK Informative Inventory Report (1990 to 2021), National Atmospheric Emissions Inventory, Ricardo Energy & Environment, https://uk-air.defra.gov.uk/assets/documents/reports/cat09/2303151609_UK_IIR_2023_Submission.pdf*.

Jenkin, M.E. (2004) 'Analysis of sources and partitioning of oxidant in the UK-Part 1: the NOx-dependence of annual mean concentrations of nitrogen dioxide and ozone. ', *Atmospheric Environment*, 38, pp. 5117–5129.

Jenkin, M.E. (2012) *Investigation of the NOx-dependence of oxidant partitioning at UK sites using annual mean data 1991-2011. Report 05-12. Atmospheric Chemistry Services, Okehampton, Devon, UK. Available upon request.*

Kent, A.J., Grice, S.E., Stedman, J.R., Bush, T.J., *et al.* (2007) *UK air quality modelling for annual reporting 2005 on ambient air quality assessment under Council Directives 96/62/EC, 1999/30/EC and 2000/69/EC. Report to the Department for Environment, Food and Rural Affairs, the Scottish Executive, Welsh Assembly Government and the Department of the Environment in Northern Ireland. AEA report. AEAT/ENV/R/2278 Issue 1. https://uk-air.defra.gov.uk/library/reports?report_id=453*.

Kent, A.J., Grice, S.E., Stedman, J.R., Cooke, S., *et al.* (2007) *UK air quality modelling for annual reporting 2006 on ambient air quality assessment under Council Directives 96/62/EC, 1999/30/EC and 2000/69/EC. Report to the Department for Environment, Food and Rural Affairs, the Scottish Executive, Welsh Assembly Government and the Department of the Environment in Northern Ireland. AEA report. AEAT/ENV/R/2502 Issue 1. https://uk-air.defra.gov.uk/library/reports?report_id=514*.

Kent, A.J. and Stedman, J.R. (2007) *UK and Gibraltar air quality modelling for annual reporting 2006 on ambient air quality assessment under Council Directives 96/62/EC and 2002/3/EC relating to ozone in ambient air. Report to Department for Environment, Food and Rural Affairs, the Scottish Executive, Welsh Assembly Government, the Department of the Environment in Northern Ireland and the Government of Gibraltar. AEA/ENV/R/2499. https://uk-air.defra.gov.uk/library/reports?report_id=526*.

Kent, A.J. and Stedman, J.R. (2008) *UK and Gibraltar air quality modelling for annual reporting 2007 on ambient air quality assessment under Council Directives 96/62/EC and 2002/3/EC relating to ozone in ambient air. Report to Department for Environment, Food and Rural Affairs, the Scottish Executive, Welsh Assembly Government, the Department of the Environment in Northern Ireland and the Government of Gibraltar. AEA/ENV/R/2681. https://uk-air.defra.gov.uk/library/reports?report_id=552*.

Kent, A.J., Stedman, J.R. and Yap, F.W. (2010) *UK and Gibraltar air quality modelling for annual reporting 2008 on ambient air quality assessment under Council Directives 96/62/EC and 2002/3/EC relating to ozone in ambient air. Report to Department for Environment, Food and Rural Affairs, the Scottish Executive, Welsh Assembly Government, the Department of the Environment in Northern Ireland and the Government of Gibraltar. AEA Technology Energy & Environment. AEA/ENV/R/3097. https://uk-air.defra.gov.uk/library/reports?report_id=595*.

Land Cover Map 2000, https://www.ceh.ac.uk/sites/default/files/LCM2000%20dataset%20information.pdf (2009).

Lee, D.S. *et al.* (2000) 'Modelling the atmospheric oxidised and reduced nitrogen budgets for the UK with a Lagrangian multi-layer long-range transport model. ', *Environmental Modelling and Assessment*, 5, pp. 83–104.

legislation.gov.uk (2010) *https://www.legislation.gov.uk/uksi/2010/1001/contents/made*.

legislation.gov.uk (2020) https://www.legislation.gov.uk/uksi/2010/1001/schedule/2/2020-12-10.

Murrells, T. *et al.* (2008) *Modelling of Tropospheric Ozone: First Annual Report. AEA Report AEAT/ENV/R/2567.* https://uk-air.defra.gov.uk/library/reports?report_id=510.

Murrells, T. *et al.* (2011) *Modelling of Tropospheric Ozone Annual Report 2010. AEA report. AEAT/ENV/R/3134 Issue 1.* https://uk-air.defra.gov.uk/library/reports?report_id=856.

NEGTAP (2001) *Transboundary Air Pollution: Acidification, Eutrophication and Ground-level ozone in the UK. Prepared by the National Expert Group on Transboundary Air Pollution (NEGTAP) on behalf of the Department for Environment, Food and Rural Affairs, the Scottish Executive, Welsh Assembly Government and the Department of the Environment in Northern Ireland. ISBN 1 870393 61 9.* https://uk-air.defra.gov.uk/library/reports?report_id=109.

NETS (2011) *The National Grid Seven Year Statement 2011,* https://www.nationalgrideso.com/sites/eso/files/documents/23109-ETYS%202012%20Document.pdf.

Personal communication from Ben Pearson, R.E.& E. (2023) 'Ricardo Energy & Environment, Harwell, UK. '.

Personal communication from Brian Underwood, A. (2009) 'AEA Technology, Harwell, UK.'

Personal communication from Clare Aston, R.E.& E. (2023) 'Ricardo Energy & Environment, Harwell, UK. '.

Pleim, J. (2006) 'A Simple, Efficient Solution of Flux–Profile Relationships in the Atmospheric Surface Layer', *American Meteorological Society*, 45(2), pp. 341–347.

Pleim, J. (2007) 'A Combined Local and Nonlocal Closure Model for the Atmospheric Boundary Layer. Part I: Model Description and Testing', *American Meteorological Society*, 46(9), pp. 1383–1395.

PORG (UK Photochemical Oxidants Review Group) (1998) *Ozone in the UK. 4th report of the UK Photochemical Oxidants Review Group, 1st Edition. The Department of the Environment Transport and the Regions.* https://uk-air.defra.gov.uk/library/reports?report_id=108.

Pugsley, K. *et al.* (2022) *Technical report on UK supplementary modelling assessment under the Air Quality Standards Regulations 2010 for 2020*.

Pugsley, K. *et al.* (2023) *Technical report on UK supplementary modelling assessment under the Air Quality Standards Regulations 2010 for 2021*.

Redlington, A.L. *et al.* (2009) 'Sensitivity of modelled sulphate and nitrate aerosol to cloud, pH and ammonia emissions.', *Atmospheric Environment* , 43, pp. 3227–3234.

Redlington, A.L. and Derwent, R.G. (2013) 'Modelling Secondary Organic Aerosol in the United Kingdom https://doi.org/10.1016/j.atmosenv.2012.09.074', *Atmospheric Environment* , 64, pp. 349–357.

Scarbrough, T. *et al.* (2017) *A review of the NAEI shipping emissions methodology,* https://uk-air.defra.gov.uk/assets/documents/reports/cat07/1712140936_ED61406_NAEI_shipping_report_12Dec2017.pdf.

Speed Limit Data Basemap (2022) https://www.basemap.co.uk/speed-limit-data/.

Stedman, J.R., Goodwin, J.W.L., *et al.* (2001) 'An Empirical Model For Predicting Urban Roadside Nitrogen Dioxide Concentrations in the UK. ', *Atmospheric Environment.* , 35, pp. 1451–1493.

Stedman, J.R., Bush, T.J., *et al.* (2001) *Baseline PM10 and NOx projections for PM10 objective analysis. AEA Technology, National Environmental Technology Centre. Report AEAT/ENV/R/0726.* https://uk-air.defra.gov.uk/library/reports?report_id=17.

Stedman, J.R. *et al.* (2003) *UK air quality modelling for annual reporting 2002 on ambient air quality assessment under Council Directives 96/62/EC and 1999/30/EC. AEA Technology, National Environmental Technology Centre. Report AEAT/ENV/R/1564.* https://uk-air.defra.gov.uk/library/reports?report_id=232.

Stedman, J.R. *et al.* (2005) *UK air quality modelling for annual reporting 2003 on ambient air quality assessment under Council Directives 96/62/EC, 1999/30/EC and 2000/69/EC. AEA Technology, National Environmental Technology Centre. Report AEAT/ENV/R/1790.* https://uk-air.defra.gov.uk/library/reports?report_id=284.

Stedman, J.R. *et al.* (2006) *UK air quality modelling for annual reporting 2004 on ambient air quality assessment under Council Directives 96/62/EC, 1999/30/EC and 2000/69/EC. AEA Technology, National Environmental Technology Centre. Report AEAT/ENV/R/2052.* https://uk-air.defra.gov.uk/library/reports?report_id=416.

Stedman, J.R. *et al.* (2007) 'A consistent method for modelling PM10 and PM2.5 concentrations across the United Kingdom in 2004 for air quality assessment.', *Atmospheric Environment*, 41, pp. 161–172.

Stedman, J.R. and Bush, T. (2000) *Mapping of nitrogen dioxide and PM10 in the UK for Article 5 Assessment. AEA Technology, National Environmental Technology Centre. Report AEAT/ENV/R/0707.* https://uk-air.defra.gov.uk/library/reports?report_id=96.

Stedman, J.R., Bush, T.J. and Vincent, K.J. (2002) *UK air quality modelling for annual reporting 2001 on ambient air quality assessment under Council Directives 96/62/EC and 1999/30/EC. AEA Technology, National Environmental Technology Centre. Report AEAT/ENV/R/1221.* https://uk-air.defra.gov.uk/library/reports?report_id=158.

Tang, Y.S. *et al.* (2015) *Development of a new model DELTA sampler and assessment of potential sampling artefacts in the UKEAP AGANet DELTA system. Report for the UK Department for Environment, Food and Rural Affairs (DEFRA) and NERC. Centre for Ecology and Hydrology (CEH).* https://uk-air.defra.gov.uk/library/reports?report_id=861.

Teletrac Navman (2021) *https://www.teletracnavman.com/homepage-b*.
Tsagatakis, I. *et al.* (2023) *UK Spatial Emission Methodology. A report of the National Atmospheric Emissions Inventory 2021, Ricardo Energy & Environment.* https://uk-air.defra.gov.uk/assets/documents/reports/cat09/2307061053_UK_Spatial_Emissions_Methodology_for_NAEI_2021_v1.pdf.

UCAR (2020) *https://www.mmm.ucar.edu/weather-research-and-forecasting-model*.
UK-Air (2023) https://uk-air.defra.gov.uk/compliance-data.

Vardoulakis, S. *et al.* (2003) 'Modelling air quality in street canyons: a review', *Atmospheric Environment*, 37(2), pp. 155–182.

Vincent, K.J., Bush, T. and Coleman, P. (2007) *Assessment of Benzo[a]Pyrene Concentrations in the UK in 2005, 2010, 2015 and 2020. Report to The Department for Environment, Food and Rural Affairs, Welsh Assembly Government, the Scottish Executive and the Department of the Environment for Northern Ireland. AEA report. AEA/ENV/R/2373 Issue 1.* https://uk-air.defra.gov.uk/library/reports?report_id=467.

Vincent, K.J., Bush, T. and Telling, S. (2010) *Preliminary Assessment for the Ambient Air Quality Directive (2008/50/EC) for the United Kingdom. Report to The Department for Environment, Food and Rural Affairs, Welsh Assembly Government, the Scottish Government and the Department of the Environment for Northern Ireland. AEA report. AEAT/ENV/R/2961 Issue 1.* https://uk-air.defra.gov.uk/library/reports?report_id=638.

Walker, H.L. *et al.* (2010) *UK modelling under the Air Quality Framework Directive (96/62/EC) and Fourth Daughter Directive (2004/30/EC) for 2009 covering As, Cd, Ni and B(a)P. Report for The Department for Environment, Food and Rural Affairs, Welsh Assembly Government, the Scottish*

Government and the Department of the Environment for Northern Ireland. AEA report. AEAT/ENV/R/3070 Issue 1. https://uk-air.defra.gov.uk/library/reports?report_id=694.

Walker, H.L. *et al.* (2011) *UK modelling under the Air Quality Framework Directive (96/62/EC) and Fourth Daughter Directive (2004/30/EC) for 2010 covering As, Cd, Ni and B(a)P. Report for The Department for Environment, Food and Rural Affairs, Welsh Government, the Scottish Government and the Department of the Environment for Northern Ireland. AEA report. AEAT/ENV/R/3216 Issue 1.* https://uk-air.defra.gov.uk/assets/documents/reports/cat09/1204301510_dd42010mapsrep_v0.pdf.

Yap, F.W. *et al.* (2009) *UK air quality modelling for annual reporting 2008 on ambient air quality assessment under Council Directives 96/62/EC, 1999/30/EC and 2004/107/EC. Report to The Department for Environment, Food and Rural Affairs, Welsh Assembly Government, the Scottish Government and the Department of the Environment for Northern Ireland. AEA Report. AEAT/ENV/R/2860 Issue 1.* https://uk-air.defra.gov.uk/library/reports?report_id=596.

Appendices

Appendix 1 - Monitoring sites used to verify the mapped estimates

Table A1.1 lists the air quality monitoring network names for the sites used to verify the 2022 model output of the pollutants, which are given in Table A1.2. Table A1.2 also lists additional monitoring sites, operated by Hanson Building Products Ltd., which are used to verify the SO_2 models, and INEOS, which are used to verify the benzene modelling.

Table A1.1 - Air quality monitoring network and URL

Air quality monitoring network/data provider	Abbreviation	URL
Air Quality England	AQE	http://www.airqualityengland.co.uk/
Welsh Air Quality Network	WAQN	https://airquality.gov.wales/
Heathrow Airwatch		http://www.heathrowairwatch.org.uk/
London Air Quality Network*	LAQN	http://www.londonair.org.uk/LondonAir/Default.aspx
Northern Ireland Automatic Urban Network	NIAUN	http://www.airqualityni.co.uk/
Scottish Automatic Rural Network	SARN	http://www.scottishairquality.co.uk/
Scottish Automatic Urban Network	SAUN	http://www.scottishairquality.co.uk/
Kent Air		https://kentair.org.uk/
Essex Air Quality Network	EAQN	https://essexair.org.uk/
Sussex Air Quality Network	SAQN	https://sussex-air.net/

***** Data extracted using OpenAir (Carslaw and Ropkins, 2012) import KCL function from a database of air quality monitoring data made available by Imperial College London, Environmental Research group (ERG). Data was extracted on 21/06/2023.

Table A1.2 - Monitoring sites available for verification of the mapped estimates (PM_{10} measurements by Osiris instruments were not included in the verification)

Site name	Site type	Network	NO_X, NO_2	PM_{10}	$PM_{2.5}$	SO_2	O_3	C_6H_6
Barnet Chalgrove School	Urban Background	AQE	Y	Y				
Barnet Tally Ho	Kerbside	AQE	Y	Y				
Barnsley A628 Roadside Site 2	Suburban	AQE	Y					
Barnsley A635 Kendray Roadside	Roadside	AQE		Y				
Bedford Lurke Street	Traffic	AQE	Y					
Bedford Prebend Street	Traffic	AQE	Y					
Birmingham Airport 2	Airport	AQE	Y	Y	Y	Y	Y	
Bolton A579 Derby Street	Roadside	AQE	Y	Y	Y			
Bradford-on-Avon Masons Lane	Roadside	AQE	Y	Y				

Breckland East Wretham	Rural	AQE	Y	Y			Y	
Breckland Swaffham	Roadside	AQE	Y					
Bury Prestwich	Roadside	AQE	Y	Y				
Bury Radcliffe	Roadside	AQE	Y	Y				
Cambridge Montague Road	Roadside	AQE	Y	Y				
Cambridge Newmarket Road	Roadside	AQE	Y		Y			
Cambridge Parker Street	Roadside	AQE	Y	Y				
Camden - Coopers Lane	Urban Industrial	AQE		Y	Y			
Camden - Euston Road	Roadside	AQE	Y	Y	Y			
Camden High Street	Roadside	AQE	Y					
Cheshire West & Chester - Helsby	Urban Background	AQE		Y	Y			
Dacorum Northchurch High Street	Traffic	AQE	Y	Y	Y			
Devizes Sidmouth Street	Roadside	AQE	Y	Y				
Ealing Green Quarter	Urban Background	AQE	Y	Y	Y			
East Herts Hertford Gascoyne Way	Traffic	AQE	Y		Y			
East Midlands Airport	Industrial	AQE	Y	Y	Y			
East Suffolk Woodbridge 2	Roadside	AQE	Y					
Farnham South Street	Roadside	AQE	Y	Y				
Gateshead A1 Dunston	Roadside	AQE	Y		Y			
Gateshead Angel of the North	Roadside	AQE	Y	Y	Y			
Gateshead Bottle Bank	Roadside	AQE	Y					
Gateshead Lychgate Court	Roadside	AQE	Y		Y			
Gateshead Tyne Bridge	Roadside	AQE	Y	Y	Y			
Godalming Ockford Road 2	Roadside	AQE	Y					
Hackney Queensbridge Road	Suburban	AQE	Y	Y				
Haringey Wood Green	Roadside	AQE	Y	Y	Y			
Hatfield West View	Roadside	AQE	Y					
Heathrow Bath Road	Roadside	AQE	Y	Y	Y			
Heathrow Green Gates	Airport	AQE	Y	Y	Y			
Heathrow LHR2	Airport	AQE	Y	Y	Y			
Heathrow Oaks Road	Airport	AQE	Y	Y	Y			
HF 4 - Shepherds Bush Town Centre	Roadside	AQE	Y	Y	Y			
HF 5 - Hammersmith Town Centre	Roadside	AQE	Y	Y	Y		Y	

Hillingdon Harmondsworth	Urban Background	AQE	Y	Y				
Hillingdon Harmondsworth Osiris	Urban Background	AQE		Y	Y			
Hillingdon Hayes	Roadside	AQE	Y	Y				
Hillingdon Oxford Avenue	Urban Centre	AQE	Y	Y				
Hillingdon Sipson	Urban Background	AQE	Y					
Hillingdon South Ruislip	Roadside	AQE	Y	Y				
Hitchin Stevenage Road	Traffic	AQE	Y					
Hitchin Stevenage Road Particulates	Roadside	AQE		Y	Y			
Hounslow Brentford	Roadside	AQE	Y	Y	Y			
Hounslow Chiswick	Roadside	AQE	Y	Y	Y			
Hounslow Feltham	Traffic	AQE	Y	Y				
Hounslow Gunnersbury	Traffic	AQE	Y	Y				
Hounslow Hatton Cross	Roadside	AQE	Y	Y				
Hounslow Heston	Roadside	AQE	Y	Y				
Ipswich St Matthews Street	Roadside	AQE	Y					
London Luton Airport	Background	AQE		Y				
Luton Airport FutureLuToN	Airport	AQE	Y	Y	Y	Y	Y	
Luton Dunstable Road East	Traffic	AQE	Y	Y	Y			
Manchester Oxford Road	Kerbside	AQE	Y	Y				
Manchester Sharston	Suburban	AQE		Y	Y	Y		
New Forest - Fawley	Urban Industrial	AQE		Y		Y		
New Forest - Lyndhurst	Traffic	AQE	Y					
New Forest - Totton	Traffic	AQE	Y	Y				
North Tyneside Coast Road	Roadside	AQE	Y	Y	Y			
Oldham Shaw Crompton Way	Roadside	AQE		Y				
Oxford High St	Roadside	AQE	Y	Y	Y			
Oxford St Ebbes (Cal Club)	Urban Background	AQE					Y	
Plymouth Moor Lane	Roadside	AQE		Y	Y			
Plymouth Mutley Plain	Roadside	AQE	Y					
Plymouth Royal Parade	Roadside	AQE	Y					
RBKC Chelsea Old Town Hall	Roadside	AQE	Y					
RBKC Cromwell Road	Roadside	AQE	Y	Y	Y			
RBKC Earls Court Road	Roadside	AQE	Y	Y				
RBKC Knightsbridge	Roadside	AQE	Y					
Reading Caversham Road	Roadside	AQE	Y	Y				

Reading Oxford Road	Roadside	AQE	Y	Y				
Redcar Dormanstown	Industrial	AQE	Y	Y	Y		Y	
Rochdale Queensway	Roadside	AQE	Y	Y	Y			
S Cambs Impington	Roadside	AQE	Y	Y	Y			
S Cambs Orchard Park School	Urban Background	AQE	Y	Y				
Salford M60	Roadside	AQE	Y	Y	Y		Y	
Salisbury Exeter Street	Roadside	AQE	Y	Y				
Slough Brands Hill London Road	Roadside	AQE	Y	Y				
Slough Lakeside 2	Urban Background	AQE	Y	Y				
Slough Lakeside 2 Osiris	Urban Background	AQE		Y	Y			
Slough Spackmans Way	Roadside	AQE	Y	Y				
Slough Town Centre Wellington Street	Roadside	AQE	Y					
Slough Windmill Bath Road	Roadside	AQE	Y	Y				
SODC Henley	Roadside	AQE	Y					
SODC Wallingford	Roadside	AQE	Y					
SODC Watlington	Traffic	AQE	Y					
South Holland Spalding Monkhouse School	Urban Background	AQE	Y	Y				
South Holland Westmere School	Rural	AQE	Y	Y			Y	
Spelthorne Sunbury Cross	Urban Background	AQE	Y	Y	Y			
Stevenage St Georges Way South	Roadside	AQE	Y		Y			
Stockport Cheadle A34	Roadside	AQE	Y	Y				
Stockport Hazel Grove	Roadside	AQE	Y	Y				
Tameside A635 Manchester Road	Roadside	AQE	Y	Y	Y			
Tameside Mottram Moor	Traffic	AQE	Y	Y				
Tower Hamlets - Blackwall	Roadside	AQE	Y	Y	Y		Y	
Tower Hamlets - Millwall Park	Background	AQE	Y	Y			Y	
Tower Hamlets - Victoria Park	Background	AQE	Y	Y	Y			
Trafford A56	Roadside	AQE	Y	Y				
Trafford Moss Park	Urban Background	AQE	Y	Y				
Trafford Wellacre Academy	Urban Background	AQE	Y					
VofWH Abingdon Stert St 2	Roadside	AQE	Y					
Wakefield Castleford	Roadside	AQE	Y					
Wakefield City - Newton Bar	Urban Background	AQE	Y					

Wakefield City - Park Street	Roadside	AQE	Y	Y	Y			
Waltham Forest Crooked Billet	Kerbside	AQE	Y	Y				
Waltham Forest Dawlish Rd	Urban Background	AQE	Y	Y	Y			
Waltham Forest Leyton	Urban Background	AQE	Y	Y				
Watford Town Hall	Traffic	AQE	Y	Y	Y			
Welwyn Hatfield	Roadside	AQE			Y			
Wigan Leigh 3	Roadside	AQE	Y	Y	Y			
Wycombe Abbey 5	Roadside	AQE	Y					
Wycombe Stokenchurch	Roadside	AQE	Y					
York Fulford Road	Roadside	AQE	Y					
York Gillygate	Roadside	AQE	Y		Y			
York Heworth Green	Roadside	AQE	Y					
York Holgate	Roadside	AQE	Y	Y				
York Lawrence Street	Roadside	AQE	Y					
York Nunnery Lane	Roadside	AQE	Y					
York Plantation Drive	Roadside	AQE		Y				
Thurrock - London Road (Purfleet)	Urban Traffic	EAQN	Y	Y				
Bradley Fen	Brick-Works	Hanson Building Products Limited				Y		
Whittlesey	Brick-Works	Hanson Building Products Limited				Y		
26 Lomond Road Grangemouth	Refinery	Ineos						Y
Abbotsinch173 Boness Road Grangemouth	Refinery	Ineos						Y
Beechwood Low Causeway Culross Fife	Refinery	Ineos						Y
KG Gate	Refinery	Ineos						Y
Kinneil Kerse near boundary fence of Kinneil Gas Plant	Refinery	Ineos						Y
Kinneil Kerse on road near Waste Tip	Refinery	Ineos						Y
Mercer Street Kincardine Fife	Refinery	Ineos						Y
Road Station Gate 1	Refinery	Ineos						Y
Stores/Poly Gate Gate 14	Refinery	Ineos						Y
Technical Building Gate 4	Refinery	Ineos						Y
Canterbury Military Road	Roadside	Kent Air	Y					

Dartford - St Clements 2	Roadside	Kent Air	Y	Y				
Dartford Town Centre Roadside	Roadside	Kent Air	Y	Y				
Dover Centre Roadside	Roadside	Kent Air		Y				
Gravesham A2 Roadside	Roadside	Kent Air	Y	Y				
Gravesham Industrial Background	Urban Background	Kent Air	Y	Y				
Maidstone Rural	Rural	Kent Air	Y	Y				
Maidstone Upper Stone Street	Roadside	Kent Air	Y	Y	Y			
Swale Newington 4	Roadside	Kent Air	Y	Y	Y			
Swale Ospringe Roadside 2	Roadside	Kent Air	Y	Y				
Swale St Pauls Street	Roadside	Kent Air	Y	Y	Y			
Thanet Birchington Roadside	Roadside	Kent Air	Y	Y				
Thanet Ramsgate Roadside	Roadside	Kent Air	Y	Y				
Tonbridge and Malling Borough Green Roadside	Roadside	Kent Air	Y	Y				
Tunbridge Wells A26 Roadside	Roadside	Kent Air	Y	Y	Y			
Barking and Dagenham - Rush Green	Suburban Background	LAQN	Y			Y		
Barking and Dagenham - Scrattons Farm	Suburban Background	LAQN	Y	Y				
Bexley - Belvedere	Suburban Background	LAQN	Y	Y	Y			
Bexley - Belvedere West	Urban Background	LAQN	Y	Y	Y		Y	
Brent - ARK Franklin Primary Academy	Urban Traffic	LAQN	Y	Y				
Brent - Ikea	Urban Traffic	LAQN	Y	Y			Y	
Brent - John Keble Primary School	Urban Traffic	LAQN	Y	Y				
Brent - Neasden Lane	Urban Industrial	LAQN	Y	Y				
City of London - Beech Street	Urban Traffic	LAQN	Y	Y				
City of London - Sir John Cass School	Urban Background	LAQN	Y	Y				
City of London - Walbrook Wharf	Urban Traffic	LAQN	Y					
Croydon - Norbury	Urban Traffic	LAQN	Y					
Ealing - Hanger Lane Gyratory	Urban Traffic	LAQN	Y	Y				
Ealing - Western Avenue	Urban Traffic	LAQN	Y	Y				
Enfield - Bowes Primary School	Urban Traffic	LAQN	Y	Y				

Enfield - Bush Hill Park	Suburban Background	LAQN	Y					
Enfield - Derby Road	Urban Traffic	LAQN	Y					
Enfield - Prince of Wales School	Urban Background	LAQN	Y					
Greenwich - A206 Burrage Grove	Urban Traffic	LAQN	Y	Y				
Greenwich - Blackheath	Urban Traffic	LAQN	Y	Y				
Greenwich - Falconwood	Urban Traffic	LAQN	Y	Y			Y	
Greenwich - Falconwood FDMS	Urban Traffic	LAQN			Y			
Greenwich - Fiveways Sidcup Rd A20	Urban Traffic	LAQN	Y	Y				
Greenwich - John Harrison Way	Urban Traffic	LAQN	Y	Y				
Greenwich - Plumstead High Street	Urban Traffic	LAQN	Y	Y			Y	
Greenwich - Trafalgar Road (Hoskins St)	Urban Traffic	LAQN	Y	Y				
Greenwich - Westhorne Avenue	Urban Traffic	LAQN	Y	Y			Y	
Greenwich - Woolwich Flyover	Urban Traffic	LAQN	Y	Y			Y	
Hackney - Old Street	Urban Traffic	LAQN	Y	Y	Y		Y	
Havering - Rainham	Urban Traffic	LAQN	Y	Y				
Havering - Romford	Urban Traffic	LAQN	Y	Y				
Islington - Arsenal	Urban Background	LAQN	Y	Y				
Islington - Holloway Road	Urban Traffic	LAQN	Y	Y				
Kingston Upon Thames - Cromwell Road	Urban Traffic	LAQN	Y	Y				
Kingston Upon Thames - Kingston Vale	Urban Traffic	LAQN	Y	Y				
Kingston Upon Thames - Tolworth Broadway	Urban Traffic	LAQN	Y	Y				
Lambeth - Bondway Interchange	Urban Industrial	LAQN	Y	Y		Y		
Lambeth - Brixton Road	Urban Traffic	LAQN	Y	Y				
Lambeth - Streatham Green	Urban Background	LAQN	Y	Y				
Lewisham - Deptford	Urban Background	LAQN	Y					
Lewisham - Honor Oak Park	Urban Background	LAQN	Y				Y	
Lewisham - Loampit Vale	Urban Traffic	LAQN	Y	Y				
Lewisham - New Cross	Urban Traffic	LAQN	Y	Y				
Redbridge - Gardner Close	Urban Traffic	LAQN	Y	Y				

Redbridge - Ley Street	Urban Background	LAQN	Y	Y			Y	
Richmond Upon Thames - Barnes Wetlands	Suburban Background	LAQN	Y	Y			Y	
Richmond Upon Thames - Castelnau	Urban Traffic	LAQN	Y	Y				
Sevenoaks - Bat and Ball	Urban Traffic	LAQN	Y	Y				
Sevenoaks - Greatness Park	Urban Background	LAQN	Y	Y		Y	Y	
Southwark - Elephant and Castle	Urban Background	LAQN	Y	Y			Y	
Southwark - Tower Bridge Road	Urban Traffic	LAQN	Y					
Sutton - Beddington Lane north	Urban Industrial	LAQN	Y	Y				
Sutton - Wallington	Urban Traffic	LAQN	Y	Y				
Sutton - Worcester Park	Urban Traffic	LAQN	Y	Y				
Wandsworth - Battersea	Urban Traffic	LAQN	Y	Y				
Wandsworth - Lavender Hill (Clapham Jct)	Urban Traffic	LAQN	Y	Y				
Wandsworth - Putney	Urban Background	LAQN	Y	Y				
Wandsworth - Putney High Street	Urban Traffic	LAQN	Y	Y				
Wandsworth - Tooting High Street	Urban Traffic	LAQN	Y	Y				
Westminster - Cavendish Square	Urban Traffic	LAQN	Y					
Westminster - Duke Street (Grosvenor)	Urban Traffic	LAQN	Y					
Westminster - Ebury Street (Grosvenor)	Urban Traffic	LAQN	Y					
Westminster - Elizabeth Bridge	Urban Traffic	LAQN	Y		Y			
Westminster - Oxford Street	Urban Traffic	LAQN	Y					
Westminster - Oxford Street East	Urban Traffic	LAQN	Y					
Westminster - Strand (Northbank BID)	Urban Traffic	LAQN	Y					
Windsor and Maidenhead - Aldebury Road	Urban Background	LAQN	Y					
Windsor and Maidenhead - Clarence Road	Urban Traffic	LAQN	Y					
Windsor and Maidenhead - Frascati Way	Urban Traffic	LAQN	Y					

Ballymena Ballykeel	Urban Background	NIAUN		Y	Y			
Belfast Newtownards Road	Roadside	NIAUN	Y					
Belfast Ormeau Road	Roadside	NIAUN	Y					
Belfast Westlink Roden Street	Roadside	NIAUN	Y					
Castlereagh Dundonald	Roadside	NIAUN	Y					
Derry Dales Corner	Roadside	NIAUN	Y					
Downpatrick Roadside	Roadside	NIAUN	Y					
Limavady Dungiven	Roadside	NIAUN	Y					
Lisburn Dunmurry Seymour Hill	Urban Background	NIAUN		Y	Y	Y		
Newry Canal Street	Roadside	NIAUN	Y	Y				
Newtownabbey Antrim Road	Roadside	NIAUN	Y					
Newtownstewart	Urban Background	NIAUN		Y	Y			
North Down Holywood A2	Roadside	NIAUN	Y	Y	Y			
Strabane Springhill Park	Urban Background	NIAUN		Y	Y	Y		
Glasgow Waulkmillglen Reservoir	Rural	SARN	Y	Y	Y		Y	
Lerwick	Rural	SARN	Y			Y		
Aberdeen Anderson Dr	Roadside	SAUN	Y	Y	Y			
Aberdeen King Street	Roadside	SAUN	Y	Y	Y			
Aberdeen Market Street 2	Roadside	SAUN	Y	Y	Y			
Aberdeen Union Street Roadside	Roadside	SAUN		Y	Y			
Aberdeen Wellington Road	Roadside	SAUN		Y	Y			
Alloa A907	Roadside	SAUN	Y	Y	Y			
Angus Forfar Glamis Rd	Roadside	SAUN		Y	Y			
Dundee Broughty Ferry Road	Urban Industrial	SAUN	Y	Y	Y			
Dundee Lochee Road	Kerbside	SAUN	Y	Y	Y			
Dundee Mains Loan	Urban Background	SAUN		Y	Y			
Dundee Meadowside	Roadside	SAUN	Y	Y	Y			
Dundee Seagate	Kerbside	SAUN	Y	Y	Y			
Dundee Whitehall Street	Roadside	SAUN	Y	Y	Y			
E Ayrshire Kilmarnock St Marnock St	Roadside	SAUN	Y	Y	Y			
East Dunbartonshire Bearsden	Roadside	SAUN	Y	Y	Y			
East Dunbartonshire Bishopbriggs	Roadside	SAUN	Y	Y	Y			
East Dunbartonshire Kirkintilloch	Roadside	SAUN	Y	Y	Y			

East Dunbartonshire Milngavie	Roadside	SAUN	Y	Y	Y			
East Lothian Musselburgh N High St	Roadside	SAUN	Y	Y	Y			
Edinburgh Currie	Suburban	SAUN	Y	Y	Y			
Edinburgh Glasgow Road	Roadside	SAUN	Y	Y	Y			
Edinburgh Gorgie Road	Roadside	SAUN	Y					
Edinburgh Nicolson Street	Roadside	SAUN		Y	Y			
Edinburgh Queensferry Road	Roadside	SAUN	Y	Y	Y			
Edinburgh Salamander St	Roadside	SAUN	Y	Y	Y			
Edinburgh St Johns Road	Kerbside	SAUN	Y	Y	Y			
Edinburgh Tower Street	Roadside	SAUN		Y	Y			
Falkirk Boness	Urban Industrial	SAUN				Y		
Falkirk Grangemouth MC	Urban Background	SAUN	Y	Y	Y	Y		
Falkirk Grangemouth Zetland Park	Urban Industrial	SAUN		Y	Y	Y		
Falkirk Haggs	Roadside	SAUN	Y	Y	Y			
Falkirk Hope St	Roadside	SAUN	Y	Y	Y	Y		
Falkirk Main St Bainsford	Roadside	SAUN	Y	Y	Y			
Falkirk West Bridge Street	Roadside	SAUN	Y	Y	Y			
Fife Cupar	Roadside	SAUN	Y	Y	Y			
Fife Dunfermline	Roadside	SAUN	Y	Y	Y			
Fife Kirkcaldy	Roadside	SAUN	Y	Y	Y			
Fife Rosyth	Roadside	SAUN	Y	Y	Y			
Glasgow Anderston	Urban Background	SAUN	Y	Y	Y			
Glasgow Broomhill	Roadside	SAUN		Y	Y			
Glasgow Byres Road	Roadside	SAUN	Y	Y	Y			
Glasgow Dumbarton Road	Roadside	SAUN	Y	Y	Y			
Glasgow Kerbside	Kerbside	SAUN		Y	Y			
Glasgow Nithsdale Road	Roadside	SAUN	Y	Y	Y			
Grangemouth Moray	Urban Background	SAUN				Y		
N Lanarkshire Airdrie Kenilworth Dr	Roadside	SAUN	Y	Y				
N Lanarkshire Chapelhall	Roadside	SAUN	Y	Y	Y			
N Lanarkshire Coatbridge Whifflet A725	Roadside	SAUN	Y	Y	Y			

N Lanarkshire Croy	Roadside	SAUN	Y	Y	Y			
N Lanarkshire Kirkshaws	Roadside	SAUN	Y	Y	Y			
N Lanarkshire Motherwell	Roadside	SAUN	Y	Y	Y			
N Lanarkshire Motherwell Adele St.	Roadside	SAUN	Y	Y	Y			
N Lanarkshire Ravenscraig Plantation Road	Roadside	SAUN	Y	Y	Y			
N Lanarkshire Shawhead Coatbridge	Roadside	SAUN	Y	Y	Y			
N Lanarkshire Uddingston New Edinburgh Rd	Roadside	SAUN	Y	Y	Y			
North Ayrshire Irvine High St	Kerbside	SAUN	Y	Y	Y			
Perth Atholl Street	Roadside	SAUN	Y	Y	Y			
Perth Bridgend	Roadside	SAUN	Y	Y	Y			
Perth Crieff	Roadside	SAUN	Y	Y	Y			
Perth Muirton	Urban Background	SAUN		Y	Y			
Renfrew Cockels Loan	Roadside	SAUN	Y					
Renfrew Inchinnan Road	Roadside	SAUN	Y					
Renfrewshire Johnstone	Roadside	SAUN		Y	Y			
South Ayrshire Ayr Harbour	Roadside	SAUN	Y	Y	Y			
South Ayrshire Ayr High St	Roadside	SAUN	Y	Y	Y			
South Lanarkshire Blantyre	Roadside	SAUN	Y	Y	Y			
South Lanarkshire Cambuslang	Kerbside	SAUN	Y	Y	Y			
South Lanarkshire East Kilbride	Roadside	SAUN	Y	Y	Y			
South Lanarkshire Hamilton	Roadside	SAUN	Y	Y	Y			
South Lanarkshire Lanark	Kerbside	SAUN	Y	Y	Y			
South Lanarkshire Raith Interchange 2	Roadside	SAUN	Y	Y	Y			
South Lanarkshire Rutherglen	Roadside	SAUN	Y	Y	Y			
South Lanarkshire Uddingston	Roadside	SAUN	Y	Y	Y			
Stirling Craigs Roundabout	Roadside	SAUN	Y	Y	Y			
West Dunbartonshire Clydebank	Roadside	SAUN	Y	Y	Y			
West Lothian Broxburn	Roadside	SAUN	Y	Y	Y			

West Lothian Linlithgow High Street 2	Roadside	SAUN	Y	Y	Y			
Chichester - Lodsworth	Rural Background	SAQN					Y	
Eastbourne - Devonshire Park	Urban Background	SAQN	Y	Y			Y	
Lewes - Newhaven	Urban Traffic	SAQN					Y	
Reigate and Banstead - A23 Hooley	Urban Traffic	SAQN	Y					
Reigate and Banstead - Horley South East	Suburban Background	SAQN	Y					
Reigate and Banstead - Poles Lane	Rural Background	SAQN	Y				Y	
Rother - Rye Harbour	Rural Background	SAQN					Y	
Wealden - Isfield	Rural Background	SAQN					Y	
Bridgend Park Street	Roadside	WAQN	Y	Y				
Caerphilly Blackwood High Street	Roadside	WAQN	Y	Y				
Caerphilly Fochriw	Roadside	WAQN		Y	Y			
Caerphilly Islwyn Road Wattsville	Roadside	WAQN	Y					
Cardiff Castle Street	Roadside	WAQN	Y	Y	Y			
Cimla Road / Victoria Gardens	Roadside	WAQN	Y					
Marchlyn Mawr	Remote	WAQN	Y				Y	
Nantgarw Road	Roadside	WAQN	Y					
Newport M4 Junction 25	Roadside	WAQN	Y				Y	
Newport St Julians Comp School	Urban Background	WAQN	Y	Y	Y			
Rhondda Mountain Ash	Roadside	WAQN	Y					
Rhondda Pontypridd Gelliwastad Rd	Roadside	WAQN	Y					
Rhondda-Cynon-Taf Broadway	Roadside	WAQN	Y					
Swansea Cwm Level Park	Urban Background	WAQN	Y				Y	
Swansea Hafod DOAS	Roadside	WAQN	Y				Y	Y
Swansea Morfa Road NOX	Roadside	WAQN	Y					
Swansea Port Tennant Roadside	Roadside	WAQN	Y		Y			
Swansea St Thomas DOAS	Roadside	WAQN	Y			Y	Y	Y
Wrexham	Roadside	WAQN		Y				
Wrexham Chirk	Urban Industrial	WAQN	Y	Y	Y			
Wrexham Chirk Community Hospital	Urban Background	WAQN	Y	Y	Y			

Appendix 2 - Monitoring sites for As, Cd, Ni, Pb and B(a)P

The monitoring stations operating during 2022 for the purpose of AQSR reporting have been listed within e-Reporting Data flow C (Assessment Regimes), which can be found on UK-Air (*UK-Air*, 2023). A summary of the annual mean As, Cd, Ni, Pb and B(a)P measurements used for calibrating and verifying the modelling used in the assessment are provided here.

Heavy Metal Monitoring sites

2022 annual mean concentrations of As, Cd, Ni and Pb are presented in Table A2.1 for heavy metal monitoring sites where data capture was at least 75%. The mass concentrations presented are rounded to two significant figures.

Table A2.1 – Summary of urban and rural heavy metal mass concentrations, 2022

EoI code	Site name	Site type*	Annual mean (ng m^{-3})				%dc
			As	Cd	Ni	Pb	
GB0048R	Auchencorth Moss	RB	0.19	0.025	0.21	0.81	98
GB0567A	Belfast Centre	UB	0.43	0.064	0.88	2.4	93
GB1046A	Chesterfield Loundsley	UB	0.65	0.12	1.0	5.2	85
GB1055R	Chilbolton Observatory	RB	0.6	0.08	0.81	3.0	85
GB0854A	Cwmystwyth	RB	0.23	0.053	0.31	1.4	99
GB0886A	Detling	RB	0.67	0.11	0.64	4.6	98
GB0002R	Eskdalemuir	RB	0.15	0.022	0.33	0.67	89
GB1048A	Fenny Compton	RB	0.63	0.085	0.4	3.1	91
GB0017R	Heigham Holmes	RB	0.52	0.074	0.64	2.8	96
GB0682A	London Marylebone Road	UT	0.84	0.12	1.6	5.7	99
GB0743A	London Westminster	UB	0.76	0.094	0.87	5.5	86
GB1015A	Pontardawe Brecon Road	SI	0.64	0.26	3.3	5.9	92
GB1016A	Pontardawe Tawe Terrace	UI	0.63	0.31	17	6.6	96
GB0906A	Port Talbot Margam	UI	0.81	0.6	1.1	7.7	94
GB1004A	Scunthorpe Low Santon	UI	0.9	0.64	1.4	23	98
GB0841A	Scunthorpe Town	UI	0.76	0.25	0.91	10	100
GB1027A	Sheffield Devonshire Green	UB	0.68	0.13	2.5	5.4	97
GB0538A	Sheffield Tinsley	UI	0.9	0.26	17	12	98
GB0981A	Swansea Coedgwilym	UB	0.64	0.29	8.1	51	79
GB0979A	Swansea Morriston	UT	0.77	0.39	10	9.3	96
GB1261A	Walsall Pleck Park	UB	0.88	0.89	0.87	6.6	94
GB0013R	Yarner Wood	RB	0.39	0.047	0.4	1.4	98

*RB = Rural Background, UB = Urban Background, UT = Urban Traffic, UI = Urban Industrial, SI = Suburban Industrial, SB = Suburban Background.

B(a)P Monitoring sites

2022 annual B(a)P mean concentrations are presented in Table A2.2 for those sites where data capture was at least 75%. The mass concentrations presented are rounded to two significant figures. All measurements were obtained using Digitel DHA-80 samplers.

Table A2.2 – Summary of B(a)P mass concentrations, 2022

EoI code	Site name	Site type*	Annual mean B(a)P, ng/m^3	%dc
GB0048R	Auchencorth Moss	RB	0.015	96
GB0934A	Ballymena Ballykeel	UB	0.49	100
GB1097A	Birmingham Ladywood	UB	0.12	99
GB0700A	Bolsover	UB	0.16	91
GB0884A	Bristol St Paul's	UB	0.27	98
GB0869A	Cardiff Lakeside	UB	0.21	100
GB1055R	Chilbolton Observatory	RB	0.093	99
GB0944A	Derry Brandywell	UB	0.6	99
GB0839A	Edinburgh St Leonards	UB	0.061	100
GB1028A	Glasgow Townhead	UB	0.078	94
GB0702A	Hazelrigg	RB	0.038	100
GB0014R	High Muffles	RB	0.029	95
GB1023A	Kilmakee Leisure Centre	UB	0.31	99
GB0705A	Kinlochleven	UB	0.14	96
GB0867A	Leeds Millshaw	UB	0.2	100
GB0777A	Liverpool Speke	UI	0.16	96
GB0849A	London Brent	UB	0.14	100
GB0682A	London Marylebone Road	UT	0.13	99
GB0583A	Middlesbrough	UB	0.17	99
GB0568A	Newcastle Centre	UB	0.1	99
GB0962A	Newport	UB	0.23	98
GB0646A	Nottingham Centre	UB	0.18	99
GB0687A	Plymouth Centre	UB	0.15	100
GB0906A	Port Talbot Margam	UI	0.63	99
GB0731A	Preston	UB	0.21	83
GB0940A	Royston	UB	0.38	99
GB1004A	Scunthorpe Low Santon	UI	0.51	100
GB0841A	Scunthorpe Town	UI	0.62	100
GB0598A	Southampton Centre	UB	0.19	97
GB0004R	Stoke Ferry	RB	0.11	89
GB0943A	Swansea Cwm Level Park	UB	0.36	99

*RB = Rural Background, UB = Urban Background, UT = Urban Traffic, UI = Urban Industrial, SI = Suburban Industrial.

Appendix 3 – Small point source model

Introduction

Small industrial sources were generally represented in early maps (Stedman, Bush and Vincent, 2002) as 1 km square volume sources. However, this approach in some cases lead to unreasonably high concentrations close to the source. A revised small point source model was developed that uses dispersion kernels that take these factors into account.

The dispersion model ADMS 3.0 was used to prepare the dispersion kernels.

Discharge Conditions

The National Atmospheric Emission Inventory (NAEI) contains limited information concerning the discharge characteristics of individual emission sources. In many cases the information is limited to data on the total annual emission of individual pollutants. It is therefore necessary to make some general assumptions concerning the discharge height, the discharge temperature, the volumetric flow rate of the discharge and the discharge velocity. The approach adopted has been to make reasonable, but generally conservative assumptions corresponding to industrial practice.

Sulphur dioxide

For sulphur dioxide, it was assumed that the plant operates continuously throughout the year. The stack height was estimated using the following equations taken from the 3rd edition of the Chimney Heights Memorandum:

If the sulphur dioxide emission rate, R_A kg/h, is less than 10 kg/h, the chimney height, U m, is given by:

$$U = 6R_A^{0.5},$$

If R_A is in the range 10-100 kg/h:

$$U = 12R_A^{0.2},$$

Emission rates in excess of 100 kg/h were not considered in this study.

No account was taken of the effects of buildings: it was assumed that the increase in chimney height to take account of building effects provided by the Memorandum would compensate for the building effects.

It was then assumed that the sulphur dioxide concentration in the discharge would be at the limit for indigenous coal and liquid fuel for new and existing plant provided by Secretary of States Guidance-Boilers and Furnaces, 20-50 MW net rated thermal input PG1/3(95). The limit is 3000 mg m^{-3} at reference conditions of 273 K, 101.3 kPa, 6% oxygen for solid fuel firing and 3% oxygen for liquid firing and dry gas. It was assumed that the oxygen content in the discharge corresponds with the reference condition. The moisture content of the discharge was ignored. It was assumed that the temperature of discharge was 373 K: higher temperatures would lead to improved buoyancy and hence lower ground level concentrations while lower temperatures usually result in unacceptable water condensation. A discharge velocity of 10 m/s was selected to be representative of most combustion source discharges. The discharge diameter d m was calculated from:

$$d = \sqrt{\frac{4qT}{273\pi cv}},$$

where: q is the sulphur dioxide emission rate, g s^{-1}
T is the discharge temperature, 373 K
c is the emission concentration at reference conditions, 3 g m^{-3}
v is the discharge velocity, 10 m s^{-1}

Table A3.1 shows the modelled stack heights and diameters.

Table A3.1 - Modelled stack heights and diameters for sulphur dioxide

Emission rate			Stack height, m	Stack diameter, m
g s^{-1}	kg h^{-1}	t a^{-1}		
0.1	0.36	3.2	3.60	0.08
0.2	0.72	6.3	5.09	0.11
0.5	1.8	15.8	8.05	0.17
1	3.6	31.5	11.38	0.24
2	7.2	63.1	16.10	0.34
5	18	157.7	21.39	0.54
10	36	315.4	24.57	0.76
20	72	630.7	28.23	1.08

Oxides of nitrogen

For nitrogen dioxide, it was assumed that the plant operates continuously throughout the year. The stack height was estimated using the following equation taken from the 3rd edition of the Chimney Heights Memorandum for very low sulphur fuels:

$$U = 1.36Q^{0.6}(1 - 4.7\times10^{-5}Q^{1.69}),$$

where: Q is the gross heat input in MW.

This relationship applies for heat inputs up to 150 MW. For larger heat inputs a fixed height of 30 m was used corresponding to an approximate lower limit derived from available data on stack heights for large sources.

The gross heat input used in the above equation was calculated from the oxides of nitrogen emission rate using an emission factor of 10600 kg/MTh (0.100 g/MJ) for oxides of nitrogen emitted from natural gas combustion in non-domestic non-power station sources taken from the NAEI.

For fuels containing significant sulphur, the actual stack height will be greater to allow for the dispersion of sulphur dioxide so that the approach taken is expected to lead to an overestimate of ground level concentrations.

The emission limits for oxides of nitrogen provided by Secretary of States Guidance-Boilers and Furnaces, 20-50 MW net rated thermal input PG1/3(95) depend on the type of fuel and are in the range 140-650 mg m^{-3} at reference conditions. A value of 300 mg m^{-3} was used in the calculation of the stack discharge diameter. Other assumptions concerning discharge conditions followed those made for sulphur dioxide above. Table A3.2 shows the modelled stack heights and diameters.

Table A3.2 - Modelled stack heights and diameters for oxides of nitrogen

Emission rate		Stack height, m	Stack diameter, m
g s^{-1}	t a^{-1}		
0.1	3.2	1.36	0.24
0.2	6.3	2.06	0.34
0.5	15.8	3.57	0.54
1	31.5	5.40	0.76
2	63.1	8.15	1.08
5	157.7	13.72	1.70
10	315.4	19.12	2.41
20	630.7	21.34	3.41
50	1576.8	30.00	5.38
100	3153.6	30.00	7.61

Particulate matter, PM_{10}

The stack heights and diameters used for oxides of nitrogen were also used to provide the kernels for particulate matter PM_{10}. This will provide a conservative assessment of PM_{10} concentrations for the

following reasons. The emission limits for total particulate matter provided by Secretary of States Guidance-Boilers and Furnaces, 20-50 MW net rated thermal input PG1/3(95) depend on the type of fuel and are in the range 5-300 mg m^{-3} at reference conditions. The emission limit for total particulate matter includes but is not limited to the contribution from PM_{10}.

Dispersion Modelling

The dispersion model ADMS 3.0 was used to predict ground level concentrations on two receptor grids:

- an “in-square” grid covering an area 1 km x 1 km with the source at the centre and with receptors at 33.3 m intervals;
- an “outer-grid” covering an area 30 km x 30 km with the source at the centre and with receptors at 1 km intervals.

A surface roughness value of 0.5 m was used, corresponding to areas of open suburbia. Meteorological data for Heathrow for the years 1993-2002 was used in the assessment, with most model runs using the 2000 data.

Results

Sulphur dioxide

Table A3.3 shows the predicted “in-square average” concentration for the 1 km square centred on the emission source for 2000 meteorological data.

Table A3.3 - Predicted in-square concentration, for sulphur dioxide

Emission rate, g s^{-1}	Average in square concentration, μg m^{-3}
0.1	0.599
0.2	0.934
0.5	1.555
1	2.19
2	2.92
5	4.57
10	6.56
20	8.86

The results shown in Table A3.3 may be approximated by the relationship

$$C = Aq^{0.5},$$

where: C is the in-square concentration, μg m^{-3} and q is the emission rate, g s^{-1}. A is a proportionality factor (2.07 in 2000).

Table A3.4 shows the predicted in-square concentration for an emission rate of 10 g s^{-1} for meteorological years 1993-2002. Table A3.4 also shows the inter-annual variation in the factor A.

Table A3.4 - In-square concentrations for 10 g/s emissions

Year	In-square concentration, μg m^{-3}	Factor *A*
1993	6.21	1.96
1994	6.01	1.90
1995	6.12	1.94
1996	6.23	1.97
1997	6.10	1.93
1998	6.18	1.95
1999	6.49	2.05
2000	6.56	2.07
2001	6.32	2.00
2002	6.51	2.06

Figure A3.1 shows the predicted "outer-grid" concentration along the east-west axis through the source for 2000 meteorological data for a range of rates of emission (in g/s). Figure A3.1 does not include results for the 1 km source square.

Figure A3.1 - Sulphur dioxide concentration on east-west axis, 2000 meteorological data

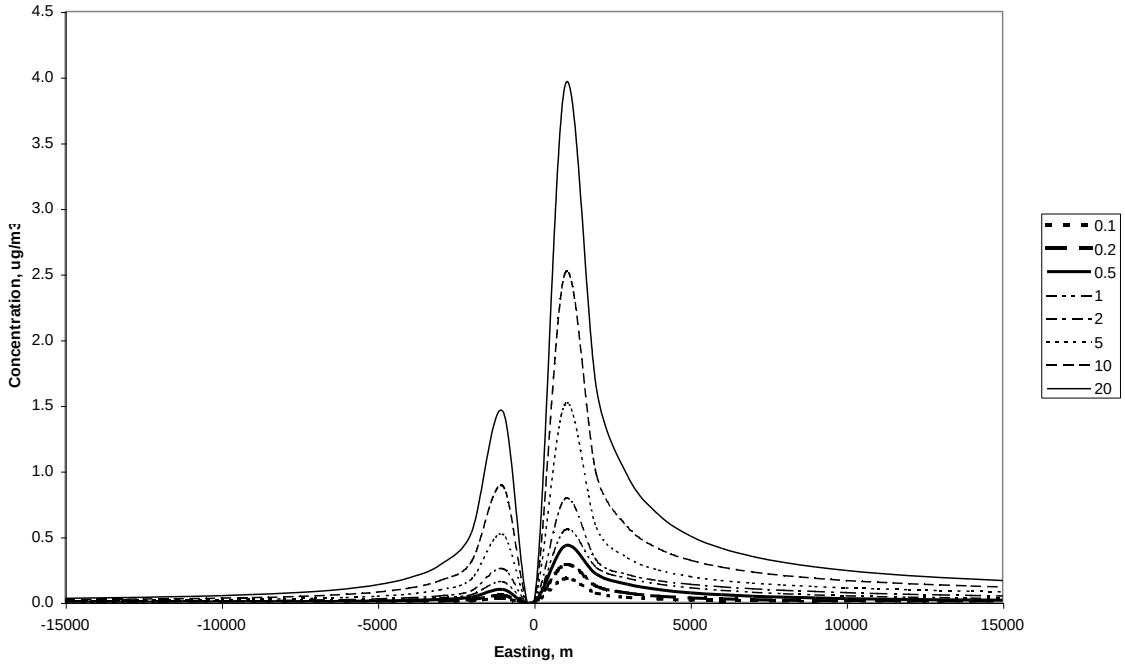

Figure A3.2 shows the same model results plotted as $C/q^{2/3}$. The spread of the model results is greatly reduced so that as a reasonable approximation all the model results may be reduced to a single line.

Figure A3.2 - Reduced sulphur dioxide concentrations on the east-west axis, 2000 meteorological data

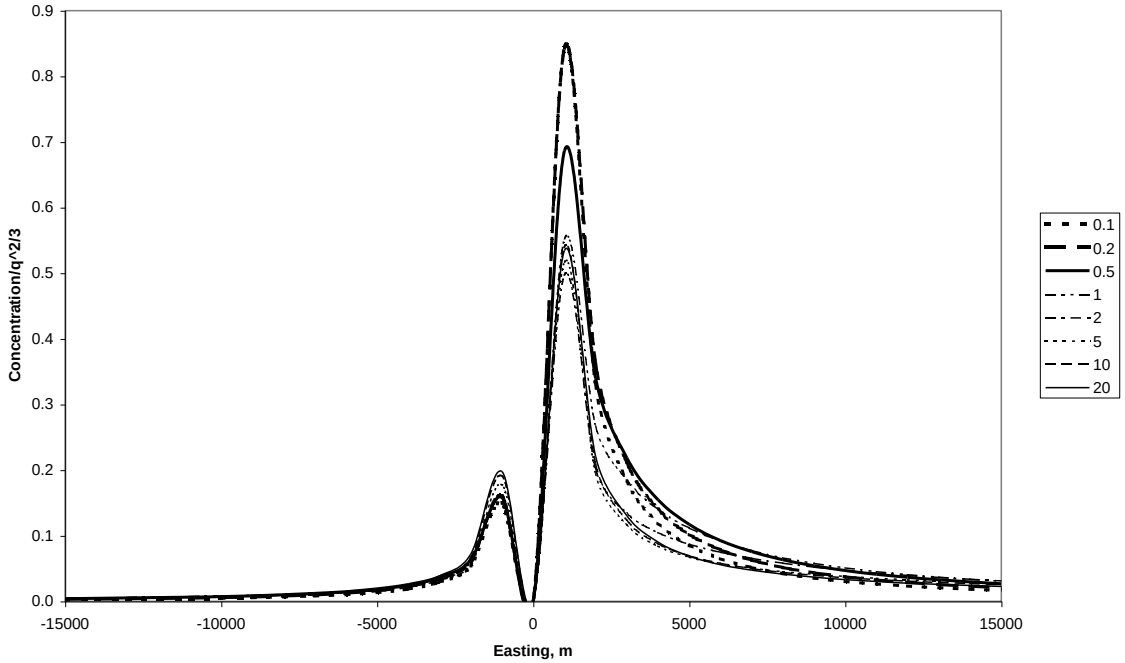

Thus, it is proposed to use the results for an emission rate of 10 g/s for all emission rates in the range 0.1-20 g/s in the preparation of dispersion kernels for industrial sulphur dioxide emissions. The dispersion kernel will be multiplied by $10.(q/10)^{2/3}$ to provide estimates of the impact of emission q (g s^{-1}) at each receptor location. Separate kernels have been created from each meteorological data year 1993-2002.

Oxides of nitrogen

Table A3.5 shows the predicted "in-square average" concentration for the 1 km square centred on the emission source for 2000 meteorological data.

Table A3.5 - In-square oxides of nitrogen concentrations, 2000

Emission rate, g s^{-1}	In square concentration, μg m^{-3}
0.1	0.464
0.2	0.764
0.5	1.37
1	1.97
2	2.6
5	3.31
10	3.58
20	4.34
50	3.745
100	4.3

The results shown in Table A3.5 may be approximated in the range 0.1-20 g s^{-1} by the relationship

$$C = B \log_{10}(10q)+0.464,$$

where: C is the in-square concentration, μg m^{-3} and q is the emission rate, g s^{-1}. and B is a numerical constant, 1.68 in 2000.

For emission rates in the range 20-100 g s^{-1}, the in-square concentration is approximately 4 μg m^{-3}.

Table A3.6 shows the predicted in-square concentration for an emission rate of 20 g s^{-1} for meteorological years 1993-2002. Table A3.6 also shows the inter-annual variation in the factor B.

Table A3.6 - Inter annual variation in in-square oxides of nitrogen concentration

Year	In-square concentration, μg m^{-3}	Factor B
1993	3.62	1.37
1994	3.88	1.48
1995	3.74	1.42
1996	4.3	1.67
1997	3.66	1.39
1998	3.64	1.38
1999	4.14	1.60
2000	4.34	1.68
2001	4.02	1.55
2002	4.68	1.83

Figure A3.3 shows the predicted “outer-grid” oxides of nitrogen concentration along the east-west axis through the source for a range of rates of emission (in g s^{-1}).

Figure A3.3 - Oxides of nitrogen concentration on east-west axis, 2000 meteorological data

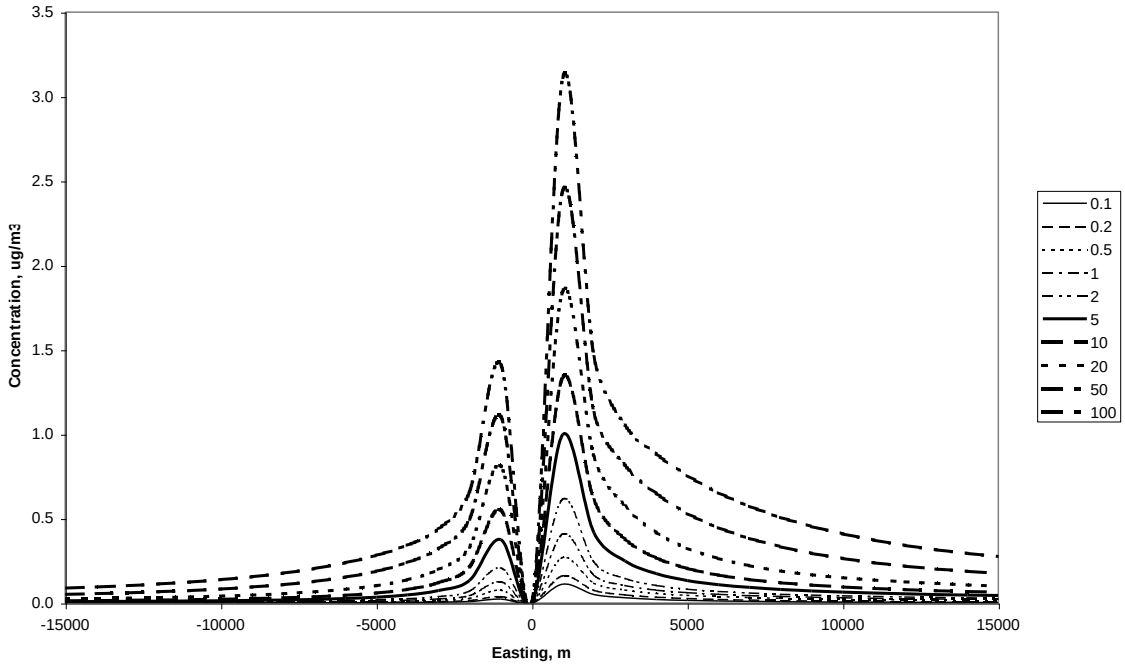

Figure A3.4 shows the same model results plotted as $C/q^{0.6}$. The spread of the model results is greatly reduced so that as a reasonable approximation all the model results may be reduced to a single line.

Figure A3.4 - Reduced oxides of nitrogen concentrations on the east-west axis, 2000 meteorological data

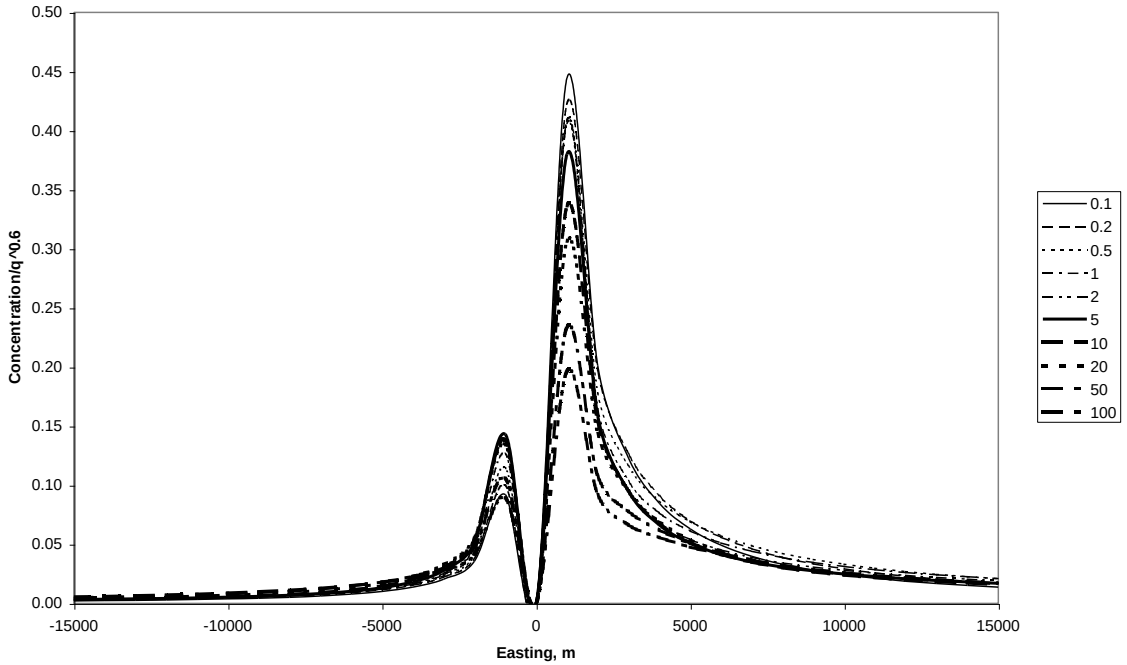

Thus, it is proposed to use the results for an emission rate of 20 g s^{-1} for all emission rates in the range 0.1-100 g s^{-1} in the preparation of dispersion kernels for oxides of nitrogen emissions. The dispersion kernel will be multiplied by $20.(q/20)^{0.6}$ to provide estimates of the impact of emission q g s^{-1} at each receptor location. Separate kernels have been created for each meteorological data year 1993-2002.

Method

Sulphur dioxide

Point sources with emissions greater than or equal to 500 tonnes per year (15.85 g s^{-1}) have been modelled explicitly using ADMS. Point sources with emissions less than 500 tonnes per year have been modelled using the small points model. This model has two components.

The in-square concentration for each source has been calculated using the following function:

$$C = 1.98.q^{0.5}$$

where C is the in-square concentration, μg m^{-3} and q is the emission rate, g s^{-1} and 1.98 is a numerical constant, calculated as the average value over the years 1993-2002 for met data at Heathrow.

The outer-grid concentration has been calculated by adjusting the emissions for each source using the function:

$$Q = 10.(q/10)^{0.667},$$

where: q is the emission rate, g s^{-1} and Q is the adjusted emissions. The sum of the adjusted emission was then calculated for each grid square and the outer-grid concentration calculated using a small points dispersion kernel (which was calculated as the average over the years 1993-2002 for met data at Heathrow).

The in-square and outer-grid concentrations were then summed to calculate the total contribution to ambient annual mean concentrations from these small point sources.

Oxides of nitrogen

Point sources with emissions greater than or equal to 500 tonnes per year (15.85 g s^{-1}) have been modelled explicitly using ADMS. Point sources with emissions less than 500 tonnes per year have been modelled using the small points model. This model has two components.

The in-square concentration for each source has been calculated using the following function:

$$C = 1.54.\ \log_{10}(10q)+0.464,$$

where: C is the in-square concentration, μg m^{-3} and q is the emission rate, g s^{-1} and 1.54 is a numerical constant, calculated as the average value over the years 1993-2002 for met data at Heathrow.

The outer-grid concentration has been calculated by adjusting the emissions for each source using the function:

$$Q = 20.\ (q/20)^{0.6},$$

where: q is the emission rate, g s^{-1} and Q is the adjusted emissions. The sum of the adjusted emission was then calculated for each grid square and the outer-grid concentration calculated using a small points dispersion kernel (which was calculated as the average over the years 1993-2002 for met data at Heathrow).

The in-square and outer-grid concentrations were then summed to calculate the total contribution to ambient annual mean concentrations from these small point sources.

PM_{10} and $PM_{2.5}$

The method for PM_{10} and $PM_{2.5}$ was the same as for NO_x, except that point sources with emissions greater than or equal to 200 tonnes per year (6.34 g s^{-1}) have been modelled explicitly using ADMS. Point sources with emissions less than 200 tonnes per year have been modelled using the small points model.

Benzene

The method for benzene was different. Point sources with combustion emissions greater than or equal to 5 tonnes per year (0.16 g s^{-1}) have been modelled explicitly using ADMS. Fugitive and process point sources have been modelled using a different small points model, as described in Section 7.3.2.

Appendix 4 – WRF meteorology

The meteorological input data for the PCM model for the 2022 compliance assessment was 50 km by 50 km gridded outputs from the Weather Research and Forecasting (WRF) numerical weather prediction modelling system (https://www.mmm.ucar.edu/weather-research-and-forecasting-model). Table A4.1 gives the options used in the WRF calculations. The WRF outputs were used in the point source modelling (detailed in Section 3.3.1, the area source model (see Appendix 5 – Dispersion kernels for the area source model) and the roads kernel model (see Appendix 8 – The PCM Roads Kernel Model). WRF meteorological data was used for the first time for the 2020 assessment.

Table A4.1 - Settings applied to WRF simulations

Parameters	Setting applied
WRF version	3.5.1
Grid resolution (domain)	50 km (Europe)
Spatial projection	ETRS89 Lambert Conformal Conic
Initial and lateral boundary conditions	Global Forecast System (GFS), 0.5 degree (GFS Forecast, 2021)
Land use	US Geological Survey land use types
Vertical layers	23
Nudging	Grid analysis nudging (U, V, Q and T), 3h nudging time interval throughout a simulation period, and nudging within PBL and above
Radiation (SW/LW)	RRTM/Dudhia
Cumulus	Kain-Fritsch
Microphysics	WSM 3
PBL	ACM2 (Pleim, 2007)
Land surface	5-layer thermal diffusion (Pleim, 2006)
Surface layer	P-X (Pleim, 2006)
Time resolution	Adaptive time step, hourly output
Year modelled	2022

Appendix 5 – Dispersion kernels for the area source model

Dispersion kernels for calculating the annual mean contribution of emissions from area sources to ambient annual mean concentrations were calculated using ADMS 5.2. Separate kernels were calculated for traffic, domestic and other area sources (which were assumed to have a constant temporal profile of emissions). Kernels were generated for the assessment year using hourly sequential meteorological data from the WRF model (see Appendix 4 – WRF meteorology). The dispersion parameters used to calculate the kernels are listed in Table A5.1. The emission profiles used to represent traffic emissions for the traffic kernels are shown in Figure A5.1a and Figure A5.1b. The profiles by hour of the day and day of the week were obtained from DfT traffic flow data for all traffic in Great Britain averaged over the period 2010-2014 (DfT, 2022a). The profile by month of the year was obtained from DfT traffic flow data for all motor vehicles in Great Britain in 2022 (DfT, 2021).

Figure A5.1a - Normalised hourly and daily temporal profiles of traffic emissions

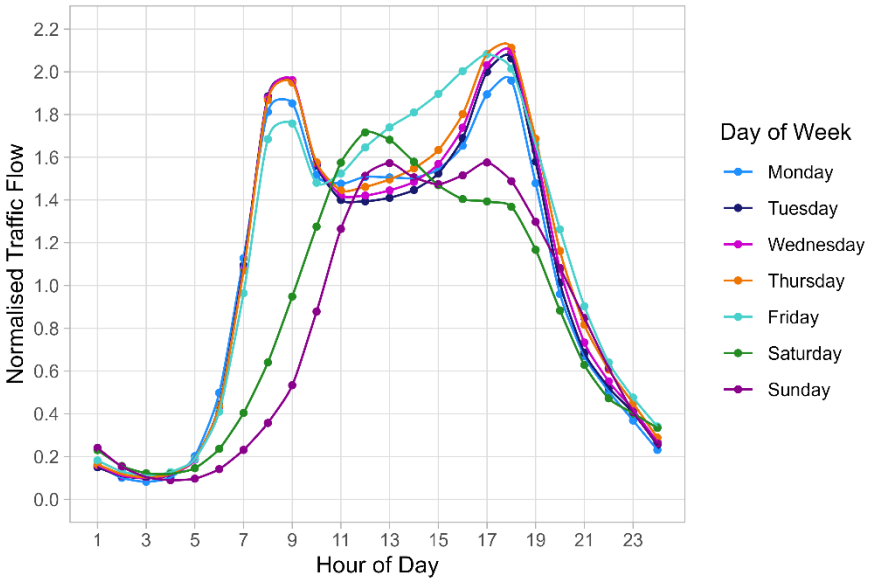

Figure A5.1b - Normalised monthly profile of traffic emissions

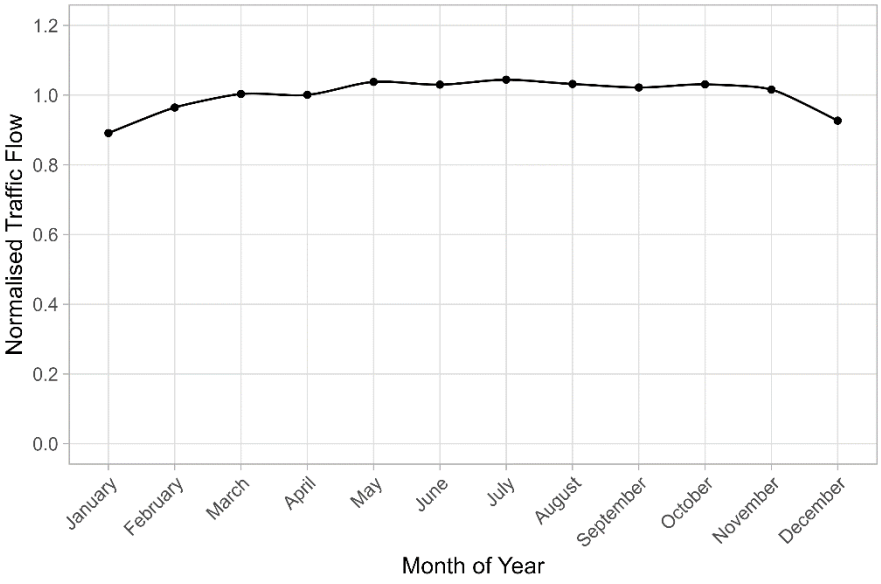

A time varying emissions profile was applied for domestic sources the first time in the 2011 assessment to better represent emissions related to domestic combustion. The 2011 – 2019

assessments used a time varying emissions profile calculated for the Waddington meteorological station. The 2020, 2021 and 2022 assessments used meteorological data from the WRF model (see Appendix 4 – WRF meteorology) and hence regional time varying emissions profiles have been applied in this work. Both seasonal and diurnal profiles have been used to weight domestic emissions. These weightings have been developed and applied following a similar method to (Coleman *et al.*, 2001). In this work a normalised diurnal profile has been superimposed onto a seasonal profile based on degree days calculated from temperature data for each WRF grid cell and the assessment year. The diurnal profile applied has been estimated from (Coleman *et al.*, 2001), see Figure A5.2. Degree days provide a simple but effective tool to relate energy use and emissions from buildings to the weather (Day, 2006). A degree day is a unit used to determine the heating requirements of buildings, representing a fall of one degree below a specified average outdoor temperature (15.5 °C, in this case). Degree days for each WRF grid cell have been calculated from the equation:

$$D_d = \frac{\sum_{i=1}^{N} \theta_b - \theta_{o,i}{}_{(\theta_b - \theta_{o,i} \geq 0)}}{N}$$

Where D_d is the daily degree days for one day, θ_b is the base temperature, $\theta_{o,i}$ is the ambient (or outdoor) air temperature and N is the number of hours of available data in a given day. Figure A5.3 shows an example seasonal profile of degree days calculated for one WRF grid cell in London for the year 2020. The seasonal profile of degree days has been verified versus National Grid, National Transmission System gas demand data.

Figure A5.2 - Diurnal profile of domestic emissions estimated from (Coleman et al., 2001)

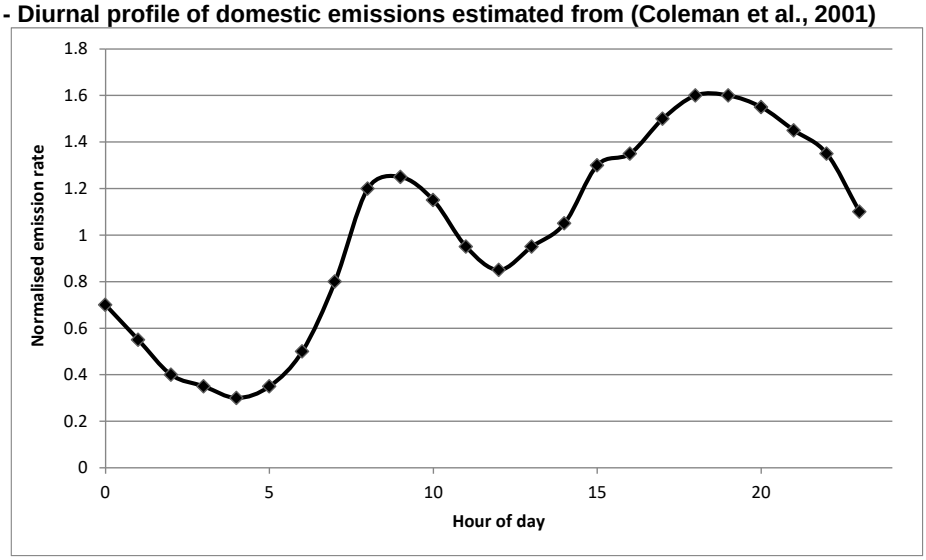

Figure A5.3 - Seasonal profile of degree days calculated for an example WRF grid cell in London in 2022 (base temperature of 15.5°C)

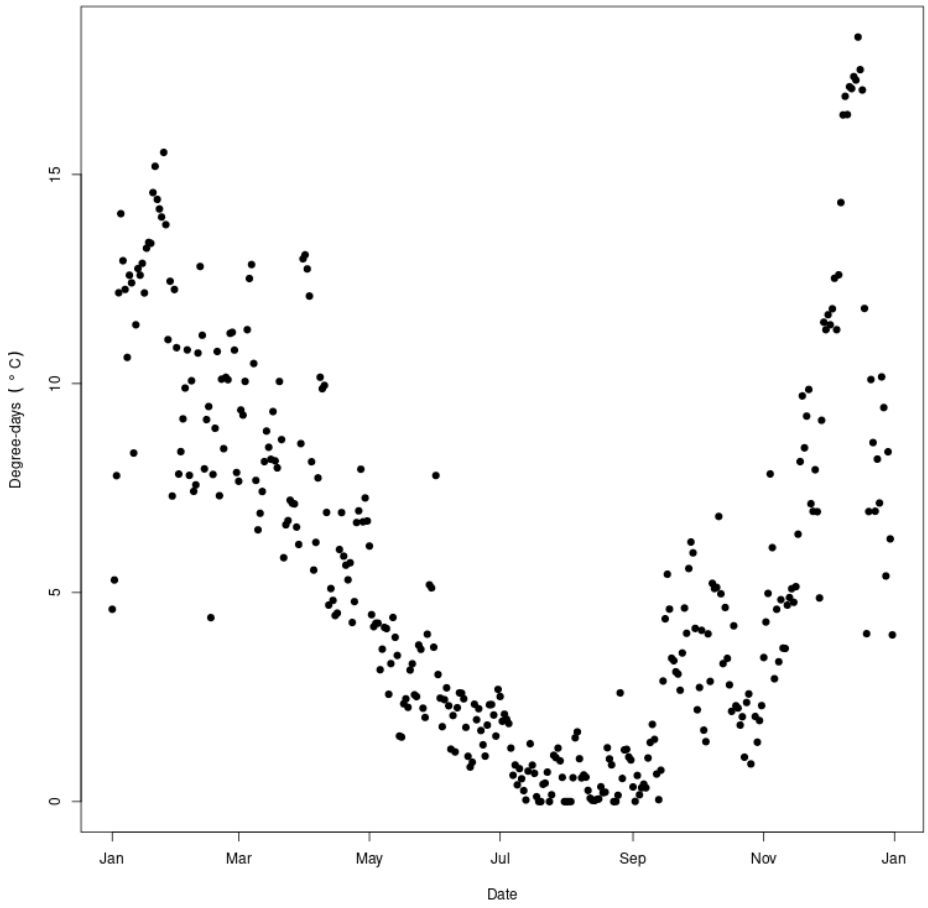

For SO_2, NO_x, NO_2, PM_{10}, $PM_{2.5}$, C_6H_6, heavy metals (Pb, As, Cd, Ni) and B(a)P the area source dispersion kernels are on a 1 km x 1 km resolution matrix and are made using ADMS 5.2. The centre squares have been scaled to remove the impact of sources within 50 m of the receptor location in that square on the basis that background sites are not located very close to specific sources such as major roads. Different kernels have been made for different area types, to take into account different dispersion conditions in urban areas of different sizes. The kernels have been made specific to different types of location by varying minimum Monin Obukhov Length (LMO) and surface roughness due to different land use (see Table A5.1). The location of the different area types are shown in Figure A5.4.

The dispersion kernels used for fugitive and process point sources of benzene are the same as the non-road transport kernels but with the values for the central receptor location calculated as described in Section 7.3.2.

Table A5.1 - Summary of inverted dispersion kernel parameters

Kernel name	Area types	Type of location	Minimum Monin-Obukhov length (m)		Surface roughness (m)		Height (m) of volume source	Variable emission profile?	Emission rate (g m^{-3} s^{-1})
			Disp. site	Met. site	Disp. site	Met. site			
Non-road transport	1,2,4	Conurbation	25	Varies by predominant area type of WRF grid cell	1.0	Varies by WRF grid cell based on USGS Land Use	30	N	3.33E-08
Non-road transport	3,4,5,6,7,8	Smaller urban	20	Varies by predominant area type of WRF grid cell	0.5	Varies by WRF grid cell based on USGS Land Use	30	N	3.33E-08
Non-road transport	9,10	Rural	10	Varies by predominant area type of WRF grid cell	0.1	Varies by WRF grid cell based on USGS Land Use	30	N	3.33E-08
Domestic	1,2,4	Conurbation	25	Varies by predominant area type of WRF grid cell	1.0	Varies by WRF grid cell based on USGS Land Use	20	Y	5.0E-08
Domestic	3,4,5,6,7,8	Smaller urban	20	Varies by predominant area type of WRF grid cell	0.5	Varies by WRF grid cell based on USGS Land Use	20	Y	5.0E-08
Domestic	9,10	Rural	10	Varies by predominant area type of WRF grid cell	0.1	Varies by WRF grid cell based on USGS Land Use	20	Y	5.0E-08
Road transport	1,2,4	Conurbation	25	Varies by predominant area type of WRF grid cell	1.0	Varies by WRF grid cell based on USGS Land Use	10	Y	1.0E-7
Road transport	3,4,5,6,7,8	Smaller urban	20	Varies by predominant area type of WRF grid cell	0.5	Varies by WRF grid cell based on USGS Land Use	10	Y	1.0E-7
Road transport	9,10	Rural	10	Varies by predominant area type of WRF grid cell	0.1	Varies by WRF grid cell based on USGS Land Use	10	Y	1.0E-7

Figure A5.4 - Map of UK area types

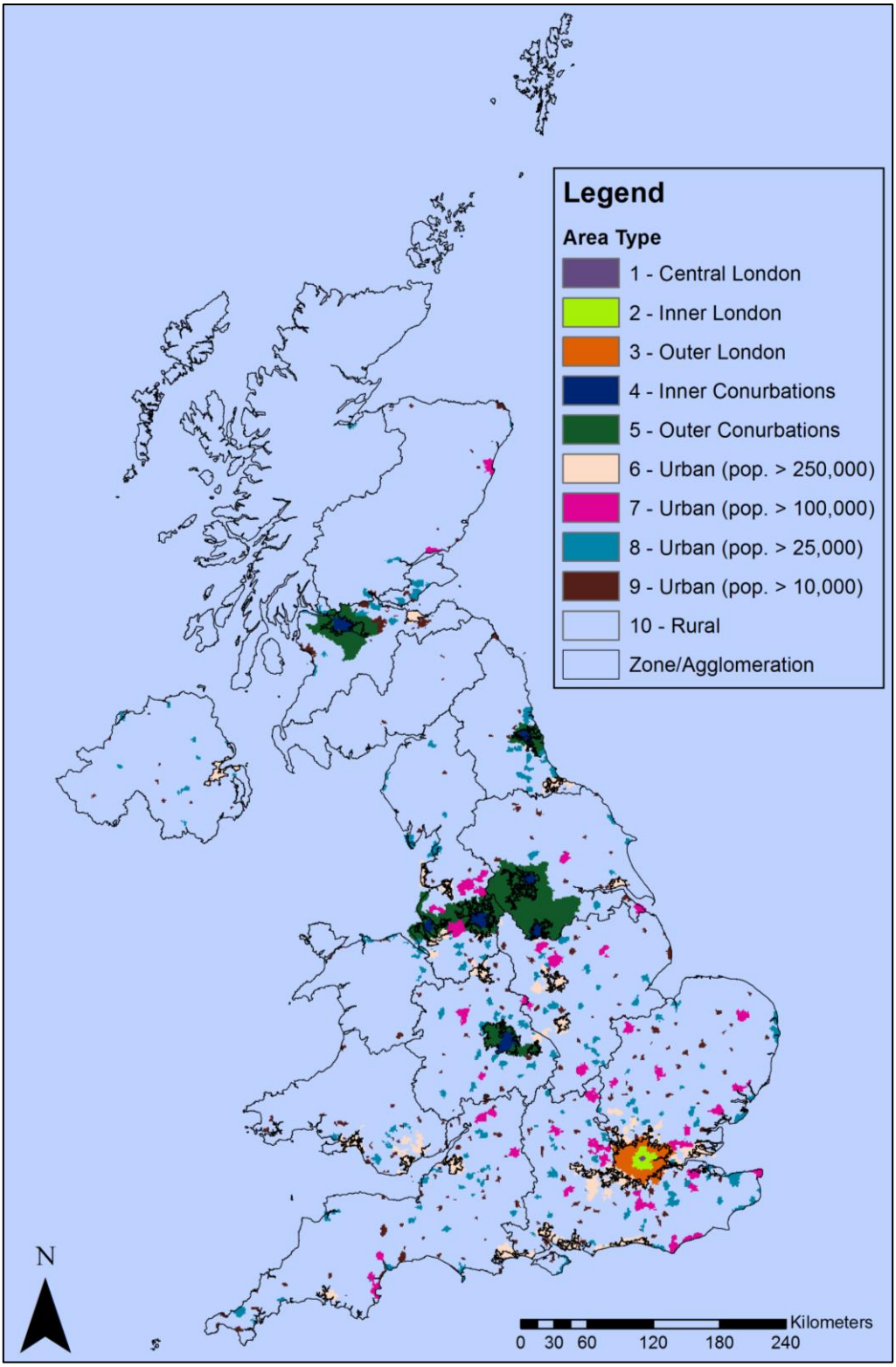

Appendix 6 – Method for calculating and mapping emissions from aircraft and shipping

Aircraft

Aircraft emissions were calculated using data obtained from the NAEI (Ingledew *et al.*, 2023) for emissions from planes in various phases of flying (e.g. take off, landing, taxiing). The NAEI provides estimates of total emissions for aircraft, which include emissions up to a height of 1000 m. Ground level emissions for use in PCM modelling were calculated on the basis of:

Ground level emissions = Taxi out + Hold + Taxi in + APU arrival + APU departure +

(0.5 x Take off) + (0.5 x Landing) + (0.5 x Reverse thrust).

The factor of 0.5 has been chosen on the basis of findings from detailed studies (Underwood, 2009). Initial climb, climb-out and approach are included in the emission inventory but excluded from ground level emissions used for the PCM model.

Figure A6.1 and Figure A6.2 show good agreement between the measured and modelled annual mean ground-level NO_X concentrations at monitoring sites in the vicinity of Heathrow and Gatwick airports for 2008, respectively, based on this approach.

Figure A6.1 - Comparison of the measured and modelled annual mean NO_X at Heathrow Airport for 2008

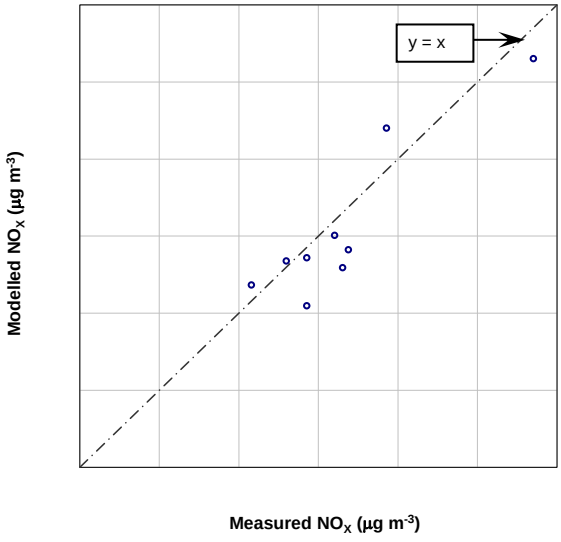

Figure A6.2 - Comparison of the measured and modelled annual mean NO_X at Gatwick Airport for 2008

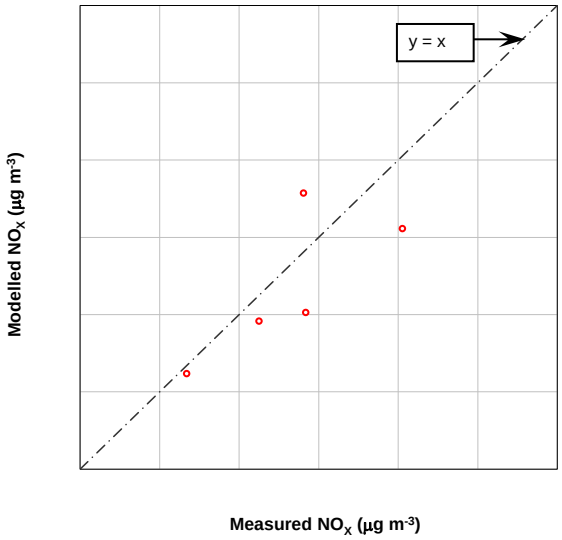

Shipping

A revised, more sophisticated, method has been used to map UK shipping emissions for the NAEI 2016, NAEI 2017, NAEI 2018, NAEI 2019, NAEI2020 and NAEI 2021. Previously, shipping emissions were estimated by modelling fuel consumption from a database of shipping activities around UK waters for different vessel, fuel and journey types (Entec, 2010). This approach provided the best available solution at that time but had some recognised issues such as the age of the dataset (dating from 2007), estimated location of vessels rather than actual locations, low spatial resolution compared with other NAEI outputs[9] and insufficient representation of shipping types other than internationally trading vessels. Improvements made to the shipping emissions modelling for the NAEI National Inventory reporting, which were first reported in (Scarbrough *et al.*, 2017), provides higher resolution and greater accuracy to shipping emissions estimates (through improved coverage of various vessel types), as well as enabling a deeper understanding of the spatial pattern of emissions compared with the previous approach.

The revised method has been developed using Automatic Identification System (AIS) data supplied by the Maritime and Coastguard Agency. AIS is an on-board ship system that transmits a message containing a vessel's position - and other information such as speed - every few seconds, to be received by other vessels, onshore or by satellites[10]. A complete set of one year's worth of AIS data received by terrestrial UK receivers was obtained and processed to give a dataset that records shipping activity at five-minute intervals for the whole of the year 2014. This was then used to calculate fuel consumption and emissions for each vessel for the year 2014 in conjunction with a second dataset of technical characteristics of individual vessels. The estimates for year 2014 were then forecast to the current NAEI year accounting for activity changes over time, the 2015 sulphur emission control area change in sulphur content limit, fleet-wide efficiency gains and additional NO_X emission factor changes to account for fleet turnover. A detailed discussion of the methodology used to develop a shipping emissions inventory from AIS data can be found in (Scarbrough *et al.*, 2017).

The process of inventory mapping seeks to spatially disaggregate NAEI inventory totals in a way that represents how those emissions are geographically distributed in the real world. AIS data are inherently spatial as they record a vessel's position, and so emissions from each ship can be easily attributed to the NAEI 1 km grid using the longitude and latitude accompanying each AIS message. A small number of messages are erroneously located upon terrestrial grid squares (Scarbrough et al., 2017, p. 10) or are legitimately in non-UK water bodies within the NAEI mapping area (e.g. vessel movements within major rivers in north-eastern France). These emissions should not exist within the UK shipping map and have been removed.

Emissions caps applied for the shipping sector for 2022 were consistent with those applied in previous years. The NAEI shipping inventory improvements have resulted in a significantly lower impact of these caps, resulting in an emissions loss of around 1% compared with 5% before the inventory improvement as a result of being more realistically distributed.

[9] NAEI maps are drawn on 1x1km resolution grid, but pre-2016 shipping emissions were based on 5x5km gridded emissions and the NAEI inherited this lower resolution limit.
[10] http://www.imo.org/en/OurWork/Safety/Navigation/Pages/AIS.aspx

Appendix 7 – Monitoring stations used in $PM_{2.5}$ AEI calculation

Table A7.1 lists the EoI codes, air quality monitoring station names, the station classification and instrument type for the sites used for the $PM_{2.5}$ AEI calculation in the 2022. The instruments that were used in the 2022 assessment were:

- Ref.eq - Reference equivalent converted from raw FIDAS
- TEOM FDMS - Tapered Element Oscillating Microbalance Filter Dynamic Measurement System
- BAM - Beta Attenuation Monitoring
- Mixed – instrument change part way through the year (in most cases from TEOM FDMS to Ref. eq)

Table A7.1 - List of urban and suburban background monitoring stations used in AEI calculation

EoI code	Station name	Station classification	Instrument type
GB0729A	Aberdeen	Urban Background	(Ref.eq)
GB0567A	Belfast Centre	Urban Background	(Ref.eq)
GB1013A	Birmingham Acocks Green	Urban Background	(Ref.eq)
GB1097A	Birmingham Ladywood	Urban Background	(Ref.eq)
GB0882A	Blackpool Marton	Urban Background	(Ref.eq)
GB0741A	Bournemouth	Urban Background	(BAM)
GB0860A	Brighton Preston Park	Urban Background	(BAM)
GB0884A	Bristol St Paul's	Urban Background	(BAM)
GB0580A	Cardiff Centre	Urban Background	mixed
GB1046A	Chesterfield Loundsley Green	Urban Background	(Ref.eq)
GB1034A	Coventry Allesley	Urban Background	(Ref.eq)
GB1005A	Eastbourne	Urban Background	(Ref.eq)
GB0839A	Edinburgh St Leonards	Urban Background	(Ref.eq)
GB1028A	Glasgow Townhead	Urban Background	(Ref.eq)
GB0776A	Hull Freetown	Urban Background	(Ref.eq)
GB0643A	Leamington Spa	Urban Background	(Ref.eq)
GB0584A	Leeds Centre	Urban Background	mixed
GB1026A	Leicester University	Urban Background	mixed
GB0608A	London Bexley	Suburban Background	mixed
GB0566A	London Bloomsbury	Urban Background	mixed
GB0586A	London Eltham	Suburban Background	(TEOM FDMS)
GB1098A	London Honor Oak Park	Urban Background	(Ref.eq)
GB0620A	London N. Kensington	Urban Background	(Ref.eq)
GB1025A	London Teddington Bushy Park	Urban Background	(Ref.eq)
GB0743A	London Westminster	Urban Background	(BAM)
GB0613A	Manchester Piccadilly	Urban Background	(Ref.eq)
GB0568A	Newcastle Centre	Urban Background	mixed
GB0962A	Newport	Urban Background	(Ref.eq)
GB1073A	Northampton Spring Park	Urban Background	(BAM)
GB0995A	Norwich Lakenfields	Urban Background	(Ref.eq)
GB0646A	Nottingham Centre	Urban Background	(Ref.eq)

EoI code	Station name	Station classification	Instrument type
GB0920A	Oxford St Ebbes	Urban Background	(Ref.eq)
GB0687A	Plymouth Centre	Urban Background	(TEOM FDMS)
GB0733A	Portsmouth	Urban Background	(Ref.eq)
GB0731A	Preston	Urban Background	(Ref.eq)
GB0840A	Reading New Town	Urban Background	(BAM)
GB1027A	Sheffield Devonshire Green	Urban Background	(Ref.eq)
GB0598A	Southampton Centre	Urban Background	(Ref.eq)
GB0728A	Southend-on-Sea	Urban Background	(Ref.eq)
GB0658A	Stoke-on-Trent Centre	Urban Background	(Ref.eq)
GB0863A	Sunderland Silksworth	Urban Background	(Ref.eq)
GB0864A	Wigan Centre	Urban Background	(Ref.eq)
GB0730A	Wirral Tranmere	Urban Background	(Ref.eq)
GB0918A	York Bootham	Urban Background	mixed

Appendix 8 – The PCM Roads Kernel Model

Description of the model

The PCM Roads Kernel Model (PCM-RKM) has been set up to calculate roadside concentrations of NO_2, NO_x, PM_{10}, $PM_{2.5}$ and benzene on urban major roads. The model uses the ADMS-Roads dispersion model[11] (Version 5.0). Individual model runs are carried out for the approximately 9000 census points covering UK urban major roads. Each model run is parameterised using specific input data for the census point. These inputs are as follows and are described below:

- Road geometry
- Traffic speeds, emissions and traffic counts
- Meteorology
- Receptor locations

Road geometry

The PCM model uses a line coverage[12] to represent the layout of UK major roads, in combination with the census point dataset which describes the traffic flows on these roads. There is one census point per major road between junctions with other major roads. The traffic flow between major road junctions is assumed to be constant based on the assumption that the majority of traffic joins or leaves major roads at junctions with other major roads.

An assessment of variation in modelled concentrations with road orientation (not detailed here) suggests that differences in road orientation can make an approximately +/- 40% change for a receptor at 4 m from the roadside. This assessment evaluated the relative change in concentration modelled for receptors at various distances from the road for all road links. For each census point, the concentration modelled for a receptor at a particular distance from the roadside was compared to the concentration modelled for an identical road link aligned due north at the same distance from the road. The relative change is largely independent of road type, traffic flow and road width; hence the orientation of a particular road is important to the modelled concentration that results. This difference is driven by the orientation of the road relative to the prevailing wind direction.

The orientation of roads within the PCM model can be described at three levels. The coarsest level is the census point level where multiple UK major road sections are associated with each census point. This level of detail corresponds to the end nodes of the road links. The major road sections level data set, which comes from Ordnance Survey data, contains major road links but has nodes at junctions with both major roads and minor roads. Finally, there is the x, y coordinate level, where the coordinates of each arc of every link which makes up the major roads GIS dataset are available, therefore several grid references correspond to each link.

The number of road links for each census point means that the stretches of road are too long to be accurately described by one orientation calculated from the end nodes of the full length of road. To best represent the road orientation the x, y coordinate level would be most accurate. However, this would produce approximately 40 records for each census point, and it would be unfeasible to resolve variations in roadside concentrations down to this level when the underlying traffic data is represented at a much coarser level. Hence to represent the orientation of road links associated with each census point the end nodes of the major road sections have been used to calculate the bearing of the road link with respect to due north. The nearest UK major road section associated with the census point is used to define the orientation for all sections associated with that census point, given that it most closely represents the situation at the census point.

Road sources within ADMS-Roads are treated as line sources of variable width. To represent road widths as accurately as possible for all roads within the UK urban major roads coverage, the width has been estimated based on lane counts provided in the census point dataset. Road widths have been calculated assuming an average width of 4 metres per lane for urban single and dual carriageway A-roads and urban motorways. The 4-metre lane width assumption corresponds to those recommended by the Design Manual for Roads and Bridges (DMRB, 2005), where a lane width of

[11] http://www.cerc.co.uk/environmental-software/ADMS-Roads-model.html
[12] A set of lines within Geographical Information System

3.65 metres is more typical and the difference in lane width takes into account the hardstrip for urban A-roads.

To provide confidence in the lane counts from the census points dataset and the lane widths calculated, these were verified for a subset of road links for the following cases:

- Where lane counts were not available
- Where only a single lane was indicated
- For road links with the highest traffic flows
- For road links where predictions indicated the highest concentrations in a zone
- For road links that were going to be included in the roadside calibration for the first time

Excluding those road links where only a single lane was indicated, for the assessed road links an average of 4 metres per lane was typical. Wider and more varied widths were observed for roads with only single lanes, but these are not characteristic of the complete dataset, typically being slip roads or small urban A-roads and carrying the least traffic (and represent less than 0.5% of the census points). All road sources are set up as line sources of length 2000 m. For road links that have not been assessed and a lane count has not been provided, the following default road widths have been assumed. The default characteristics are summarised in Table A8.1.

Table A8.1 - Default road source characteristics

Road type	Assumed number of lanes in each direction	Total width (m)	Length (m)
Single carriageway A-road	1	8	2000
Dual carriageway A-road	2	16	2000
Motorway	3	32	2000

Traffic speeds, emissions and traffic counts

ADMS-Roads uses traffic speeds and flows by vehicle category to estimate vehicle induced turbulence. The PCM-RKM uses traffic emissions for major road links in the UK provided directly by the NAEI and incorporates the vehicle induced turbulence as calculated by ADMS-Roads. Unitary emissions of 1 g/km/s are applied such that output concentrations profiles can be treated as kernels providing weightings for the pollutant specific road link emissions from the NAEI. The roadside increment concentration is calculated by multiplying concentrations modelled for unit emissions by the emissions rate for each road link. Traffic flows (annual average daily flows, AADFs) by census point have been aggregated into 2 vehicle categories i.e. light and heavy-duty vehicles for the calculation of vehicle induced turbulence.

Previously, traffic speed assumptions by vehicle category were applied following categories based upon UK area type and road type taking data from DfT congestion statistics to estimate the speeds. NAEI traffic speed assignments have been applied defined by region, land use and speed limit, see Section 3.3.6.

Emissions are assumed to be time varying, with temporal profiles varying by hour of the day, day of the week and having a seasonal monthly variation. The time varying emissions profiles for traffic are the same as those used for treating area source emissions from traffic in the PCM area source model (see Figure A5.1a and Figure A5.1b, Appendix 5 – Dispersion kernels for the area source model).[13] The profiles were obtained from DfT traffic flow data for all traffic in Great Britain averaged over the period 2010-2014 (DfT, 2022a).

[13] A 2022 specific monthly profile was used for 2022.

Meteorology

Hourly sequential meteorological data from the WRF model in the reference year has been used in the setup of the ADMS-Roads model runs (see Appendix 4 – WRF meteorology). Table A8.2 shows the other assumptions applied for details of the meteorological conditions at the roads, which are dependent on the area type and meteorological site. These are in common with the setup for the area source dispersion kernels in the PCM model (see Appendix 5 – Dispersion kernels for the area source model).

Table A8.2 - Summary of meteorological parameters applied by area type

Area types (from Table A7.2)	Types of location	Minimum Monin–Obukhov length (m)		Surface roughness (m)	
		Dispersion site	Meteorological site	Dispersion site	Meteorological site
1,2,4	Conurbation	25	Varies by predominant area type of WRF grid cell	1.0	Varies by WRF grid cell based on USGS Land Use
3,5,6,7,8	Smaller urban	20	Varies by predominant area type of WRF grid cell	0.5	Varies by WRF grid cell based on USGS Land Use
9,10	Rural	10	Varies by predominant area type of WRF grid cell	0.1	Varies by WRF grid cell based on USGS Land Use

Receptors locations

Model runs are set up with a road source for each major road link nearest to a census point. This road source represents the link at the road angle determined from the coordinates of its end nodes. Concentrations are modelled for 49 receptors, with one at the road centre line of the road link, and 24 each side perpendicular to the road link. Close to the road receptors are spaced at 1 m intervals, after 15 m from the roadside the receptor spacing progressively increases to a maximum of 200 m from the roadside. A diagram illustrating the position of receptors and road source is given in Table A8.1.

Figure A8.1- Schematic diagram of road source (blue) and receptors (red)

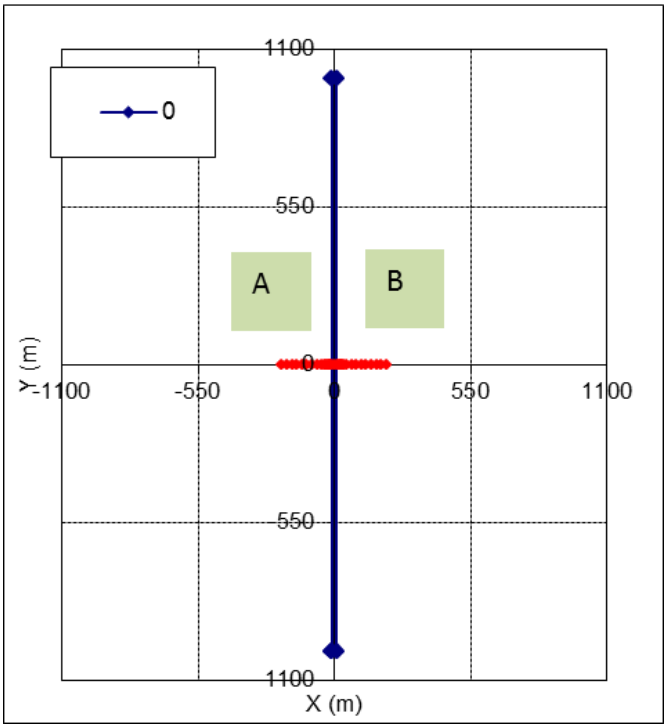

Model outputs

Modelled concentrations can be derived from the ADMS-Roads model outputs for all receptor locations specified. In the PCM-RKM modelling the average concentration across each side of the road at a distance of 4 m from the kerb for all census points has been selected for comparison with the measured concentrations at roadside (traffic) stations for model calibration. The same output has also been used for the compliance assessment modelling for roadside (traffic) concentrations. To illustrate the variation in concentration modelled with distance from the road a normalised concentration profile is presented in Figure A8.2.

Figure A8.2 - Example normalised concentration profile

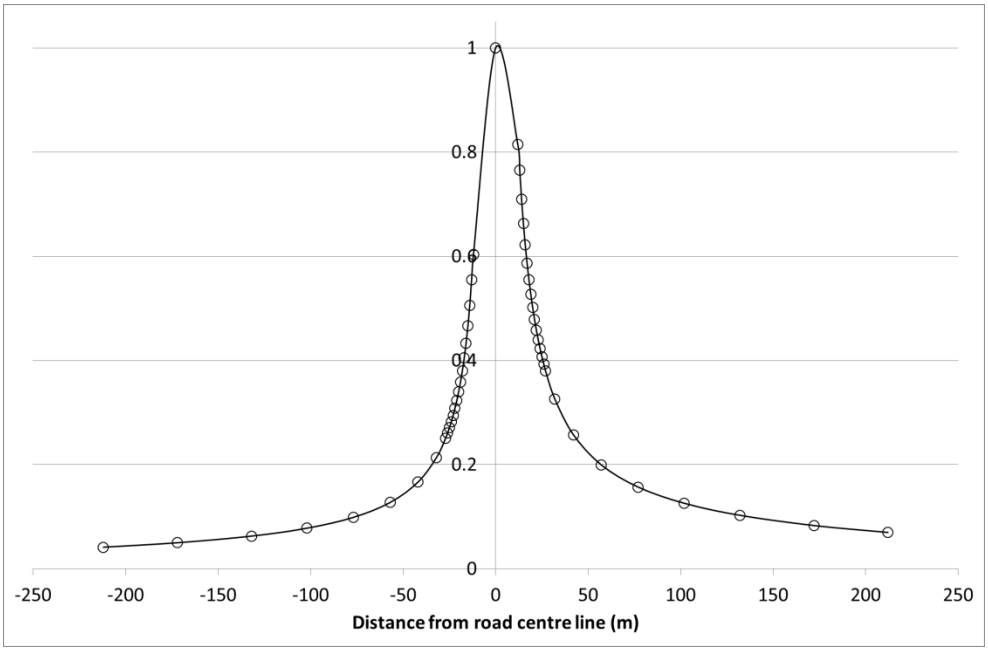

Model calibration

The PCM-RKM uses the PCM roadside increment approach for the prediction of the local contribution to total concentrations at the roadside. As such the annual mean concentration at roadside locations has been assumed to be made up of two parts: a background concentration (excluding local sources) and a roadside increment.

Roadside concentration = background concentration + roadside increment.

To calibrate the model, modelled concentrations are compared to measured roadside increment concentrations (i.e. measured roadside concentration minus modelled background concentration) at AURN roadside traffic stations. Figure 3.9 in Chapter 3 presents the calibration plot for NO_X for 2022 for the PCM-RKM.

Adjustment factors applied to road link emissions

The effect of street canyons has not been explicitly included in the PCM-RKM model. Instead, the model calibration based on the comparison of measured and modelled roadside concentration increments implicitly includes some influence of street canyon effects, dependent on how much the local environment of the AURN road traffic stations used to calibrate the model can be characterised as street canyons. Street canyons are typically characterised in terms of aspect ratio, the ratio of the road width to the height of buildings lining the road. Vardoulakis et al. (2003) characterised avenue canyons as those with aspect ratios (AR) < 0.5, and deep canyons as those where AR = 2.

Motorways are expected to have a more open aspect than the urban streets where the AURN road traffic stations used to calibrate the model are situated. An adjustment factor has therefore been derived for motorways.

The AURN road traffic stations used to calibrate the model have been characterised in terms of AR from estimates of the average road widths (building façade to building façade) and average building heights determined by examining the roads within ArcMap, Google Earth and Google Streetview.

In development of the PCM-RKM, comparison of roadside modelling results to the previous PCM model output indicated significant increases in the modelled concentrations for roads with high traffic flows predicted by using ADMS-Roads. These increases are not thought realistic and indicate under-prediction of dispersion for the widest and highest flow roads since dispersion is likely to be most efficient on these roads. To address this, adjustment factors have been developed to apply to the road link emissions for motorways and A-roads where the traffic flow exceeds an annual average daily flow of 75,000.

The combined traffic flow and motorway adjustment factors as a function of traffic flow are presented in Figure A8.3.

Figure A8.3 - Combined adjustment factors applied to road link emissions for 2022

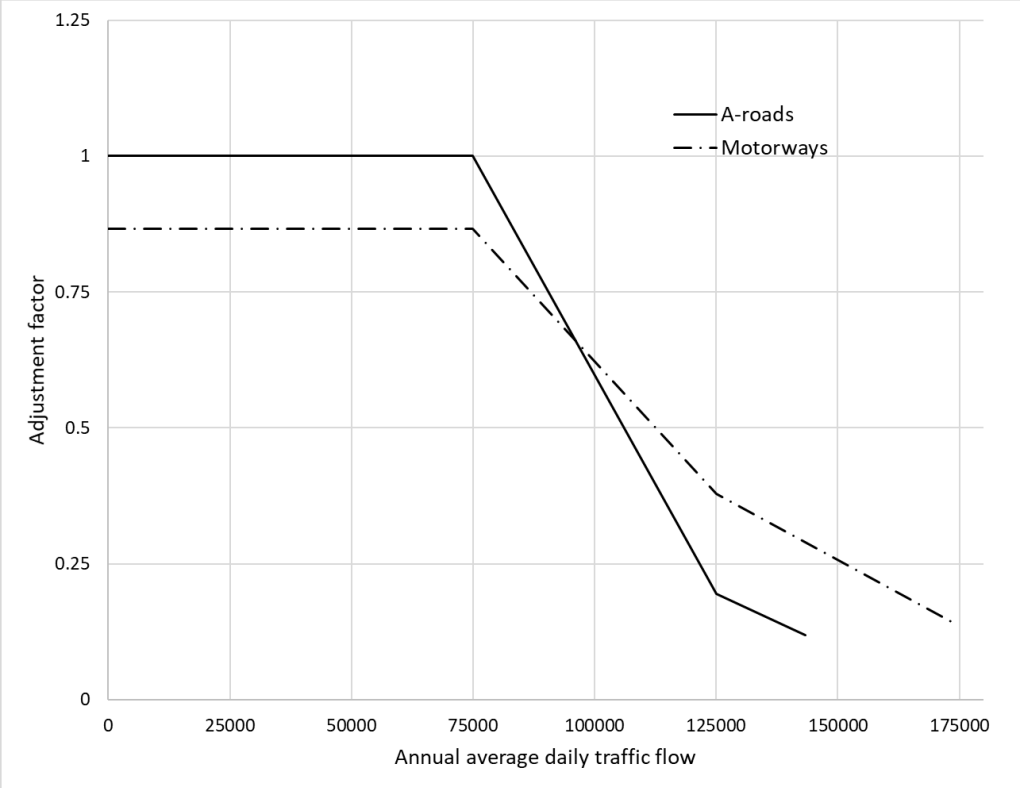

Model verification

Verification of the PCM-RKM for NO_X, NO_2, PM_{10}, $PM_{2.5}$, and benzene for the assessment year is discussed in the body of this report.

Appendix 9 – Selected acronyms

ADMS	Atmospheric Dispersion Modelling System
AEI	Average exposure indicator
AGANet	UK Acid Gases and Aerosols Monitoring Network (UK)
AOT40	Accumulated exposure index above a threshold concentration of 40 ppb
APU	Auxiliary power unit (aircraft)
AQD	Directive on ambient air quality and cleaner air for Europe (2008/50/EC), known as the 'Air Quality Directive'
AQDD4	The fourth Daughter Directive 2004/107/EC (AQDD4) under the Air Quality Framework Directive (1996/62/EC)
AQUILA	European Network of Air Quality Reference Laboratories
AQSR	Air Quality Standards Regulations 2010
As	Arsenic
AURN	Automatic urban and rural network (UK)
B(a)P	benzo(a)pyrene, a polycyclic aromatic hydrocarbon
BEIS	Department for Business, Energy & Industrial Strategy
Cd	Cadmium
CL	Critical level
CO	Carbon monoxide
COPERT	Software tool used to calculate air pollutant emissions from road transport
Defra	Department for Environment, Food & Rural Affairs
DQO	Data quality objective
ECO	Exposure concentration obligation
EEP	Energy and emissions projections
EMEP	European Monitoring and Evaluation Programme under the Convention on Long-range Transboundary Air Pollution
ERG	Environmental Research Group, Kings College London
ERT	Exposure Reduction Target
ETS	Emissions Trading Scheme
f-NO_2	The fraction of NO_x emissions emitted as primary NO_2 (by volume)
HDV	Heavy duty vehicles
IDW	Inverse Distance Weighting
IED	Industrial Emissions Directive (2010/75/EU)
IPR	Implementing Provisions on Reporting (Decision 2011/850/EU)
LAQN	London Air Quality Network
LEZ	Low Emission Zone
LMO	Monin Obukhov Length
LTO	Long term objective
LV	Limit value
MAAQ	Modelling Ambient Air Quality
NAEI	National Atmospheric Emissions Inventory (UK)

NAME	Numerical Atmospheric-dispersion Modelling Environment
NAMN	National Ammonia Monitoring Network (UK)
NERT	National Exposure Reduction Target
Ni	Nickel
NO	Nitrogen monoxide
NO_2	Nitrogen dioxide
NOx	Oxides of nitrogen
O_3	Ozone
Pb	Lead
PCM	Pollution Climate Mapping
PCM-RKM	Pollution Climate Mapping Roads Kernel Model
PM	Particulate Matter
PM_{10}	Particulate matter 10 micrometres or less in diameter
$PM_{2.5}$	Particulate matter 2.5 micrometres or less in diameter
SIA	Secondary inorganic aerosol
SNAP	Standardized Nomenclature for Air Pollutants (emissions inventory sector splits)
SO_2	Sulphur dioxide
SOA	Secondary organic aerosol
TEOM	Tapered element oscillating microbalance
TEOM FDMS	Tapered element oscillating microbalance and Filter Dynamics Measurement System
TRACK	A receptor oriented, Lagrangian statistical air quality model
TV	Target value
UKEAP	United Kingdom Eutrophying & Acidifying Network
ULEZ	Ultra-Low Emission Zone
UUNN	UK Urban NO_2 Network
VCM	Volatile correction model
WRF	Weather Research and Forecasting

The Gemini Building
Fermi Avenue
Harwell
Didcot
Oxfordshire
OX11 0QR
United Kingdom
t: +44 (0)1235 753000
e: enquiry@ricardo.com

ee.ricardo.com